Coventry University

Coventry University

DOCTOR OF PHILOSOPHY

Decision making on mitigating a possible collision of an autonomous vehicle on a motorway

Gilbert, Alexander

Award date:
2019

Awarding institution:
Coventry University

[Link to publication](#)

Decision Making on Mitigating a Possible Collision of an Autonomous Vehicle on a Motorway

Alexander Gilbert
BEng. (Hons), MScR

A thesis submitted in partial fulfilment of

the University's requirements for the

degree of Doctor of Philosophy.

September 2018

Coventry University

Certificate of Ethical Approval

Applicant:

Alexander Gilbert

Project Title:

Control of Autonomous Vehicles in Highway Driving Situations to Improve Safety

This is to certify that the above named applicant has completed the Coventry University Ethical Approval process and their project has been confirmed and approved as Low Risk

Date of approval:

05 July 2018

Project Reference Number:

P72931

Abstract

Autonomous vehicles are fast becoming one of the major areas of research for automotive engineering. When the vehicle is fully in control of its actions, this raises questions concerning automotive safety, such as what an autonomous vehicle will do when faced with an imminent collision. Assuming that autonomous vehicles cannot crash is a dangerous over-estimation, and so systems need to be in place to limit the potential risks to vehicle occupants.

The aim of this research is to develop a control strategy for an autonomous vehicle, called the Host Vehicle, to avoid or mitigate collisions on longitudinal multiple carriageway roads. These multiple carriageway roads are arterial roads, called motorways. The potential collisions must be assessed from the perspectives of all vehicles involved in the impact, to prevent a selfish decision being made by the Host Vehicle. The main scenario of this thesis is of an autonomous vehicle driving on a three-lane motorway, with potential collisions in each lane. Therefore, each lane is a possible choice for the autonomous vehicle to select. This thesis proposes a system that selects the safest possible crash for an autonomous vehicle when faced with multiple possible collisions. This system aims to avoid or mitigate potential collisions.

This system requires expertise from several different areas. Autonomous highway platooning systems have been developed and tested to demonstrate that autonomous vehicles can crash. If a potential lane-change manoeuvre is required to avoid or mitigate a collision, the manoeuvre must be planned and assessed to ensure the risk to the autonomous vehicle safety is not increased. The potential collisions must be assessed for severity, requiring modelling of these collisions to produce metrics for a decision-making process. The severity of a collision is greatly influenced by the impact velocity, which therefore requires the impact velocity of the potential collisions to be simulated. Two simulators are developed for the case when Vehicle-to-Vehicle communication is available, and the case when this communication is not available. These two cases influence the available parameters for calculating the severity of the collision. Once all the required outputs from the simulators and modelling are produced, describing the potential collision severity of each available lane, these are used to select the lane with the least severe collision scenario. Multi-Attribute Decision Making (MADM) is used to assess the outputs from the simulators, and make the decision of which lane the autonomous vehicle should

drive into. MADM has not been applied to this type of problem before. The MADM methods which are investigated for this research problem are the Technique for Order of Preference by Similarity to Ideal Solution (TOPSIS), the Analytical Hierarchy Process (AHP), and the Analytical Network Process (ANP).

The novelty of the proposed system includes the application of Multi-Attribute Decision Making to select the least severe collisions for the Host Vehicle to take, therefore an autonomous decision is made to improve the safety and survivability of vehicle occupants. This system is supported by the development of a new two stage collision modelling to describe the severity of multiple vehicle collisions. These two stages are two separate rear-end collisions, the Host Vehicle collides into a vehicle ahead, and a vehicle behind collides into the Host Vehicle. A steering and braking trajectory planner is developed to give the Host Vehicle multiple actions to select from.

The proposed simulation methods are tested and evaluated with respect to the decisions they make. This includes simulating several scenarios in which the simulated vehicles vary their behaviours. The result is a recommended lane choice, so the car decides on the safest collisions to have. The scenarios vary the input parameters such as initial velocity, available headway distance and braking of vehicles. Each scenario is tested, and the lane selection is presented. The parameters are varied in a sensitivity analysis to demonstrate how the lane selection can change based on the inputted scenario. The TOPSIS and AHP methods generated good decisions in line with the decisions made by the subject expert. The ANP method would require further parameter tuning. The proposed system is intended to be an evolution of the current Adaptive Cruise Control and Collision Avoidance/Warning systems including Automatic Emergency Braking.

Acknowledgements

Finally, I would like to express my gratitude to my family who have supported me with massive amounts of patience every year, whilst I have not reciprocated that patience.

Alex Gilbert

2018

Contents

List of Figures

List of Tables

Nomenclature

a	m/s^2	Acceleration
A_F	m^2	Largest cross sectional area of the vehicle
a_x	m/s^2	Longitudinal acceleration
a_y	m/s^2	Lateral acceleration
$a_{x.max}$	m/s^2	Maximum longitudinal acceleration
$a_{y.max}$	m/s^2	Maximum lateral acceleration
C_d		Aerodynamic drag coefficient
C_r		Coefficient of rolling resistance
CoM		Centre of mass
$C_{\alpha f}, C_{\alpha r}$	N/rad	Tyre cornering stiffness front and rear respectively
D	m	Platoon spacing constant
d		Euclidean distance
DoF		Degrees of freedom
E	J, kJ	Energy absorbed by vehicle in collision
F	N	Force
F_a	N	Laplace transform of f_a
f_a, f_b	N	Linear force acting on Vehicles a and b, respectively
F_{aero}	N	Aerodynamic drag force
f_{k_a}	N	Reaction force acting through the crash structures of Vehicle a
F_{Long}	N	Force to accelerate vehicle (accelerate or brake)
f_{pa}	kN	Failure Point
$F_{Resistance}$	N	Resistance forces acting on vehicle
F_{xf}, F_{xr}	N	Longitudinal tyre forces at the front and rear respectively
F_{yf}, F_{yr}	N	Lateral tyre forces at the front and rear respectively
FEA		Finite Element Analysis

g	m/s^2	Acceleration due to gravity
h	m	Perpendicular distance to the COM of the vehicle from the line of action of the principle direction of force
I_z	$kg.m^2$	Moment of inertia in yaw
J	$Joules$	Unit of energy
k_a, k_b	kN/m	Crash structure stiffness of Vehicles a and b, respectively
kg	$kilogram$	
kJ	$kiloJoules$	
km	$kilometres$	
km/h	$kilometres/hour$	
kN	$kiloNewtons$	
kN/m	$kiloNewtons/metre$	
kr	m	Radii of gyration described by $I_i = M_i k_i^2$
L	m	Vehicle length (highway platooning report)
l	m	Vehicle wheelbase length (steering controller report)
l_f, l_r	m	Distance from COM to front and rear axles respectively
m	m	Unit of distance
M	kg	Mass
M_z	$kg.m^2/s$	Moment of yaw
M_a, M_b	kg	Mass of Vehicles a and b, respectively
M_c	kg	Mass of datum point
mph	$miles/hour$	Unit of Speed
ms	$milliseconds$	Unit of time
m/s	$metres/second$	Unit of Speed
m/s^2	$metres/second^2$	Unit of acceleration
N	$Newtons$	Unit of force
nm	$nanometres$	Unit of distance
P	$kg.m$	Momentum
R	m	Radius of curvature
R_x	N	Rolling resistance force

R_{xf}, R_{xr}	N	Rolling resistance force for front and rear axles respectively
s	m	Displacement
t	$seconds$	Time
u	m/s	Initial velocity
u_b		System input to bilinear modelling
u_i		Input control for Vehicle i
v	m/s	Forward velocity
V_a, V_b		Vehicles a and b, respectively
v_a, v_b	m/s	Velocity of Vehicles a and b, respectively
V_H		Host Vehicle
v_i	m/s	Velocity of vehicle i in platoon
$\dot{v}_i$	m/s^2	Derivative of velocity for Vehicle i, acceleration
v_{wind}	m/s	Velocity of headwind
v_x	m/s	Velocity x component
v_y	m/s	Velocity y component
x	m	Displacement in x axis
X_a	N	Laplace transform of x_a
x_a, x_b	m	Distance of Vehicles a and b, respectively
$\dot{x}_i$	m/s	Derivative of displacement for Vehicle $i = v_i$
$\ddot{x}$	m/s^2	Second derivative of longitudinal displacement
x_s		Simulated value for Euclidean Optimization
y	m	Displacement in y axis
$\ddot{y}$	m/s^2	Second derivative of lateral displacement
y_b		System input to bilinear modelling
y_{FEA}		FEA data value for Euclidean Optimization
β	$radians$	Sideslip angle
β		coefficient of the linear part of the Bilinear system
γ	$metres^{-1}$	Curvature of radius
γ_a		Scaled stiffness value
γp		Collision velocity parameter
δ	$radians$	Steering angle
δ_a	m	crash structure deformation along the longitudinal x axis
ε_i	metres	Spacing for platoon vehicles

η		coefficient of the bilinear product term involving the input and output
θ	$radians$	Angle of incline
μ		Coefficient of friction
ρ	kg/m^3	Density of air
ψ	$radians$	Yaw angle
$\dot{\psi}$	$radians/s$	Yaw rate
o	$degrees$	Angle of rotation

Chapter 1

Introduction

1.1 Introduction

Automotive engineering is an ever-developing industry, researching new technologies to further the capabilities of transport in the modern world. For decades, one of the main research areas has been safety. Moving vehicles at high speeds increases the risks to those around, and so safety technologies have developed to reduce the risks to human life.

One of the newest research areas is autonomous vehicles, with automotive manufacturers, research groups, universities and governments investing in the developing methodologies that will result in self-driving cars. This thesis concerns an autonomous vehicle development which supports the continual need to improve automotive safety. Allowing the vehicle to drive itself, in theory means that human error can be eliminated as a cause of automotive collisions. However, humans have

intuition, a natural behaviour that acts when facing an imminent danger. If an autonomous vehicle is facing an imminent collision, what should it do? The idea of this research and that of the industrial collaborator is to consider the risk to all vehicles involved in potential collisions, and not just itself.

1.2 Motivation for Research

Existing collision avoidance technologies focus on braking control, to reduce the vehicle's velocity to either avoid or mitigate a collision (Moon, Moon, and Yi, 2009). There is an existing research which evaluates steering as an option to avoid a collision, and even employ steering and braking to slow a vehicle's velocity whilst also steering around a hazard. However, these steering avoidance systems will only steer the vehicle if an avoidance is possible. Existing research from Anderson et al. (2010) and Hayashi et al. (2012) focuses on collision avoidance, but what if all actions the autonomous vehicle can take will result in a collision?

This thesis asks a question which is related to the trolley problem, which theorizes only two possible lanes for a trolley to take, both resulting in collision. If there are separate unavoidable collisions ahead, which should be selected? Bleske-Rechek et al. (2010) surveyed people's responses to the ethical thought experiment of the trolley problem, and personal factors that may influence the decision. Nyholm and Smids (2016) use the trolley problem to demonstrate the ethical decisions that autonomous vehicles will need to make, which may result in harming people involved in one collision over another. This thesis addresses the question of which collision will be the safer to have. An evaluation is also needed to determine the severity of possible secondary collisions, in case the actions of the autonomous vehicle move it into the path of a vehicle behind itself. This calls for a development of an autonomous collision mitigation system.

1.3 Preliminary Background Information

The research conducted in this thesis draws from the science of vehicle dynamics, which can describe the vehicle's ability to perform the intended manoeuvres. This is informed by the works of Milliken and Milliken (1995) to calculate the Ackermann steering angle, Blundell and Harty (2004) to calculate the yaw capabilities of a

vehicle, and Rajamani (2011) to calculate a lateral acceleration used to determine a safe braking value that won't result in tyre over-saturation during a steering manoeuvre. If there are avoiding or mitigating actions for the Host Vehicle to select from, then there are different manoeuvres which must be planned and evaluated. Vehicle dynamics is critical in determining the safety of any actions the Host Vehicle can or cannot take.

The different options the Host Vehicle can take may result in a need to mitigate collisions. The assessment of the severity of a collision is informed by the modelling technique introduced by Kamal (1970), by using a lumped-mass model to simulate the collision. Pickering et al. (2018) have further developed this modelling technique for simulating collisions between two vehicles. It is adapted by this thesis. Whilst this research area will require further development, it is intended that the develop system be able to work in real-time for future applications.

A decision must be made with these different potential collisions and they will be described by parameters. Different parameters can be used to measure the severity of the collision such as impact velocity between the autonomous vehicle and vehicle ahead or the required braking for the vehicle behind to avoid a collision with the autonomous vehicle. These parameters can also be in conflict with one another, such as the impact velocity ahead in one lane may be a very low value whilst the required braking behind in the same lane is very high. A mathematical decision making method is employed to make an unbiased decision. For this Multi-Attribute Decision Making (MADM) methods are investigated, and in particular the methods AHP (Saaty, 1980), TOPSIS (Hwang and Yoon, 1981), and ANP (Saaty, 1996). The problem is that an autonomous vehicle is following another vehicle which comes to a sudden stop. The MADM methods are employed to assess the proposed collisions, and determine the best lane for the Host Vehicle to drive into, effectively selecting the safest collision. A MADM method has not yet been applied to this type of problem.

This research problem is described under collision avoidance. Existing collision avoidance technologies such as Ammoun and Nashashibi (2009) aim to avoid a collision. Hayashi et al. (2012) and Anderson et al. (2010) even proposed methods to introduce steering to avoid a collision. However, there is a need for improvement when addressing what an autonomous vehicle should do when avoidance is not available.

1.4 Research Objectives

The overall aim of this research is to develop a control strategy for an autonomous vehicle, the Host Vehicle, to avoid or mitigate collisions on longitudinal multiple carriageway roads (motorways). The potential collisions must be assessed from the perspectives of all vehicles involved in the impact, to prevent a selfish decision being made by the Host Vehicle. A selfish decision will only assess the simulation results which describe the severity of the collision for the Host Vehicle, but this may also conflict with the severity for the other motorway vehicles. Simulation results describing the collision severity for the other vehicles on the motorway will need to be considered by the Host Vehicle. The Host Vehicle will then decide on the safest collision.

This aim is supported by the following objectives:

- Analyse the current developments in the area of mitigating collisions.
- Investigate the potential that autonomous vehicles can collide.
- Develop a simulator to evaluate the impact of a collision.
- Develop a decision-making method to decide on the best action that the autonomous vehicle should take in order to mitigate a possible collision.

This research programme aims to develop a decision making system for an autonomous vehicle to select the least severe collision on a motorway. This aim requires addressing several issues. First, highway platooning will demonstrate that an autonomous system can be made unstable, resulting in collision. The aim of this is to demonstrate that there is a need for autonomous vehicles to have a system which will make a decision on mitigating collisions, as it cannot be assumed that collisions are always avoidable. The models will further develop the exiting research on highway platooning, and further developments will be undertaken to analyse the impact of vehicle spacing on the platoon performance. The developed models will also be tested with vehicle speeds which more closely represent UK motorway speeds, and the platooning itself will be stressed to observe at what point the platoon becomes unstable, and results in collisions. The platoons will be further stressed by introducing time delays, to slow the reactions of the vehicles, and the platoon size will be increased.

The autonomous vehicle may need to perform a lane-change manoeuvre, requiring this manoeuvre to be planned and assessed. A lane-change trajectory planner must be developed and tested. The steering controller aims to demonstrate that the trajectory planned can be implemented by a steering controller. In order to accomplish the aim of performing a steering manoeuvre into an adjacent lane whilst also slowing the vehicle down, a sinusoidal wave will be used as a trajectory plan. A tyre saturation model will be used. A kinematic model will be used to demonstrate the manoeuvre, but is the trajectory and braking planner which is important for later parts of the thesis.

Collision modelling which can simulate the zero lateral offset collisions described in the scope of this thesis needs to be developed. The aim of this research is to develop an accurate and useable model which can produce results describing the collisions, and which can be used to assess severity of the collisions. The modelling technique does need tuning, to best reproduce available FEA data. A tuning method will be developed based on Euclidean geometry, as to optimise the key properties. The modelling will consider one vehicle impacting another at the rear. This modelling will be further developed to simulate a second collision stage, by considering three cars colliding in one lane.

The proposed scenario of a 3 lane motorway and multiple potential collisions must be simulated by motorway simulators. The aim of this objective is to develop simulators which can reliably and accurately produce results describing the severity of multiple possible collisions. Multi-Attribute Decision Making (MADM) methods will be investigated to support decision making on selecting the best lane for the autonomous vehicle to drive into. The simulators will need to use developments from earlier sections in the thesis. This intends to simulate the impact velocities of multiple collisions in multiple lanes, but also calculate if a manoeuvre into any given lane is viable or not. If not, then this manoeuvre, and so this lane, will be disqualified from the decision process. The simulators must ensure that any action taken will result in a safer outcome for all involved, and must not increase the danger to the vehicle occupants.

The proposed system will need to be tested to demonstrate that the main aim of an autonomous vehicle selecting the least severe collision can be achieved. The sensitivity analyses to be carried out will demonstrate the impact of the decisions made, and will determine what parameters can affect this lane selection. Limitations in the developed simulators and decision making processes will be identified.

1.4.1 Scope

Autonomous vehicle safety is a research problem that will be in continuous development for decades to come. Therefore, it is critical to limit the scope of this research programme, aiming to give a meaningful contribution to one defined area, as opposed to accomplishing very little in the larger research area.

The project will be focusing on motorways. These are multiple carriageway roads, sometimes referred to as arterial roads. Although slower urban roads have statistically more collisions, the higher speeds operating on motorways are more likely to result in severe injury or fatal accidents. The most severe collisions occur on rural roads, as given in accident statistics by the House of Commons (2013), but this is not included in the scope of this research problem. The monotonous driving on motorways is a key assumption for autonomous vehicles, as is demonstrated by the already existing Adaptive Cruise Control technologies, and highway platooning technologies in development to form convoys of automated vehicles driving closely together.

The project will only be addressing potential impacts with cars. Collisions with pedestrians, cyclists, motorbikes and larger heavy vehicles such as lorries and buses will not be included. The focus on motorways also allows for the assumption of straight roads. In reality, even motorways are not completely straight, but will be assumed to be so. This is agreed with the industrial support for this research problem. Calculating the velocities and displacements of the vehicles on a curved road increases the complexity of the simulators to be used in the decision making processes. This is a development to be considered in the future. This thesis focuses on the decision making of the autonomous vehicle on the straight motorways. This thesis aims to present a control strategy concept, which could be further developed at a later stage to include other potential collision scenarios and in different environments.

Allowing an autonomous vehicle to take control of the vehicle's safety raises ethical questions. This is a considerably large debate, which will not be addressed in this thesis. This thesis assumes that it is the ethical responsibility of the autonomous vehicle to minimise the risks to its occupants as much as possible, whilst also limiting the potential risks to others. If the autonomous vehicle chooses to change lanes, it is also effectively choosing other victims with which to have the crash. If the overall risk in one lane is lower than another, then the autonomous vehicle is ethically

responsible to select the lowest overall risk. In this way it gives an overall benefit to all vehicles involved, even those which will not be involved in the selected collisions. The proposed control strategies will only be simulating vehicles, and not the occupant inside, but the collision severity for a vehicle is assumed to directly influence the severity for the vehicle's occupants.

1.5 Research Methodology

Existing models are the inspiration for further development into highway platooning. The platooning analysed involves a single lead vehicle with 5 following vehicles. The models of the lead vehicle and following vehicles will be constructed in MATLAB/Simulink. Improving the performance of the existing platooning model will be investigated by introducing PI control for platoon stability. The model will be further tested by introducing time delays, and increasing the size of the platoon.

To assess the viability of a steering manoeuvre into an adjacent lane, a steering and braking trajectory planner is to be developed, also using MATLAB/Simulink. This model needs to plan a steering trajectory and calculate an available braking value to slow the vehicle without oversaturating the tyres. The steering and braking manoeuvre will use a kinematic model to demonstrate its performance.

Collision modelling is to be developed to assess the severity of zero lateral offset rear-end collisions between two or more vehicles. A mass-spring system is the initial inspiration for a new modelling technique to measure the deformation and acceleration of a defined mass. This mass-spring model is to be adapted into a bilinear lumped mass model. It will be constructed in MATLAB/Simulink. The bilinear model aims to reproduce collision data from a vehicle model, and will use a Euclidean optimization to geometrically tune the bilinear parameters by comparing the model's simulation results with the collision data.

As there are multiple lanes, and therefore multiple vehicles for the Host Vehicle to collide with, a motorway simulator needs to be developed. This will calculate the positions and velocities of multiple vehicles on a multiple lane road. These lanes and their vehicles will be simulated in MATLAB/Simulink, to calculate the potential impact velocity of the Host Vehicle and any of these potential vehicles. Each lane will have a vehicle ahead of the Host Vehicle, and a vehicle behind. This

means that in any of the 3 lanes, there are potentially 2 collisions, therefore 6 potential collisions must be simulated in total. The MADM methods which assess these simulation results are to be selected and applied in the problem. They will recommend which of the 3 possible lanes is the most appropriate for the Host Vehicle to drive into. The MADM methods will be developed in MATLAB/Simulink.

The developed simulator and decision making processes will need testing, and so sensitivity analyses will be performed, after benchmark scenarios are set. As one parameter will be varied in each sensitivity analysis, it will be observed how that one parameter will influence the simulation results, and the decision made. A number of different parameters will need varying, to evaluate which of the parameters has the influence on the decision. The decision is the lane into which the Host Vehicle will drive into, to avoid or mitigate collisions.

1.6 Outline of Thesis

The research objective of selecting the safest collision, is a complex problem requiring research and development in several areas. To begin, a literature review is conducted in Chapter 2. This gives an overview of the existing research on which this thesis employs to develop the contributions in this field. Chapter 3 reviews the MADM methods which will be appropriate for the research problem.

Chapter 4 demonstrates that even autonomous vehicles can still crash, and therefore demonstrates a need for a safety control system. In this chapter highway platooning models are created, influenced by the works of Cook (2007). Highway platooning is a system that is intended for use on motorways, which is the same environment considered in this thesis. Chapter 4 demonstrates that the autonomous system can become unstable, and therefore can result in collisions. Highway platooning inspired the format of the motorway adapted in this research. This research considers 3 lanes of a motorway.

Chapter 5 addresses the need for a lane-change manoeuvre. This thesis is looking at selecting the safest lane for the Host Vehicle to drive into, whether this results in collision avoidance or mitigation. If a different lane other than its current lane is selected, the Host Vehicle will need to perform a lane-change manoeuvre. This manoeuvre may not be safe to complete, and therefore, Chapter 5 develops a lane-change trajectory planner and evaluates whether the manoeuvre can be

completed safely. A steering controller is developed to evaluate whether the proposed trajectory can be completed. The steering controllers also employ braking to achieve the slowest speed possible at the end of the manoeuvre, in case a collision avoidance is not possible.

Chapter 6 adapts existing modelling techniques to determine the severity of collisions. A collision avoidance may not be possible and whichever lane is selected may still result in an impact. Due to a car's crash structure being designed to absorb as much of the collision energy as possible, and deforming in the process, a collision is not a simple evaluation of impact velocity. The collisions need to be modelled and Chapter 6 develops the models which can describe the severity of the collisions. Using Finite Element Analysis (FEA) data to tune the models, an accurate approximation is reproduced to simulate collisions. These models are used to evaluate a car in a rear-end collision.

Chapter 7 develops the simulators which calculate potential impact speeds. The behaviours of the Host Vehicle and all other vehicles on the motorway, including the vehicles ahead and behind in the 3 simulated lanes are calculated. Two separate simulators are developed, one which will not depend on Vehicle-To-Vehicle (V2V) data, and the second which will depend on V2V data, such as vehicle mass and dynamic braking parameters. The V2V simulator will have more available parameters to perform more complex calculations on vehicle braking and collision modelling. The simulator without V2V data does not have these data sets available, and so will need to make its decisions based on simpler calculations.

Chapter 8 applied MADM methods which use the outputs from the simulators described in Chapter 7, and make a decision on which lane the Host Vehicle should drive into. These methods use mathematical algorithms which rank preferences, i.e. lanes in which the Host Vehicle can be. These decisions can be influenced by inputted criteria weights, so some of the outputs from the simulators can be deemed more important for the decision than others. The criteria on which the decision is based are different for the two simulators. The Non-V2V simulator uses impact velocity ahead, required braking of the vehicles behind, and a maximum deceleration describing the severity of the manoeuvre. The V2V simulator uses the collision accelerations of the impacts as well as manoeuvre acceleration and Time-To-Collision (TTC).

Chapter 9 tests the amalgamation of Chapters 5 to 8. The developments and findings from these chapters are used to make the whole control strategy by

simulating and assessing the simulated problem. Chapter 9 presents the simulation results, demonstrating the decision made for a range of different scenarios. First, benchmark scenarios are defined for both the V2V and Non-V2V simulators. Then the one parameter will be varied incrementally in a sensitivity analysis to observe whether a decision changes on which lane is preferred. The limits of the simulators and decision making processes are evaluated, and demonstrates how one parameter can affect the decision made.

Chapter 10 discusses the conclusions of this thesis by reviewing the findings of each chapter. This also includes the further work that this thesis could introduce.

1.7 Research Contribution

This thesis develops and applies different modelling techniques to develop a control strategy for a new application, such as collision mitigation for autonomous vehicles. Public attention is often attracted when autonomous vehicles are discussed, especially regarding safety. This thesis contributes in this area which will need further development before it can be employed, as the majority of the findings demonstrated here are simulation based. However, the findings are encouraging, as it is demonstrated that a control system can simulate potential collisions, and select the safest collision to have with the aim of reducing the risks to vehicle occupants. Therefore, the control strategy proposed could have a very dramatic effect on saving the lives of roads users.

Automotive safety devices such as seat belts, airbags, and crumple zones are common devices now. And even active safety systems such as Automatic Emergency Braking (AEB) or Collision Warning systems are increasing in popularity. The proposed control strategy is an evolution of these technologies, giving AEB systems further versatility by allowing for more options to be available for the vehicle. Current technologies focus on reducing impact speed as much as possible, but as this research demonstrates, selecting the safest collision can also be a possibility.

The research included in this thesis will put forward novelties for achieving the aim of selecting the least severe collision. Highway platooning will develop on from an existing platooning model. The new developments will include introducing PI control to better maintain the vehicle spacing. This system will be further tested by introducing time delays, increasing the lead vehicle input speed to that representing a

UK motorway, and increasing the size of the platoon. This all contributes to finding the limits of this platooning system, and demonstrating that autonomous vehicles can still collide.

A novel steering and braking trajectory planner will be developed, which will use a sinusoidal wave as an initial starting point, from which an appropriate braking value can be calculated using a 'g-g' vehicle acceleration model. Determining the steering trajectory before the braking ensures that a lane-change manoeuvre can be completed without oversaturating the tyres. This will also prevent the controlled Host Vehicle from colliding into multiple vehicles ahead.

A new bilinear lumped mass modelling technique is to be developed to simulate vehicle collisions. The modelling will reproduce FEA data results quickly and with satisfactory accuracy. The collision modelling will be developed with a Euclidean tuning method to best capture the FEA results.

Two motorway simulators will be developed which are to be used to provide the results as inputs to the decision making processes. Two simulators will be developed for when Vehicle-to-Vehicle (V2V) communication is available, and when it is not available. Without V2V to communicate vehicle parameters, it will not be possible to perform certain calculations. Therefore, a Non-V2V simulator will perform simulations, relying more on assumptions. These are novel simulators, as they will allow for the motorway simulations to be adjusted quickly, making them suitable for sensitivity analyses. The second of these two simulators will work with the collision modelling developed in this thesis.

The application of MADM to a decision process involving real-time autonomous vehicles is novel. Using the results from the simulators, there will be metrics describing the severity of multiple potential collisions. Several different MADM methods will be investigated for use with the developed simulators. These MADM methods will be demonstrated to be a suitable decision making method, to select a lane for the Host Vehicle to drive into.

Chapter 2

Vehicle Dynamics and Collision Research - Literature Review

2.1 Introduction

The research problem under consideration will require understandings from several different disciplines. A literature review of some of these disciplines is contained in Chapter 2. Firstly, a review of Advanced Driver-Assistance Systems (ADAS) will evaluate technologies available for current vehicles that are related to the research

problem. Vehicle Dynamics is important for verifying whether an autonomous vehicle can maintain control through driving manoeuvres, and so an evaluation of vehicle dynamics and vehicle dynamic systems will be included. This is followed by vehicle models used to represent the car.

Collision Avoidance technologies are evaluated for their current capabilities, and how they can be improved upon. This will also investigate Collision Mitigation technologies. The literature review will be completed by a review of Automotive Collision Research to describe why this research programme is important. A review of automotive collision statistics will show the importance of introducing autonomous systems to automotive safety, and assessing the vehicle itself will show how the vehicle performs during a crash.

A conclusion of the literature review will define the current capabilities of cars and why the development of automotive safety technologies must continue. The literature review will demonstrate areas to improve upon, and discuss the improvements that this thesis aims to achieve.

2.2 Current Advanced Driver Assistance Systems and Autonomous Safety Systems

Advanced Driver Assistance Systems (ADAS) are becoming more and more popular on road vehicles. A review of some of these technologies which are relevant to the research problem is included. These technologies are the currently available features on cars which this research problem may either work with or improve upon. An overview of levels of automation is also included.

2.2.1 Adaptive Cruise Control

The car maintains a speed determined by the driver, and the driver can take over at any point, as is the basis for cruise control systems. Adaptive cruise control (ACC) maintains a set distance to the vehicle ahead by using sensors to detect the position and velocity of vehicles in front. It can then control the car speed to match the vehicle in front (Bosch 2014).

The ACC controls engine and transmission in order to control the vehicle speed and the Electronic Stability Programme (ESP). The ESP controls the brakes, so if the car detects that a vehicle in front is slowing or detects an obstacle that will not move out of the car's path, the brakes will be applied. To detect obstacles in front many cars use radar, Lidar, light detection and cameras.

The control of the vehicle can usually be divided into 3 main control modules (Bosch 2014). Cruise control algorithm controls vehicle speed if radar has not detected obstacles or traffic in front. Tracking control algorithm maintains a time gap from a vehicle in front when the radar sensor has sensed a moving vehicle in the field of vision of the car. Cornering control algorithm is essential when the car turns a corner. Radar has a limited range of vision, and the vehicle in front can move out of this range. Until that vehicle is detected again, or the standard cruise control is activated, the cornering control algorithm needs to keep a constant lateral acceleration.

2.2.2 Automatic Parking

Obstacles around the car are detected using ultrasonic parking sensors. The sensors have a detection range of $20 - 450cm$. Firstly the parking space needs to be measured to ensure the vehicle can fit safely without damaging itself. The driver will be informed if the space is large enough, and then a confirmation from the driver is required so that the parking procedure can take place.

For a system where the driver still parks, space geometry is mapped, and a trajectory is displayed to the driver as instructions. This trajectory is re-calculated constantly. Signals from the steer-angle sensor are required to measure if the driver is following the suggested trajectory.

For automatic systems the steering system must be electrically activated power steering. Once the car has measured the space, the driver just needs to engage reverse gear and then let go of the steering wheel. The driver can slow the vehicle by still controlling the brake, but the system will take control of the steering action and accelerator function (Bosch 2014).

2.2.3 Night Vision and Blind Spot Detection

The average low-beam headlamp has a range of 40 to $50m$, which is increased with high-beam headlamps to 120 to $150m$. Zhang et al (2016) note that at night the driver's field of vision becomes narrower with decreasing recognition capability of objects. Dangers increase as high or full-beam light from the headlights of oncoming cars dazzle drivers. Night vision systems have improved visibility and safety, with two main systems described by Bosch (2014), which are Far-infrared and Near-infrared systems.

A thermal-imaging camera detects thermal radiation in a range of wavelengths from 7 to $12\mu m$. Far-infrared systems are passive, not needing additional sources of radiation to illuminate objects. The camera is pyroelectric thermal. The camera image is then transferred to an Electronic Control Unit (ECU), which is then displayed for the driver to see. The image is unusual for the observer, as images do not represent a normal reflected image. Hot objects are shown as light contours against dark. The more of a contrast displayed the more of a temperature difference.

Near-infrared systems are based on the technology used for far-infrared systems, but are based near the visible light spectrum, hence the name near-infrared. Radiation is not emitted by objects at this wavelength, so the vision area is illuminated by infrared headlamps, meaning that the near-infrared systems are active. The scene is recorded by an infrared-sensitive camera and transferred to the ECU. The ECU processes that image, displaying it for the driver to see.

Illuminating the scene with infrared radiation can be easily done by halogen lamps, which have a high infrared content. Because of this, the halogen bulbs are usually integrated into the headlamp module. $380nm$ to $1,100nm$ is the wavelength range that the road scene is illuminated with. The most useful wavelengths for infrared cameras are between 900 and $1,000nm$. This provides a useful signal that the imager of the camera can detect, as the visible light spectrum for humans is $380nm$ to $700nm$.

Near-infrared systems provide a higher image quality that can identify pedestrians, and an image that is easier for the driver to understand. For this reason, near-infrared systems are furthering video-based assistance, and involved in other safety systems such as automatic braking.

There are areas around a vehicle which cannot be viewed by the driver directly or in the mirrors. These are the blind spots, into which another vehicle can move, causing a potential hazard. Blind spot detection uses either an electronic electromagnetic wave (radar) sensor, or computer processed vision images to detect a car. When another vehicle is detected, an audible warning sounds, or flashing light in the driver's peripheral vision will alert the driver to the blind spot hazard. More advanced systems will even engage lane departure to steer the vehicle within the highway lanes, away from the hazardous vehicle.

2.2.4 Automatic Braking

Automatic braking is an active predictive system which monitors a vehicle path and any obstacles in front that will cause a collision. The basic system is an audio or visual alert that tells the driver to apply the brakes, called predictive collision warning. Emergency brake assist arms the brakes, boosting the brake pressure so that when the brake pedal is pressed, the full braking force is applied meaning that the time is not lost when pushing the pedal to the floor. The driver can also be alerted by a "braking jerk" when the car applies the brakes for split seconds. More advanced systems apply the brakes automatically.

Automatic Emergency Braking (AEB) performs predictive collision warning and brake assist, but when the driver fails to act on these alerts (including a braking jerk) partial braking is applied giving the driver more time to react. Partial braking is increased if the driver does not react or if it is only the accelerator pedal that has been released. When the radar sensors detect that a collision is unavoidable full braking is applied to mitigate the crash.

The vehicle can be brought to a standstill before the crash, or at least reduce the speed of the crash, reducing the impact speed. This provides a major benefit to crash safety (Bosch, 2014).

2.2.5 Collision Avoidance Systems

Collision avoidance systems are built on the existing sensors at the front of the car for ADAS systems such as adaptive cruise control. The collision avoidance system performs calculations to detect whether there are potential obstructions ahead. If the

system calculates that the speed differential between the vehicle and potential hazards is too great, the system engages the avoidance measures.

The most basic method is an audible warning alerting the driver into making an emergency manoeuvre. The car could also pre-charge the brakes, in order to provide optimal braking force immediately when the brake pedal is pressed. More advanced systems activate the brakes automatically, even engaging the Anti-lock Braking System (ABS) and Electronic Stability Control (ESC) to maintain vehicle control.

2.2.6 Levels of Automation

To determine the level of automation, several organisations have set out definitions of autonomous capabilities. BASt is the German Federal Highway Research Institute which has defined 5 levels of automation. The following definitions are quoted from Gassner and Westhoff (2012).

0 – "*Driver Only: Human driver executes the driving task manually*"

1 – "*Driver Assistance: The driver permanently controls either longitudinal or lateral control. The other task can be automated to a certain extent by the assistance system.*"

2 – "*Partial Automation: The system takes over longitudinal and lateral control, the driver shall permanently monitor the system and shall be prepared to take over control at any time.*"

3 – "*High Automation: The system takes over longitudinal and lateral control; the driver is no longer required to permanently monitor the system. In case of a take-over request, the driver must take-over control within a lead time.*"

4 – "*Full Automation: The system takes over longitudinal and lateral control completely and permanently. In case of a take-over request the driver does not respond to, the system will return to the minimal risk condition by itself.*"

2.3 Control Engineering for Vehicle Dynamics

Vehicle dynamics is described by Schramm, Hiller and Bardini (2014) as a branch of vehicle mechanics which deals with the necessary motional actions of moving road vehicles and resulting forces under the considerations of the natural laws. Vehicle dynamics references are found in many development areas of automotive vehicles, vehicle systems and components.

Vehicle dynamics is becoming more influenced by Control Engineering. This is because of more active systems being used in the vehicle architecture. The science is expanding into electronic steering, brake by wire, torque vectoring and even autonomous vehicle control. It is therefore important to analyse the relationship between vehicle dynamics and control engineering.

2.3.1 Tyre Saturation

It is important to understand what the tyres are capable of in an emergency situation. For this tyre saturation needs to be analysed.

Friction circles are models that illustrate the forces on the car, Longitudinal (Acceleration and Braking) and Lateral (turning left or right). Figure 2-1 shows how a friction circle works. They represent the dynamic relationship between the tyres of a vehicle with the road surface.
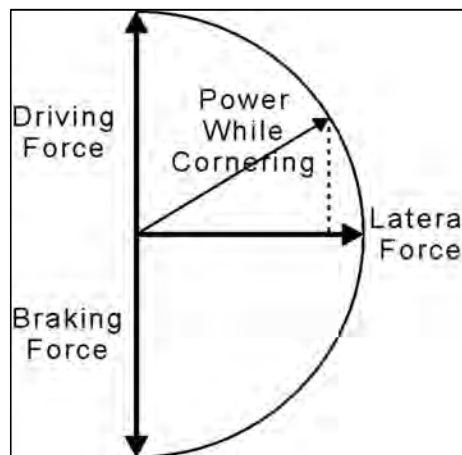
Figure 2-1 - Friction Circle - Haney (2003)

The three bold arrows show the direction of the forces, although some friction circles will reverse the driving and braking forces. Figure 2-1 demonstrates that when

there is a combination of forces such as accelerating whilst turning or braking whilst turning, neither of the maximum forces are available, i.e. the driving or braking force and the lateral force. The combined longitudinal (driving or braking) and lateral (turning) forces create a vector, and the maximum length of that vector should not exceed the limits of the tyre forces, as represented by the friction circle. The example of Figure 2-1 shows how adding a longitudinal force such as driving force to the tyre whilst turning will reduce the lateral force of the tyre. This example represents driving out of a slow corner when driving force will be increasing.
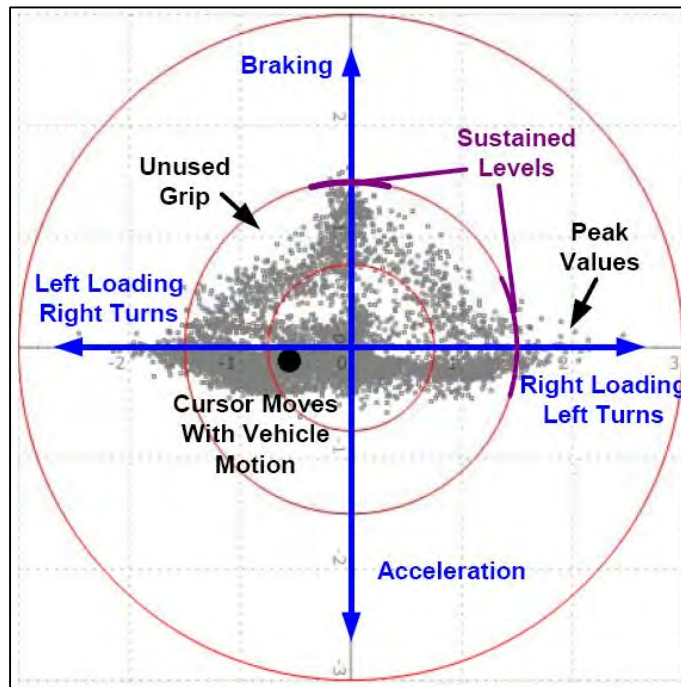
Figure 2-2 - Friction Circle Data Collection - Trackpedia (2010)

Figure 2-2 is an example of an actual Friction Circle for a race car driving around a race track. The first observation shows that the car is far more effective at braking than it is as accelerating, but this can be said of almost all ground vehicles.

Figure 2-2 demonstrates the largest lateral and braking forces occur when there are no other forces acting on the vehicle. When there is a combination of forces there are limited values for both forces acting on the vehicle. It is also called a 'g-g' diagram when the principle is used to measure accelerations.

The tyre becomes saturated with the forces it must act on the road, and once this limit is met there will be a negative effect on tyre grip, as the tyre cannot maintain grip with the road when these forces exceed the limits of the tyre. When the

autonomous vehicle performs an emergency manoeuvre whether to avoid a crash or mitigate it, it must have full control of the car's tyres. The capabilities of the tyre must be respected, specifically the tyre saturation.

2.3.2 Vehicle Stability

A car's stability can be described in terms of Oversteer and Understeer. The meaning of these terms is often unclear as they have different meanings for different researchers. Blundell and Harty (2004) describe these terms with great use to control engineering. It is the relationship between the tyres of the front and rear axles and the dynamics of Yaw Rate Gain (YRG) and Lateral Acceleration Gain (AyG) for each tyre.

The images of Figure 2-3 are summarized as:

(a) YRG reduces further than AyG

(b) AyG and YRG reduce proportionally

(c) AyG reduces further than YRG
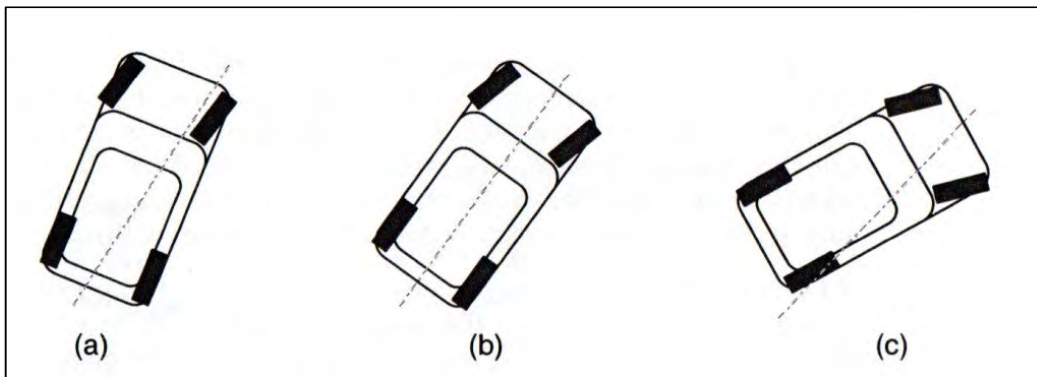
Figure 2-3 - Departures from Linearity Possibilities - Blundell and Harty (2004)

Starting with image (b) of Figure 2-3, YRG reduces proportionally to AyG, allowing the car to maintain along its driver controlled intended path. This is called Neutral Steer. At the limit of adhesion there is reduced stability and control. The response of the steering will be satisfactory to enthusiastic drivers and vehicle speed can influence path radius, without losing driver confidence. The car will experience

progressive departure which is unsafe for less experienced and inattentive drivers. This vehicle behaviour poorly reacts to road disturbances.

Image (a) shows YRG reducing more than AyG, meaning the car cannot achieve the intended path instructed by the driver, needing a new wider line. This is called Understeer. The limit of adhesion control is reduced, but this system is inherently stable. The stability of understeer is demonstrated when the driving inputs of driving force and steering input are too great for the vehicle to respond as instructed. Control is re-gained by reducing these inputs, i.e. when the car takes a wider line the response of the driver is to reduce speed and steer more. Many road cars are setup for understeer as it is considered safe. Understeer is considered safe, as this increases the probability of a frontal collision, should a collision occur. This results in the front crash structure performing its intended purpose of deforming and protecting the passenger cell. Haney (2003) gives another definition for understeer when a higher slip angle is achieved by the front tyres than the rear tyres.

Image (c) shows AyG reducing more than YRG, meaning the car rotates more than it turns. Even though the car will take an objectively understeer path departure from the neutral line, this is Oversteer causing the car to drive a wider line than the neutral steer line. The system is unstable requiring more speed and steering input to maintain control once the limit of adhesion is passed. Oversteer is considered unsafe for most drivers but preferred by more enthusiastic drivers as vehicles which can preserve their yaw rate gain when loosing linearity are generally regarded to be fun and sporty to drive. Haney (2003) gives another definition for oversteer when a higher slip angle is achieved by the rear tyres than the front tyres.

2.3.3 Control of Vehicle Dynamics

The science of vehicle dynamics is expanding to include control systems to improve vehicle performance behaviours. An understanding of these systems is vital, as they will possibly be used to provide better control over autonomous vehicles in driving situations.

Electronic Stability Programme (ESP) monitors vehicle and driver behaviour, comparing this with target states. Braking and drivetrain systems are developed to intervene, stabilising vehicle motion. Assistant Braking Systems and Traction Control brake individual wheels and control engine torque (Bosch 2014).

Braking individual wheels, considers rear inside wheel when understeering through bends, or front outside wheel when oversteering through bends. Tyre slip influences intrinsic vehicle motions (longitudinal and lateral), and steering angle determines braking force as precisely as possible.

At the vehicle's limits, the control of handling characteristics intends to maintain the three degrees of freedom for the vehicle in the plane of the road. Linear velocity v_x, lateral velocity v_y, and yaw rate $\dot{\psi}$ about the vertical axis are the degrees of freedom to be maintained within the limits of control. Dynamic vehicular response is translated from operator inputs, which is adapted to the road characteristics in an optimization process designed to ensure maximum safety.

Active steering stabilization adds an additional steering angle to the driver's steering angle, with use of an override gearbox. Yaw rate is automatically controlled with steering intervention, maintaining set point values in oversteer manoeuvres. Yaw motion is compensated for on roads with differing grip factors for braking. Active steering stabilization reduces Electronic Stability Programme (ESP) workload, as yaw compensation is automatic and significantly faster than a typical driver's steering operation, which reduces the yaw-moment build-up delay of ESP. This also helps to reduce braking distances (Bosch 2014).

Pioneered by McLaren in the development of Formula 1, the inside rear wheel brakes assisting the car's steering input to maintain turning trajectory. Cars.mclaren.com (2015) state that speed and steering angle are factored to work out the perfect cornering trajectory by the system. An exact amount of braking force required is applied to the inside rear wheel when cornering, which effectively allows the car to pivot around the desired path. Traction is managed by the innovative brake steer technology, whilst minimising mid-corner understeer and, when at speed, controls oversteer.

The system operates at relative states of understeer maintaining trajectory. Supercars.net (2010) inform that brake steer prevents 'wash out' tendencies maintaining car's direction. When accelerating out of corners, rear inside wheels tend to spin which is combated by braking that inside wheel, causing the rate of yaw to increase, allowing a quicker application of power. This performs the same task as limited slip differentials, removing the need for heavy components and saving weight.

In a conversation for Motorsport Magazine October 2006, Adrian Newey states that "*The biggest effect on set-up was that you could run the car more*

`understeery', more stable, so that you were less likely to have entry oversteer problems. And you could have better traction because you'd set the car up more towards understeer [less roll stiffness at the rear]."

This technology may work with ESP, maintaining high speed vehicle direction, when factors such as tyre saturation make control difficult. Rear wheels affecting steering reduces loads on the front.

As analysed in Bosch (2014), drive torque distributes between the front and rear axles to increase or reduce understeer tendencies. Agility of lateral dynamics can increase without inducing oversteer. Drive torque distributes between left and right wheels of an axle, improving agility.

For understeer, outside wheel drive torque increases through turns, and reduces for inside wheel. An additional yaw moment acts on the vehicle though the turn, reducing understeer. For accelerating on roads with differing grip factors, drive torque distributes to wheel with greatest grip factor. This reduces the need for traction control brake interventions on wheels with low grip factors. For oversteer, wheel torque shifts partly reduce needs for brake interventions reducing speed loss.

For torque distribution without braking force, a differential allows one wheel on an axis to rotate at a different speed to the other. Torque vectoring systems are greatly effective on Front Wheel Drive, Rear Wheel Drive and 4 Wheel Drive vehicles, all able to utilise active differentials.

The Electric Dynamic Control (eDC2) differential described by patents of Pinto, Aldworth, Franco-Jorge, and Watkinson (2015a and 2015b), give torque vectoring control by using electric motors to independently control the torque applied to different wheels from the powertrain. This technology developed by Horiba Mira is intended for use with electric and hybrid powertrains. This system is able to improve the handling responses of a vehicle increase agility and reduce understeer by assessing the yaw rate and yaw rate error of the vehicle. The overall benefit is improved handling control. This is an example of how control engineering is applied for this purpose, and is already considered for application with autonomous vehicles in the patent of Kentley (2017).

In 2015, both Porsche and Ferrari unveiled cars utilising 4-Wheel-Steering (4WS) with the 911 GT3 and F12 Berlinetta respectively. The system described by Porche.com (2015) turns the rear wheels in the opposite direction to that of the front wheels at speeds up to $50km/h$. This effectively shortens the wheelbase, as it

reduces the turning circle which makes steering into corners more dynamic and parking manoeuvres are noticeably easier. For speeds of $80km/h$ and greater, the rear wheels are steered in the same direction by the system as the front wheels. This has the effect of increasing the wheelbase length as well as increasing stability, for manoeuvres such as on high-speed motorways. For speeds between $50km/h$ and $80km/h$ the driving conditions dictate a constantly changing steering direction for the rear wheels.

Due to the stabilising properties of rear-axle steering, the front axle's steering ratio has been made more direct around the central position. This gives the advantage of greater agility without losing stability at high speeds. There is no contradiction between stability and agility of the rear-wheel steering system, as there can be without the system. The result of the rear-wheel steering system is improved manoeuvrability in day-to-day driving, and a noticeable increase in the maximum performance, i.e. speed and stability in extreme driving manoeuvres.

2.3.4 Vehicle Dynamics and Control in Car Handling

Abe (1999) evaluated chassis controls with the aim of improving a vehicle's handling performance and with that active safety. 4WS uses tyre lateral force which is proportional to the control command of steer angle, in a range where lateral acceleration is small. 4WS is a chassis control system relating to improving handling performance. However, when working with high lateral acceleration, the lateral force that is achieved is not necessarily proportional to the steer angle. This is due to the saturation property in respect to the slip angle. The control law is sensitive to environmental conditions and vehicle motion, as lateral force is strongly dependant on tyre longitudinal force and vertical load.

Direct yaw moment control (DYC) is a promising method of chassis control. The distribution of the longitudinal tyre forces actively generates a yaw moment which controls vehicle motion. DYC has a major advantage as long as tyre longitudinal force is within the tyre capacity limit with respect to the vertical load. It has no feedback from vehicle lateral motion.

In the non-linear range of tyre characteristics and vehicle dynamics it has been emphasized by Abe (1999) that DYC is more effective for vehicle motion control, and that its control law should be introduced in the non-linear dynamics

assumption. Overall, a higher vehicle handling limit performance is achieved with the integration and coordination of 4WS and DYC control systems.

It is also clear that control laws are used to great effect in vehicle handling performance. One of the models used by Abe (1999) was a 2 DoF bicycle model, which was deemed sufficient to derive a control law for DYC. Using a relatively simple mathematical model to directly affect vehicle handling for the better is encouraging for developing a vehicle model that can essentially drive the car itself.

An adaptive integrated chassis control for a vehicle with rear-wheel drive is proposed by Bianchi et al. (2010), with the use of Rear Torque Vectoring (RTV) and Active Front Steering (AFS) available, when there are uncertainties in the parameters. An additional steering angle is applied over the one defined by the driver by the AFS. Torque applied to left or right wheels on the rear axle is applied asymmetrically by the RTV. The lateral tyre stiffness provides the parameter uncertainties.

A linearization control utilising adaptive feedback for the vehicle dynamics is designed by Bianchi et al. (2010). This control is then used as a reference to the actuators, by using a classical control scheme. This will impose the linearizing control actively. This gives the advantages that it is less complex to implement by using a control scheme respecting a linearizing of the dynamics as a whole (vehicle and actuator). This will prevent over-parameterisation, resulting in a control structure which is easier to use. It is unnecessary for the driver-imposed wheel angle to be measured or evaluated.

Combining AFS with the RTV with the aim of improving stability of the vehicle throughout various situations is another goal of this investigation. This means situations that not only include deviation from nominal values for vehicle parameters, but also rapid variations of road conditions, weather conditions including dry, wet or icy. An adaptive feedback linearization technique accomplishes this, where cancelling nonlinear terms robustly uses parameter adaptation.

Kritayakirana and Gerdes (2012) use racing drivers to develop a driving style for autonomous vehicles at the limits of handling. Racing drivers keep control of the vehicle at the limits of friction without losing control. When designing controllers, they prove to be ideal models and their behaviour should be mimicked.

Racing drivers maximise tyre force, whilst following the racing line governed by friction between the road surface and tyres, sometimes referred to as 'grip'. To

display maximising of tyre forces in a mathematical model a 'g-g' diagram is used as illustrated in Figure 2-1. The circle represents the friction limit, and the driver's responsibility is to operate the car within this limit, preferably very close to the limit. The tyres have limits, therefore applying the maximum braking or acceleration whilst also applying maximum steering will exceed the tyre friction limits, and control will be lost. Braking can be maximized without cornering, and vice versa. Or a combination of longitudinal and lateral forces which generate maximum tyre forces can be utilised, as concluded by Kritayakirana and Gerdes (2012).

The driver modulates inputs of steering, braking and throttle within the limits of the friction circle. Before the corner entry, the maximum braking is applied, and no lateral force as the car is not yet turning. Longitudinal forces are not applied through the pure cornering aspect of the apex, so tyre forces are maximised by applying lateral cornering forces. The maximum acceleration is applied at corner exit, when lateral forces are not required. The challenging driving components are the transitions between corner entry and corner exit, where steering and longitudinal inputs must be coordinated using techniques such as trail-braking or throttle-on-exit (Kritayakirana and Gerdes, 2012). Trail-braking is the transition phase where the driver slowly decreases braking input whilst increasing the steering input. Throttle-on-exit is the opposite, steering input is reduced whilst throttle input increases. The challenge of these driving behaviours is described by the friction circles of Figure 2-1 and Figure 2-2, where driving and steering forces must be balanced, as not to over-saturate the tyres.

This balance between lateral and longitudinal forces is vital. Controlling braking before the corner greatly affects steering input that can be introduced. Critically, a higher cornering force is required by higher vehicle speeds, which results in reducing the available braking force. Therefore, as the radius of curvature of the corner becomes smaller, when the vehicle travels at excessive speed it will prematurely use all of the friction capability and become unable to track the desired racing line. Braking points and steering inputs must be controlled perfectly by the controller to achieve the optimal racing line, as stated by Kritayakirana and Gerdes (2012).

The controller developed by Kritayakirana and Gerdes (2012) separates path generation from path tracking at the limits. Vehicle limits are described by a 'g-g' diagram friction limit circle, imitating the driver's racing line. The controller uses priori

knowledge of friction relying on variations of track surface handled by the controller's robustness. Aligning moment or tyre slip could estimate real-time friction estimations.

2.3.5 Steering Controllers

In this section existing research on steering controllers is reviewed, focusing on kinematic controllers, their capabilities and limitations. Kinematic steering models describe the geometric motion of the vehicle without consideration of the forces acting on it. Kinematic models use velocity as an input to the system, as with Rajamani (2011). Dynamic steering models evaluate the forces and moments which cause the vehicle movement.

Ahmed and Yüksel (2013) used forward velocity and angular acceleration as control inputs to develop a proportional input-scaling feedback controller which follows a desired path. Kinematic simulation results are stored in a look-up table and applied to a programmable vehicle, capable of replicating the simulation. The realistic simulations proved the simulation results to be accurate for a double lane change at $2.8m/s$, stating that "*the controller is robust and converges giving good performance provided that the car starts sufficiently close to the desired path.*"

Snider (2009) discussed the use of a bicycle model, described in Section 2.3.6. The author claims that a simple kinematic bicycle model used for the vehicle system is a common approximation used in motion planning for robots, simple vehicle analysis and deriving control laws for geometric methods. Snider developed and simulated several steering controllers, concluding that a kinematic model was sufficient for slow driving or parking manoeuvres. The author also concludes that for highway driving at moderate speeds a simple dynamic model will suffice. The kinematic model used by the author was stable up to $15m/s$, and used a path tracking controller. A kinematic controller was capable of accurately directing a vehicle up to a certain velocity.

The collision avoidance steering controller developed by Shah et al. (2015) generated reference values, namely yaw rate. It used a PI feedback controller to better track the planned path. This controller was tested in simulation and with a real vehicle. The results demonstrated the possibilities of applying it in real world applications. The controller itself used a polynomial-based path planning method with

real-time evaluation of the path constraints. The controller developed was tested at speeds up to $70 km/h$.

Kong et al. (2015) compared the use of kinematic and dynamic bicycle models for autonomous driving. They concluded that a discretized kinematic model at $200 ms$ has similar performance as a dynamic model discretized at $100 ms$. The kinematic model even forecasted errors better than the dynamic model. Due to the kinematic model not including tyre and road interaction calculations, less computational power was required, and could be operational at a wide range of speeds. The authors shared the conclusion that at higher speeds the use of a tyre model reduced the reference errors. To provide better performance, the authors suggested limiting the reference velocity, so that the lateral acceleration could not exceed a certain value.

Kong et al. (2015) discuss a disadvantage of dynamic steering models, which is the computational effort required and that tyre models become singular when vehicle speed is low. A tyre slip angle estimation term is used for tyre models, which has vehicle velocity in the denominator. The use of the same control design for stop-and-go scenarios is therefore prohibited, which is a common scenario in urban driving. A method for slip angle estimation was proposed by Lee et al. (2013). This method provided reliable slip angles for use with vehicle stability control. This method used measured yaw rate and lateral acceleration from the vehicle as it was performing manoeuvres. The proposed slip angle estimator is derived from a kinematic bicycle model. It was not to rely on dynamic tyre modelling.

Nam et al. (2013) also developed a slip angle estimator. However, this model relied on measurements from lateral tyre force sensors. Whilst the use of a Kalman filter did provide reliable estimations, the authors do state that this model is based on linear tyre dynamic models, and so errors may occur with severe manoeuvres on low friction roads.

2.3.6 Bicycle Model

Abe (1999) used a bicycle model to implement a DYC, as discussed in Section 2.3.4. The bicycle model is a simplified kinematic model of a four wheeled vehicle. It combines the two front wheels and two rear wheels in assuming they behave identically. Figure 2-4 demonstrates this simplification given in Takacs and Stepan (2013).
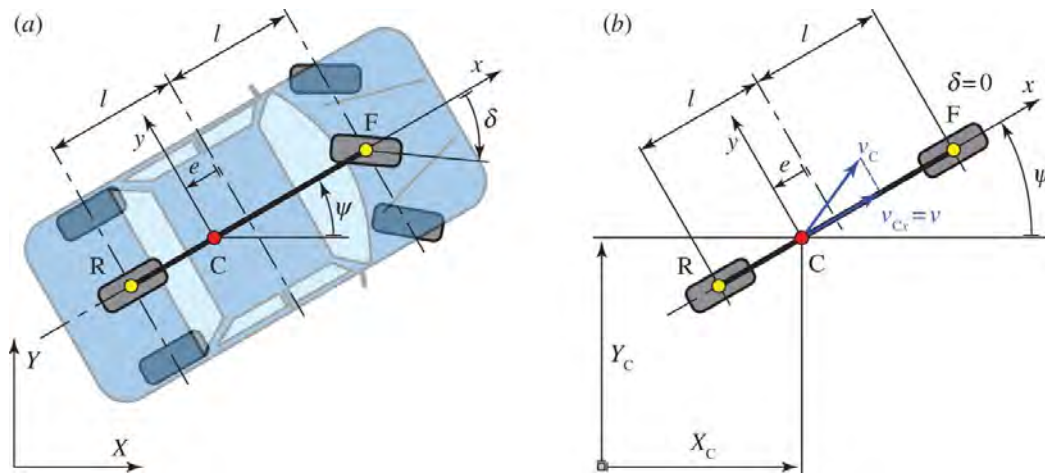
Figure 2-4 - Bicycle Model - Takacs and Stepan (2013)

where F and R denotes the centre points of the front and rear axles repectively, C denotes the Centre of Mass (CoM), l denotes the wheelbase length divided by 2, e denotes the position of the CoM from the half wheelbase length, x and y denote the longitudinal and lateral directions the vehicle is travelling, X_c and Y_c denote the Cartesian coordinates of the x and y positions of the CoM, v denotes the vehicle velocity in the vehicle's longitudinal direction, also denoted by v_{Cx}, v_c is the velocity in direction of travel, δ denotes the steering angle, and ψ denotes the yaw angle.

Figure 2-4(a) shows how the two wheels on each axle of a 4 wheeled vehicle are represented by a single wheel, and Figure 2-4(b) is the simplified bicycle model. The bicycle model has been adapted to numerous applications including Kong et al. (2015) developing both kinematic and dynamic bicycle models for an autonomous steering, braking and acceleration model.

The bicycle model is described by Blundell and Harty (2004) as a 2 degree-of-freedom model with lateral acceleration and yaw rate as the degrees-of-freedom. the equations which govern the bicycle model are given as:

$$\Sigma M_z = I_z \dot{\psi} \qquad\qquad (2\text{-}1)$$

$$\Sigma F_y = M(\dot{v}_y + v_x \psi) \qquad\qquad (2\text{-}2)$$

where the yaw rate $\dot{\psi}$ multiplied by the yaw inertia of the vehicle I_z gives the applied yaw moment M_z. The applied lateral forces F_y is given by the lateral acceleration $\dot{v}_y$ and the longitudinal acceleration v_x multiplied by the yaw angle, all multiplied by the vehicle mass M.

2.4 Highway Platooning

Highway platooning is a control strategy which could be applied to motorway driving situations, with the aim of improving traffic flow and safety, and also reduce aerodynamic resistance of the platooning vehicles. It is a method of grouping vehicles together in single file, effectively forming a train. The vehicles are driven with small spacing distances between them, meaning the control of these vehicles must be automated, as a human driven vehicle will not be able to react quickly enough to avoid collisions between the vehicles. Bergenhem et al. (2012) reviewed five highway platooning systems. The systems reviewed by Bergenhem et al. (2012) demonstrate the popularity of this system, and the importance of introducing it to highways.

These platooning systems include SARTRE from Sartre-project.eu (2012) which was a European Commission co-funded project which sought a change in transport utilization. The intention of this project was to develop and integrate solutions which allowed vehicles to drive in platoons on public motorways without the need to modify the infrastructure, such as creating dedicated lanes. PATH (Michael et al., 1998) was a project that looked into increasing highway capacity whilst requiring minimum infrastructure modification. PATH concludes that platoons of up to 10 cars could result in a highway capacity increase of factor two or three.

The Grand Cooperative Driving Challenge (GCDC.net, 2016) challenged researchers to improve traffic throughput by reducing the spacing distances between vehicles, and investigated multiple vehicle types, i.e. passenger cars and heavy goods vehicles.

Energy ITS was a project of the Japanese Ministry of Economy, Trade and Industry from Tsugawa, Kato, and Aoki (2011) which aimed to improve the energy saving of truck platoons and mitigating the impact of unskilled drivers. Energy

reductions were observed and a reduction in emitted CO2 when a three-truck platoon was driven at 80km/h.

SCANIA-Platooning is a collaboration between Scania and KTH (The Royal Institute of Technology) from Sweden, investigating the operation of a single vehicle in a platoon without compromising safety.

2.5 Motorway Simulation Methods

Motorway simulation methods calculate a vehicle's future position, by assessing the vehicle's current behaviour. The simulation methods described in this section focus on collision prediction and collision avoidance research. Anderson et al. (2010) proposed a framework for planning vehicle trajectory and assessing threats for a vehicle with semi-autonomous control to avoid hazards. The framework planed a trajectory with the limitations set by a dynamic vehicle model. This model focuses on the vehicle's performance. It is based on an iterative method which assesses the hazards and adjusts the vehicle control accordingly. The controller calculated a best-case trajectory for a lane-change manoeuvre to avoid a hazard ahead. The method developed must calculate the best action before any action is taken. This framework was semi-autonomous, because it was designed to work with the human driver, to avoid a hazard in the vehicle's path.

Ammoun and Nashashibi (2009) present an estimation of vehicular collision risk by calculating collisions and their "dangerousness". The vehicles are modelled to predict collisions at a crossroad junction. The authors described the methods by which the vehicle trajectories can be modelled. First, they describe a geometric approach. The advantage of a shape-based trajectory generation is the reduced time of estimation assured by the low computational effort required. It can also predict some of the trajectory before the manoeuvre has begun. The approach taken by these authors is dynamic. Collisions are detected by modelling an elliptical shape constructed from 4 circles around each vehicle, which accounts for uncertainty of the vehicle dimensions and position. In this model a collision was detected if one of the circles of the vehicle intersected at least one of the other vehicles circles. A Time-To-Collision (TTC) is calculated as the time period between the current time and the instant of the first impact between the vehicles. It is assumed that the respective vehicles are keeping their current speed. As a collision is unavoidable, a decisive action needs to be taken autonomously.

Eidehall et al. (2007) present an automotive safety system Emergency Lane Assist (ELA). ELA included a threat assessment module in a conventional lane guidance system that tried to activate the lane guidance interventions according to the actual lane departure risk level. The goal was to prevent dangerous lane departure manoeuvres only. Vehicle Position was described by Cartesian Coordinates and used to calculate the vehicle states. Positions of Host and Target Vehicles were simulated, which then required a decision on whether a dangerous situation would result from a lane-change manoeuvre. The simulation evaluates traffic around the vehicle and define lane markings which are used to assess whether a manoeuvre is dangerous. The decision process follows steps which evaluate the possibility of a collision, including Times to cross the defined lane markings, and identifying objects in the intended lane. This system is appropriate as a preventative control strategy which prevents dangerous lane change manoeuvres. It simulates vehicle positions using a Cartesian coordinate system and assess other lanes for traffic. However, the ELA system is a preventative method, and does not assess imminent collisions.

Hayashi et al. (2012) proposed a collision avoidance system which utilized not only braking, but also steering. A constant deceleration was assumed to determine velocity. A vehicle trajectory is plotted geometrically by generating two circular radii. This has the benefit of creating a trajectory that can maintain vehicle speed and steering input closer to the limits of yaw. However, the steering trajectory must be limited by the vehicle's yaw rate, but this model did not consider it.

The collision avoidance system instructs full braking to be applied through the steering manoeuvre, but this may not be possible and result in oversaturation of the tyres. When the system calculated that a collision is unavoidable, the vehicle is instructed to only apply the maximum braking, no steering input. The avoidance strategy proposed was tested for whether a braking only or steering manoeuvre would be the best course of action. The results are promising but do demonstrate areas which should be improved. This is an avoidance only system. The mitigation control is limited, as it appears to be the case in many existing avoidance systems.

Future autonomous vehicles computational architecture is a developing research area. Liu, Tang, Zhang, and Gaudiot (2017) discussed the future requirements of processing large data sets for autonomous vehicles and the costs of employing current computer systems. The authors conclude that the processing of all necessary data for an autonomous vehicle to function will require considerable

computational effort. This conclusion is supported by the advantages stated by Ammoun and Nashashibi (2009) regarding the geometric approach.

2.6 Vehicle Collisions

A number of technologies currently work towards collision avoidance. Many new cars are equipped with automatic braking, which uses front facing radar to detect a potential hazard, and either alert the driver or apply the brakes automatically. These are the beginnings of technologies applied to autonomous safety.

Autonomous cars will be equipped to avoid crashes occurring. However current technologies to limit hazards of unavoidable collisions are still in their infancy. Assuming autonomous cars will prevent all collisions is a dangerous over-estimation. The car needs to know how to behave in imminent collisions. Currently, the best strategy is to apply the brakes, assuming that it will be enough. However, the vehicle dynamics and collision situation may not result in collision avoidance if only full braking is applied.

2.6.1 Collision Avoidance

The current trend of autonomous vehicles is to avoid collisions from happening. This requires planning ahead. Wang et al. (2012) proposed an avoidance strategy at roundabouts. The car protects itself by creating an imaginary force field, into which nothing can travel. To describe the collision area, the rectangle and coordinate system are introduced. The dimensions of the rectangle are determined by the size of the collision area. The rectangle's centre is the merging point for the target trajectory. The rectangular collision area is dependent on the length and speed of the vehicle.

When autonomous vehicles at the same time enter a conflict area along their trajectories, a collision may occur. The collision area and the distance between the vehicles are modelled by probability concepts. For the collision avoidance process using the rectangle conflict area, a force field function is implemented. To achieve collision avoidance a concept of force-fields and warning functions are introduced. When a vehicle is close to the rectangle conflict area (the force-field) of another

vehicle and a warning signal is received, autonomous vehicles would adjust their speed to move away from the conflict area.

Moon, Moon, and Yi (2009) outlined the development of adaptive cruise control with a collision avoidance system. The control system is designed to avoid rear-end collisions completely when following another vehicle. The system operates by dividing driving situations into 3 groups named safe, warning, and dangerous. Moon, Moon, and Yi (2009) note that little work has been published on integrating an ACC system with collision avoidance.

For the vehicle to track a desired deceleration, the controller has to manipulate the throttle and brake actuator. Reverse dynamics is the basis for the control principles of throttle or brake, with feed-forward Proportional-Integral-Derivative (PID) control principle being utilised (Moon, Moon, and Yi, 2009).

Many of the existing avoidance systems manipulate longitudinal control to slow the vehicle into avoiding a collision such as the technologies discussed by (Moon, Moon, and Yi, 2009) and Wang et al. (2012). A more advanced system would introduce lateral control, steering away from collisions such as the developments of Eidehall et al. (2007) and Hayashi et al. (2012).

2.6.2 Collision Mitigation

When a collision is unavoidable by an action taken by the driver it calls to reduce the Collison speed by braking. This is the aim of the system named Collision Mitigation by Braking (CMbB). Non-probabilistic decision criterion were the first commercial systems used for CMbB. Jansson and Gustafsson (2008) incorporate CMbB into their collision avoidance system.

Radar, LIDAR, and a dSpace Autobox running with a Kalman filter for Gaussian motion discrete time linear model and conflict function are equipped on the demonstrator vehicle used by Jansson and Gustafsson (2008). Relative longitudinal, lateral and orientation are provided by Gaussian posterior distribution with Kalman filter. A more complex model includes brake and steering dynamics model for prediction. Evasive braking and steering manoeuvres were used to calculate a collision probability for each instant by simulation.

The system developed by Jansson and Gustafsson (2008) aims to reduce the impact speed of a head-on collision, and achieves a collisions speed reduction in all

cases of between $10km/h$ to $15km/h$. Using accident statistics and Bayesian analysis, motivated by Jansson (2005), this system has the capability of reducing the number of head-on accidents that are fatal by 15%. This paper demonstrates a collision avoidance and collision mitigation system using Monte Carlo simulation. Here the mitigation and avoidance system only control the brakes. This will of course be useful as it has proven to reduce the impact speed when a collision is unavoidable, but there are still improvements to be made as this system is still highly reliant of the driver being in control of steering, especially for the avoidance manoeuvre.

2.6.3 Steering Control to Avoid Collision

One method for collision avoidance is to introduce a steering input. This is best described by a lane-change manoeuvre, investigated by Best (2012). The author considers a high-speed emergency lateral manoeuvre to avoid a collision, controlled by an autonomous vehicle controller. It investigates whether vehicles can autonomously change from one lane of a motorway to another. While other autonomous crash research studied a little bit about the handling characteristics of the vehicle, instead assuming that all control commands will be executed perfectly without considering limitations of the vehicle's handling capabilities, this investigation explores the optimal behaviour of the vehicle to avoid a crash. This is done by optimising the lateral characteristics of the vehicle's handling balance rather than the longitudinal, as discussed with the tyre saturation in Section 2.3.1.

Generalised Optimal Control (GOC) is an iterative simulation-based method which will achieve optimality of the collision avoidance (Best, 2012). This method allows simultaneous optimisation of time-varying control of braking, acceleration and steering with fixed model parameters. The avoidance manoeuvre does not use a reference path, instead the optimal path evolves as the simulation calculates a vehicle position, cost functions on the obstacle, and final stable vehicle position and orientation. Unfortunately, this system is not appropriate for real vehicle applications as this technique is very expensive computationally, and is not suitable for real-time applications.

An aggressive manoeuvre with high g is the optimal rapid lane-change which destabilises the vehicle. Much of the effort of the control is placed for the destabilisation after the initial steer, generating a high yaw moment and reducing the

speed. Adding braking or acceleration control results in a small decrease in headway. Combining braking and steering control will reduce the speed by a noticeable amount, but the difficulty is in the reliability of a controller that can control both steering and braking in the critical first seconds of the manoeuvre.

Best (2012) states that coupling the destabilising step-steer open-loop inputs would be an appropriate route to design a practical real-time controller, which would probably be scaled according to road friction estimations. Vehicle stability in the safe lane would be recovered by a suitable closed-loop yaw controller.

2.6.4 Automotive Collision Testing

The dangers of automotive collisions are assessed in this section, focusing on collisions occurring on roads which are defined in the scope of this project. These are limited to dual carriageways and motorways, where the traffic travels in the same direction, and the speed is around a constant $70mph$ ($112kph$). A rear-end collision refers to the situation when the front of a vehicle collides with the rear of a vehicle in front.

The Insurance Institute for Highway Safety (IIHS) is a research organisation, working with the Highway Loss Data Institute (HLDI) which studies insurance data. IIHS-HLDI (2017) publish collision test information, useful in describing the importance to potential autonomous systems.

IIHS test 2 main types of frontal collisions at $40mph$: 1. a moderate overlap collision where 40% of the front of a vehicle impacts with a deformable barrier, and 2. a small overlap collision where 25% of the front of the vehicle impacts with the rigid barrier. IIHS-HLDI states that the forces of these tests are similar to 2 vehicles of the same weight colliding head-on at just under $40mph$ impact speed. Whilst a head-on collision will have a greater impact speed than a rear-end collision, the vehicle crash structure at the rear of the vehicle behaves in the same way as the front, a deformable structure designed to dissipate energy from the collision.

The design of modern cars have safety cages which encapsulate the passenger cell (Marzbanrad and Ebrahimi, 2011). These are built to protect the passenger cell from head-on and moderate overlap collisions by reducing the deformation of a crash. Crash structures manage the energy of a collision reducing the forces which reach the passenger cell. The design of the vehicle means the main

crash structures are located in the middle 50% of the front crash structure. The passenger cell is protected from intrusion due to these structures. Passenger are further protected with safety belts and airbags.

A small overlap collision behaves differently, as the front crash structure often does not cover the full width of the vehicle. Areas that are not well protected by the front crash structures are vulnerable to small overlap collisions which can impact the front wheel and suspensions as well as the firewall. Some vehicles even allow the front wheel to intrude into the passenger cell's footwell causing serious injury to legs and feet.

IIHS-HLDI note that offset crashes only utilise one side of the vehicle's front-end crash structure, not the full width as the vehicle impacts the barrier. Due to this, a smaller section of the crash structure is all that is available to manage the crash energy, with a more likely intrusion into the passenger cell. Offset testing is more demanding on the vehicle's crash structure than full-width testing. However, due to the reduced crushing of the vehicle structure resulting in greater decelerations of the full-width test, additional restraints such as safety belts and airbags are in greater demand.

2.6.5 Collision Testing Results

Definitive conclusions to collision testing cannot always be possible. This is due to the difference in vehicle types and performance. However, by analysing the collision results of 3 separate vehicles in IIHS.org (2017) general observations can be made.

The 3 vehicles are a 2017 Audi Q7 Large Sports Utility Vehicle (SUV), a 2015 Subaru Legacy Midsize Car, and a 2014 Mini Cooper Minicar. They are all different sizes and masses and were selected due to all being awarded a 2017 Top Safety Pick+ by IIHS and all vehicles achieved a Good rating for crashworthiness (small overlap front, moderate overlap front, side, roof strength and head restraints & seats). The following observations are made based on the size of the vehicle by the author of this thesis:

- Larger vehicles experience less intrusion to safety cell.

- The three tested vehicles have similar driver injury test measurements in areas such as neck tension and chest compression.

- The larger the vehicle the less force exerted on feet and tibia for the moderate overlap test.

- For small overlap the midsize vehicle does experience less forces exerted on the driver, but largest vehicle experiences the maximum force.

- The largest vehicle does experience the largest HIC-15 values, which suggests they are more likely to result in Head Injury. Midsize vehicle result is best for both tests. HIC-15 is the Head Injury Criterion measurement stating the likelihood of injury in $15ms$ between the peaks of the accelerations of the head in a collision (Bertocci et al., 2003).

The following observations are made based on the differences between collision types:

- Generally greater forces are exerted on driver in femur and tibia in small overlap test, possibility of intrusion to safety cell as suggested by notes from IIHS-HLDI (2017).

- Moderate overlap test will result in a larger maximum chest compression, which suggests more reliance on the seat belt also suggested by IIHS-HLDI (2017).

- Similar forces are exerted on the driver's necks between both tests and for all vehicles, but the small overlap test does have a higher HIC-15 value, especially for the large SUV.

- More intrusion to passenger cell is recorded with a small overlap test.

2.6.6 Rear-End Collisions

Rear-end collisions are a common collision type on motorways, and so the control strategies developed in this thesis will focus on mitigating these impacts. The National Transportation Safety Board (2015) stated that FOR 2012 in the USA "*more than 1.7 million rear-end crashes occurred on our nation's highways, resulting in more than 1,700 fatalities and 500,000 injured people. Many of these crashes could have been mitigated, or possibly even prevented, had rear-end collision avoidance technologies been in place.*" The study also included 2011 where it is stated that rear-end collisions rarely result in fatality, approximately 1 in every 100, but the potential for injury is high the data from the study for the last two available years,

2011 and 2012, states that 3,491 people were killed in rear-end crashes and more than 1 million others were injured.

The IIHS.org (2016) provide statistics on the types of collisions that resulted in fatality in 2015 in USA. For rear-end collisions, the number of automotive collisions that resulted in fatality was 1,044, which accounted for 9% of all highway deaths in 2015. In comparison, frontal impacts accounted for 56%, and side impacts accounted for 33% of fatalities on the roads in the USA. These statistics suggests that limiting potential collisions to rear-end collisions only would prove beneficial. The autonomous control must not allow side impacts or frontal collisions. The study also reports that passengers in lighter vehicles are more at risk when colliding with heavier vehicles, and in multiple-vehicle collisions heavier vehicles will better protect their occupants with fewer fatalities.

2.6.7 Zero-Lateral Offset Collisions

Jula, Kosmatopoulos, and Ioannou (2000) model lane-change manoeuvres and assess the risks of collisions of other vehicles on the road using a time-to-collision analysis. Three types of collision may occur during the lane-change manoeuvre, including rear-end, angle or side-swipe. A side swipe collision, also called "T-bone" collision, is the collision where one vehicle impacts the left or right-hand side of another vehicle. This is a serious collision due to the lack of crash safety structures. An angle collision is similar to a head-on or rear-end collision, but the vehicle behind impacts the vehicle ahead at an angle, and possibly at one side of the vehicle. A car crash will not be an elastic collision, as the crash structures are designed to dissipate the kinetic energy of the collision.

A two-dimensional analysis of an inelastic collision between two vehicles evaluates the resultant velocity and direction. These equations are given by Stanbrough (2006):

$$v_x = \frac{m_1 v_{1x} + m_2 v_{2x}}{m_1 + m_2} \qquad v_y = \frac{m_1 v_{1y} + m_2 v_{2y}}{M_1 + M_2} \qquad (2\text{-}3)$$

$$v = \sqrt{v_x^2 + v_y^2} \qquad (2\text{-}4)$$

$$\theta = \tan^{-1}\left(\frac{v_y}{v_x}\right) \qquad (2\text{-}5)$$

where m denotes Vehicle Mass, v is velocity, v_x and v_y are the x and y components of the velocity respectively, and θ is the angle of velocity vector with the x axis. Subscripts 1 and 2 identify the vehicle.

The danger of a side-swipe or angle collision is that the vehicles may be pushed into another lane. This would introduce a risk of another collision with another vehicle in that lane. A rear-end collision with zero-lateral offset and no v_y component at the point of impact will have the minimum risk of this occurring. Due to this undesirable after-effect, any collision that cannot limit the impact to one lane must be prevented. A rear-end collision lends itself better to predictability, as it can be described as a one-dimensional collision. This means fewer variables can influence the modelling such as angle of impact.

2.6.8 Crash Statistics

The following statistics are relevant to dual carriageway and motorway collisions in the UK, providing an insight into the need for autonomous systems. Many of the statistics are provided by the Department for Transport, developed by information reported to police forces across the country. These figures are incomplete of all accidents and casualties, however the fatalities are widely recognised to be robust.

The Department of Transport (2012) states that the number of road deaths reported to police decreased from 1,901 in 2011 to 1,754 in 2012, this is an 8% fall of 147. All severities reduced for motorway casualties (killed and seriously injury were down 17% and 12% respectively). This is in respective of an increase of 0.4% in traffic. Slightly injured casualties also decreased by 5%. In 2012 5,615 motorway accidents were reported to police, which is a 4% reduction than 2011.

The Department for Transport (2014) reports 96 fatalities on motorways, 4 less than in 2013. However, casualties described as seriously injured on motorways increased by 8.8% to 718. Slightly injured casualties also increased by 5.3%. It is noted that even though motorways are responsible for 21% of traffic, they are only responsible for 5.4% of fatalities, and 4.7% of injured causalities.

Accident statistics provided by the House of Commons (2013) show that in 2012 the number of road deaths is one-third that of in 1990, that is a 66% reduction. A similar conclusion is given for serious injuries, which has decreased 62%, and slight

injuries is down by 38%. Higher speed limits have a higher risk of accidents being fatal, 1.0% of casualties on motorways (up to $70mph$) in 2012 resulted in a fatality. This is compared with 0.6% on built up roads (30 to $40mph$) and 1.9% on rural roads. Motorways do have safer casualty rates, as only 5% of casualties in 2012 occurred on motorways.

The House of Commons report (2013) does provide insight into the severity of motorway collisions. A $30mph$ road accident will have a probability of only 0.6% of it resulting in a fatality. Rural $60mph$ roads have a 2.8% fatality rate, and $70mph$ motorways have a 2.0% fatality rate.

The United Kingdom is amongst the safest driving countries in the world as demonstrated by statistics provided by the House of Commons (2013). Across the UK, Northern Ireland is the safest with 26 deaths per million population. England has 28 per million, Wales has 30 per million and Scotland has 32 per million. The UK records an average of 28 deaths per million population. The only EU country with a lower rate is Malta at 22 per million. The United States fatality rate is approximately 4 times higher, at 108 per million. Comparing with two EU countries that also have extensive road networks, France has a death rate of 56 per million, and Germany 44 per million.

The Think Road Safety Annual Survey Gov.UK (2013) states that 60% of the survey participants reported that they "*know people who drive at 90mph on the motorway with no traffic*". Whilst 37% of drivers (cars, vans and lorries) admitted to driving when too tired. Smart Driving (2008) provide two statistics highlighting the importance of a driver error. Firstly, 90% of motorway accidents are due to driver error, only 10% being due to mechanical failure. Secondly, it takes over half a second for most drivers to react before they press the brake pedal.

It can be observed that with an increase in traffic levels, there follows an increase in road accidents. Between 2013 and 2014 the Department for Transport (2015) noted an increase of 2.4% in vehicle traffic levels. The Department for Transport (2014) reports that in the year ending in June 2014, there was an increase of 1.7% of motor vehicle traffic compared to that time 1 year previously. The Department for Transport (2015) reports that over the last ten years motorway traffic has grown 27% faster than any other road type. Furthermore, there were also 1,775 road deaths in 2014, a 4% increase compared to 2013.

2.6.9 Optimising the Collision

Stigson, Kullgren and Rosen (2012) describe the factors which influence the severity of the crash for vehicle occupants. Factors such as the relative velocity between the vehicles, impact angle, the structure and mass of the vehicles, and the crash situation all affect the severity for the human inside the vehicles. Crash tests with volunteers, animals, dummies and numerical models are amongst the approaches undertaken before to estimate the response from the occupants. Unfortunately, there is still limited knowledge on human tolerance. Human injury risk is influenced by, and can differ depending on parameters such as age, gender, crash type, restraint system type and road user groups. Analysing real world crashes has increased the understanding of crash severity and how it correlates with factors such as impact speed, injury outcome and the type of object being impacted with. This demonstrates the difficulty of determining an exact assessment for crash severity, but assumptions could be made to simplify the assessment by assuming all vehicle occupants will behave the same way. The use of numerical models is encouraging to simulate the severity of a collision. It also demonstrates the importance of factors influencing the collision other than impact velocity, such as vehicle masses and crash structures.

If a collision is to occur, there are preparations to make the impact as safe as possible for the occupants of the vehicle. Mitigating a collision can be done in different ways, usually by reducing vehicle velocity as much as possible as investigated by Jansson (2005). Autonomous vehicles will have the ability to better optimise the use of their crash structures by deciding on which collision to have.

Crash structures are part of a vehicle's chassis designed to deform, dissipating energy before it reaches occupants. Xu et al. (2010) evaluated the crashworthiness of a frontal crash structure stating that the most important members in frontal collisions are the frontal rails. Approximately 50% of the crash energy is absorbed by the frontal rails during the crash process.

Huang and Dong (2015) investigate the effects of using all of the vehicle frontal area versus only 40% of the frontal area in a collision. They evaluated FRB (100% Front Rigid Barrier) impacts and OBD (40% Offset Deformable Barrier) impacts. In FRB impacts the whole front of the car body participates, which results in high passenger cell accelerations, but relatively smaller body deformations. The main factor which causes harm is the strong impacts on the occupant head and chest caused by the huge impact inertia force. Only one side of the vehicle is involved in

OBD impacts, which results in large deformations which can cause invasions into the passenger compartment. This means that the main factor which results in harm to vehicle occupants is external components intruding into the passenger compartment for OBD impacts.
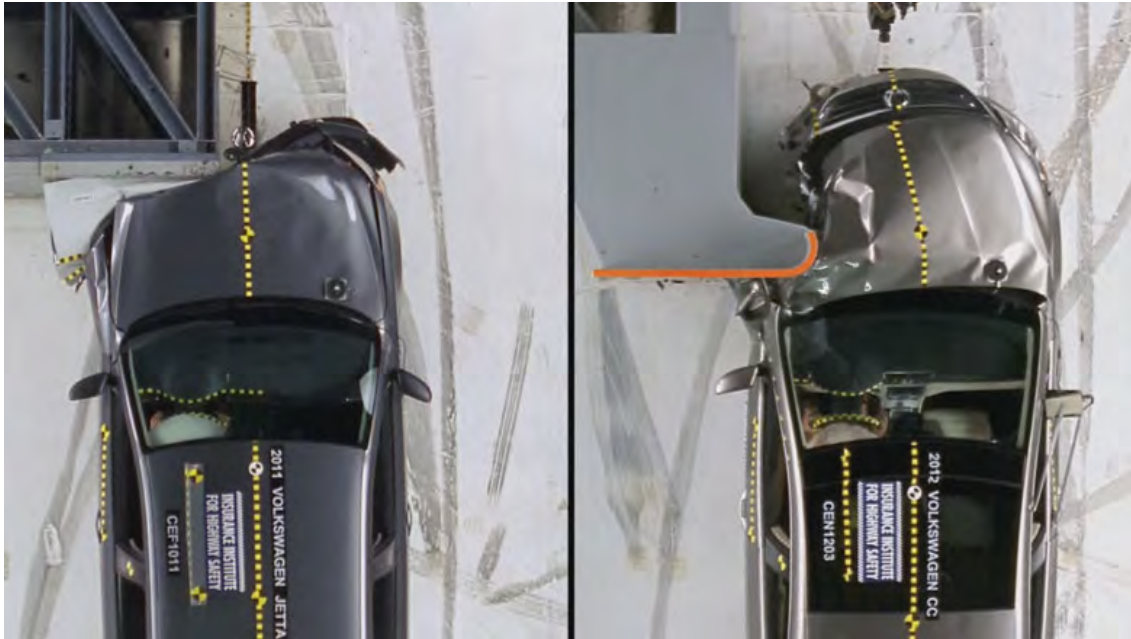
Figure 2-5 - 40% Offset vs. 25% Offset - Safety.TRW.com (2013)

Figure 2-5 demonstrates the need to optimise crash. For occupant safety, it is better to maximise the use of frontal crash structures in frontal impacts. More of the structure can dissipate more of the impact energy. The Insurance Institute for Highway Safety (IIHS) investigated what happens when a small area of the crash structure is used. Figure 2-5 shows the effects of a 40% offset collision (40% of vehicle frontal area impact) against a 25% offset collision (25% of vehicle frontal area impact), with two similar vehicles.

Whilst not utilising all of the crash structure, the 40% collision uses its crash structure to absorb impact energy. The vehicle has stopped quickly, the barrier with which the car impacted has not reached the occupancy cell. The 25% offset collision is very different. The crash structure has not dissipated the impact energy as well, the vehicle has travelled so that the barrier is much closer to the occupancy cell.

Autonomous vehicles will need to decide on the safest collision to have, which may involve the car aiming to have a 100% frontal impact to better optimise the use of the crash structure.

ConsumerReports.org (2013) reports a study conducted by the University of Buffalo highlighting the importance of crash compatibility, where vehicles of similar mass and crash structure collide. The laws of physics dictate that when mismatched vehicles collide, the lighter vehicle will suffer greater deformations and accelerations. This study demonstrates the real dangers. In car vs. SUV head-on collisions, the study concluded that the probability of death for the car's driver were 7.6 times greater than for the SUV driver. In collisions with cars that had a better front-crash test rating than the SUV, the car did fare slightly better than before, but the probability of death was still four and a half times greater for the car driver than the SUV driver.

2.6.10   Literature Review Conclusions

The literature review demonstrates the different disciplines upon which the research problem will rely. Firstly, a review of ADAS shows the technologies currently available for vehicles. The research problem aims to avoid or mitigate collisions on high-speed motorways, and an understanding of vehicle dynamics demonstrates the importance of the autonomous vehicle maintaining control through emergency manoeuvres. Building on from the vehicle dynamics, the vehicle will need to be modelled, and the bicycle model discussed in Section 2.3.6 will be the starting point.

Highway platooning methods are reviewed as an example of autonomous driving systems on motorways. There are also examples of motorway simulators to review if any methods can be adapted for this thesis. A review of collision avoidance and mitigation technologies highlights the limitations of these systems, with little research focused on mitigating unavoidable collisions.

Collision avoidance and mitigation technologies were discussed, but also demonstrated that research for a decision process for an autonomous vehicle to decide on the best action to take is certainly in its infancy. There is a clear novelty to the aims of this thesis to construct a decision process to support collision mitigation.

Adaptive Cruise Control is capable of bringing a car to a complete stop, and Automatic Emergency Braking can stop the car if an imminent collision is ahead. But these systems have only one objective which is to slow the car as much as possible, aiming to avoid or mitigate a collision directly ahead. These systems could be improved upon by introducing steering as another factor in either avoiding or

mitigating imminent collisions. Steering manoeuvres to avoid collisions have been addressed in the literature, but this does not address the possibility that whatever action is taken will still result in collision. The literature review was completed with an overview of automotive collision research to demonstrate the importance of the research to be completed in this thesis.

This research programme aims to evolve from these technologies and develop a simulator and decision-making method that can select the best action for an autonomous vehicle to take, with the aim of improving safety on high-speed motorways.

Chapter 3

Multi-Attribute Decision Making - Literature Review

3.1 Introduction

The autonomous vehicle will need to make a decision based on available information about imminent collisions. Generally, this decision can be made based on different types of information. The application of Multi-Attribute Decision Making (MADM) methods is discussed, due to the suitability of MADM to the research problem. MADM selects the best alternative by assessing results from defined criteria. The

severity of a collision will be described by the criteria, whilst the available lanes are the alternatives. MADM methods are mathematical processes which rank the alternatives. These decision making methods will work with simulators which produce the attribute values, with the aim of selecting the least severe collisions when faced with multiple potential imminent collisions.

3.2 Multi Attribute Decision Making (MADM)

MADM problems are associated with a decision problem of the choice or ranking of existing alternatives. MADM is described by Kahraman (2008) as a general class of operation research models dealing with decision problems with the consideration of a number of decision criteria. MADM requires that the selection be made among decision alternatives which are described by their individual attributes. MADM methods are suited to decisions with a limited number of decision alternatives. Sorting and ranking of alternatives is how a MADM problem is solved. A final ranking or selection of alternatives is determined by combining information from the problem's decision matrix with additional information from the decision maker. Besides decision matrix, all but the simplest MADM techniques use additional information from the decision maker to calculate the final rankings or selection. This additional information is the criteria weights, meaning that certain criteria can be made more influential over the final decision.

A discrete number of metrics on which to base the decision, called criteria, will need to be calculated. Also, the MADM methods considers a discrete number of possible decisions, i.e. alternatives. The discrete criteria and alternatives lends well to the capabilities of MADM. Kahraman (2008) concludes that discrete decision spaces are a necessity for MADM decision making processes, which focus on the selection or ranking of different predetermined alternatives. The alternatives and criteria must be determined before the decision process begins, as comparing the alternatives i and criteria j forms a matrix of size i by j. However, one or more alternatives can be disqualified from the decision process if required, by simply not including it with the decision process. Therefore, a MADM method would suit the problem of selecting a collision with the least severe impact, where a lane on which the autonomous vehicle should collide has to be selected considering a number of criteria. However, MADM refers to a range of decision making methods, not one specific technique.

48

There are many different MADM techniques, and each will be better suited to some situations over others. Chamblás and Pradenas (2018) use AHP, ELECTRE and TOPSIS to select the best method for desalinating seawater. In this example, all MADM methods showed the same preference with no major discrepancies in the results.

The decision-making problem should apply a MADM method best suited to a situation. Drawing on the findings and experience of other authors help, as Thor, Ding, and Kamaruddin (2013) summarise the benefits and disadvantages of four popular MADM methods including AHP, TOPSIS, ELECTRE, and SAW.

3.3   MADM Methods

3.3.1 SAW

SAW (Simple Additive Weighting) described by Yoon and Hwang (1995) is a commonly used MADM method which determines the best option by normalizing all alternative values, and weighting them for each criterion. The best alternative has the highest summed value of normalized and weighted attribute values.

Afshari, Yusuff, and Derayatifar (2012) use SAW with fuzzy logic to select the best candidate for a project manager job. The fuzzy logic is used to convert linguistic variables into numerical values, such as height can be described with fuzzy logic as very low, low, medium, high, very high.

3.3.2 ELECTRE

ELECTRE ELimination Et Choix Traduisant la REalité (ELimination and Choice Expressing REality) is described by Yoon and Hwang (1995) as a method that establishes outranking relationships by the dichotomization of preferred alternatives and non-preferred ones. ELECTRE normalizes attribute values and determines normalized weight values. Then each alternative is compared against another alternative and allocated into two sets, concordance and discordance sets. When one alternative A_p is preferred over another alternative A_q, then A_p is compiled into

the concordance set. The discordance set is composed of all alternative values whereby A_p is not preferred over another alternative A_q.

Concordance and discordance indexes are calculated as a measure of confidence of the pairwise judgements. The dominance of one alternative A_p over alternative A_q is stronger when there is a higher concordance index. An evaluation is made between each alternative's concordance and discordance indexes in such a way as they are compared against the average concordance and discordance indexes. Each alternative is compared against all other alternatives pairwise for preference, the best alternative is selected with outranking relationships.

Wang and Triantaphyllou (2008) explain that partial pre-ordering only puts the alternatives in an order of preference, whereas a complete pre-order includes the rank value of each alternative. In order for ELECTRE to achieve a complete pre-order with the rank value of alternatives, further analysis is required. The partial pre-ordering will only state that one alternative is preferred over another, not giving specific values as to how much that alternative is preferred.

Comaniţă et al (2015) use ELECTRE to select the best bioplastic material for packaging taking six criteria including economic and environmental factors into account for the decision. ELECTRE is also used by Shanian and Savadogo (2006) to select the most appropriate material for a particular application, in this example a loaded thermal conductor is the application needing a suitable material. The considered material are ranked after a criteria sensitivity analysis is performed to determine the optimal weights of the criteria.

3.3.3 TOPSIS

The Technique for Order of Preference by Similarity to Ideal Solution (TOPSIS) is set up similarly to AHP, where criteria are weighted according to their importance and the alternatives are ranked based on their similarity to the ideal solution. It is originally developed by Hwang and Yoon (1981). TOPSIS calculates the Ideal solution by selecting the best result for each criterion. It also calculates the Negative Ideal solution by selecting least desirable results for all criteria. These two solutions effectively form two artificial alternatives. Each alternative is then compared to these artificial alternatives for their geometric distances. The decision made by TOPSIS is the alternative which has the shortest geometric distance to the Ideal solution, and

the longest geometric distance to the Negative Ideal Solution. Finding the geometric distances relies on the attribute values to be standardised, by the following equation:

$$r_{ij} = \frac{x_{ij}}{\sqrt{\sum_{i=1}^{m} x_{ij}^2}}, \quad i = 1,..,m; \quad j = 1,..,n.$$

(3-1)

where x_{ij} is the attribute value, r_{ij} is the standardised value of each attribute value, i and j refer to the attribute that corresponds to alternative i and criterion j.

One benefit of this method is that defining the optimisation of criteria is simple, as it is a simple case of selecting either the maximum or minimum attribute values for each criterion to create the artificial alternatives.

Behzadian et al (2012) review publications of TOPSIS applied to various problems. TOPSIS has been used in fields such as supply chain, management and logistics, business and marketing management, health, safety and environment management, and human resources management. The authors also review the applications of TOPSIS in design, engineering and manufacturing systems.

This review includes Zhang et al (2010) using TOPSIS as a method to determine the standard outputs of decision values. The paper actually develops a new method for evaluating vehicle performance using fuzzy logic to numerically represent the numerical value of a linguistic variable. TOPSIS is used as the method to compare all other methods with. The optimal decision method created by the authors is the one that most closely represents the results of TOPSIS.

Wang and Chang (2007) use TOPSIS to select the optimal aircraft for initial training at the Taiwan Air Force Academy. Fuzzy logic is also used to give numerical values to linguistic variables when describing the performance of the aircraft.

Many TOPSIS methods use fuzzy logic to represent linguistic variables as numerical values, but that will not be necessary for this research application as the collisions will be described numerically.

3.3.4 Analytical Hierarchy Process

The AHP method is a widely used decision making technique proposed by Saaty (1980). It uses a process of pairwise comparisons, both for the weighting of priorities and assessing the decision matrix. However, as the values for each alternative and

criteria are crisp numbers, pairwise comparison can be replaced by simply normalizing these matrices. The AHP method is similar to SAW (Section 3.3.1), but introduces pairwise comparisons. The pairwise comparison method allows for human made judgements to be objectively assessed for consistency. Vector normalization is a major component to structuring the decision process, and AHP uses the following equation:

$$\hat{x} = \frac{x}{\sum x} \tag{3-2}$$

where $\hat{x}$ is the normalized attribute value, $\sum \hat{x}$ is 1, and $\sum x$ is the sum of all alternative values x.

Saaty (1996) describes consistency using an eigenvector evaluation of the judgements made in the pairwise matrices. Consistency is measured by comparing the matrix of judgements with the right eigenvector derived from that same matrix. It is only subjective assessments, which are the assessments made by a person that need to be assessed for consistency.

Harker (1989) describes the calculation of consistency as a measurement of the judgement errors made when completing the matrices. The author also states the benefit of adapting a normally human-made decision, by introducing a mathematical process. A decision made by a group instead of an individual can also be done using AHP, using the Delphi technique, which surveys the group to produce a statistically analysed preference.

Harker (1989) discusses the benefits of employing AHP, and gives examples of when it has been used. AHP was used in Finland in a parliamentary debate as to whether a new nuclear power-plant should be constructed, as discussed by Hämäläinen and Seppäläinen (1986). The AHP method was praised for removing the unimportant arguments which at the time fuelled debates, and was able to focus on the information that was important.

The nature of AHP is to structure a decision making problem into a mathematical process. This method is often applied to social problems such as Hämäläinen and Seppäläinen (1986), and Handfield et al. (2002) to introduce environmental factors to the decision made by purchasing managers. However, the AHP method has also been applied in engineering decision problems by Triantaphyllou and Mann (1995) to assess resource allocation for cloud computing, Omasa et al. (2004) to evaluate tissue engineering and regenerative medicine,

Pörtner et al. (2005) to evaluate and compare tissue engineering reactors, and Yang and Kuo (2003) to optimise the layout of a manufacturing or service industry system, by using a computer-aided-layout planning tool to generate many different layout alternatives. These layouts were then evaluated using AHP.

3.3.5 Analytical Network Process

The Analytical Network Process (ANP) first published by Saaty (1996) is considered to be a more generalized form of the AHP method. Instead of making the decision based on a hierarchy structure, where each step leads onto the next, ANP introduces feedback. ANP is based upon AHP, and therefore, the first few steps are the same. Once the weighted ranks of the AHP are calculated, the network feedback process begins. This decision-making process makes use of a Supermatrix, where alternatives and criteria are assessed.

Assessing the importance of the alternatives does not itself introduce a feedback, this is included in the Supermatrix. The feedback is an assessment of how influential the criteria have been on each attribute value. It is the matrix power iteration, i.e., the raising of the matrix to power k that causes the matrix to converge, creating the Limit Supermatrix. The matrix convergence allows for the resulting eigenvector to be assessed for the rank of alternatives.

It is the power iteration method that allows for the weights of criteria to influence alternative values, and then the influence of alternative values on the decision made to influence the weights of criteria. It is noted that power iteration is a slow method to achieve convergence, hence why the value of k needs to be high. Instead of squaring the Supermatrix repeatedly until the matrix converges, it is faster to raise the Supermatrix to the power k, such as with Equation (3-3).

$$Limit\ Supermatrix = (Supermatrix)^k \qquad (3\text{-}3)$$

AHP is a hierarchy where the criterion weights determine the importance of alternatives. The feedback of ANP not only uses criteria weights to determine the alternative importance, but also the importance of alternatives to determine the importance of each criteria, (Saaty, 1996). It is the Supermatrix method that employs this feedback.

Carlucci (2010) describes the advantage ANP has, noting that AHP is a top-down decision process performed by judging the performance of the alternatives on the criteria. Decision making does not strictly fit this top-down idea, as the criteria are frequently dependent on the alternatives available to the decision making process. A form of iteration or feedback dependencies is called for among decision elements.

Gencer and Gürpinar (2007) use ANP to select a supplier for an electronics company. The authors praise ANP for including the assessment of how the criteria affect the suppliers, but also what criteria are important for those suppliers. ANP was used by Cheng and Li (2005) to prioritise potential projects in construction. ANP was able to state which projects should be considered more important for developers.

3.4 Decision Making Conclusions

The research problem included in this thesis is an engineering decision problem, one which will not benefit from a human opinion. Therefore, the objective and consistent mathematical method is suitable for the problem of selecting a motorway lane to optimise the outcomes for all involved.

The autonomous vehicle will need to make a decision on the least severe collision. The review of MADM demonstrates the suitability of this approach. MADM is a general term for a type of decision making involving a finite number of alternatives available, and a finite number of criteria by which to assess the decision. This chapter includes a review of 5 MADM methods. The methods are described, and applications in existing research are discussed.

MADM is suitable for the research problem, due to the finite alternatives and criteria. The research problem is for an autonomous vehicle to select the least severe lane of a motorway to drive into, when facing multiple imminent collisions in all lanes. The lanes of the motorway are the alternatives available, and the metrics which describe the severity of the collisions in each lane are the criteria.

Chapter 4

Highway Platooning

4.1 Introduction

The overall objective of this investigation is to demonstrate that autonomously driven vehicles can still have collisions, and that there is a need for an autonomous collision mitigation control, to limit the dangers to the vehicle occupants. For the aim of developing an autonomous collision avoidance strategy, it is beneficial to demonstrate a need for such methodology. Autonomous vehicles have the potential to improve automotive safety by preventing collisions from happening. However, assuming that autonomous vehicles cannot crash is a dangerous over-estimation.

Highway Platooning considers the behaviour of road vehicles acting like trains. Vehicles will join platoons, all heading in the same direction at identical speeds. This has the effect of potentially increasing traffic flow, reducing the aerodynamic drag on the vehicles in the platoon, and managing safety. Highway

platooning is investigated due to the similar research scenario of motorway safety, which is of vehicles travelling at high speed on multiple-lane roadways. The control strategy developed in this thesis could potentially be applied to a highway platooning scenario.

The aim of this investigation are to test platooning control systems, and demonstrate their limitations. For this the work of Cook (2007) is heavily drawn upon. This research provides the control strategies for two main platooning methods, Bidirectional Control and Asymmetrical Control. The systems are developed and tested in this chapter, demonstrating what can cause these systems to fail, resulting in collisions between the platooning vehicles.

The simulations presented in Cook (2007) are repeated with a new input signal, and similar results are observed. The author of this thesis then adds a new feedback control to better manage the vehicle spacing. The platooning model is further stressed by time delays. Increasing the platoon size is simulated by the author of this thesis, to observe the limits of the new control.

4.2 Lead Vehicle First Order Velocity

A first order system will be used as the input signal for all models presented in this chapter. This first order system will represent the lead vehicle velocity. It can be simulated quickly and tuned to the desired behaviour. The following scenario will be simulated. The lead vehicle will accelerate from $10m/s$ up to $30m/s$. After driving at $30m/s$ for $50s$, the lead vehicle will then decelerate from $30m/s$ back to the original $10m/s$. The lead vehicle velocity is represented in Figure 4-1. This input is similar to that from Cook (2007), but the maximum velocity is increased to $30m/s$, to represent the UK motorway speed limit of $70mph$ ($31.29m/s$). The velocity profile simulates sudden velocity changes from a low speed to high, and then a high speed to low.
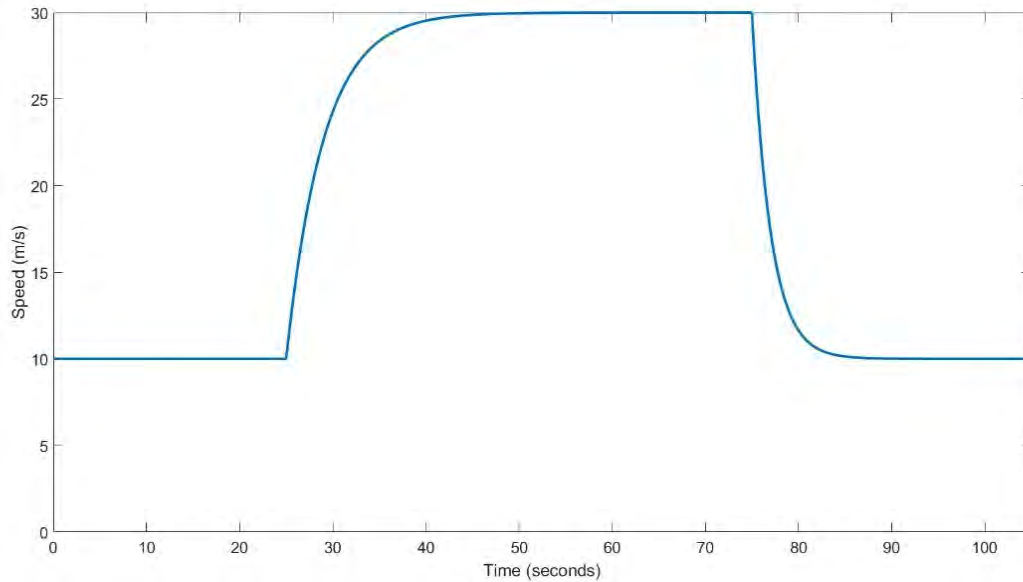
Figure 4-1 - Lead Vehicle Velocity

In order to stress the control systems of the following vehicles, the acceleration of the lead vehicle will take only $4s$, and the braking will take $2s$. Sudden changes in velocity will increase the risk of the following vehicles colliding into the back of the lead vehicle. They will need to avoid such an eventuality.

Autocar.com (2017) gives the fastest accelerating road cars of the year to accelerate from 0 to $60mph$ (0 to $26.82m/s$) a time of $2.3s$. A $10m/s$ to $30m/s$ velocity change represents traffic that is slow moving, accelerates up to the UK national speed limit ($70mph$, $31.29m/s$), and then decelerates back to slow moving traffic. The $4s$ to accelerate represents a fast accelerating vehicle. These are values given by Autocar.com (2017) which suggest are feasible. The braking time of $2s$ is assumed from a CarAndDriver.com (2008) article examining braking performance from $100mph$ to 0. The best performing car, a Porsche 911 road-car stopped consistently over 35 emergency stopping manoeuvres with only $20s$ between tests. The stopping distance is given as $305feet$ ($92.964m$).

This equates to an average rate of deceleration of $10.75m/s^2$, given by Equation (4-1).

$$a = \frac{(v^2 - u^2)}{2s} \qquad\qquad (4\text{-}1)$$

where s is stopping distance (m), u is initial velocity (m/s), v is final velocity (m/s), and a is deceleration (m/s^2).

Braking time t is calculated by Equation (4-2):

$$t = \frac{v - u}{a}$$

(4-2)

With an initial speed of $30m/s$, final speed of $10m/s$, and a rate of deceleration of $10.75m/s^2$, a stopping time of $1.8605s$ is calculated. The calculation of $10.75m/s^2$ deceleration is from the static SUVAT equations, and so that value is assumed as an average rate of deceleration.

4.3 Highway Platooning

Highway platooning is to be used on a long roadway with little to no steering required. This is a control technology which will likely be reliant on V2V communications, and is used to demonstrate that the system can be stressed to a point where the platoon is unstable, resulting in collisions. The highway platooning models were first published by Cook and Sudin (2003). Cook continued to develop the platooning control.

The model by Cook (2007) uses the velocity and spacing data from the vehicles immediately ahead and behind, not the whole platoon. Each vehicle could therefore rely on its own sensors to provide the inputs to its own control law. Vehicle-to-Vehicle (V2V) communication is theoretically not required and could therefore be used when V2V is not available. This leads to the following assumptions:

- It is assumed that all vehicles in the platoon can match the accelerations and decelerations of the lead vehicle
- Vehicle-To-Vehicle (V2V) communication is not used, it is assumed that no information is passed between vehicles, the system will be relying on visual data obtained by each vehicle. Each vehicle in the platoon will use on-board sensors to determine the velocities and displacements of other vehicles.

4.3.1 Bidirectional Control

A model published by Cook (2007) simulates longitudinal dynamics of a platoon of vehicles. It can be used to demonstrate an important issue that even autonomously controlled vehicles can crash. This model replicates the Bidirectional Controller of Cook (2007), where vehicles control velocity based on values for the vehicle immediately in front, and immediately behind. The bidirectional control has the effect of maintaining the distance between the vehicle in front and behind equally. This is due to the issue of reducing vehicle spacing propagating through the platoon. The further along the platoon, the less reaction time the vehicles will have. The model presented here is constructed in Simulink.

The bidirectional control law is stated as in Equation (4-3).

$$u_i = k_p(\varepsilon_i - \varepsilon_{i+1}) + k_v(v_{i-1} - 2v_i + v_{i+1}) \tag{4-3}$$

where u is the control signal for each vehicle's acceleration, v is the velocity, ε is the separation distance, the subscripts $i-1$ and $i+1$ refer to the vehicles ahead and behind the control vehicle i respectively, and k_p and k_v are constant gains. The separation distance is described by:

$$\varepsilon_i = x_{i-1} - x_i - L \tag{4-4}$$

where x is the vehicle's longitudinal displacement, and L is the vehicle length. Each vehicle is assumed to have identical lengths.

The vehicle motion control law is defined by a Laplace transfer function $G(s)$:

$$G(s) = \frac{k_v s + k_p}{s^2 + 2(k_v s + k_p)} \tag{4-5}$$

where s denotes the Laplace transformation representing velocity and s^2 represents acceleration.

As the final vehicle in the platoon will not have a velocity input for a vehicle behind it, a separate control is required given by:

$$\dot{v}_z = k_p(\varepsilon_z - D) + k_v(v_{z-1} - v_z) \tag{4-6}$$

where D is the desired separation distance between the vehicles, and subscript z denotes the final vehicle in the platoon.

For the simulations all vehicles will have length $5m$, and the separation distance will also be set to $5m$. The bidirectional control of each vehicle in the platoon uses the velocity of the vehicle immediately ahead, and immediately behind to determine its own velocity control.

4.3.1.1　　　Five Vehicle Platoon

The Bidirectional control will be assessed for platoon stability. Stability will be assessed on how each vehicle can follow the lead vehicle's velocity. Stability will also be assessed by the acceleration of each vehicle to match the lead vehicle's velocity, and the separation distance between each vehicle. It can be assessed if a collision does or does not occur. The lead vehicle will use the velocity defined in Section 4.2 as the input to the system, and 5 vehicles will follow the lead vehicle, as presented in Figure 4-2.
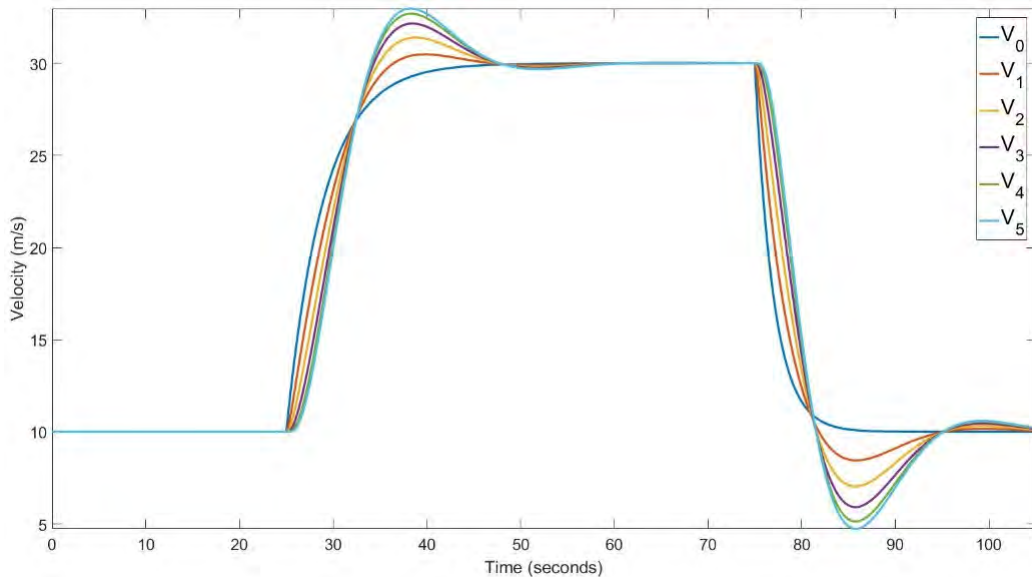
Figure 4-2 - Five Vehicle Platoon Velocity

The lead vehicle's velocity is represented by line V_0. The velocity plot of all vehicles demonstrates that each vehicle overshoots the vehicle ahead's velocity, for both the acceleration and deceleration. The overshoots demonstrated in Figure 4-2 do work to maintain the separation between the vehicles and there is little oscillation, but a further look at the acceleration and separation plots will determine this system's performance.
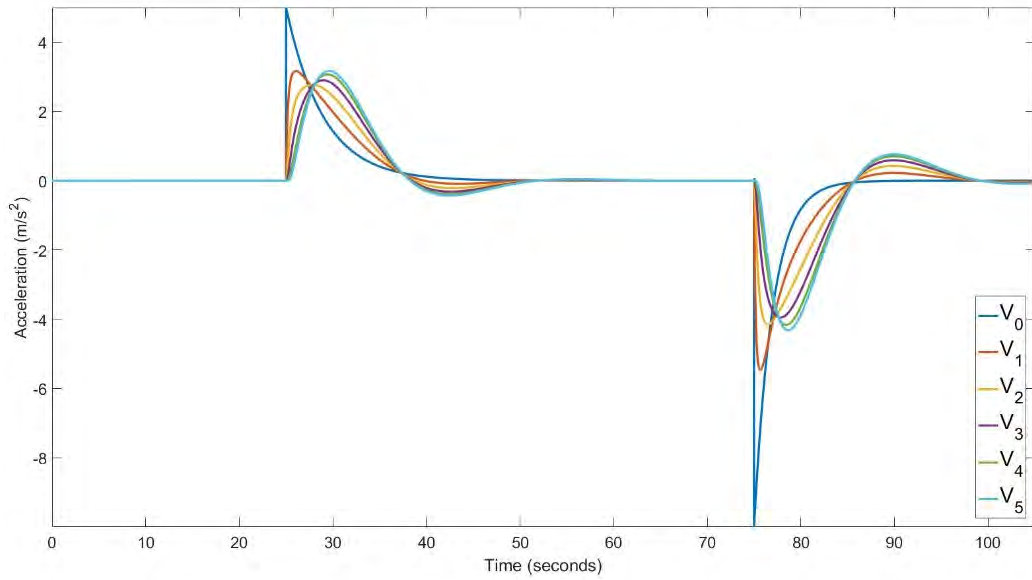
Figure 4-3 - Five Vehicle Platoon Acceleration

The acceleration results presented in Figure 4-3 demonstrates a similar result to the velocity. No vehicle exceeds the lead vehicle's maximum accelerations, but there is a noticeable oscillation following the inputs from the following vehicles (V_1 to V_5).
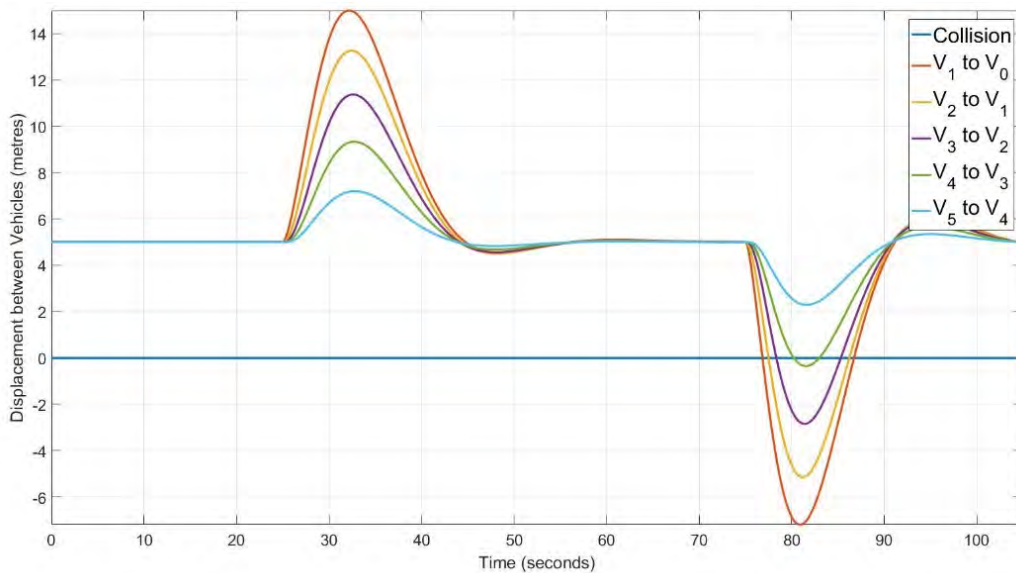
Figure 4-4 - Five Vehicle Platoon Separation Displacement

The separation results presented in Figure 4-4 is the most concerning. The collision line represents the point at which a collision occurs from vehicles 1 to 5, by impacting the rear of their respective vehicles ahead. Vehicles 1 to 4 have all crossed that collision line, indicating a collision. Only vehicle 5 avoided collision. It is observed that the further down the platoon (higher number vehicles), the least severe the separation appears to be, for both the increasing and decreasing velocity motions. Vehicle 1 must react immediately to the lead vehicle's sudden accelerations, and the following vehicles have more and more ability to dampen these changes. Each collision is considered separate from all other collisions, and so the effect of collisions ahead of any given vehicle, and this affecting the velocity and spacing of those vehicles ahead is not taken into account.
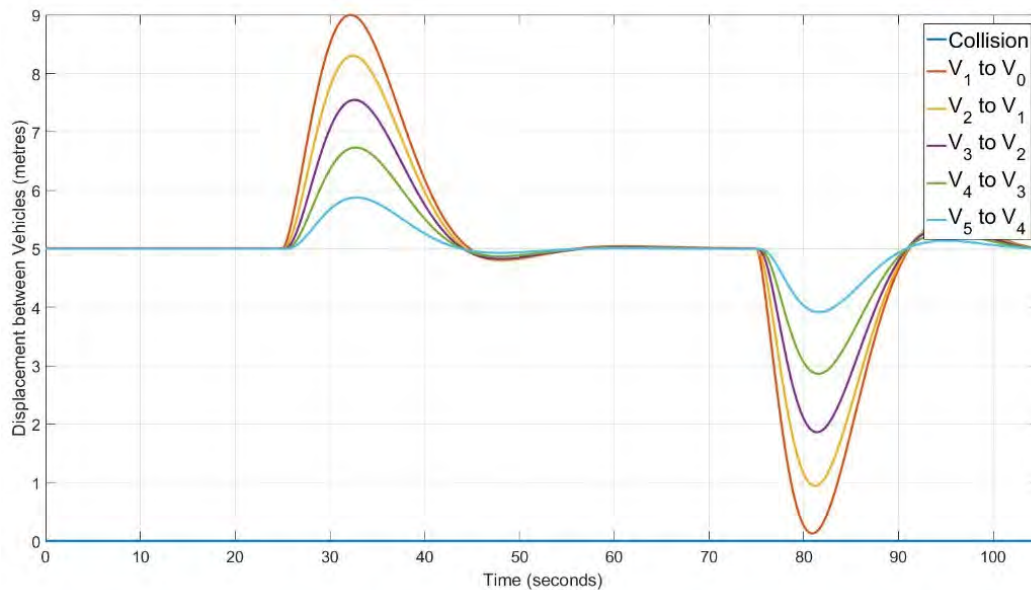
Figure 4-5 - Five Vehicle Platoon Separation Displacement, 18m/s maximum speed

Adjusting the maximum velocity of the lead vehicle, whilst still using the same acceleration and deceleration transfer function, results in preventing collision, as presented in Figure 4-5. It is found that the maximum speed without resulting in collision is $18m/s$. And even with this reduction in velocity change, a collision is only $0.1282m$ away. One can conclude that the lead vehicle's sudden deceleration are too severe for the bidirectional control alone, with the separation distance set to $5m$. Increasing this distance to $13m$ will also maintain platoon stability without resulting in collisions. These results reflect the original results from Cook (2007).

4.3.1.2 Five Vehicle Platoon with PI Control

Due to the poor performance of the bidirectional control, the author of this thesis introduces a Proportional-Integral (PI) controller to improve the separation distance control of the vehicles. The PI controller is introduced with feedback from the vehicle's velocity to control the error in this signal, which is then tuned and fed back into the vehicle's control laws.
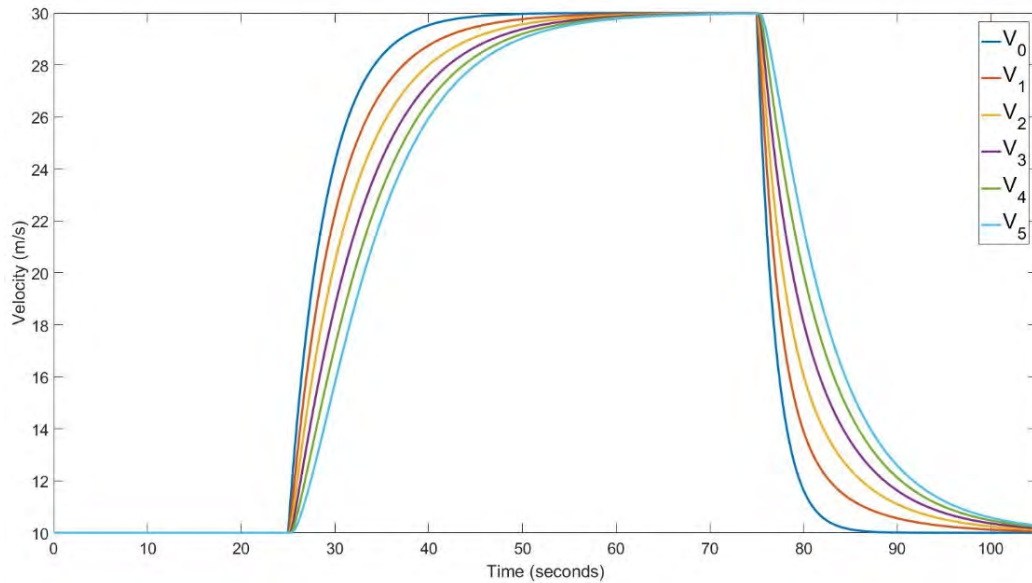
Figure 4-6 - Five Vehicle Platoon with PI Velocity

As one can see in Figure 4-6 the PI control has removed any overshoot and oscillation in the platooning vehicle's velocity plots, as observed in Figure 4-2.
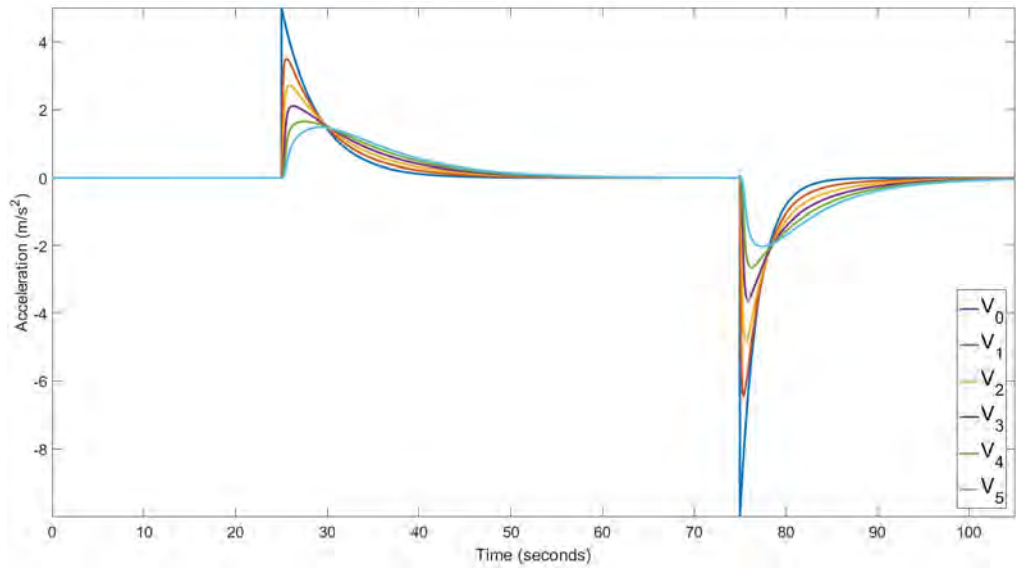
Figure 4-7 - Five Vehicle Platoon with PI Acceleration

Again, the acceleration results presented in Figure 4-7 demonstrates no oscillations as seen with the previous acceleration results, Figure 4-3. The further along the platoon, the lower the maximum acceleration peak, but does maintain an acceleration that is not zero for longer.
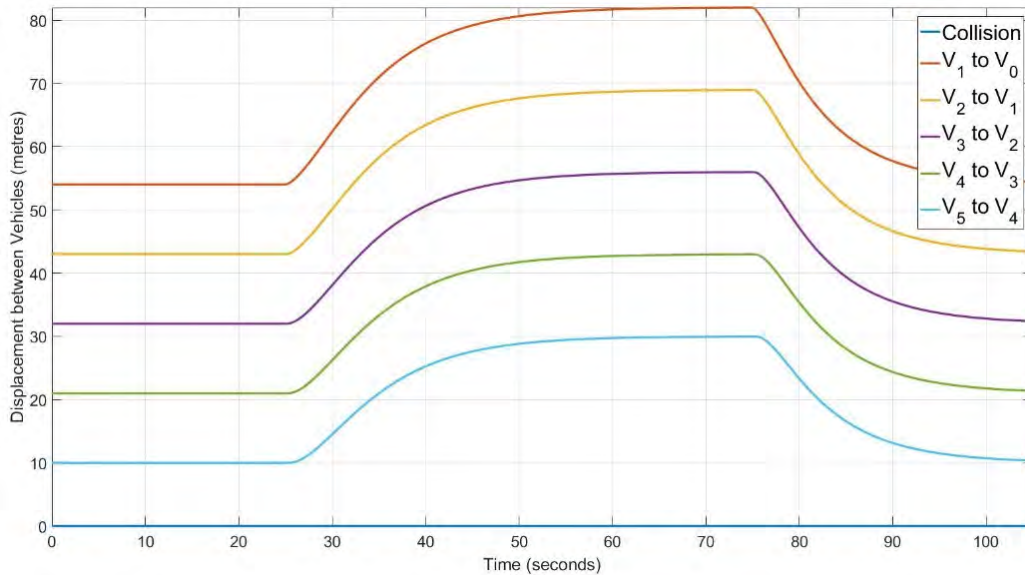
Figure 4-8 - Five Vehicle Platoon with PI Separation Displacement

The separation displacement results presented in Figure 4-8 reveals a new behaviour. As the velocity increases, so does the spacing, effectively creating a

velocity-dependent spacing control. This can be considered a benefit to safety, as with increased speed, an increased spacing gives more time to react to the vehicle ahead. However, there is a clear disadvantage to this PI control. Each plot still represents the separation distance of each vehicle to the vehicle ahead. Vehicle 1 at times is spaced over $80m$ away from the lead vehicle, and vehicle 2 is spaced nearly $70m$ from vehicle 1. It is also observed that the further along the platoon, the lower the separation distance. The integral controls the separation, but needs to be maintained before the spacing control becomes unstable. The PI control, whilst demonstrating some desirable effects needs to be further considered.

4.3.2 Asymmetrical Control

One issue with the simple bidirectional control of Cook (2007) is that the positioning of v_i is treated as relative to the car immediately in front and behind. It is possible to split these, and have more specific control for the relationship with the vehicle in front, and the relationship with the vehicle behind, effectively having truly asymmetrical control. Cook (2007) also developed an asymmetrical strategy, which is to be evaluated here.

The asymmetrical control law approaches v_{i-1} and v_{i+1} separately by the following control parameters:

$$((x_{i-1} - x_i) - D) \quad (v_{i-1} - v_i) \qquad ((x_{i+1} - x_i) + D) \quad (v_{i+1} - v_i)$$

where D is the separation distance input, to form the following equation:

$$u_i = Kp1(x_{i-1} - x_i - D) + Kv1(\dot{x}_{i-1} - \dot{x}_i) + Kp2(x_{i+1} - x_i + D) \\ + Kv2(\dot{x}_{i+1} - \dot{x}_i)$$

(4-7)

where $Kp1$ and $Kv1$ are constant gains for the vehicle ahead $i - 1$ control, and $Kp2$ and $Kv2$ are constant gains for the vehicle behind $i + 1$ control. Which can be redefined as:

$$\dot{v}_i = \ddot{x}_i = Kp1(x_{i-1} - x_i - D) + Kv1(\dot{x}_{i-1} - \dot{x}_i) \\ + Kp2(x_{i+1} - x_i + D) + Kv2(\dot{x}_{i+1} - \dot{x}_i)$$

(4-8)

The derivative of Equation (4-8) is produced:

$$\ddot{v}_i = Kp1(v_{i-1} - v_i) + Kv1(\dot{v}_{i-1} - \dot{v}_i) + Kp2(v_{i+1} - v_i) \\ + Kv2(\dot{v}_{i+1} - \dot{v}_i)$$

(4-9)

The differentiation causes the D values to disappear, and the equations is expanded to:

$$\ddot{v}_i = Kp1v_{i-1} - Kp1v_i + Kv1\dot{v}_{i-1} - Kv1\dot{v}_i + Kp2v_{i+1} - Kp2v_i \\ + Kv2\dot{v}_{i+1} - Kv2\dot{v}_i$$

(4-10)

to be rearranged as:

$$\ddot{v}_i + Kv1\dot{v}_i + Kv2\dot{v}_i + Kp1v_i + Kp2v_i \\ = Kv1\dot{v}_{i-1} + Kv2\dot{v}_{i+1} + Kp1v_{i-1} + Kp2v_{i+1}$$

(4-11)

A Laplace Transformation creates the following equations:

$$s^2 v_i + sKv1v_i + sKv2v_i + Kp1v_i + Kp2v_i \\ = sKv1v_{i-1} + sKv2v_{i+1} + Kp1v_{i-1} + Kp2v_{i+1}$$

(4-12)

which is formatted as:

$$v_i\left(s^2 + s(Kv1 + Kv2) + (Kp1 + Kp2)\right) \\ = v_{i-1}(sKv1 + Kp1) + v_{i+1}(sKv2 + Kp2)$$

(4-13)

to develop the following control law of Equation (4-14).

$$v_i = \frac{v_{i-1}(sKv1 + Kp1)}{s^2 + s(Kv1 + Kv2) + (Kp1 + Kp2)} \\ + \frac{v_{i+1}(sKv2 + Kp2)}{s^2 + s(Kv1 + Kv2) + (Kp1 + Kp2)}$$

(4-14)

The stated control laws from Cook and Sudin (2003) are given as:

$$\dot{v}_i = Kp(\varepsilon_i - \varepsilon_{i+1}) + Kv_+(v_{i-1} - v_i) - Kv_-(v_i - v_{i+1})$$

(4-15)

$$G_\pm(s) = \frac{Kv_\pm s + Kp}{s^2 + (Kv_+ + Kv_-)s + 2Kp}$$

(4-16)

The notation $\pm$ refers to two different control laws, when $G_-(s)$ and $Kv_-(s)$ are selected, this refers to the control law and constant gain for the vehicle ahead respectively, whilst $G_+(s)$ and $Kv_+(s)$ refer to the vehicle behind.

4.3.2.1 Five Vehicle Platoon with PI Control

The asymmetrical control will also use PI control, as proposed by the author of this thesis in Section 4.3.1.2, but this time the velocity ahead data will have a different PI tuning to the velocity behind. Also, the altered control laws described in Section 4.3.2 are introduced.
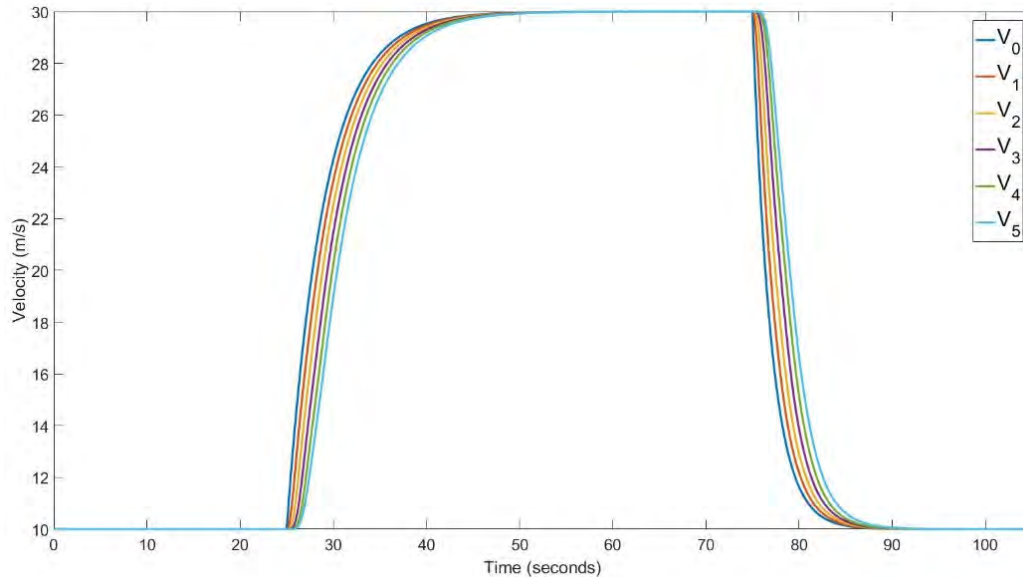
Figure 4-9 - Five Vehicle Asymmetrical Platoon Velocity

The asymmetrical control with PI control maintains a steady velocity for all vehicles in the platoon, as presented in Figure 4-9. There are no overshoots or oscillations.
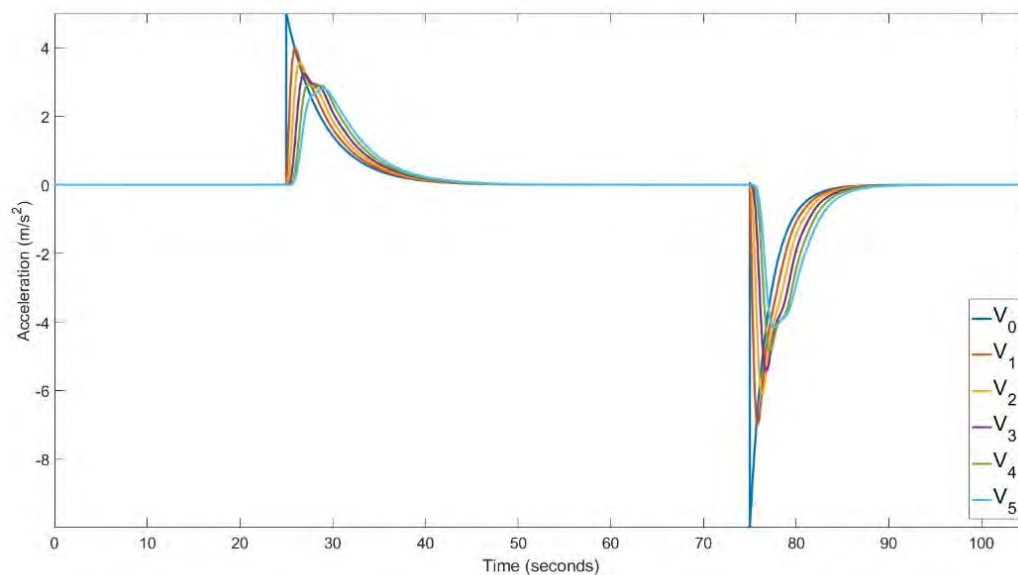
Figure 4-10 - Five Vehicle Asymmetrical Platoon Acceleration

67

Figure 4-10 demonstrates a similar behaviour to the previous PI acceleration in Figure 4-7. However, this demonstrates a noticeable reduction in the time of non-zero acceleration for the platooning vehicles. The plots of the platooning vehicle also seem to be closer to each other, demonstrating more similar acceleration behaviours.
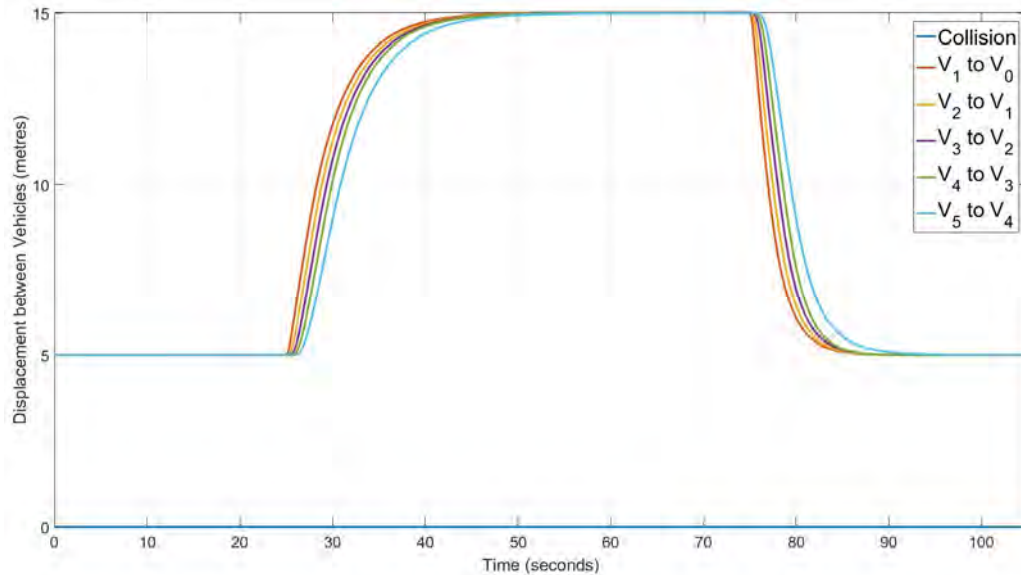
Figure 4-11 - Five Vehicle Asymmetrical Platoon Separation Displacement

It is observed that the velocity dependent spacing whilst maintained is different as presented in Figure 4-11, compared to Figure 4-8. Displacement increases by a factor of three at the velocity change, as velocity also increases by a factor of three. This is due to the integral control of the PI controller. This controls the velocity dependent spacing, and tuning it to maintain a $5m$ displacement at $10m/s$, results in the different displacement at $30m/s$. Adjusting the integral will influence the spacing control, as well as increasing the value of the integral reduces the maximum delay before the system fails.

The velocity dependent spacing has been maintained, and there are no concerns about collisions. The velocity dependent spacing increases the separation displacement by $20m$, when the speed increases by $20m/s$. The plots are stable, with no overshoots or oscillations.

The separation displacement of the last vehicle in the platoon, V_5 does behave slightly differently to the other platooning vehicles. This is due to V_5 having the $\dot{V}_z$ control given by Equation (4-6). This vehicle also has its own PI control. The

five vehicle asymmetrical control with PI behaves satisfactorily, and now must be stressed to examine limitations by making the conditions more challenging.

4.3.2.2   Five Vehicle Platoon with PI Control and Time Delay

The Asymmetrical control will be assessed using the same scenario observed in Section 4.3.2.1, but now the system will be stressed by introducing a time delay for the incoming velocity data. The time delay represents anything that may delay the information being processed, such as computational and measurement speed. The time delay is added by the author of this thesis to further stress the model to observe its capabilities at adapting to the proposed situation. A delay may cause the vehicles to collide, as they are incapable of reacting immediately to sudden velocity changes. A delay could be caused by processing times, or by V2V communication. The control system will still need to maintain stability.

Simulating a delay introduced to each platooning vehicle in increments of $0.05s$, the platoon maintained stability up to $0.15s$. At $0.2s$ it is observed that oscillations are exponentially increasing in all simulation plots: Velocity, Acceleration and Separation Displacement.

Instead, the stability of the platoon will be assessed if only 1 vehicle has a disruptive delay. All but one vehicles will have a standard delay time of $0.001s$. V_2, which is near the front of the platoon, will have an increased delay, and the effects of this will be observed. The maximum delay V_2 can experience before the system becomes unstable is $0.45s$.
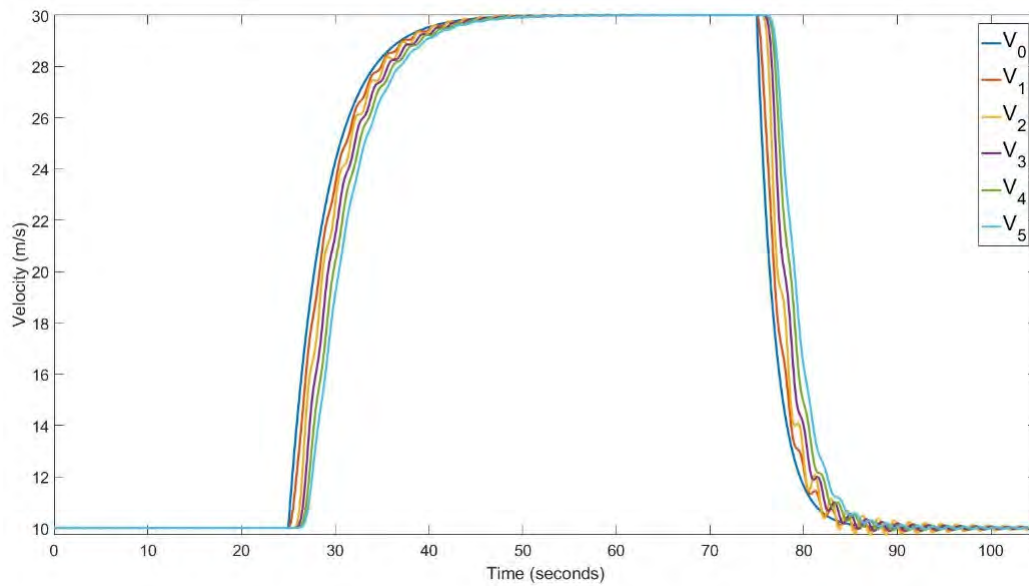
Figure 4-12 - Vehicle 2 with 0.45s Delay Velocity

The velocity results presented in in Figure 4-12 shows that velocity is maintained, but oscillations are observed on all velocities, except for lead vehicle V_0. These oscillations are most evident at velocity changes, especially at times, 30s to 40s, and 80s to 100s.
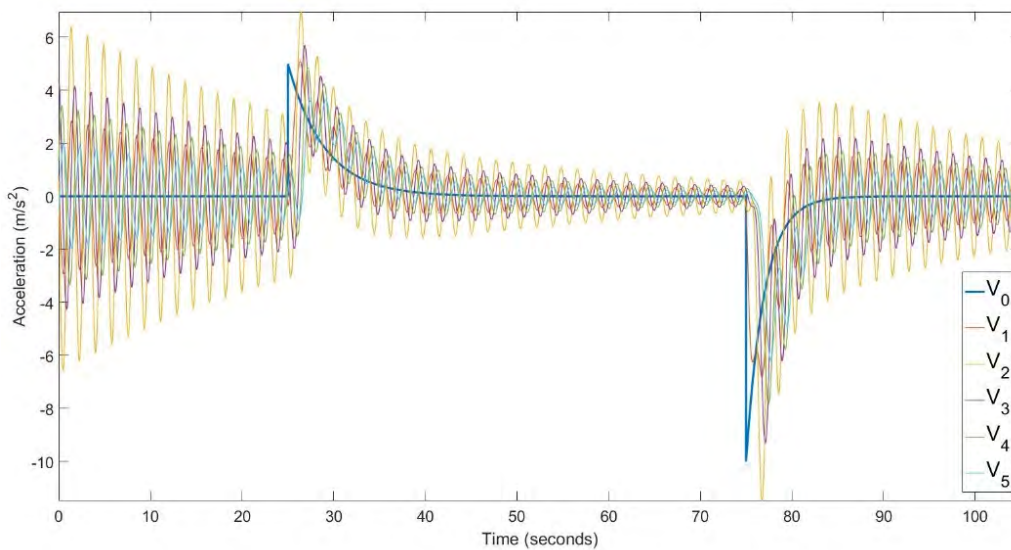
Figure 4-13 - Vehicle 2 with 0.45s Delay Acceleration

The oscillations in vehicle accelerations is very evident in Figure 4-13. This would produce an uncomfortable experience for the occupants of the platoon, as it cannot maintain a steady acceleration, and therefore velocity. Whilst platoon stability can be considered to be maintained, this performance would indicate a failing

stability due to the acceleration oscillations. However, the acceleration oscillations do not drastically affect the velocity and displacement graphs of Figure 4-12 and Figure 4-14.
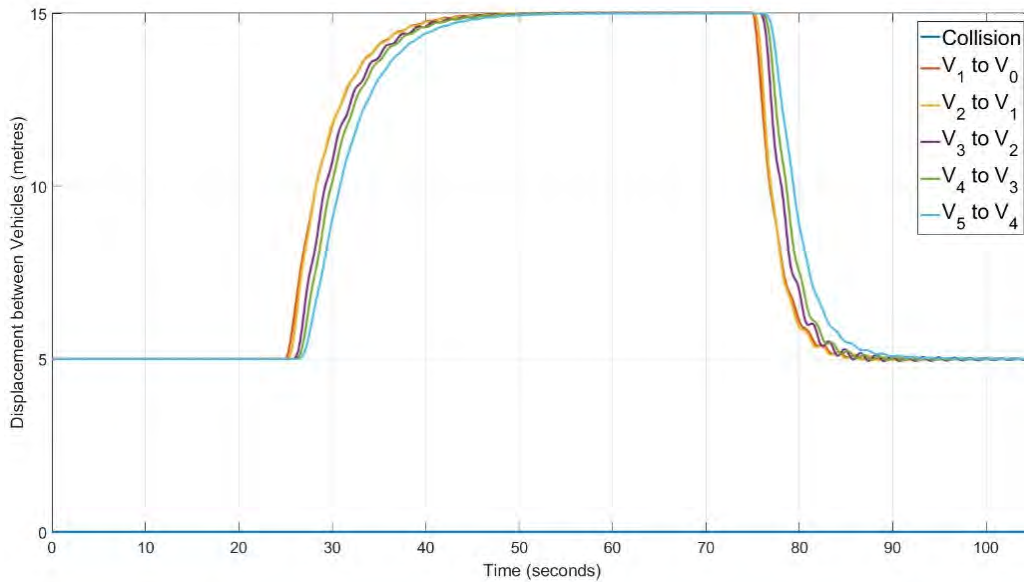
Figure 4-14 - Vehicle 2 with $0.45s$ Delay Separation Displacement

The separation displacement presented in Figure 4-14 does look fairly stable, with only minor oscillations observed at the velocity changes. However, whilst separation displacement has been maintained and therefore platoon stability maintained, the performance of the acceleration in Figure 4-13 demonstrates that this platoon is on the verge of becoming unstable.
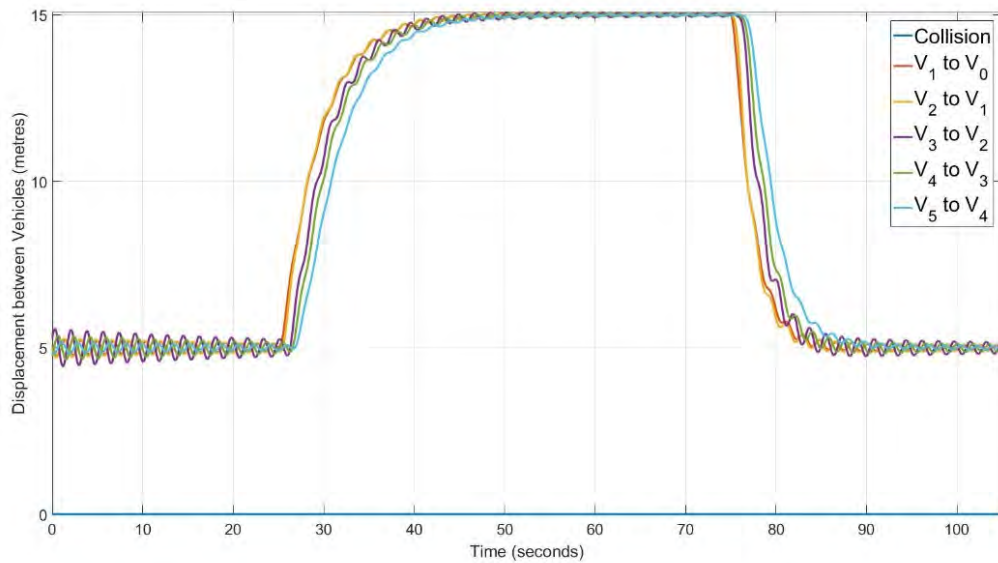
Figure 4-15 – Vehicle 2 with 0.5s Delay Separation Displacement

The separation displacement results, when vehicle 2 has a delay of 0.5s is given in Figure 4-15.

The velocity and acceleration plots exhibited large oscillations, which would be severely uncomfortable for the occupants of those vehicles. This is translated to the separation displacement plot, where even though spacing is maintained, the plots also show oscillations, suggesting an unstable platooning control, for all vehicles, not just V_2. Another observation is that increasing the delay for all other vehicles in the platoon, reduces the maximum delay that can be applied to V_2 before the platoon becomes unstable.

4.3.2.3   Ten Vehicle Platoon with PI Control and Time Delay

As the Asymmetrical control has proven to maintain platoon stability well, more vehicles are simulated, to observe how stability is maintained, and how the effects of delay will affect more vehicles. The maximum time delay applied to all vehicles equally before exponentially increasing oscillations are observed is 0.15s. This is the same maximum time delay as demonstrated in Chapter 4.3.2.2 for a five vehicle platoon.

Repeating the scenario with all vehicles set to time delay of 0.001s, except for 1 vehicle yields the following results. This time, with more platooning vehicles, the

increased delay is applied to V_4, as to better observe how this disruption propagates not only to the following vehicles, but also propagates forwards, to the vehicles ahead. The maximum time delay before platoon instability is observed is $0.4s$, which is $0.05s$ lower than the previous simulation in Section 4.3.2.2. Although only a small difference, this suggests that the larger the platoon, the more vulnerable it is to time delays.
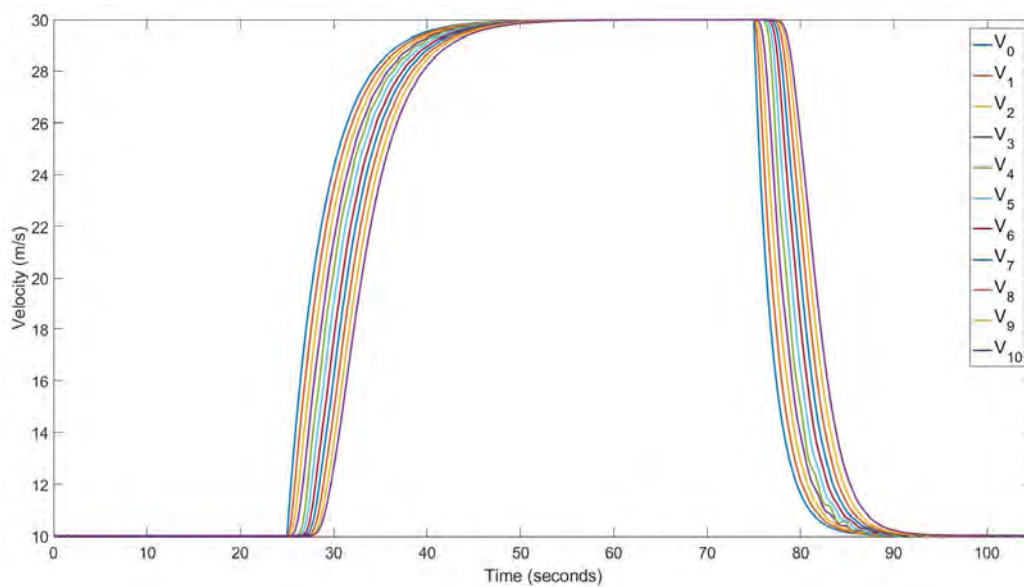
Figure 4-16 - Vehicle 4 with $0.4s$ Delay Velocity

The velocity plot in Figure 4-16 shows that even with the increased delay applied to V_4, the velocity of all vehicles in the platoon maintains stability. Small oscillations are observed, but these can be considered minor and will not de-stabilise the platoon.
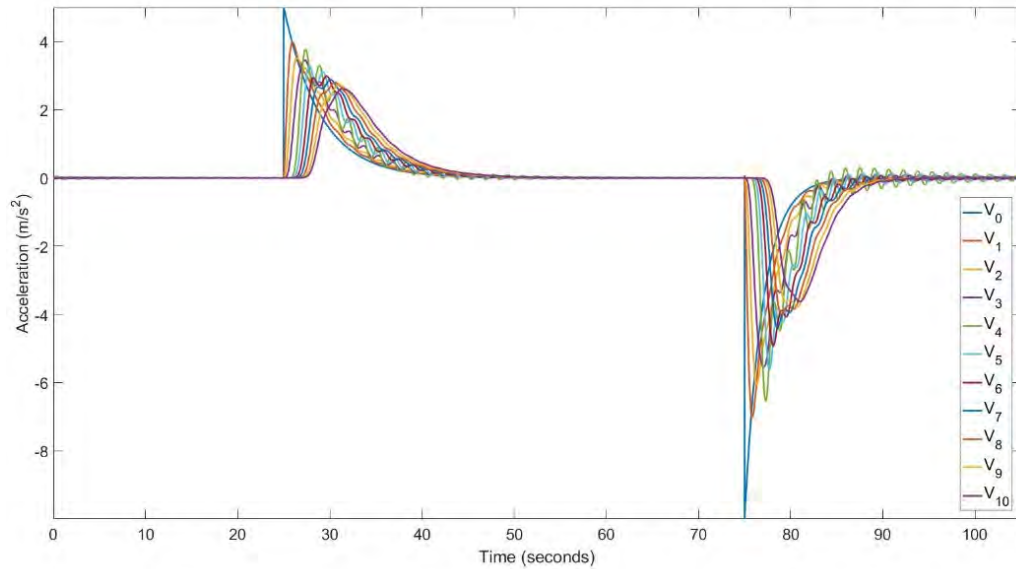
Figure 4-17 - Vehicle 4 with 0.4s Delay Acceleration

The acceleration of the 10 vehicle platoon with delay presented in Figure 4-17 demonstrates a different behaviour. Oscillations are clearly evident for many vehicles in the platoon. Again, this alone is not enough to de-stabilise the platoon, but it is the first sign that stability is reducing.
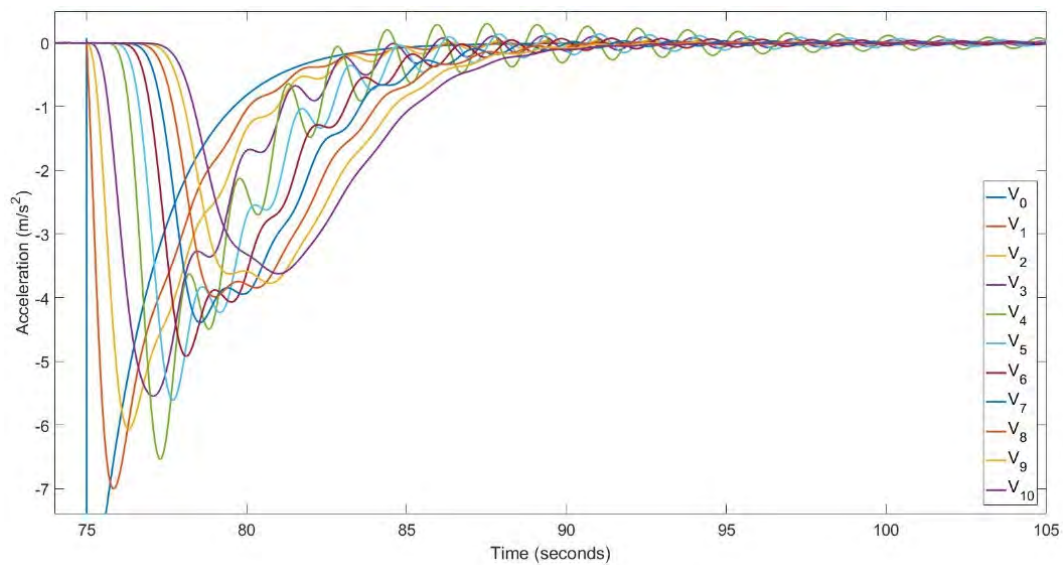
Figure 4-18 - Vehicle 4 with 0.4s Delay Acceleration Magnified

A magnified look at the deceleration in Figure 4-18 demonstrates how the oscillations propagate through the platoon. The delay is caused with V_4, and

oscillations are observed for vehicles 1 to 7. The oscillations of vehicles 8 to 10 are very minor. The oscillations are most severe for V_4, and the vehicles immediately surrounding it. As each vehicle experience the oscillations, it appears that the effects are dampened for the nest vehicle along.
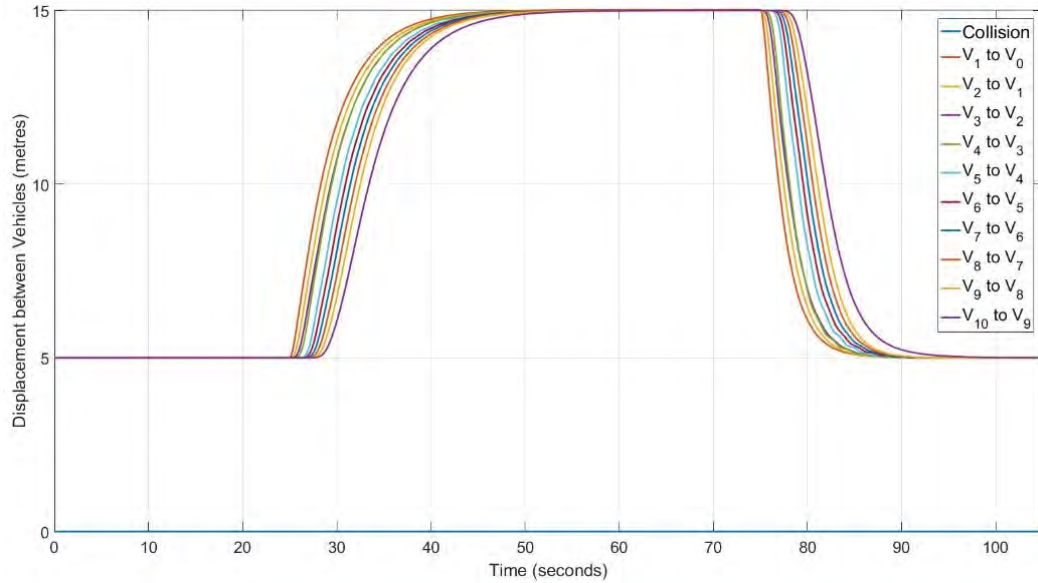
Figure 4-19 - Vehicle 4 with 0.4s Delay Separation Displacement

Figure 4-19 demonstrates that the separation displacement of the entire platoon is maintained.
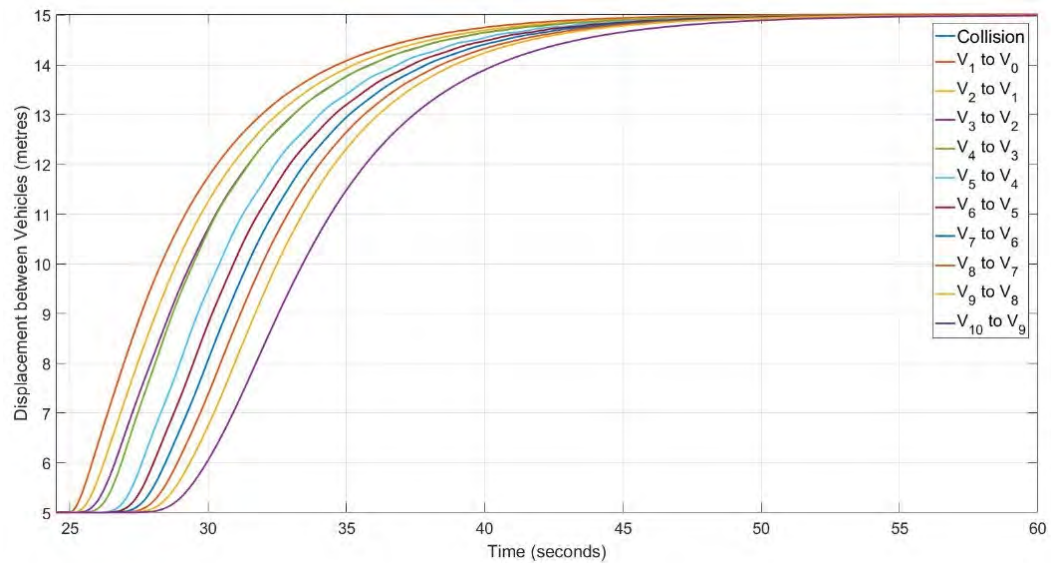
Figure 4-20 - Vehicle 4 with 0.4s Delay Separation Displacement Magnified

Magnifying the separation displacement in Figure 4-19, as given in Figure 4-20, to focus on one velocity change from $10m/s$ to $30m/s$ shows how the behaviour of V_4 differs from the others, at it follows a similar plot to the vehicle in front V_3, however the vehicle behind V_5 has a noticeable space.

The single large delay is then applied to vehicles 2, 6 and 8 separately, to observe when platoon instability occurs. Like V_4, V_6 and V_8 were able to manage a delay of $0.4s$ before destabilising at $0.45s$. Vehicle 2 was able to maintain stability with a delay of up to $0.5s$ before destabilising at $0.55s$. This suggests that the effects of large delays with a single vehicle are better dampened closer to the front of the platoon.

4.4 Conclusions

Autonomous highway platooning systems developed by Cook (2007) were modelled and tested to demonstrate that an autonomous system can be forced beyond its limits and result in vehicle collisions. A bidirectional controller was developed and tested, but the separation displacement proved difficult to control when treating the input velocities of the vehicles ahead the same as the vehicles behind. An asymmetrical control was developed from the bidirectional controller, but this time managing the information from the vehicle behind differently to the information from the vehicle in front. This proved better at maintaining steady velocities and accelerations. The added benefit of the introduced PI controller was the velocity dependent spacing. The asymmetrical platoon proved to maintain stability, even when controlling 10 vehicles.

One of the influential factors capable of destabilising the platoon control was delays to the processing of the information. With a large enough delay, a single vehicle proved capable of destabilising the platoon. Each of the systems developed could result in platoon instability, which would mean that the autonomously driven vehicles can possibly collide into one another.

All of the highway platooning methods investigated by Bergenhem et al. (2012) state the importance of utilising V2V communication. With V2V communication it would be possible to network all platooning vehicles, and have control over all vehicles operating as one platoon, as opposed to each vehicle

controlling itself. Networking has not been investigated, as the platooning model proposed by Cook (2007) can theoretically operate without V2V.

Predictive control could be applied, as this could help mitigate the overshoots and oscillations of the following vehicles when the lead vehicle's velocity changes. The PI control was capable of controlling the accelerations and spacing distances of the vehicles until a large enough delay was simulated. Model Predictive Control (MPC) models a dynamic system to predict future states, which in this application would be the dynamics of the other platooning vehicles. MPC therefore has the potential to better control the vehicle spacing by predicting the changes in velocity. However, the demonstrated PI control was sufficient to make initial observations which inform later chapters. The following chapters look at controlling just one vehicle, and so the introduction of MPC for controlling multiple vehicles will need to be addressed in future research problems. This raises the question as to whether V2V communication is needed to provide accurate inputs to these models, from the vehicles in the platoon which are being modelled, or if an average vehicle model can be used to represent all vehicles. With V2V assumed to be unavailable, an average vehicle model would be the only possibility, but the accuracy of this model to represent the longitudinal vehicle dynamics of any vehicle in the platoon must be tested.

It is the nature of engineers to develop and test, so these limitations can be assessed and prevented from occurring. However, these simulations show that further safety systems are required to be developed with autonomous vehicles, as assuming they cannot crash would be naïve, especially in motorway scenarios where the vehicle speeds are high.

Chapter 5

Steering Controller

5.1 Introduction

The aim of this research project is to evaluate the possibility of a vehicle steering itself to a safer outcome when facing an imminent collision. In this chapter development of a steering controller is presented and used to evaluate the possibility that an autonomous car can steer itself to complete a lane-change manoeuvre. The development of a steering controller is not new, but it has to be analysed as the characteristics of the steering controller may influence the possible actions the vehicle can take in certain emergency situations.

The aim of this chapter is to develop a method for planning a lane-change manoeuvre, which could be employed to steer a vehicle for collision avoidance. The trajectory planning is tested by use of a kinematic bicycle model steering controller. A combined steering and braking controller is also evaluated.

The investigation is based on a kinematic bicycle model. The kinematic bicycle model is used when discussing vehicle dynamics. Kinematic models are robust in estimating vehicle states geometrically which will be used to determine if a vehicle has accomplished a steering manoeuvre. A required longitudinal distance to complete the manoeuvre and required lateral distance to avoid the hazard ahead, are used to analyse it. Vehicle limitations need to be evaluated, to ensure that such a manoeuvre can be completed without a loss in vehicle control. The steering controller evaluates a required distance to complete the lane-change, and this is compared with an average braking stopping distance. Tyre saturation properties are evaluated, and the controller is simulated to assess the performance. The steering controller is further developed to combine the steering and braking control.

5.2 Bicycle Model

The Bicycle model is a common steering model. It assumes an average steering angle for the front wheels, and can therefore be assumed to be one wheel. Milliken and Milliken (1995) described the model which had 2 degrees of freedom, lateral velocity and yaw rate. The Ackermann Steering Angle (radians) is given by Milliken and Milliken (1996) in Equation (5-1).

$$\delta_{rad} = \frac{l}{R} \qquad\qquad (5\text{-}1)$$

where l is the vehicle's wheelbase length (m), and R is the turning radius (m).

The Ackermann steering angle is a geometric calculation, and so it is limited in its application. Blundell and Harty (2004) state that the geometric steering behaviour for passenger vehicles is limited to speeds up to 15mph. The Ackermann steering angle does not account for tyre dynamics. The Ackermann angle assumes the car will travel in the direction the wheels are pointing, which at speeds of 15mph and higher does not necessarily occur due to the behaviour of pneumatic tyres. It is important to note that this research project is not developing a new steering controller. A simplistic kinematic steering controller which relies on the Ackermann angle calculations is used to test the trajectory planner.

An issue considered by simple steering controllers is the effect that velocity has on the steering effect. At lower velocities, the vehicle will turn as predicted, but

as speed increases the turning radius also increases. This is represented by a 2-degree-of-freedom steering model, the 2 degrees being lateral and longitudinal velocity, which by integrating give lateral and longitudinal positions.

The model formed by Equations (5-2) and (5-3) is informed by a model constructed by Compere (2016). This model has 3 inputs: Forward Velocity, Wheelbase Length and Steering Angle. The velocities are calculated by the following kinematic model:

$$v_x = [v.\cos(\psi_{heading}) - \left(\frac{l}{2}\right).\dot{\psi}.\sin(\psi_{heading}))] \tag{5-2}$$

$$v_y = [v.\sin(\psi_{heading}) + \left(\frac{l}{2}\right).\dot{\psi}.\cos(\psi_{heading}))] \tag{5-3}$$

where v is forward velocity (m/s), $\dot{\psi}$ is yaw rate (rad/s), $\psi_{heading}$ is yaw angle (rad), v_x is velocity in x direction (m/s), and v_y is velocity in y direction (m/s). For these simulations the wheelbase length is set to $2.6m$.

The author of this thesis uses the 2D terrain frame model of Compere (2016) which is used to provide an image of vehicle trajectory in which the issue of velocity is evident. This model was simulated with a fixed velocity value, and plots the x and y coordinates of a vehicle with several different steer angles. The steer angles increased incrementally by $0.001 rad$. This simulation was limited to a maximum yaw rate of $100°/s$ ($1.7453 rad/s$). This was selected due to it being far greater than the expected yaw rate capabilities of ground vehicles and it demonstrated the limitations of what steer angles were achievable. This value is validated by the yaw rate simulations in Section 5.3.
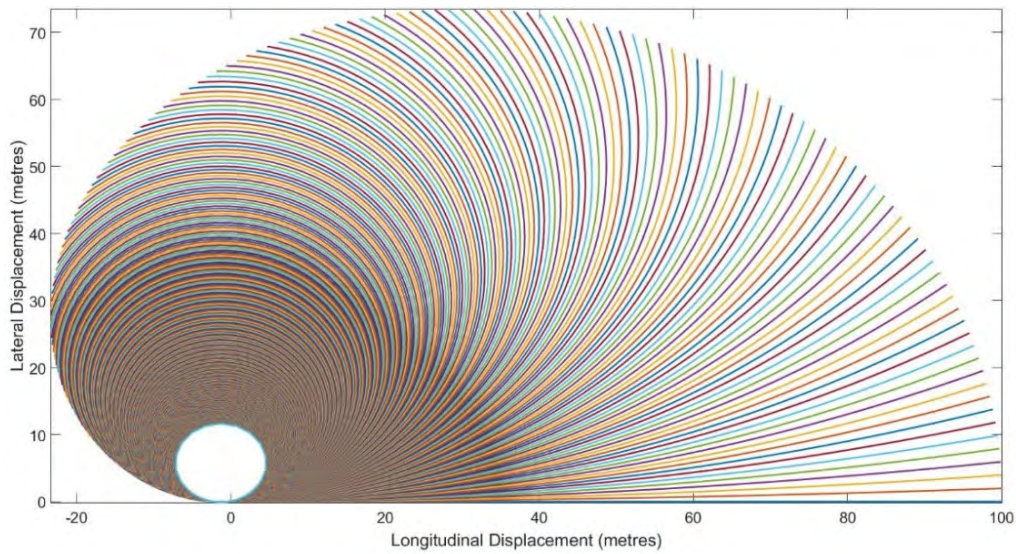
Figure 5-1 - Simulated Vehicle Trajectories at 10m/s
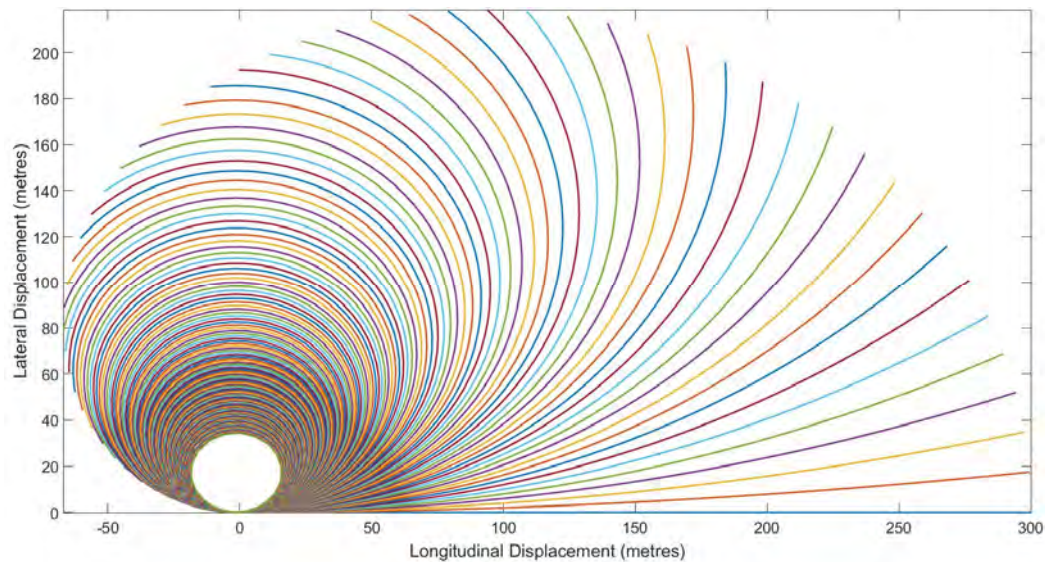
Figure 5-2 - Simulated Vehicle Trajectories at 30m/s

The plots in Figure 5-1 and Figure 5-2 represent a vehicle's trajectory for different steering angles. Both figures represent a constant velocity, and it is observed that at lower speeds the vehicle can achieve many steering angles, more plots are presented on Figure 5-1 at $10m/s$ than on Figure 5-2 at $30m/s$. Also, the smallest radius turn of the $10m/s$ plot achieves a radius of $10m$, whilst the $30m/s$ plot has a minimum radius of $30m$. These values are limited by a yaw rate limiter. The yaw rates of the velocities show that without limitations the values are

82

unrealistic, so the importance of limiting the capabilities of the vehicles steering with respect to yaw are necessary.

Table 5-1 demonstrates the maximum steering angles that can be achieved at certain velocities.

Table 5-1 - Maximum Steering Angles to Achieve Limited Yaw Rate Value

Velocity (m/s)	Steering Angle ($radians$)	Steering Angle ($degrees$)
10	0.453	25.955
20	0.226	12.949
30	0.151	8.6517

The higher the velocity, the lower the required steering angle to achieve a desired Yaw Rate. However, the trajectory plots (Figure 5-1 and Figure 5-2) show that the radius of the turn increases with velocity. Velocity has a significant influence over a vehicle's ability to turn.

5.3 Vehicle Yaw Rate

5.3.1 Calculation of Vehicle Yaw Rate

Some of the values for steering angle in Figure 5-2 seem to be unrealistic, as a vehicle would be unable to achieve such a high steering angle at high speed without losing control. Further investigation was required, which the work of Blundell and Harty (2004) provided. When a car turns it is limited by many factors, one being yaw rate. Blundell and Harty (2004) gave two equations which calculated the maximum possible yaw rate. The first is the geometric yaw rate, which is the maximum yaw rate of a vehicle due to the steering geometry, described by Equation (5-4).

$$\dot{\psi}_{geom} = \frac{v.\delta}{l}$$
(5-4)

δ is the average steering angle, which calculated from Ackermann steering geometries is $\frac{(\delta_{inner} + \delta_{outer})}{2}$.

The second yaw rate equation is limited by friction, and is given by Equation (5-5).

$$\dot{\psi}_{friction} = \frac{\mu.g}{v} \tag{5-5}$$

where μ is the coefficient of friction, and g is acceleration due to gravity ($9.81 m/s^2$). The example in Blundell and Harty (2004) gave the coefficient of friction μ as 0.9. Jones and Childers (2001) give examples of coefficients of friction between a tyre and the road. For a dry road a μ value of 0.7 to 0.9 was reported, depending on the tyre. For a wet road this μ value reduces to 0.4. This value reduces further for ice conditions. To demonstrate the steering manoeuvre, the highest value of 0.9 is used. This gives the greatest potential for the manoeuvre to be completed. Simulation of 4 different steering angles is presented in Figure 5-3.
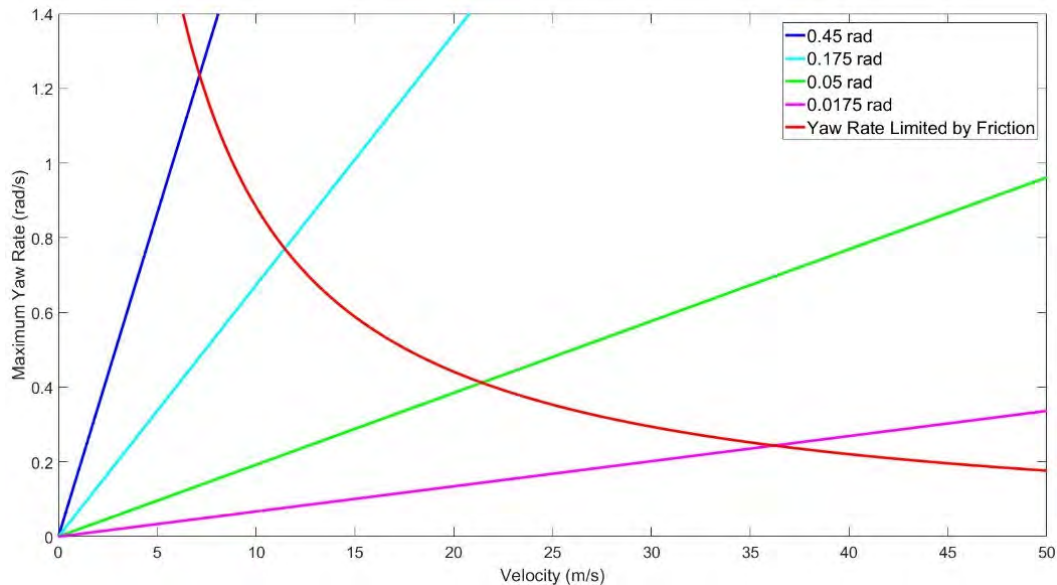
Figure 5-3 - Maximum Yaw Rates of Differing Steering Angles vs Velocity

Figure 5-3 is the yaw limitation described by Blundell and Harty (2004), which plots the maximum yaw rates described by Equations (5-4) and (5-5). It is noticed that all 4 steering angle plots meet the same friction limit. The maximum yaw rate achieved for a given steering angle at a given velocity is where the two yaw limiting plots meet. The trend of these plots is that the higher the steer angle the higher the maximum yaw rate, the maximum yaw rate is higher at lower velocities. Table 5-2 summarises the main findings presented in Figure 5-3, i.e. the velocity at which the maximum yaw rate is achieved with the 4 steering angles considered.

Table 5-2 - Maximum Yaw Rates and Velocities of Steering Angles

Steer Angle (rad)	Maximum Yaw Rate (rad/s)	Velocity (m/s)
0.45	1.2375	7.15
0.175	0.77135	11.46
0.05	0.41212	21.43
0.0175	0.24379	36.22

This yaw limitation model is now modified, in line with the model in Section 5.2, as a novel approach to limit yaw rate with respect to steer angle not velocity. This model is modified to have a fixed velocity and varying steer angle, which produces the results displayed in Table 5-3.

Table 5-3 - Maximum Yaw Rates and Velocities of Steering Angles

Velocity (m/s)	Maximum Yaw Rate (rad/s)	Steering Angle (rad)
10	0.88462	0.229
20	0.44615	0.057
30	0.3	0.025
40	0.23077	0.014

Table 5-3 gives the maximum yaw rates and steering angles of the velocities that can be achieved with 4 fixed velocities. Comparing these 4 plots graphically can be done using Figure 5-4.
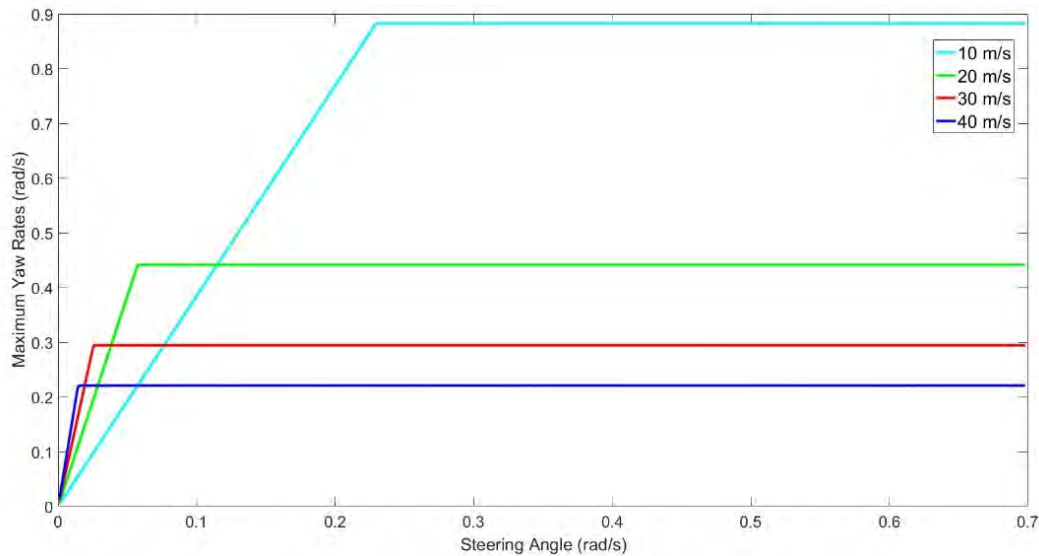
Figure 5-4 - Maximum Yaw Rates of Differing Steering Angles vs Steering Angle

The benefit of the plot in Figure 5-4 is that it gives a fixed steering angle once the maximum yaw rate limited by friction is reached. This is the point where the maximum steering angle is, so the steering controller can be limited to calculate steer angles up to this point. Increasing the steer angle beyond this maximum yaw rate will not provide a greater yaw rate and so will not provide an increased turning rate. It is at this point that the vehicle will begin to lose steering ability, referred to as a loss in grip. Here the vehicle stability characteristics of understeer and oversteer, discussed in Section 2.3.2 are experienced. The steering controller proposed in this chapter intends to avoid these stability characteristics, and maintain neutral steer.

The maximum yaw rate simulated was $0.88462 rad/s$ at $10 m/s$. This equates to $50.682°/s$, so the maximum yaw rate previously used of $100°/s$ was a significant over-estimation.

5.3.2 Steering Control with Yaw Limiter relative to Velocity

With the new yaw limitation model inspired by Blundell and Harty (2004) providing a limit to the yaw capabilities of a vehicle, and from that the limit of the maximum steering angle before a loss in traction with the road is experienced, a new model calculating vehicle trajectories is created. The model introduced in this chapter works as the previous heading angle calculation, but with a maximum yaw rate based on the vehicle limitations in the yaw model.

By limiting the maximum yaw rate of a vehicle at the simulated velocities the maximum steering angle is also limited, which limits the possible vehicle trajectories as presented in Figure 5-5.
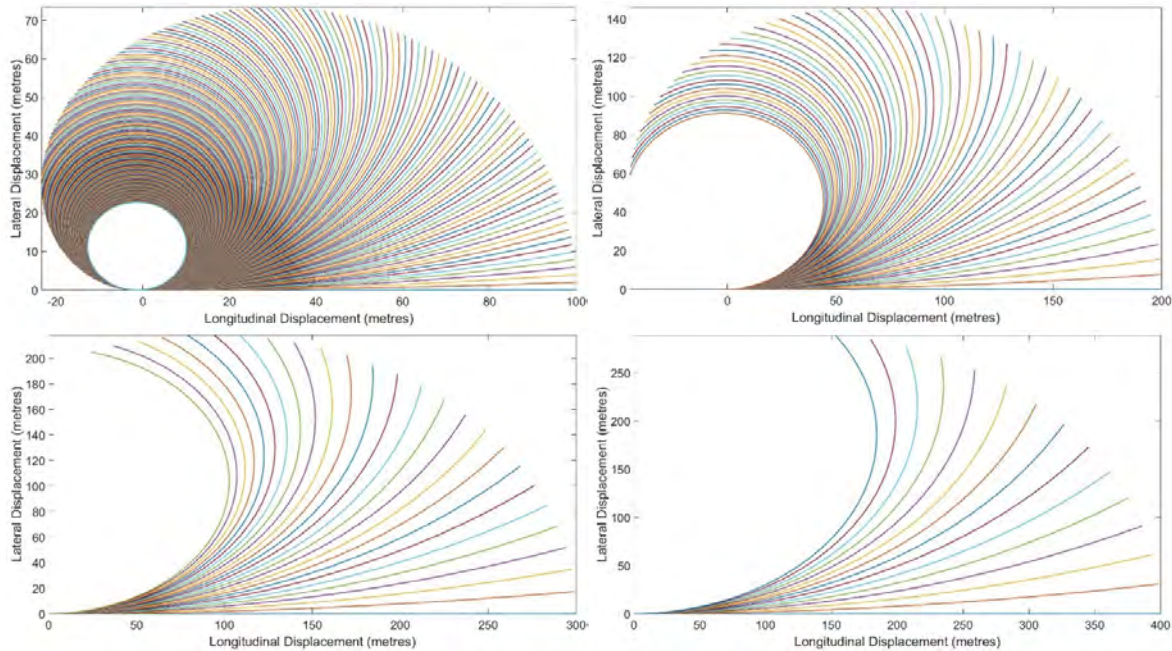
Figure 5-5 - Simulated Vehicle Trajectories with Limitations in Yaw Rate

Top Left Velocity 10m/s, Top Right Velocity 20m/s, Bottom Left Velocity 30m/s, Bottom Right Velocity 40m/s

5.4 Desired Trajectory

A desired trajectory or path has to be determined. For this a sinusoidal curve is created. This requires only an x and y value, or a longitudinal and lateral displacement. The longitudinal displacement refers to how much distance is required to make the manoeuvre. The lateral displacement refers to how much the car needs to turn. The benefit of a sinusoidal curve is that the vehicle can finish the manoeuvre in a parallel heading to where it began. This is a very useful feature, especially if the road is straight and the vehicle needs to be heading in the same direction to all other road traffic.

The sinusoidal shape is created by an S-function which has the ability to add longitudinal distance, without lateral distance. For a longitudinal displacement of $10m$, and lateral displacement also at $10m$, the S-function is demonstrated in Figure 5-6. The S-function begins at $0.5m$ longitudinal distance, and ends with a given

87

safety displacement of 10%. This means the vehicle will reach its lateral displacement with 10% of the longitudinal displacement still to drive. This can be adjusted, but is introduced in the model to ensure the vehicle is on the correct lateral displacement with no steering input at the final stages of the manoeuvre, in case a corrective steer input is required.
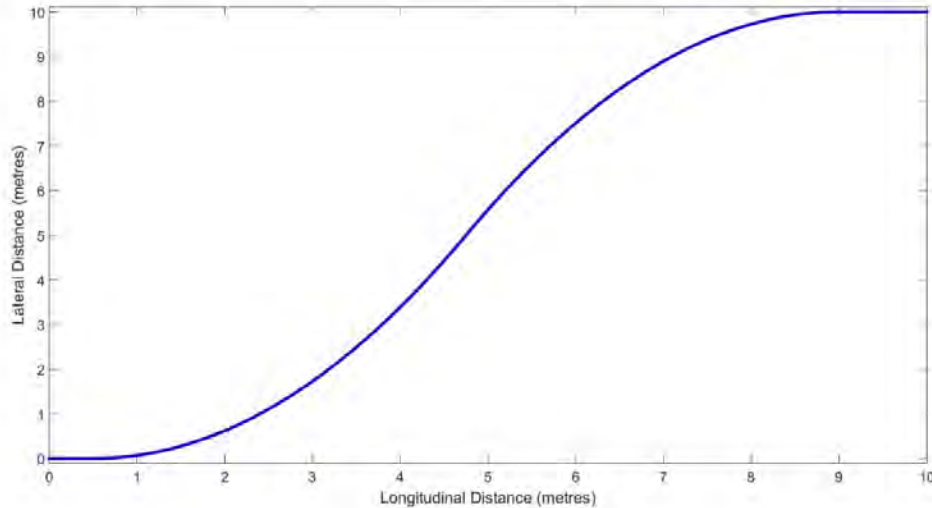
Figure 5-6 - Vehicle Trajectory - Longitudinal Displacement 10m, Lateral Displacement 10m

The kinematic steering controller needs an input of either steering angle or yaw rate. As yaw rate is a limiting factor of how fast a car can turn, this will be calculated from the desired vehicle course. Using an equation proposed by Houenou et al. (2013), Equation (5-6) can calculate the required yaw rate:

$$\dot{\psi} = \gamma . v \tag{5-6}$$

where $\dot{\psi}$ is the yaw rate, γ is the curvature of radius and v is the vehicle's velocity.

As the x and y displacement values of the planned course are given parametrically, the radius (R) of the turns, and the curvature of radius (γ) will also be calculated parametrically using Equations (5-7) and (5-8), given in Mathworld.Wolfram.com (2016).

$$R = \frac{(x'^2 + y'^2)^{3/2}}{|x'.y'' - y'.x''|} \tag{5-7}$$

$$\gamma = \frac{1}{R} \qquad (5\text{-}8)$$

where $x' = \frac{dx}{dt}, y' = \frac{dx}{dt}, x'' = \frac{d^2x}{dt^2}, y'' = \frac{d^2y}{dt^2}$

Using Equations (5-6), (5-7), and (5-8) the necessary yaw rate to complete the manoeuvre is calculated. The Longitudinal displacement is set as not to require a yaw rate higher than the maximum yaw rate calculated for the given speed.

Leics.gov.uk (2016) gives the minimum width of a carriageway lane (dual carriageways and motorways) as $3.7m$. This is supported by the Federal Highway Administration for the U.S. Department of Transportation (2014) giving a Freeway lane width of $3.6m$. For the simplicity of demonstrating a lateral manoeuvre, this lateral distance will be rounded up to $4m$, as even a slight increase in lateral distance will require a higher yaw rate, which is the limiting factor. This will ensure that the vehicle can make a single lane change manoeuvre.

5.5 Kinematic Steering Controller

5.5.1 Model of Kinematic Steering Controller

Now that the necessary yaw rate $(\dot{\psi})$ has been calculated, the required steering angle (δ) is calculated by rearranging equations from Rajamani (2011):

$$\dot{\psi} = \frac{v}{R} \qquad R = \frac{l}{\delta} \qquad (5\text{-}9)$$

$$\dot{\psi} \cong \frac{v\delta}{l} \qquad (5\text{-}10)$$

$$\delta \cong \frac{\dot{\psi}}{v/l} \qquad (5\text{-}11)$$

where l is the vehicle's wheelbase length.

For these calculations, the steering angle is a calculated approximation due to the lack of slip angle (β) available. Therefore β is assumed to be zero and not included in these calculations. β would assume small slip angles, and so would not drastically change the steering angle.

This steering angle signal is now simulated using the model formed by Equations (5-2) and (5-3), as represented in Figure 5-7 and Figure 5-8.
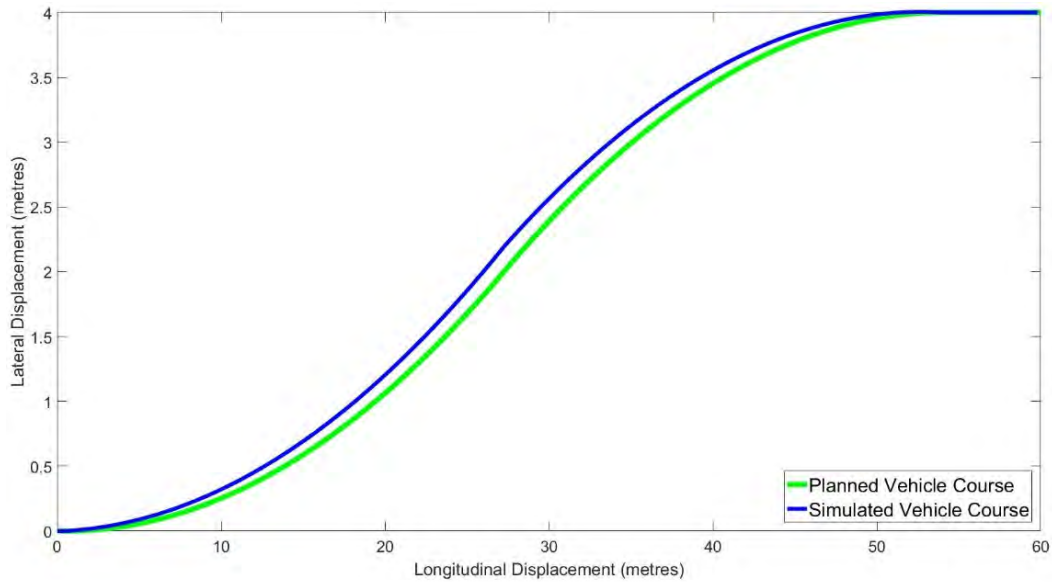
Figure 5-7 – Four metres Lateral Movement at 40m/s Simulation
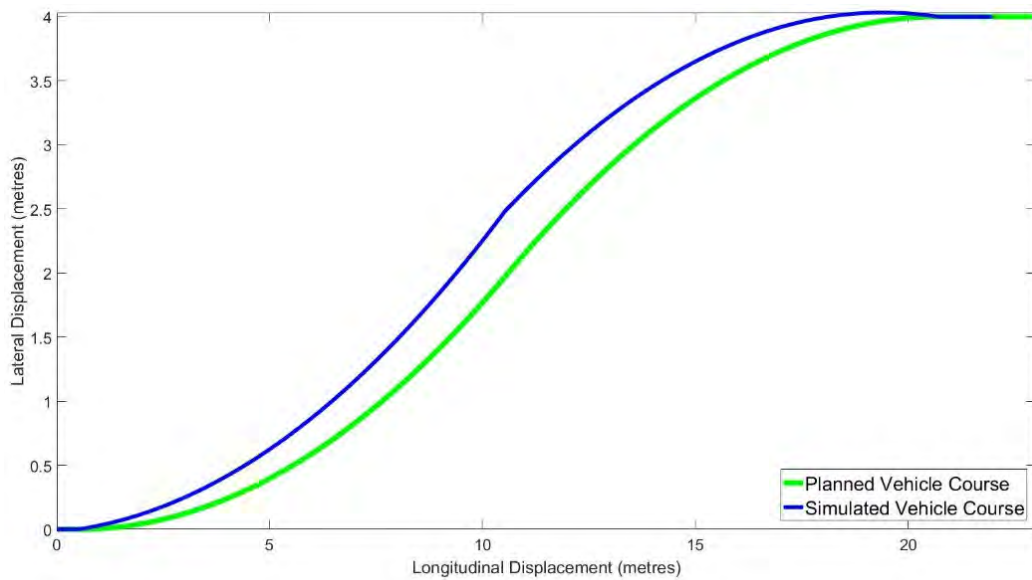
Figure 5-8 – Four metres Lateral Movement at 15m/s Simulation

One can conclude that the inputted steering angle can follow the planned vehicle course. It does not follow the planned trajectory exactly, and at lower speeds there is an evidence of overshoot as the simulation runs wider than 4m, but the simulated trajectory follows the planned trajectory when the steering input is zero.

The final position of the vehicle is as intended. The simulations show that with a small lateral displacement to achieve, and the behaviour of the vehicle kept in the linear region by limiting the maximum yaw rate, the autonomous steering controller can steer a vehicle to an intended final position.

5.5.2 Feedback with PI Controller

To aid with the path tracking, a feedback controller is analysed in this research. It will adjust the input steering angle relative to a calculated error. This is a similar kinematic method that Lee et al. (2013) employed, but here will not estimate slip angle. The input to the steering manoeuvre is the steering angle, which was calculated by a desired yaw rate. The steering angle error will need to be calculated from the simulated vehicle's lateral acceleration. On a real vehicle, acceleration would be measured using an accelerometer, but for the simulation this needs to be simulated using the derivative of the lateral velocity result. Using the following equation given in Shah et al. (2015), a yaw rate calculated from the trajectory simulation is also achieved.

$$\dot{\psi} = \frac{a_y}{v} \tag{5-12}$$

This yaw rate is then equated to steering angle using Equation (5-11). The resulting simulated steering angle is used to determine the error compared with the desired steering angle input. This steering angle error is then controlled via a PI controller. Simulation shows that with velocity dependant values for the PI controller, the kinematic steering controller tracks the planned vehicle course very closely.
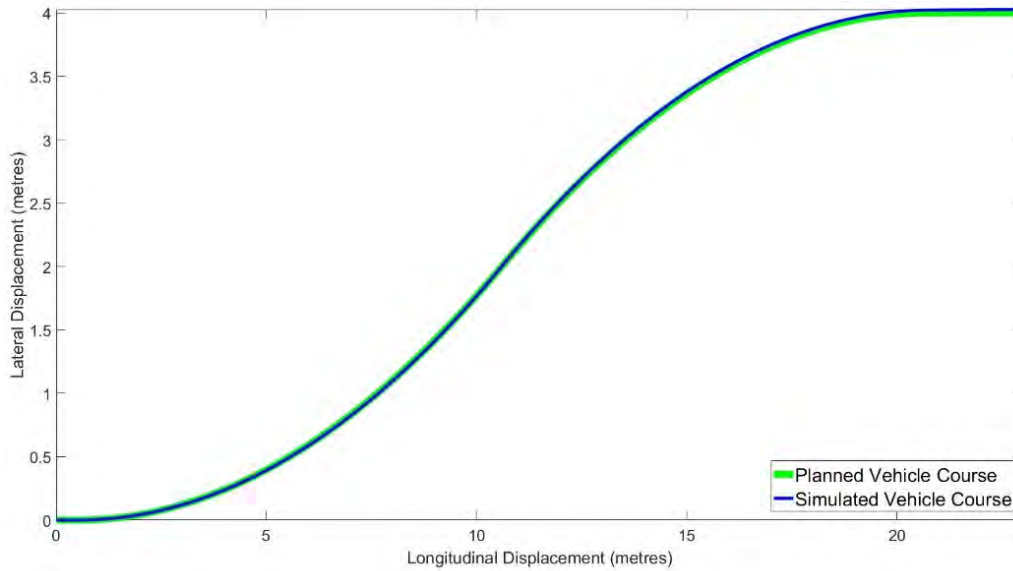
Figure 5-9 – Four metres Lateral Movement at 15m/s Simulation with PI Controller
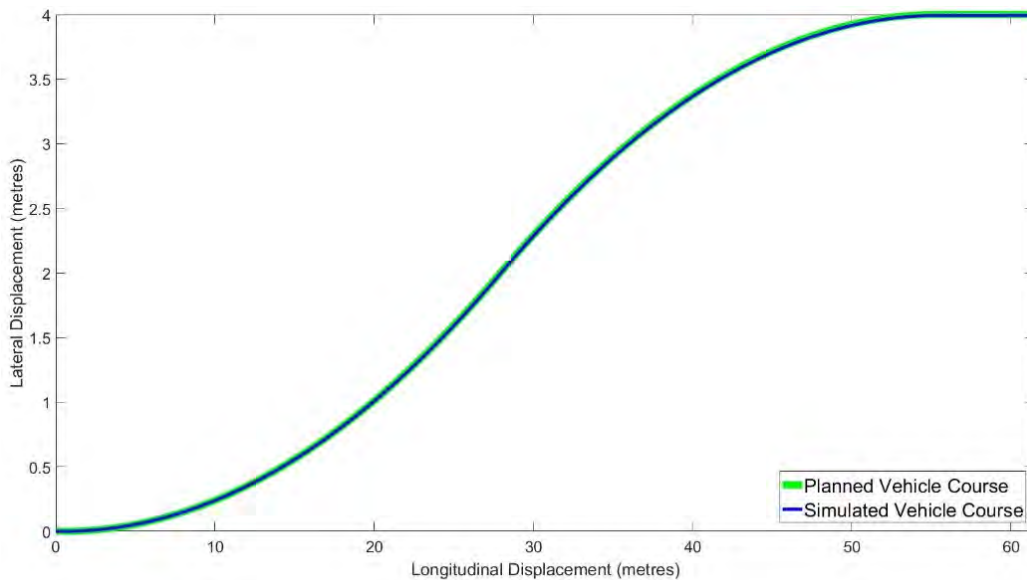
Figure 5-10 – Four metres Lateral Movement at 40m/s Simulation with PI Controller

Figure 5-9 and Figure 5-10 demonstrate the simulated trajectory of the kinematic steering controller tracking the planned course very closely. A Closer inspection shows that with velocity dependent PI variables, the controller can track the path with less than a $0.01m$ error. The feedback helps to minimise the limitations of relying on kinematic control alone without more complex dynamic inputs. Due to the effectiveness of PI control, it is unnecessary to introduce a PID control, as this requires extensive tuning to achieve even a minimal improvement in tracking performance.

PID control is explained by Asif and Webb (2015), "*It is a generic controlled loop feedback controller. In PID P (Proportional) determined by present error in the system, I (Integral) is the accumulation of past error and D (Derivative) is the prediction for future error.*" It is also explained that a PID controller can use just P with I, or P with D, or even just the individual P, I or D based on the requirements of the system to be controlled. It is a simple design for a controller, but is widely relied upon due to its "*Robustness, performance, stability and noise/disturbance rejection are some of the advantages of using PID controller.*" It also only requires slight adjustments to improve the system performance.

It might be worth mentioning that Model Predictive Control (MPC) has been applied to steering controllers by Falcone et al. (2008) and Falcone et al. (2007). MPC has the benefit of predicting future events and making control adjustments as required, and so would benefit a steering controller to maintaining accurate tracking of the desired trajectory. However, Asif and Webb (2015) describe stability, model uncertainty and limited variations of model as disadvantages for MPC. It is important to note that this research programme does not involve developing a new steering controller but testing the trajectory planning for deciding if a lane-change manoeuvre is possible or not. It is the robustness and stability of PID controllers described by Asif and Webb (2015) are what is needed to test the trajectory. Therefore, as the simulation results showed, the PI control will be sufficient to test this.

5.6 Effectiveness of Steering Manoeuvre

This steering controller of Section 5.5 simulates a lane change manoeuvre. It needs to be investigated whether a steering manoeuvre will reduce the risk of collision compared to a braking only manoeuvre. A braking only manoeuvre means the vehicle will apply full braking force and remain driving in a straight line, possibly towards the hazard.

5.6.1 Braking Distances

Braking distances includes a complex calculation because brakes do not behave linearly. For simplicity the best performance scenario is assumed:

- Assume that full braking force is applied,
- Assume there is no wheel slip or need for Anti-lock Braking System (ABS).

The calculation of braking distance in the Bosch Automotive Handbook (2014) gives the following equation:

$$s = \frac{u^2 + v^2}{2a} \qquad\qquad (5\text{-}13)$$

Where s is stopping distance (m), u is initial velocity (m/s), v is final velocity (m/s), and a is deceleration (m/s^2) For this calculation the deceleration is assumed to be constant and equal to $10.75 m/s^2$, as discussed in Section 4.2, using Equation (4-1). This is of course a static equation, and does not consider the resistance forces acting on the vehicle. Equation (5-13) is used as a guide. The braking value in Section 4.2 is an average value calculated from a real stopping distance test.

5.6.2 Steering Manoeuvre Distances

As presented in Section 5.3.2, four velocities are simulated to determine the maximum yaw rate. These yaw rates are then used as the limiting factor when simulating those velocities again in the model in Section 5.4. The maximum longitudinal distances are simulated to the nearest $0.5m$ for the steering manoeuvre, and compared against the braking only stopping distances as tested using Equation (5-13). The results are given in Table 5-4.

Table 5-4 - Steering Manoeuvre Distances

Velocity (m/s)	Yaw Rate (rad/s)	Distance to End of Manoeuvre (m)	Stopping Distance Braking only (m)
10	0.88462	16	4.65
15	0.59423	23	10.47
20	0.44615	31	18.6
25	0.35577	38.5	29.07
30	0.3	46	41.86
35	0.25577	54	56.98
40	0.23077	61.5	74.42
45	0.20769	69	94.19

The results in Table 5-4 show that a braking only manoeuvre results in a shorter stopping distance, than the distance required to complete a steering manoeuvre for velocities of $30m/s$ and lower. However, from $35m/s$ and higher, the steering manoeuvre is completed before the braking manoeuvre. These results are represented graphically in Figure 5-11.
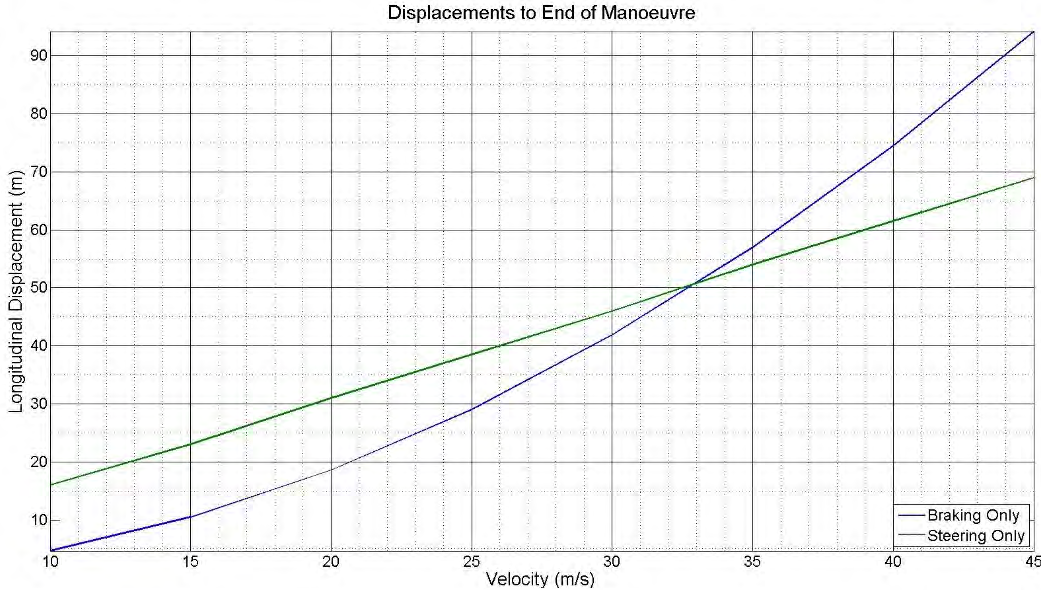
Figure 5-11 - Comparison of Displacement to End of Manoeuvre

Figure 5-11 demonstrates that up to approximately $33m/s$ ($118.8km/h$ or $73.8mph$) a braking only manoeuvre will result in the shorter displacement compared to end of manoeuvre. However, this assumes a perfect braking performance and after this point the steering manoeuvre will accomplish the task of avoiding the object by performing a single lane change manoeuvre. The best avoiding manoeuvre for slower speeds is braking, whilst at higher speeds it is steering that provides the better avoiding manoeuvre, is a conclusion shared with Jansson (2005).

This displacement to end of manoeuvre also gives a 10% safety factor, which is that the lateral distance must be accomplished with 10% of the available longitudinal left, and does not account for a loss in speed due to tyre scrub or braking. The displacement to end of manoeuvre may be further improved if a reducing velocity is simulated. Combining a steering manoeuvre with braking force may result in an even shorter displacement, with the benefit of a steering manoeuvre being evident at velocities lower than $33m/s$. This is however a more complex simulation, as the saturation properties of the tyres needs to be considered.

However, this comparison has demonstrated the need for a steering controller as it has the potential to improve upon the reliance of automatic emergency braking systems giving more and potentially safer options for collision avoidance and mitigation. Torque vectoring and brake assist steer would increase the maximum possible yaw rates, which would allow for faster turns and hence a shorter displacement.

5.6.3 Discussion

The model developed is an analytical kinematic steering controller, using equations of motion which are based on the linear behaviour of vehicle dynamics and PI controlled feedback. The limiting yaw rate aims to keep the vehicle behaviour in the linear region, which suits the limitations of a kinematic model as not to require the use of dynamic modelling techniques.

Further research would include development of a dynamic steering controller. This would require more input parameters such as mass (kg), yaw moment of inertia (kg.m^2), and tyre cornering stiffness (N/deg). From these parameters tyre lateral forces and slip angles are used to calculate the desired outcomes. However, introducing these parameters comes with an additional complexity. It is most evident

with the tyre cornering stiffness. Tyres do not always behave in a linear manner, but would for simplicity need to be assumed as linear. Gillespie (1992) describes cornering stiffness as the negative lateral force rate of change with respect to change in slip angle, which is usually evaluated at a slip angle of zero. This relationship between lateral force and slip angle is linear at low slip angles. The tyres for a typical passenger car begin to behave in a non-linear manner at sideslip angles of 4° ($0.07 rad$), and fully saturate at 8° to 10° ($0.14 rad$ to $0.17 rad$) as given by Abe (2009). Therefore, a dynamics model would rely heavily on non-linear parameters making the model itself non-linear and complex.

For real world applications a dynamic model would be better suited, but for the purposes of demonstrating the requirements of an autonomous steering controller the 2 Degrees of Freedom (DOF) kinematic model is sufficient. A kinematic steering controller is also concluded to be accurate to a point, namely the linear region of vehicle handling dynamics, appropriately limiting with maintaining the maximum yaw rate.

5.7 Steering and Braking Manoeuvre

The steering controller described in Section 5.5 completes a lane change manoeuvre whilst maintaining the set speed. The potential for improving safety further is to combine a steering and braking controller. The aim of this is to avoid or mitigate a collision. The final velocity of the steering manoeuvre will be evaluated.

5.7.1 Determine Braking Force

As the steering manoeuvre is the main manoeuvre taking place, it must be completed. A 'g-g' diagram is used as the braking controller. The inspiration for this is taken from Kritayakirana and Gerdes (2012) who used a 'g-g' diagram for a racing controller. The principle is that the overall g-force exerted on the car cannot exceed a set value.

Calculating Lateral Acceleration using the 'g-g' principle is given by Rajamani (2011), in Equation (5-14).

$$a_y = \ddot{y} + v_x\dot{\psi} \tag{5-14}$$

Assuming a unit circle for the maximum lateral $a_{y.max}$ and longitudinal $a_{x.max}$ accelerations (and decelerations), the resultant braking after steering can be determined by Pythagorean Theorem:

$$a_x = \sqrt{a_{max}^2 - a_y^2} \tag{5-15}$$
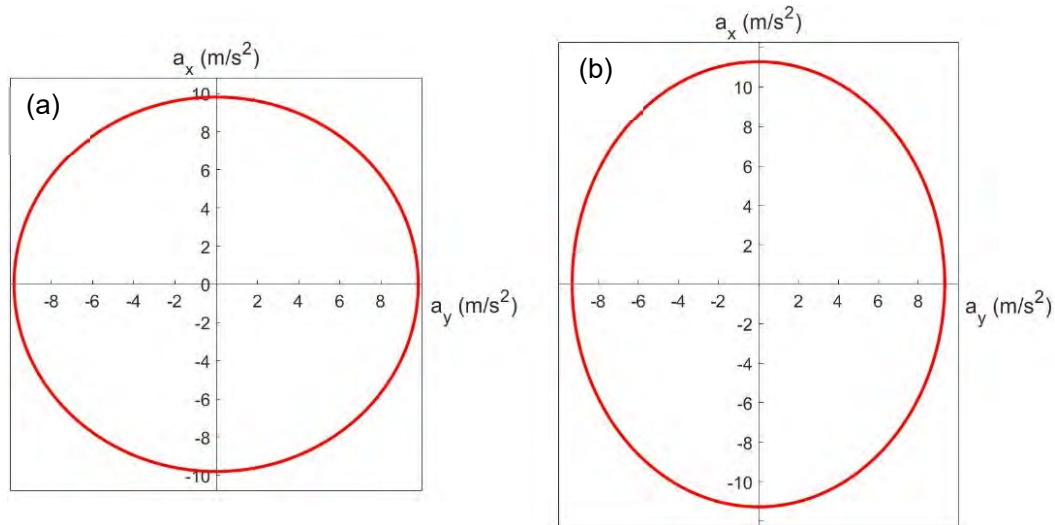
Figure 5-12 - Tyre Saturation Diagrams (a) Unit Circle, (b) Elliptical Shape

Figure 5-12(a) represents a Tyre Saturation diagram as discussed in Section 2.3.1, where the maximum longitudinal acceleration is equal to the maximum lateral acceleration. Figure 5-12(a) represents a vehicle where the maximum acceleration is $1g$ which equates to $9.81 m/s^2$. Figure 5-12(b) represents a vehicle unequal longitudinal and lateral accelerations. For example, a vehicle can achieve a maximum longitudinal acceleration (and deceleration) of $1.15g$ which equates to $11.28 m/s^2$, but only $0.95g$ in lateral acceleration equating to $9.32 m/s^2$.

An elliptical shape results if the $a_{x.max}$ and $a_{y.max}$ are unequal, described by:

$$\frac{a_x^2}{a_{x.max}} + \frac{a_y^2}{a_{y.max}} = 1 \tag{5-16}$$

Calculating a_x is done by finding angle t which subtends the vector of a_x and a_y from the following equations:

$$a_y = a_{y.max}\sin(t) \tag{5-17}$$

$$a_x = a_{x.max}\cos(t) \tag{5-18}$$

The benefit of using a simple sinusoidal wave for the trajectory from Section 5.4 is evident here. The lateral acceleration is used to calculate the available longitudinal acceleration. This method prioritises the steering manoeuvre over the braking, which ensure the steering manoeuvre is completed, which ensures the braking does not compromise the steering. If braking had been determined first and lateral acceleration afterwards, it cannot be guaranteed that the hazard ahead be avoided given the available longitudinal distance.

A correction step when calculating the Velocity and Distance Travelled needs to be applied. The steering manoeuvres will have a slightly greater distance to travel, as the lateral component of the vehicle's displacement increases the distance travelled by the vehicle from the longitudinal distance only, allowing the vehicle more distance to reduce velocity. This velocity is also in the direction of travel, which is not always entirely longitudinal. Using the planned trajectory and yaw rate, a required yaw angle is determined. Using trigonometry, velocity values for x and y direction can be calculated, where v_x is the longitudinal velocity. Then a longitudinal rate of deceleration is determined. This will be slightly greater than the previously calculated rate of deceleration due to the extra distance and v_y component of velocity.

The kinematic equations of motion are used to determine the velocities of the vehicles and the stopping distances. Equations used are as follows:

$$v = u + at \tag{5-19}$$

$$v^2 = u^2 + 2as \tag{5-20}$$

and to calculate distance:

$$s = \frac{t}{2}(u + v) \tag{5-21}$$

where a is acceleration, s is distance, t is time, u is initial velocity, and v is final velocity. A time sampling rate is set, and the calculations are performed for every time sample.

99

The v_x and v_y velocities are determined by equations from Abe (2009):

$$v_x = v \cos(\psi + \beta) \qquad (5\text{-}22)$$

$$v_y = v \sin(\psi + \beta) \qquad (5\text{-}23)$$

As this is required velocity calculations and the vehicle is assumed to achieve the desired yaw rate, slip angle (β) is be assumed to be zero again. The equivalent braking calculates the rate of deceleration in the longitudinal direction only, using Equation (4-1), with v_x as the initial velocity. v_x is used for the distance calculations using Equation (5-21), which therefore will consider the effect of a greater distance the steering manoeuvre makes.

The rate of deceleration calculated by Equation (5-18) could calculate dynamic braking for every time sample, as the reducing velocity will result in a reducing a_y. As a_y lowers, Equations (5-17) and (5-18) calculate an increasing a_x. However, it is the minimum a_x that is applied to the velocity calculations. This is a safety consideration to guarantee tyre grip. Otherwise keeping the braking on the limit of tyre saturation increases the risk of over-saturation.

The vehicle will reduce velocity faster in the longitudinal direction, with greater distance to do so, as a proportion of its velocity will be in the lateral direction. Another consideration is that when the steering manoeuvre is complete, it assumes the higher rate of deceleration. This is not a concern, however, as the vehicle will have no lateral manoeuvre after this point, and greater braking force can now be applied. The vehicle will just have to maintain the rate of deceleration.

The simulated Lateral Acceleration is used as the error, in the PD feedback to maintain tracking of the intended course. PD improves the control but still needs a speed dependant value for the derivative. Maintaining the intended course proved difficult due to the now changing velocity and steering inputs. This demonstrates the limitations of the steady-state bicycle model relying on PD control to maintain tracking of the trajectory.

5.7.2 Simulation Results

The simulation uses a unit circle maximum peak acceleration of 1g, or $9.81m/s^2$. This value is used for demonstration purposes as it is a rounded integer based on the maximum braking deceleration of $10.75m/s^2$ ($1.01g$) and the maximum lateral acceleration recorded by the maximum speed tested $8.52m/s^2$ ($0.87g$). A real vehicle would require a detailed study of the longitudinal and lateral dynamics for the 'g-g' principle, where the elliptical shape of Figure 5-12(b) is likely to be reproduced. For the purposes of demonstrating the 'g-g' braking controller, the unit circle will be sufficient.
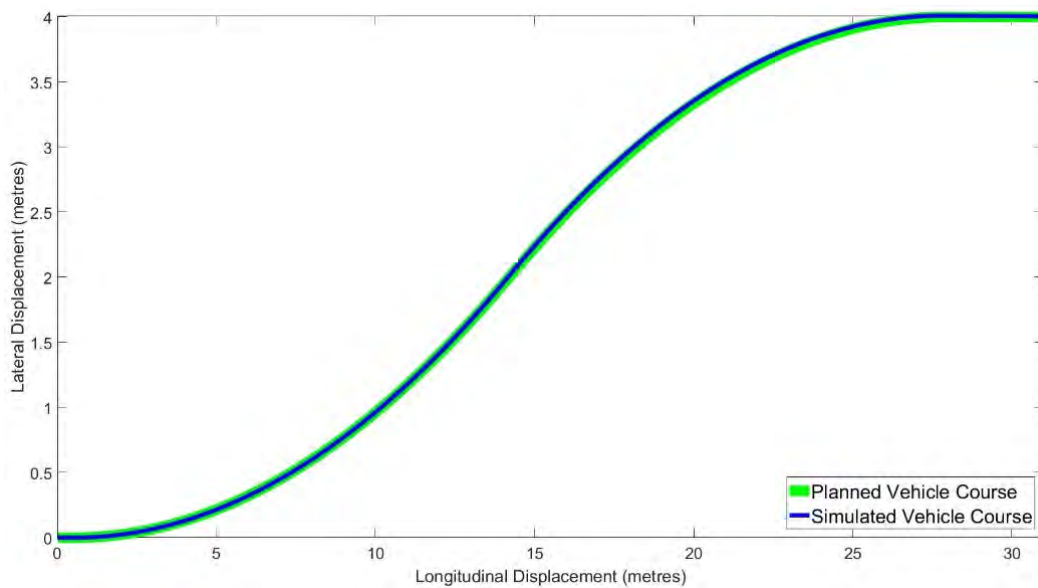
Figure 5-13 – Four metres Lateral Movement at 20m/s Simulation with PD Controller and Reducing Speed
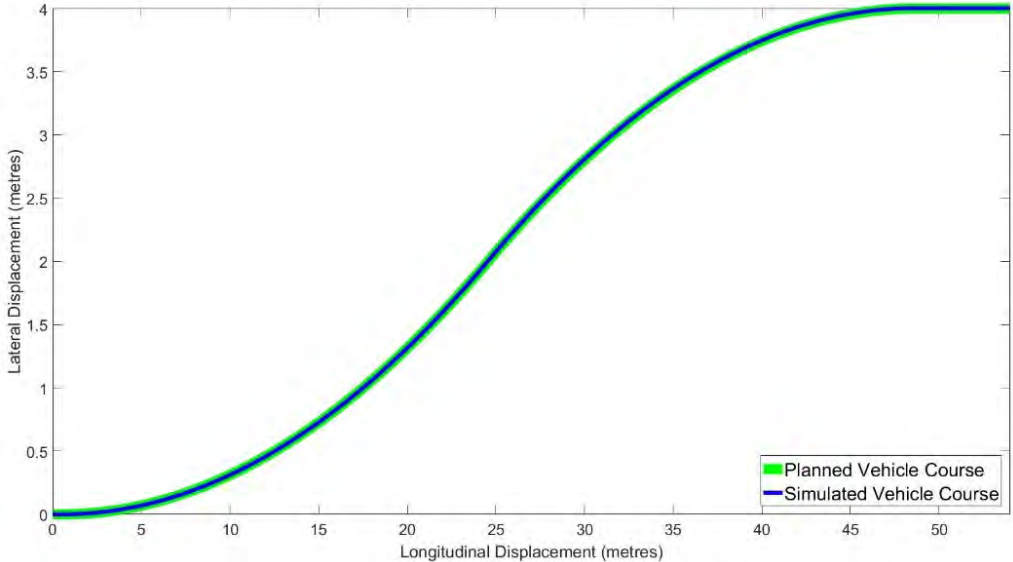
Figure 5-14 – Four metres Lateral Movement at 35m/s Simulation with PD Controller and Reducing Speed

With velocity dependent PD control the plots of the $20m/s$ and $35m/s$ simulations show that the simulated vehicle can follow the intended course closely. As shown in Figure 5-13 and Figure 5-14, it is noted that the slower the vehicle speed, the more difficult for the vehicle to track this path.

The reduction in speed achieved by the combined Steering and Braking controller is presented in Table 5-5.

Table 5-5 - Speed reduction of Steering and Braking Controller

Initial Velocity (m/s)	Distance (m)	Final Velocity (m/s)	Velocity Reduction (m/s)	Applied Braking (m/s^2)
15	23	4.8666	10.13	4.2804
20	31	11.1348	8.87	4.3974
25	38.5	16.32	8.68	4.6203
30	46	21.74	8.26	4.6203
35	54	26.27	8.73	4.9306
40	61.5	31.95	8.05	4.6916
45	69	36.93	8.07	4.7788

The distance to complete the steering manoeuvre is the same as in the case of the Steering only controller. Furthermore, the steering manoeuvre could not be completed for $10m/s$ as the velocity reduced to $0m/s$ before the end of the manoeuvre. An average of $4.6171m/s^2$ was applied as braking for the steering manoeuvres, which resulted in an average velocity reduction of $8.6843m/s$ at the instant the steering manoeuvre was completed.

5.7.3 Effect of Coefficient of Friction

For comparing the braking distances versus the combined steering and braking distances the values for the maximum braking and coefficient of friction have remained constant. The coefficient of friction will change dynamically depending upon variables such as rainfall, temperature, tyres etc. Therefore, the coefficient of friction is a vital parameter which affects the performance of both the braking and steering.

The constant values are $10.75m/s^2$ for maximum braking a_x, and a constant coefficient of friction μ of 0.9. μ can be determined from the braking performance and conservation of energy equations. Revaluating Equation (4-1) gives Equation (5-24).

$$a = \frac{(v^2 - u^2)}{2.s} = \frac{F}{M} \tag{5-24}$$

where M is the vehicle mass, F is force, which is calculated with g as the gravitational constant.

$$F = \mu.M.g \tag{5-25}$$

$$\mu = \frac{F}{M.g} = \frac{u^2}{2.g.s} \tag{5-26}$$

$$a = \mu.g \tag{5-27}$$

Therefore, the coefficient of friction μ required to decelerate from an initial speed to 0 over a set distance can be calculated using Equations (5-25) to (5-27). Now varying deceleration and coefficient of friction values can be simulated, to evaluate the effect of different braking and steering performances. For a comparison,

a μ=0.7 can achieve a maximum average deceleration of $6.867m/s^2$. These values of μ (0.7 and 0.9) are simulated for calculation of braking distances and combined steering and braking distances. Using a coefficient of friction of μ=0.9, a maximum deceleration of $8.829m/s^2$ can be achieved. Comparing the braking and steering distances to end of manoeuvre for these two coefficients of friction demonstrates its effect on the vehicle's ability to complete the manoeuvres.
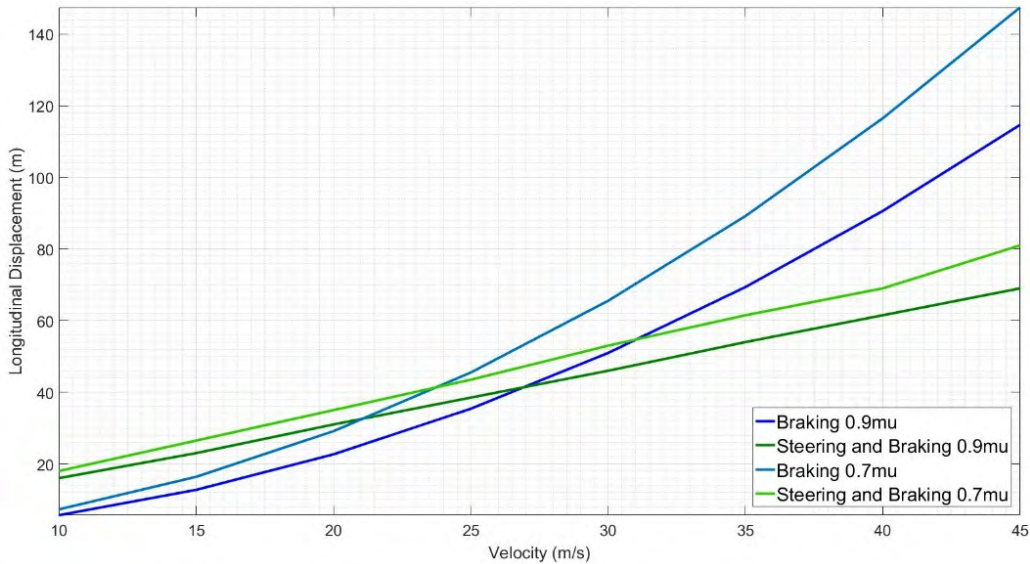
Figure 5-15 - Comparison of Displacement to End of Manoeuvre

Figure 5-15 demonstrates that with a lower coefficient of friction, a combined steering and braking manoeuvre completes the manoeuvre in a shorter distance after speeds of $24m/s$, compared to $27m/s$ of the 0.9 friction coefficient plots. The coefficient of friction does still affect the steering manoeuvre's distance to completion, but not as drastically as on the braking only manoeuvre. The coefficient of friction would also have an effect on the 'g-g' braking controller, as in the lateral dynamics of the tyres would also be affected which would require more extensive modelling. The yaw rate limited by friction in Equation (5-5) is how the coefficient of friction limits the steering controller from performing a steering manoeuvre.

5.8 Active Vehicle Dynamics Systems

The limiting factor of the kinematic steering controller is the maximum yaw rate. Active vehicle dynamics systems aim to improve performance of the steering controllers. These systems include Brake Steer and four-wheel-steering (4WS), as discussed in Section 2.3.3. Pilutti, Ulsoy, and Hrovat (1995) developed a steering intervention system using differential braking. It is noted that similar issues with maximum yaw rate were observed. Due to available yaw rate saturation, the brake steer manoeuvre was most effective at low steering angles ($0.5 degrees$) and only minor braking can be applied at higher angles ($2.3 degrees$). Exceeding these limits caused the vehicle to spin. Simulations showed "*that the maximum differential braking is found at low speeds and zero steering angle, and the minimum is found at high speed and high steering angle.*" For an emergency steering manoeuvre at high speed, whilst an advantage would be gained, it would only be minimal.

Song (2012) developed a controller using fuzzy logic to control an integrated brake pressure and rear-wheel steering. Song concluded that a body slip angle was reduced, and the simulation could track the reference yaw rate. It was also noted that adhesion limit was extended increasing the vehicle's controllability and stability.

Falcone et al. (2008) proposed two controllers utilising active front steering and braking. The first was a tenth order five input controller, which was noted for the best performance when following the desired path. The inputs were steering angle and the four-wheel braking torques. However, this model was computationally heavy and difficult to tune, demonstrating the need for a simpler lower order model. The second model was based on a two input sixth order simplified bicycle model. The four braking torques were simplified to a single braking yaw moment. This simpler model was more attractive for real-time applications, but a loss in stability at high entry speeds was observed, which would include emergency manoeuvres.

A study into the capabilities of four-wheel steering kinematic models was conducted by Spentzas, Alkhazali, and Demic (2001). It is concluded that "*A 4WS vehicle has a manoeuvring advantage over a 2WS vehicle only if its rear wheels can turn in the opposite direction to its front wheels, because only in that case we have a relative reduction of the turning radius.*"

Potential active vehicle dynamical systems such as differential braking or rear-wheel steering would provide a benefit to vehicle handling, and so would be able to complete a lateral manoeuvre faster and allow for higher yaw rates. However, a

higher order model required for accurate simulation would prove computationally heavy. There is also a question of how much the maximum yaw rate is increased by, which requires both complex dynamic modelling and physical testing. Due to the added complexity of active vehicle dynamics systems, this research programme will progress without modelling these systems, as to focus on the defined objectives.

5.9   Conclusions

A new trajectory planner using a sinusoidal wave to plan a vehicle's trajectory is proposed here. This sinusoidal trajectory planner is tested with the use of kinematic steering controllers. The steering controllers are based on existing models, but adapted to suit the intended purpose in this PhD research, including introducing the sinusoidal lane change manoeuvre and better tracking the intending course with PI control.

A kinematic steering controller is developed in this research based on the 2D bicycle model to perform a single lane change manoeuvre. PI control was introduced to the kinematic steering controller using lateral acceleration error as feedback to better track the intended trajectory. The simulation results are satisfactory, as the simulated trajectory followed the planned trajectory closely. A braking only manoeuvre is then evaluated, to compare the end of manoeuvre distances between a single lane change manoeuvre and full braking. It is concluded that at lower speeds, with the aim of avoiding a collision, a braking only manoeuvre would be more successful. The braking only manoeuvre does assume a high rate of deceleration only achievable by high performance road cars.

A novel combined steering and braking controller with the aim of avoiding or mitigating an imminent collision was introduced in this chapter. Using the kinematic steering controller, a reducing velocity (deceleration) is introduced. However, an appropriate rate of deceleration needs to be calculated first, and this utilizes tyre saturation properties to reduce the risk of the vehicle losing control. The lateral and longitudinal accelerations of the vehicle are evaluated. It is demonstrated that the reducing velocity applied to the steering controller does not reduce the distance to the end of the manoeuvre, but does provide a reduction in velocity once the steering manoeuvre has been completed.

The steering and braking controller required a PD controller to track the planned trajectory. Again, the simulated trajectories followed the planned trajectory closely, but performed better at higher speeds. It has been shown from existing research that dynamic controllers would have a better performance in tracking and simulating, however they do require greater computational effort making them slower to complete the required calculations. This is a concern for an emergency manoeuvre, and tracking of the kinematic controller proved satisfactory. The kinematic steering controller would require further testing with a real vehicle to validate the trajectory tracking performance.

A kinematic Bicycle model is limited in its capability of simulating a dynamic situation with a changing velocity brought by the combined steering and braking, which would explain why the PD controller is required to maintain tracking of the planned trajectory.

The combined steering and braking controller gives another option for avoiding or mitigating a collision. The steering controllers developed all use the same trajectory planning method. The aim of this research is not developing a new steering controller, but investigating means to plan a manoeuvre for an autonomous vehicle in an emergency situation. A method is now needed to evaluate what the best manoeuvre plan is. The steering trajectory planner gives the inputs required to determine if a steering manoeuvre is possible. It is demonstrated that the trajectory planner will be suitable for analyses of whether lane-change manoeuvres are possible for the autonomous vehicle, as all steering controllers developed and tested in this research have used the same sinusoidal trajectory planner and its outputs.

Chapter 6

Collision Modelling

6.1 Introduction

This chapter describes a modelling technique which is able to replicate in simulation a vehicle collision scenario. It is based on existing research, which can be found in the literature, as well as more recent models that capture the nonlinearity which is observed in practice. Recognising that all models are approximations, the model is required to be sufficiently representative as well as computationally efficient. This is a key issue with Finite Element Analysis (FEA) simulations, which, depending on their complexity, can take hours to simulate. Should a collision model be required for use within a specific on-line application, such as a vehicle simulating its own imminent collision, then rapid simulation is required.

Modelling of the collisions allows metrics to be produced whereby the severity of the collision can be assessed. Using FEA data of a vehicle collision to compare

the accuracy of the simulations, a collision model may be created to test a number of scenarios. The modelling technique uses lumped mass models to represent the colliding vehicles. The lumped mass model is developed from an initial linear model, to a bilinear model, as proposed by Pickering et al., (2018).

The bilinear model requires tuning, to best represent the FEA data. A Euclidean optimization process is developed to compare the simulated results with the FEA data. A range of model parameters are simulated and a Euclidean optimization selects the best performing simulation, i.e. the closest model fit to the FEA data. A limited number of scenarios are tested to produce relevant outputs. To assess the performance of the lumped mass modelling, four key properties comprising peak deformation, peak acceleration, collision energy and collision duration time are used to assess the efficacy of the lumped mass models.

6.2 Single Vehicle Collision Modelling

This Section introduces the background to vehicle crashworthiness, with focus given to the current testing legislation authorities. A finite element analysis (FEA) model is set-up based on the current testing legislation involving a collision into an immovable rigid barrier. Based on the FEA model, linear and nonlinear (bilinear) dynamic lumped mass and spring models are set-up to capture the key features of the collision, i.e. peak deformation, peak acceleration and collision energy. To tune the bilinear model, a Euclidean optimization process is developed. The key features obtained from the linear and bilinear lumped mass-spring models are compared to the features from the corresponding FEA simulation to provide a basis for a suitable model to be selected.

6.2.1 Background to Vehicle Crashworthiness

A vehicle body structure is typically made up of three compartments, namely the front crash structures, the passenger cell and the rear crash structures. In the event of a collision, the design requirement of the passenger cell is to remain rigid and prevent any intrusion. The crash structures (front and rear) on the other hand are designed to fail/buckle in a controlled passive manner. The role of the crash structure is therefore to increase the collision duration, which minimises the accelerations/decelerations

experienced by the passenger(s), as discussed by Du Bois et al. (2004). As detailed, in MacDonald (2013) the buckling of the crash structure must not exceed the crash structure design deformation length, which would result in an intrusion in to the passenger cell. Bastien et al. (2013) examined the kinematics of occupants in collisions by comparing crash tests of a vehicle into a rigid wall at $25mph$ against a vehicle decelerating at $1g$ until the vehicle reaches $25mph$, and then impacting a rigid wall. The chest accelerations resulting in this study were in the order of magnitude between $41g$ and $64g$.

A measure of a vehicle's crash performance is known as crashworthiness. In Europe the crashworthiness authority is known as the European New Car Assessment Programme (Euro NCAP), see (Euro NCAP, 2017) and in the United States of America (USA), the crashworthiness authority is known as USA NCAP. In the case of both authorities, vehicles are tested against various crashworthiness tests. Relevant to this research is the full-frontal impact test. In the Euro NCAP test, this involves the vehicle being driven at $31mph$ ($13.8582m/s$) into an immovable rigid barrier (Euro NCAP, 2017), whereas the US NCAP test involves the vehicle being driven at $35mph$ ($15.6464m/s$) into an immovable rigid barrier (US NCAP, 2017).

Considering the full-frontal impact tests of the Euro/US NCAP, the Vehicle, denoted a of mass, denoted M_a, is driven into an immovable rigid barrier with an impact collision velocity, denoted v_a. Due to Newton's Second Law which states that a force, denoted f_a acting on an object, here Vehicle a, is proportional to the time rate of change of its linear momentum (velocity). The momentum is the product of mass and velocity, i.e. $M_a v_a$, so that the force expressed as a function of time may be alternatively represented by:

$$f_a(t) = M_a \frac{dv_a(t)}{dt} = M_a \frac{d^2 x_a(t)}{dt^2} = -k_a x_a(t) \tag{6-1}$$

where x_a denotes the deformation of the crash structure of Vehicle a, k_a denotes the crash structure stiffness and t denotes time. From Equation (6-1), it is evident that an increased structural stiffness of the crash structure would result in lower deformation, hence higher accelerations, experienced by the occupant(s) on-board the vehicles. Therefore, a lower stiffness value of the vehicles structure would result in higher deformations and lower accelerations experienced by the occupant(s) on-board the vehicle.

The original equipment manufacturers (OEMs) design their vehicles to satisfy the Euro/US NCAP frontal impact tests, hence the structures are designed to absorb a pre-determined amount of collision energy. The collision energy must be absorbed within the deformation length of the crash structure. This is designed such that some pre-determined collision energy is absorbed within a pre-determined collision time to allow pre-determined accelerations/decelerations to be experienced by the occupants, as discussed by Du Bois et al. (2004). Therefore, if the OEMs know the vehicle's laden mass and collision test velocity, the collision energy can be pre-determined and taken into account at the design stage. The pre-determined collision energy is given by:

$$\Delta E_a = \frac{M_\mathrm{a}(v_\mathrm{a})^2}{2}$$

(6-2)

where, for a given vehicle, denoted Vehicle a, ΔE_a is the pre-determined collision energy, M_a is the vehicle collision test mass and v_a is the vehicle collision test impact velocity. Equation (6-2) is later used to verify the FEA model and the developed single vehicle lumped mass-spring collision mathematical models.

6.2.2 Finite Element Analysis (FEA)

To develop an initial understanding of the 'input' (force due to collision impact velocity) and 'outputs' (peak deformation, peak acceleration and collision energy), i.e. the key properties of a collision, a Toyota Yaris Sedan FEA model is employed. The developed 2010 Toyota Yaris Sedan model is available on 'open-access' from the Centre for Collision Safety and Analysis (CCSA) website, see (Centre for Collision Safety and Analysis, 2017). The CCSA is a research organisation at George Mason University which focuses on understanding vehicle collisions and developing methods to avoid or mitigate collisions. It can be seen in Marzougui et al. (2012) that the FEA model matches the crashworthiness performance of the actual vehicle very closely. The FEA Toyota Yaris Sedan collision simulation is set-up based on the US NCAP, i.e. a collision impact velocity of $35 mph$ into an immovable rigid barrier.

The outputs from the FEA Toyota Yaris Sedan simulation are illustrated in Figure 6-1 and the key properties (peak deformation, peak acceleration and collision

energy) of interest in this research are documented. The top-left plot illustrates deformation versus time up to the end of the first ¼ cycle, as this is the point of maximum deformation, as detailed by Du Bois et al. (2004). Hence, the time period to reach maximum deformation is used for the rest of the graphical outputs. The top-right plot illustrates acceleration versus time and the bottom-left illustrates force versus deformation. In the case of the force versus deformation plot, the area under the curve represents the collision energy. The collision energy in Table 6-1 has been determined by making use of the trapezoidal rule to calculate the area under the curve. The trapezoidal rule is the method used in the MATLAB function, as it is MATLAB/Simulink in which these simulations. The trapezoidal rule uses the FEA data of displacement and force to calculate collision energy. This calculation is completed for every time sample in the data set. The time sampling rate of the FEA data is not constant, but is between $9e^{-6}$ and $1.01e^{-5}$ seconds. The trapezoidal rule is sufficient for the modelling in this thesis, but future developments could investigate the potential benefits of employing Simpson's rule for integration. Note that for this study the coefficient of restitution is not taken into account, i.e. the 'restored' energy through the rebound of the collision structure which is typically 10-15%, see Batista (2005) for further details, is effectively ignored.
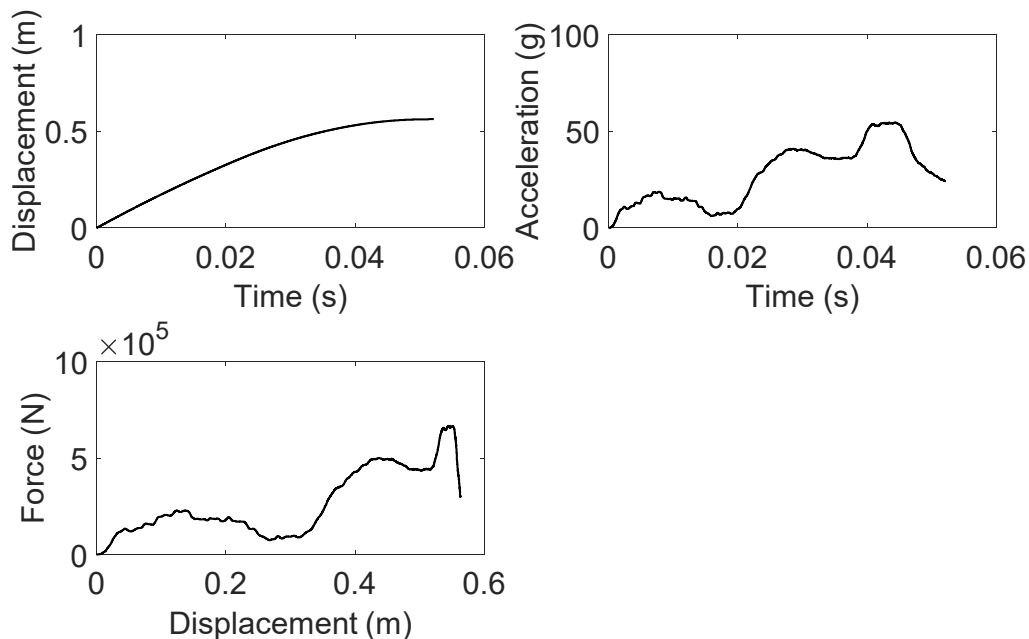
Figure 6-1 - FEA Data of Toyota Yaris Sedan

Table 6-1 - FEA Data comparison with Actual Vehicle Collision Results

Collision property	Actual vehicle	FEA model
Mass (kg)	1271	1247
Impact Velocity (m/s)	15.6464	15.6464
Peak Deformation (m)	0.5620	0.5625
Peak Acceleration (g)	~ 52.000	54.5232
Collision Deformation Energy (without restitution) (kJ)	---	148
Collision Duration (s)	---	0.0522

The results of the FEA model are close to the actual vehicle collision data, as given in Table 6-1. The peak deformation has a difference of 0.0005m for the two sets of data. The peak acceleration of the actual vehicle is an estimation based on the available data, but the FEA model produces an acceleration value with a 2.5g difference, which is an error of 4.85%. These values demonstrate the validity of the FEA modelling, compared to the results of the actual vehicle.

6.2.3 Linear Lumped Mass Modelling and Simulation

Lumped mass dynamic modelling offers a simplified approach to understanding the dynamics of a collision to that of an FEA simulation, e.g. reduced computational effort. There are a number of linear collision modelling approaches for single one-dimensional lumped mass models representing a collision into an immovable rigid barrier, such as the methods proposed by Kim and Arora (2003), Deb and Srinivas (2008), Cheva et al. (1996), Klausen et al. (2014), Lim (2015) and Lim (2017), where the initial motivation for this initial modelling came from.
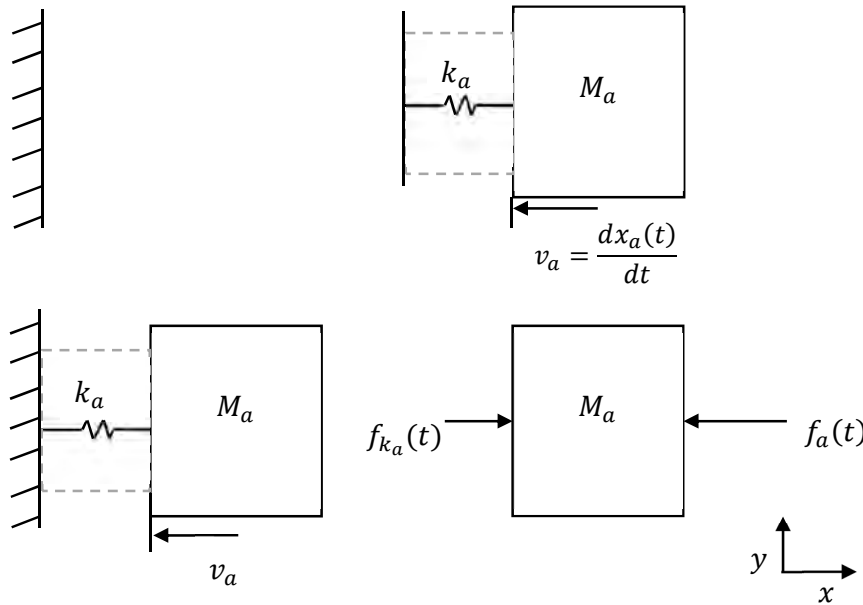
Figure 6-2 - Vehicle Mass Travelling at a Constant Velocity Consisting of Crash structures with an Immovable Rigid Barrier in Sight (Top) and Single Mass and Spring (Bottom - Left) Indicating Forces (Bottom - Right)

When a vehicle of a certain mass travels at a known velocity (see Figure 6-2) and collides into an immovable rigid barrier, the vehicle crash structure, modelled as a lumped mass model, opposes the forces created by the collision. The corresponding free body diagram of the lumped mass model is given in Figure 6-2. The reaction force is given by the spring stiffness force, denoted f_{k_a}. Due to Newton's Third Law, the reaction force from the immovable rigid barrier acting through the vehicle's crash structure is given by $f_{k_a} = -f_a(t)$, where $f_a(t)$ is related to the vehicle crash structure deformation, $x_a(t)$, so that $f_a(t) = k_a x_a(t)$. The differential equation representation of the dynamic collision scenario is given by:

$$M_a \frac{d^2 x_a(t)}{dt^2} + k_a x_a(t) = f_a(t) \tag{6-3}$$

The differential equation may be converted from the time-domain to the frequency-domain via the Laplace transform, with this being given by:

$$M_a s^2 X_a(s) + k_a X_a(s) = F_a(s) \tag{6-4}$$

Equation (6-4) is rearranged to give the following transfer function form:

$$G(s) = \frac{F_a(s)}{X_a(s)} = \frac{1}{M_a s^2(s) + k_a(s)}$$

(6-5)

Later in this Section, the stiffness value in Equation (6-5), i.e. k_a , will be tuned using a linear least squares fit to the force versus deformation FEA data detailed in Section 6.2.2, therefore, the gradient of the best straight line becomes a first estimate of the stiffness value. Linear least squares is used to effectively determine the 'best' fit to the force versus deformation data by minimising the error between the data points and the resulting model fit. When calculating the best fit for the linear least squares optimization, an offset is produced and is known as the failure point f_{p_a}. This is the initial value of the force to be overcome prior to the commencement of deformation. The linear force versus deformation model originally used by Watson (1967) is given by the following:

$$f_a = f_{p_a} + k_a \delta_a$$

(6-6)

where, equivalently, $\delta_a = x_a$ is the crash structure deformation along the longitudinal x axis.

Using Least squares, the stiffness value is estimated using the following general formula:

$$\hat{\beta} = (X'X)^{-1}X'y$$

(6-7)

where the quantity $(X'X)^{-1}X'$ is known as the pseudo inverse, (Watson, 1967).

In Figure 6-3, the force versus deformation from the FEA model is plotted with the corresponding linear least squares stiffness estimate.
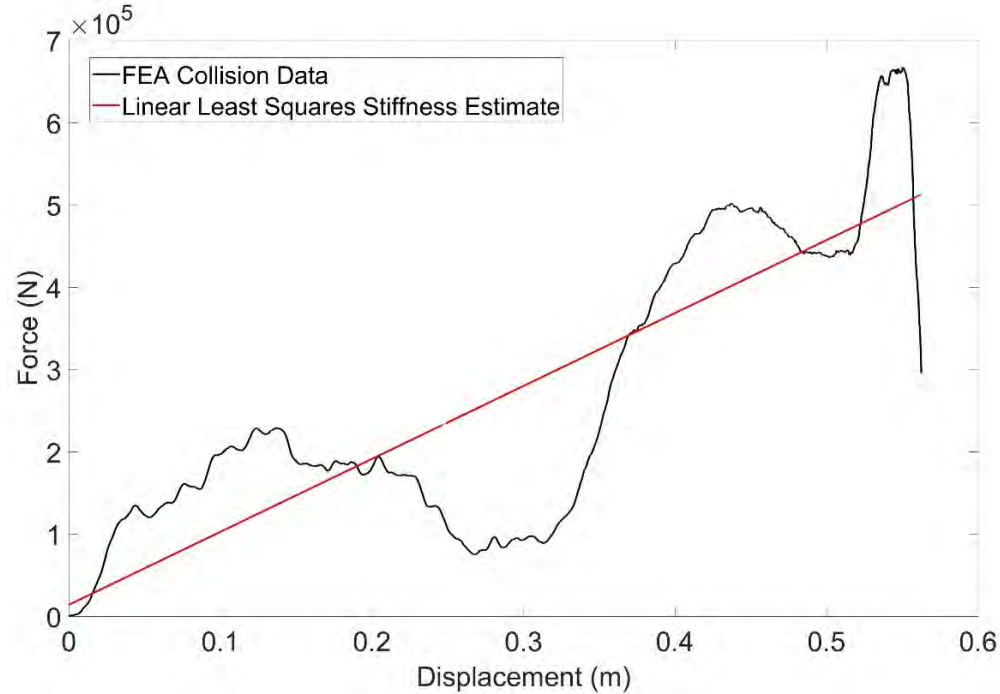
Figure 6-3 - Linear Lumped Mass Modelling Comparison with FEA Data

Table 6-2 - Linear Least Squares Estimates of Crash Structure Stiffness

Model type	Estimate of stiffness (kN/m)	Estimate of failure point (kN)
Linear single	886.009	13.968

The MATLAB/Simulink phase variable form block diagram representation of Equation (6-4) is given in Figure 6-4, where the initial condition of collision velocity to the model is applied to the left-hand integrator, i.e. corresponding to an unforced model.
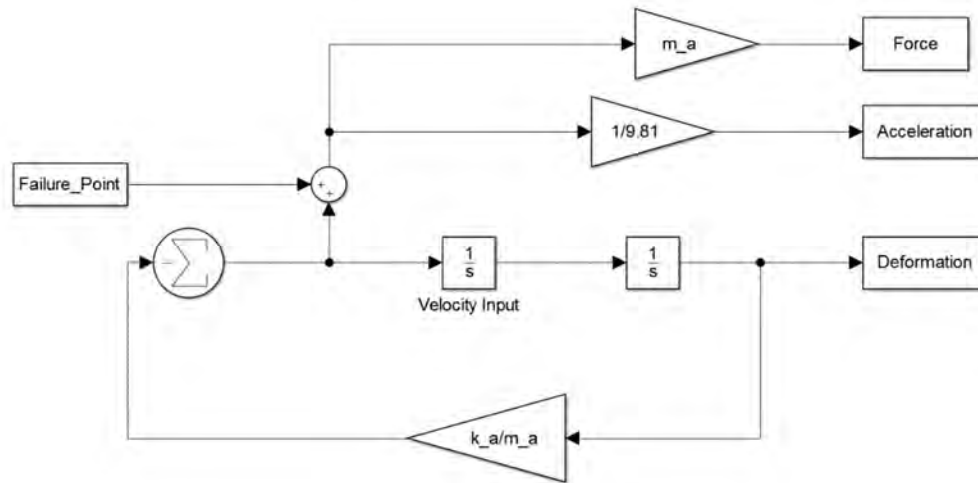
Figure 6-4 - MATLAB/Simulink Block Diagram of a Single Lumped Mass Collision Model

Using the estimated stiffness value and failure point value given in Table 6-2, the MATLAB/Simulink simulation is undertaken. The unforced free dynamic response of the linear lumped mass model is simulated for the time period up to the maximum deformation, this corresponds to the first quarter cycle of the dynamic response and the point at which the relative velocity becomes zero (or the final combined velocity becomes constant). The relevant data to be captured from the simulation is deformation versus time, acceleration versus time and force versus deformation, as discussed in Section 6.2.2. Figure 6-5 illustrates the lumped mass simulation results compared to that of the FEA simulation data. The top-left plot shows deformation versus time, the right-hand plot shows acceleration versus time and the bottom-left shows force versus deformation. The output data of interest is given in Table 6-3, where the lumped mass model key properties are compared to that of the FEA model (i.e. peak deformation, peak acceleration and collision energy). To compare the accuracy of the lumped mass simulation model results, a discrepancy between the FEA model data and lumped mass model outputs is determined using:

$$\frac{FEA\ Data -\ Lumped\ Mass\ Result}{FEA\ Data} \tag{6-8}$$
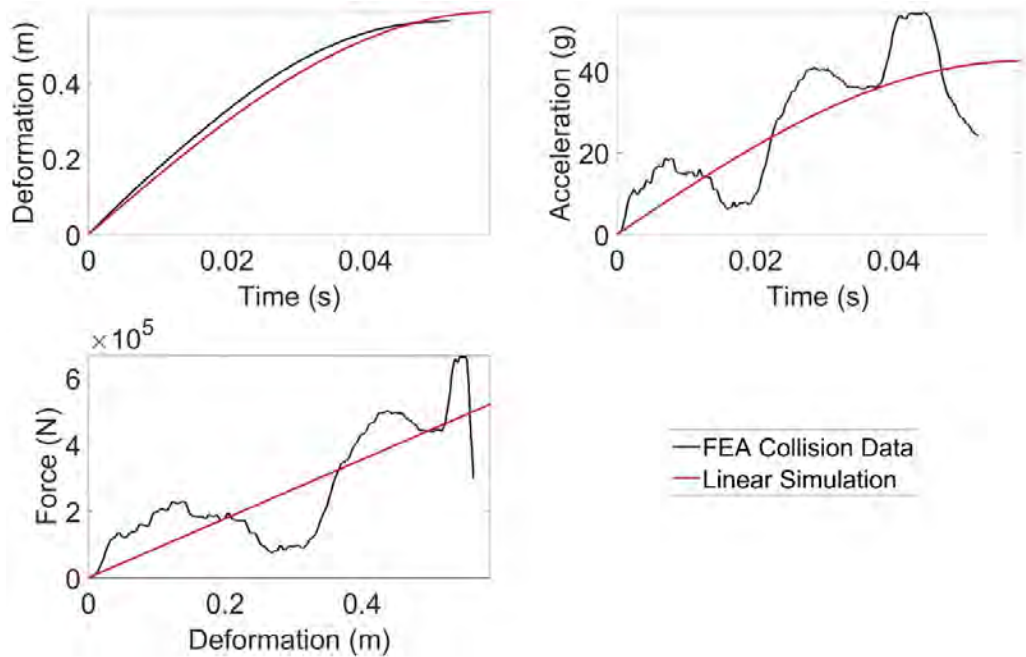
Figure 6-5 - Linear Lumped Mass modelling of Collision Comparison with FEA Data

Table 6-3 - Linear Lumped Mass Modelling of Collision Comparison with FEA Data

Key properties	FEA model	Lumped mass model	Discrepancy (+/-)	Error (%)
Peak deformation (m)	0.5625	0.5868	-0.0432	4.32
Peak acceleration (g)	54.5232	42.5010	0.2205	22.05
Collision energy (without restitution) (kJ)	147.693	152.546	-0.0329	3.29
Simulation time (t)	0.0522	0.0580	-0.1111	11.11

The results presented in Table 6-3 demonstrate that the linear modelling produced results with a low error percentage compared to the FEA data for peak deformation and collision energy. However, the peak acceleration of the lumped mass modelling is $12g$ lower than the FEA data, which is an error of 22%. This demonstrates that the linear modelling needs to be improved upon.

6.2.4 Bilinear Lumped Mass Modelling

In this research, a class of nonlinear lumped models known as bilinear systems models will be considered. Previous work in the area of modelling nonlinear spring stiffness elements is sparse. Elmarakbi and Zu (2007) have modelled the spring stiffness using a cubic approximation. In (Pickering, et al., 2018), the convoy collision scenario has been considered and modelled using a bilinear lumped mass model.

Bilinear systems modelling and control has witnessed various applications, in areas such as ecology, engineering, medicine and socioeconomics. A bilinear system modelling approach offers a first step when attempting to capture nonlinear behaviour that arises. For a comprehensive overview of applied bilinear systems and control, see for example, Mohler (1973), Bruni, DiPillo and Koch (1974), Mohler and Kolodziej (1980), Burnham (1991) and Ekman (2005).

The bilinear lumped mass collision model is now developed step by step by first considering the general second order bilinear representation:

$$\ddot{y}_b + \beta y_b + \eta y_b u_b = 0 \tag{6-9}$$

where u_b and y_b denote the arbitrary system input to the bilinear modelling (based on initial conditions) and system output, β denotes the coefficient of the linear part of the system and η denotes the coefficient of the bilinear product term involving the input and output (the output here being regarded as an internal system state, i.e. deformation). The bilinear lumped mass collision model to be used in this research is given by:

$$M_a \ddot{x}_a + k_a x_a + \eta x_a f_a = 0 \tag{6-10}$$

where the output of the lumped mass model is deformation, denoted x_a and the input of the lumped mass model is force, denoted f_a. The force input is derived from the initial impact velocity differential which is the internal input to the left derivative in the phase variable model, see Figure 6-6.

Simplifying Equation (6-10), noting that x_a is common to both the constant coefficient of the linear term and the input dependent coefficient of the bilinear term, leads to:

$$M_a\ddot{x}_a + (k_a + \eta_a f_a)x_a = 0 \qquad (6\text{-}11)$$

i.e. a system having an input dependent dynamic and steady state response.

Dividing Equation (6-11) through by m_a gives:

$$\ddot{x}_a + \left(\frac{k_a}{M_a} + \eta_a \frac{f_a}{M_a}\right)x_a = 0 \qquad (6\text{-}12)$$

As the force is derived from the initial collision impact velocity is given by $f_a = M_a\ddot{x}_a$, the following relationship is given:

$$\ddot{x}_a + \left(\frac{k_a}{M_a} + \eta_a \frac{M_a\ddot{x}_a}{M_a}\right)x_a = 0 \qquad (6\text{-}13)$$

which can be simplified as:

$$\ddot{x}_a + \left(\frac{k_a}{M_a} + \eta_a |\ddot{x}_a|\right)x_a = 0 \qquad (6\text{-}14)$$

From initial tuning of the bilinear term η_a, it was determined that an additional scaling factor of k_a was needed to 'better' capture the key properties (i.e. peak deformation, peak acceleration and collision energy) from the FEA data, with the following given:

$$\ddot{x}_a + \left(\frac{\gamma_a}{M_a} + \eta_a |\ddot{x}_a|\right)x_a = 0 \qquad (6\text{-}15)$$

where $\gamma_a = \beta_a k_a$ and β_a is the stiffness scaling factor. There are now two parameters within the bilinear collision model that can be tuned to capture the FEA collision data.

This may be configured for simulation in the phase variable form with the additional nonlinear multiplicative bilinear term, as given in Figure 6-6.
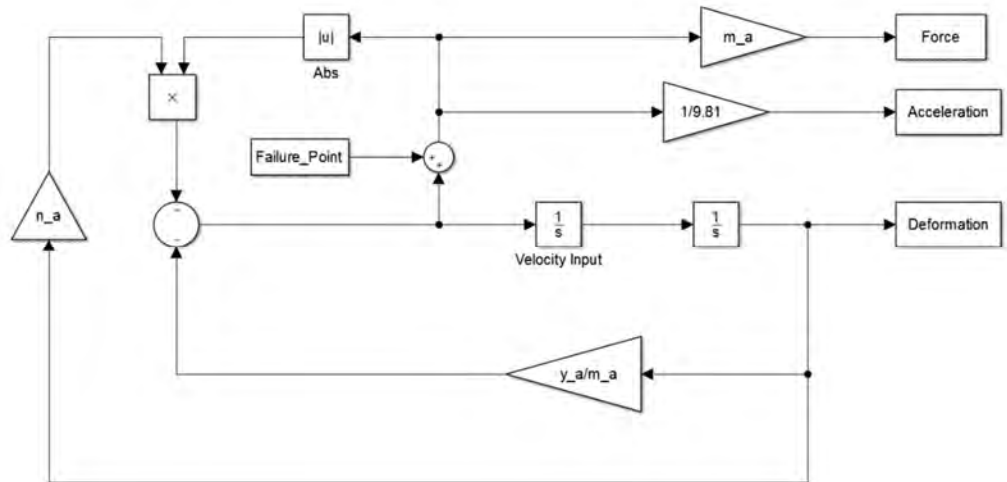
Figure 6-6 - Simulink Diagram for a Bilinear Lumped Mass Model

6.2.5 Bilinear Lumped Mass Model Tuning and Simulation

In the tuning process of the terms η_a and β_a, the key properties of peak deformation, peak acceleration and collision energy, with consideration also given to the collision duration time captured from the FEA collision model are used as benchmarks for assessing the 'goodness' of the bilinear model fit, as with the linear model, discussed in Section 6.2.4. A Euclidean norm tuning metric/approach is used to compare the key properties from the FEA model data to the bilinear simulation model results. The stiffness k_a value used in the tuning process of Equation (6-15) is taken from the linear least squares process, as discussed in Section 6.2.4. The linear spring stiffness value of $886,009 N/m$ given in Table 6-2 is used.

For the initial simulation tuning process, a range of values for β_a of between 0.1:0.1:5 are used and a range of values for η_a between -1.5:0.1:1.5. The values giving the closest Euclidean norm tuning metric to the FEA model data are selected for the bilinear simulation model.

A range of bilinear terms and multiples of stiffness are simulated and plotted on the three-dimensional plot in Figure 6-7, where each blue data point represents a single simulation of the bilinear model's key properties, i.e. peak deformation, peak acceleration and collision energy (note: collision time duration is not plotted). The

green rhombus/point represents the FEA data and the red dot is the simulation which has the closest Euclidean distance i.e. metric to the FEA data point.
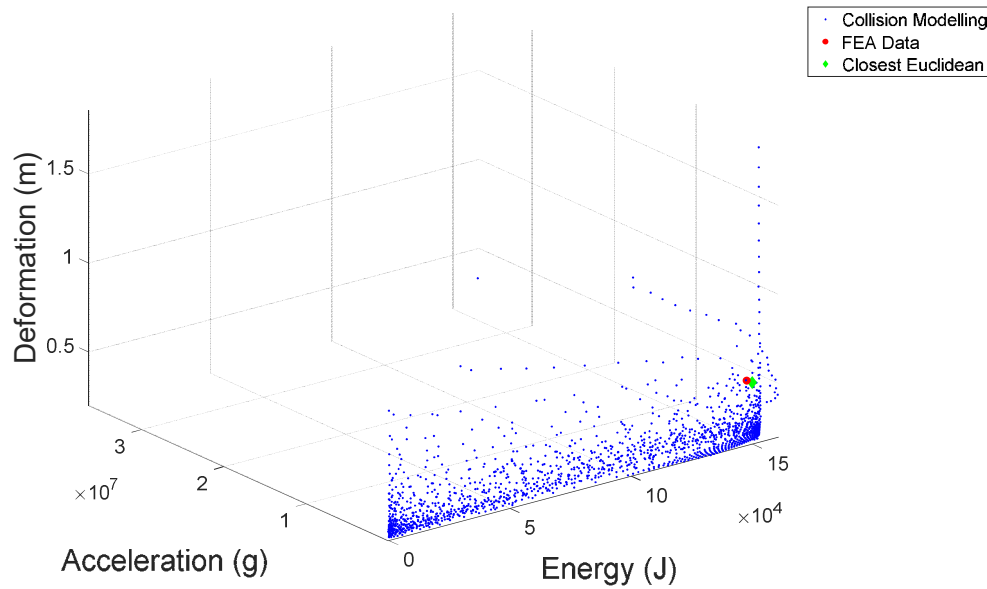
Figure 6-7 - Euclidean Optimization of Collision Modelling Results using 1/10

In order to complete the optimization of the Euclidean metric, the simulated and captured peak deformation, peak acceleration, collision energy and collision duration time values must be vector normalized. This is undertaken to re-scale the simulation results, e.g. acceleration is in units of 10, whilst deformation is in units of 0.1. The vector normalisation is given by:

$$\hat{x} = \frac{|x_s - y_{FEA}|}{\sum(|x_s - y_{FEA}|)} \tag{6-16}$$

and the Euclidean distance metric is given by:

$$d = \sqrt{\hat{x}_{acceleration}^2 + \hat{x}_{deformation}^2 + \hat{x}_{energy}^2 + \hat{x}_{time}^2} \tag{6-17}$$

where x_s denotes the simulated value, y_{FEA} is the FEA value, and d is the Euclidean distance metric. The closest simulation is given by bilinear term 1.40, and multiple of stiffness 0.5, described in Table 6-4. Using these values, the bilinear model

123

discussed above is simulated, with the graphical output given in Figure 6-8. From initial observations, the peak acceleration from the bilinear model is not captured accurately, with a value of $83.03g$, compared to a value of $54.52g$ from the FEA simulation. This led to the further refinement in the tuning process, with ranges of values for β_a between 0.57 : 0.01 : 0.97 were used and a range of values for η_a between 0.56 : 0.01 : 0.96.

These values were selected based on the initial tuning process and also trial and error. As with the initial tuning process, the range of bilinear terms and multiples of stiffness are simulated and plotted on the three-dimensional plot given in Figure 6-9. The Euclidean distance metric optimisation is undertaken with the new ranges of values, with the closest bilinear term being 0.77 and the multiple of stiffness being 0.76, stated in Table 6-4. Figure 6-10 represents the simulation results of the bilinear model where it is visibly clear that the bilinear model now captures the peak features of the FEA data more accurately. The full results are given in Table 6-5, where as in the case of the linear model simulation, the discrepancies have been determined between the bilinear model and the FEA collision data. The discrepancies of the three key features (i.e. peak deformation, peak acceleration and collision energy) are much lower for the bilinear model than for the linear model, see Table 6-3.

The simulation duration time is slightly longer for the bilinear model than that of the linear model, with both models' results being of a longer duration than that of the FEA collision data.

Table 6-4 - Euclidean Optimization Tuned Parameters

Model type	Bilinear Term (η)	Multiple of Stiffness (γ)
Bilinear – 1/10	1.40	0.50
Bilinear – 1/100	0.77	0.76
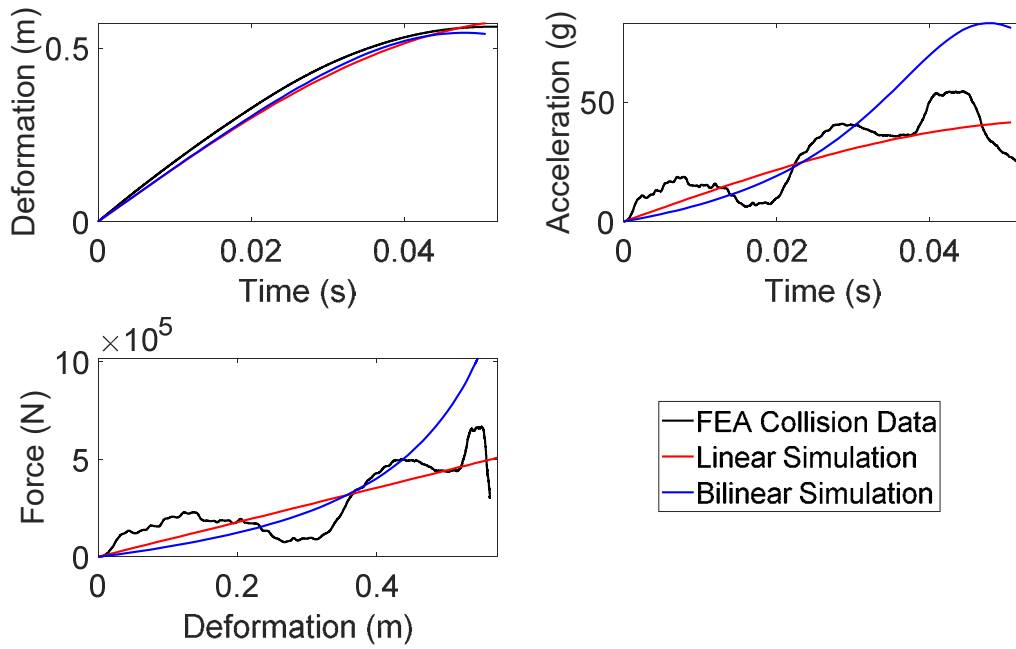
Figure 6-8 - Bilinear Lumped Mass Modelling of Collision Comparison with FEA Data and Linear Modelling using 1/10 Tuning Values
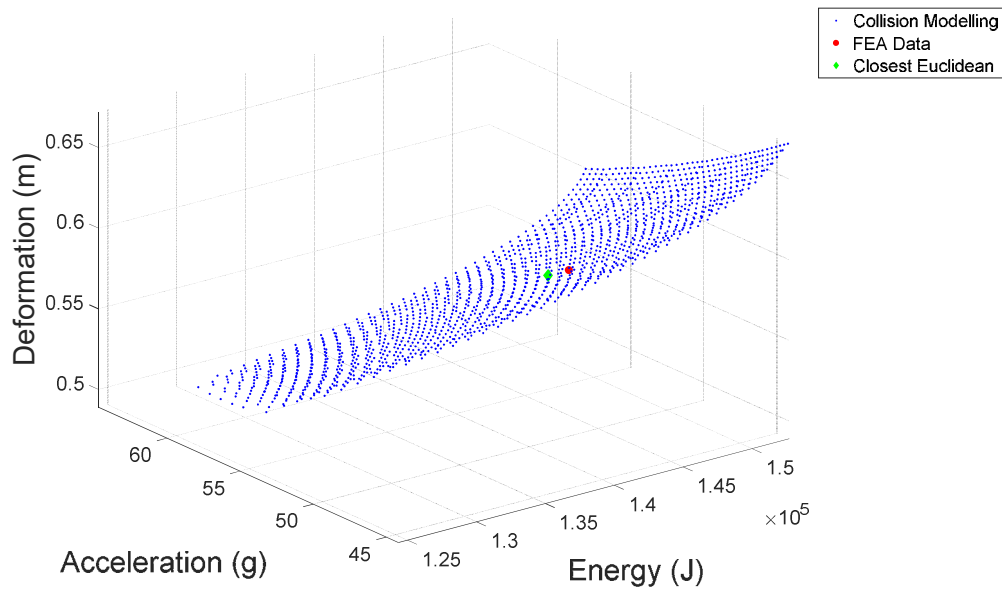
Figure 6-9 - Euclidean Optimization of Collision Modelling Results using 1/100 Tuning Values
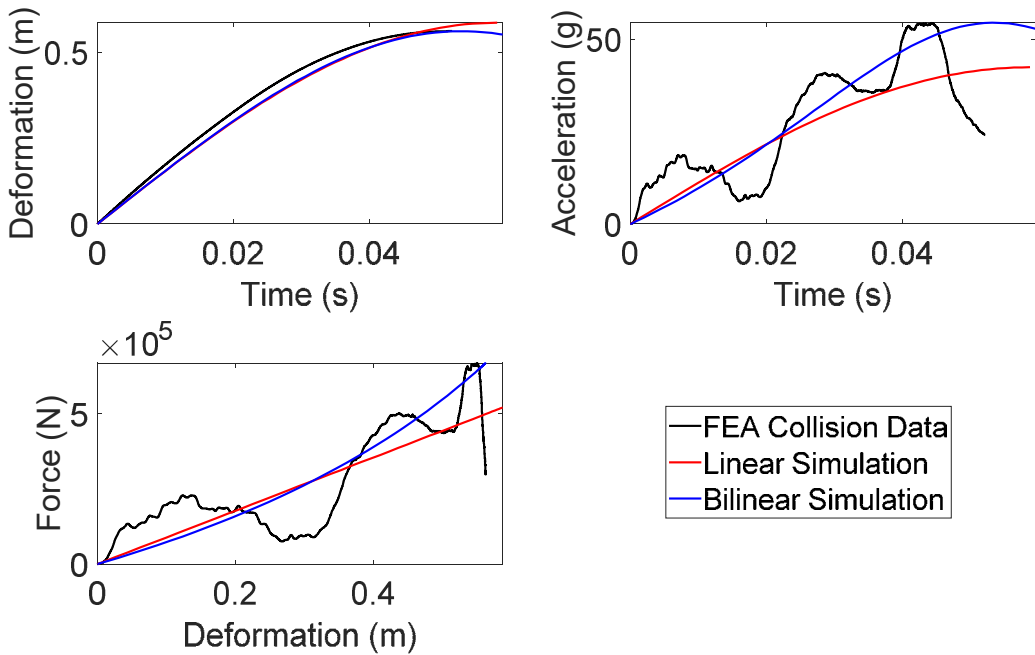
Figure 6-10 - Bilinear Lumped Mass Modelling of Collision Comparison with FEA Data and Linear Modelling using 1/100 Tuning Values

Table 6-5 – Linear and Bilinear Lumped Mass Modelling of Collision Comparison with FEA Data Results

Key properties	FEA	Linear model	Discrepancy (+/-)	Bilinear model	Discrepancy (+/-)
Peak deformation (m)	0.5625	0.5868	-0.0432	0.5623	0.0004
Peak acceleration (g)	54.5232	42.5010	0.2205	54.5829	-0.0011
Collision energy (kJ)	147.693	152.546	-0.0329	146.240	0.0098
Simulation time (t)	0.0522	0.0580	-0.1111	0.0596	-0.1418

6.3 Highway Vehicle Collision Modelling

This Section introduces the three-lane highway scenario and the basic physics between two colliding bodies, i.e. vehicles. The need for simplified lumped mass

models was introduced in Sections 6.1 and 6.2, therefore in this Section a linear and bilinear two-lumped mass model is developed and simulated. For each of the modelled vehicles, it is assumed that the rear and front crash structures of the vehicle have identical stiffness. It is further assumed, to simplify the problem that all the vehicles in the simulation have the same structural stiffness values. Therefore, the tuning parameters captured for the linear and bilinear models from Section 6.2 are used for the corresponding models developed in this Section. An example scenario of the three-lane highway scenario is given at the end of the Section to demonstrate the effectiveness of the approach.

6.3.1 Three-Lane Highway Scenario

To investigate the collision outcomes of three highway collision scenarios, the collision modelling is undertaken in two stages. The first stage of the collision event involves the Host Vehicle, denoted V_H colliding into a vehicle ahead, denoted V_{a_n} where n is the lane number, i.e. 1, 2 or 3, as illustrated in Figure 6-11. It is the role of the Host Vehicle to determine the collision path, i.e. steering into either V_a, V_{a_2} or V_{a_3}. It is assumed within this research that the Host Vehicle can undertake the steering manoeuvre to achieve a full frontal-rear collision, i.e. with no offset. This has the effect of maximising the frontal crash structure area which deforms in the collision. It is assumed that this collision then leads to a secondary collision with a vehicle behind colliding into the primary stage of the collision, as illustrated in Figure 6-12. It is further assumed that the vehicles involved in the first stage are combined and share a common final velocity, denoted v_a. An example is given in Figure 6-12, where the Host Vehicle has made a decision to steer and collide into V_{a_1}. In this case, the secondary collision will involve V_{b_1} colliding into the combined vehicle mass and velocity of V_H and V_{a_1}. This is an example of one possible two-stage collision, with a total of three given in Table 6-6, where the example given is Collision 1.
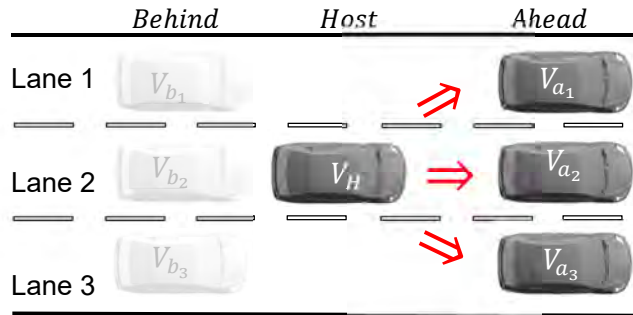
Figure 6-11 - Host Vehicle with Three Possible Collision Paths
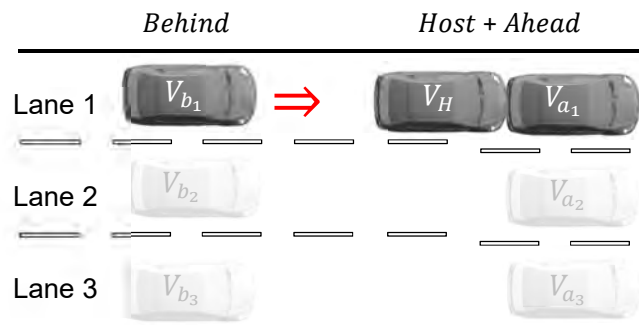
Figure 6-12 - Secondary Collision Involving a Vehicle Behind Colliding into Two Combined Vehicles

Table 6-6 - Autonomous Vehicle Collision Paths

Collision	First Collision Stage	Secondary Collision Stage
1	$V_H \Rightarrow V_{a_1}$	$V_{b_1} \Rightarrow \left(V_H + V_{a_1}\right)$
2	$V_H \Rightarrow V_{a_2}$	$V_{b_2} \Rightarrow \left(V_H + V_{a_2}\right)$
3	$V_H \Rightarrow V_{a_3}$	$V_{b_2} \Rightarrow \left(V_H + V_{a_3}\right)$

6.3.2 Physics of Two Colliding Vehicles

This sub-section builds on Section 6.2.1, where an introduction into vehicle crashworthiness is given. The physics of two colliding inelastic bodies that represent a vehicle to vehicle collisions is introduced, i.e. conservation of momentum and energy, and the total combined energy absorption of two colliding inelastic bodies. The physics of the highway collision scenario in Section 6.3.1 is checked to ensure the verification of the highway collision model for use in the later Sections.

It is well known from Newtonian dynamics that when two bodies collide, as in the case illustrated in Figure 6-12, the resulting momentum of the combined body is given by the momenta of the two bodies prior to the collision, i.e. the momentum of the two moving bodies, is conserved within the single combined moving body. This may be expressed as follows:

$$M_a\overrightarrow{v_a} + M_b\overrightarrow{v_b} = M_{a+b}\overrightarrow{v_f} \qquad (6\text{-}18)$$

where M_a and M_b denote the masses of two colliding vehicles (namely Vehicles a and b), $\overrightarrow{v_a}$ and $\overrightarrow{v_b}$ denote the velocities of the two vehicle masses and $\overrightarrow{v_f}$ denotes the final velocity of the combined vehicle mass, denoted M_{a+b}, where $M_{a+b} = M_a + M_b$. The pre- and post-impact conditions are illustrated in Figure 6-13 (Top) and Figure 6-13 (Bottom), respectively.

Pre-collision

Post-collision
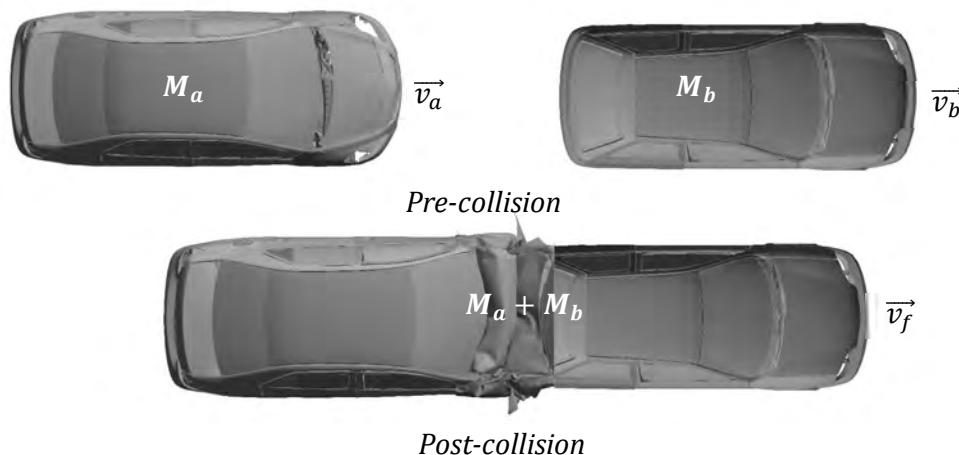
Figure 6-13 – Illustrating Pre- and Post-Impact Conditions of Two Colliding Vehicles

The arbitrary illustrative example given by Equation (6-18) and shown in Figure 6-13 indicates that the momentum $M_a\overrightarrow{v_a}$ is greater than $M_b\overrightarrow{v_b}$ and, noting the same direction of motion of the two moving vehicles, it is clear that $M_{a+b}\overrightarrow{v_f}$ has the same sign as $M_a\overrightarrow{v_a}$, hence the same direction of travel for the combined body. Rearranging Equation (6-18), the final velocity of the combined mass can be expressed as follows:

$$\overrightarrow{v_f} = \frac{M_a\overrightarrow{v_a} + M_b\overrightarrow{v_b}}{M_{a+b}} \tag{6-19}$$

The principle of conservation of energy states that the kinetic energy pre- and post-collision must be identical. This may be expressed as follows:

$$\frac{1}{2}M_a\overrightarrow{v_a^2} + \frac{1}{2}M_b\overrightarrow{v_b^2} = \frac{1}{2}M_{a+b}\overrightarrow{v_f^2} + \Delta E \tag{6-20}$$

where ΔE denotes the collision deformation energy. It is possible from Equation (6-20) to deduce and pre-determine the collision energy from a two vehicle collision scenario.

In the event of a two vehicle full-frontal impact collision, when the vehicles collide, equal and opposite forces are applied to the two vehicles collision structures. The following is given:

$$f_a = M_a a_a \tag{6-21}$$

and

$$-f_b = -(M_b a_b) \tag{6-22}$$

where a_a and a_b represent the two vehicle's accelerations and f_a and f_b represent the two vehicle's opposing forces, respectively. In the case of an increase in one of the vehicles mass values (due to passenger numbers and luggage) and assuming the two colliding vehicles have identical collision structures (i.e. stiffness and geometry), this would result in a lower acceleration being experienced by that vehicle and a higher acceleration experienced by the other vehicle.

As with the single vehicle case, detailed in Section 6.2.1, the amount of deformation to each of the vehicles' collision structures will depend on the structural stiffness, vehicle mass and initial impact velocity. Considering the structural stiffness, the following equations are given for the two vehicles:

$$f_a = k_a x_a \tag{6-23}$$

and

$$-f_b = -(k_b x_b) \tag{6-24}$$

where k_a and k_b denote the structural stiffness values of the two vehicles respectively, and x_a and x_b denote the two vehicle's deformations respectively. Assuming the vehicles have identical structural stiffness, the result of a two vehicle collision would result in equal deformation. Considering the case when the vehicles have the same structural stiffness properties and considering the following for Vehicle a:

$$\Delta E_a = f_a x_a \tag{6-25}$$

informs us that the collision energy share between the two colliding vehicles must also be equal, as the forces and deformations are equal on both vehicles.

6.3.3 Linear Lumped Mass Modelling and Simulation

Building on the single vehicle lumped mass modelling in Section 6.2, a two-stage highway platoon model is developed, as detailed in Section 6.3.1. To the knowledge of the author, collision modelling of multiple convoy vehicles using lumped parameter models have not been undertaken to represent such a collision.

Each vehicle is described as a single lumped mass and a linear spring element, modelled as a dynamic second-order system. The first stage involves the host vehicle V_{Hf}, where subscript f refers to the front spring stiffness of this vehicle, colliding with the rear of a vehicle ahead V_a. The second stage is when a Vehicle Behind V_b collides into the rear of the Host Vehicle V_{Hr}, where subscript r refers to the rear spring stiffness of this vehicle, after the collision with V_a. The free-body representations of the two-

stage collisions are represented in Figure 6-14 and Figure 6-15, respectively, where the Host Vehicle is described as V_H, Vehicle masses are denoted by M_{V_n}, and spring stiffness k_{Hfr_n}, where n denotes the vehicle identification for a multiple lane scenario (nodal representation). The contact between the colliding vehicles is represented by mass M_c which is set to be arbitrarily low. With the 3 individual masses, the system is now a 6th order mathematical model. Simulating a full frontal-rear collision, the spring sections both compress, with mass M_c acting as the datum point. This is the reference point for the vehicle deformations. It must be noted that depending on the combined two vehicle structure's momentum, within its own reference frame this datum point shall move. Using the first stage collision (Figure 6-14) the degrees of freedom are given by deformations x_H, x_c and x_a.
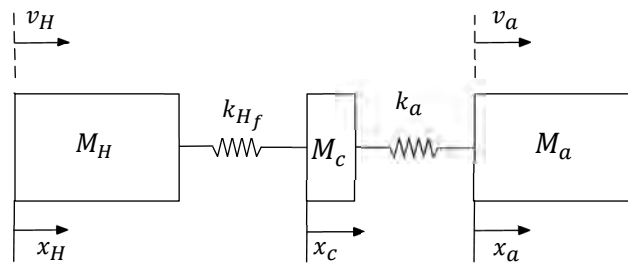
Figure 6-14 - Lumped Mass Model of Rear-End Collision Stage One
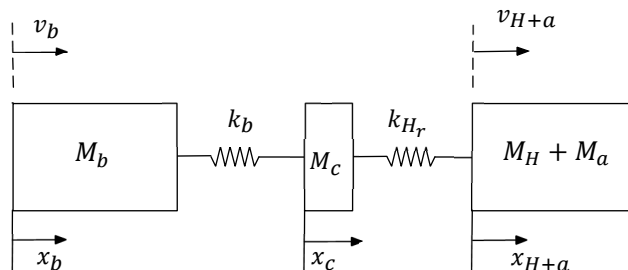
Figure 6-15 - Lumped Mass Model of Rear-End Collision Stage Two

The following coupled differential equations describe the first stage of the two vehicle collisions from Figure 6-14:

$$M_H \ddot{x}_H + k_{Hf}(x_H - x_c) = 0 \qquad (6\text{-}26)$$

132

$$M_c\ddot{x}_c + k_{H_f}x_H + \left(k_a - k_{H_f}\right)x_c + k_a = 0 \qquad (6\text{-}27)$$

$$M_a\ddot{x}_a + k_a(x_a - x_c) = 0 \qquad (6\text{-}28)$$

The second stage detailed in Figure 6-15 results in the following coupled differential equations:

$$M_b\ddot{x}_b + k_b(x_b - x_c) = 0 \qquad (6\text{-}29)$$

$$M_c\ddot{x}_c + k_b x_b + \left(k_{H_r} - k_b\right)x_c + k_{H_r} = 0 \qquad (6\text{-}30)$$

$$(M_H + M_{V_a})\ddot{x}_H + k_{H_r}(x_H - x_c) = 0 \qquad (6\text{-}31)$$

This two stage collision assumes the Host Vehicle V_H impacts the Vehicle Ahead V_a first, then the Vehicle Behind V_b impacts the Host Vehicle V_H. If the collisions occurred the other way, it is a simple matter of re-ordering the terms in the same equations. Stage one would use the terms of the Vehicle Behind V_b and Host Vehicle V_H, and the second stage would use the combined mass of the Host Vehicle V_H and Vehicle Behind V_b colliding with the Vehicle Ahead V_a.

A second order matrix differential equation for the 1st stage of the collision can represent the unforced collision of two vehicles in nodal coordinates, given by:

$$M_n\ddot{x} + K_n x = 0 \qquad (6\text{-}32)$$

where the mass and stiffness matrices are given, respectively, by the following:

$$M_n = \begin{bmatrix} M_H & 0 & 0 \\ 0 & M_c & 0 \\ 0 & 0 & M_a \end{bmatrix} \qquad (6\text{-}33)$$

$$K_n = \begin{bmatrix} k_{H_f} & -k_{H_f} & 0 \\ -k_{H_f} & (k_{H_f} + k_a) & -k_a \\ 0 & -k_a & k_a \end{bmatrix} \qquad (6\text{-}34)$$

and x and $\ddot{x}$ denote the vector quantities, given by:

$$x = \begin{bmatrix} x_H \\ x_c \\ x_a \end{bmatrix} \text{ and } \ddot{x} = \begin{bmatrix} \ddot{x}_H \\ \ddot{x}_c \\ \ddot{x}_a \end{bmatrix} \tag{6-35}$$

Equation (6-32) is multiplied by the matrix inverse of M_n in Equation (6-33) to give:

$$\ddot{x} + \widetilde{K}_n x = 0 \tag{6-36}$$

where the normalised nodal stiffness to mass ratio matrix is given by $\widetilde{K}_n$ of the collision model for the two vehicles is given by:

$$\widetilde{K}_n = - \begin{bmatrix} \dfrac{k_{H_f}}{M_H} & -\dfrac{k_{H_f}}{M_H} & 0 \\ -\dfrac{k_{H_f}}{M_c} & \dfrac{(k_{H_f} + k_a)}{M_c} & -\dfrac{k_a}{M_c} \\ 0 & -\dfrac{k_a}{M_a} & \dfrac{k_a}{M_a} \end{bmatrix} \tag{6-37}$$

Figure 6-16 illustrates the MATLAB/Simulink modelling of the two vehicle collision model. Subscript a denotes the vehicle ahead, whilst subscript b denotes the vehicle behind, m and k represent the mass and spring stiffness of the vehicles. Subscript c denotes the datum point. Both the vehicle ahead and behind have three outputs which are Force, Acceleration and Deformation. The velocities of the vehicles are input to the simulation as the initial conditions on the first integrals, illustrated in Figure 6-16. These initial conditions are the impact velocities of the vehicle collisions.
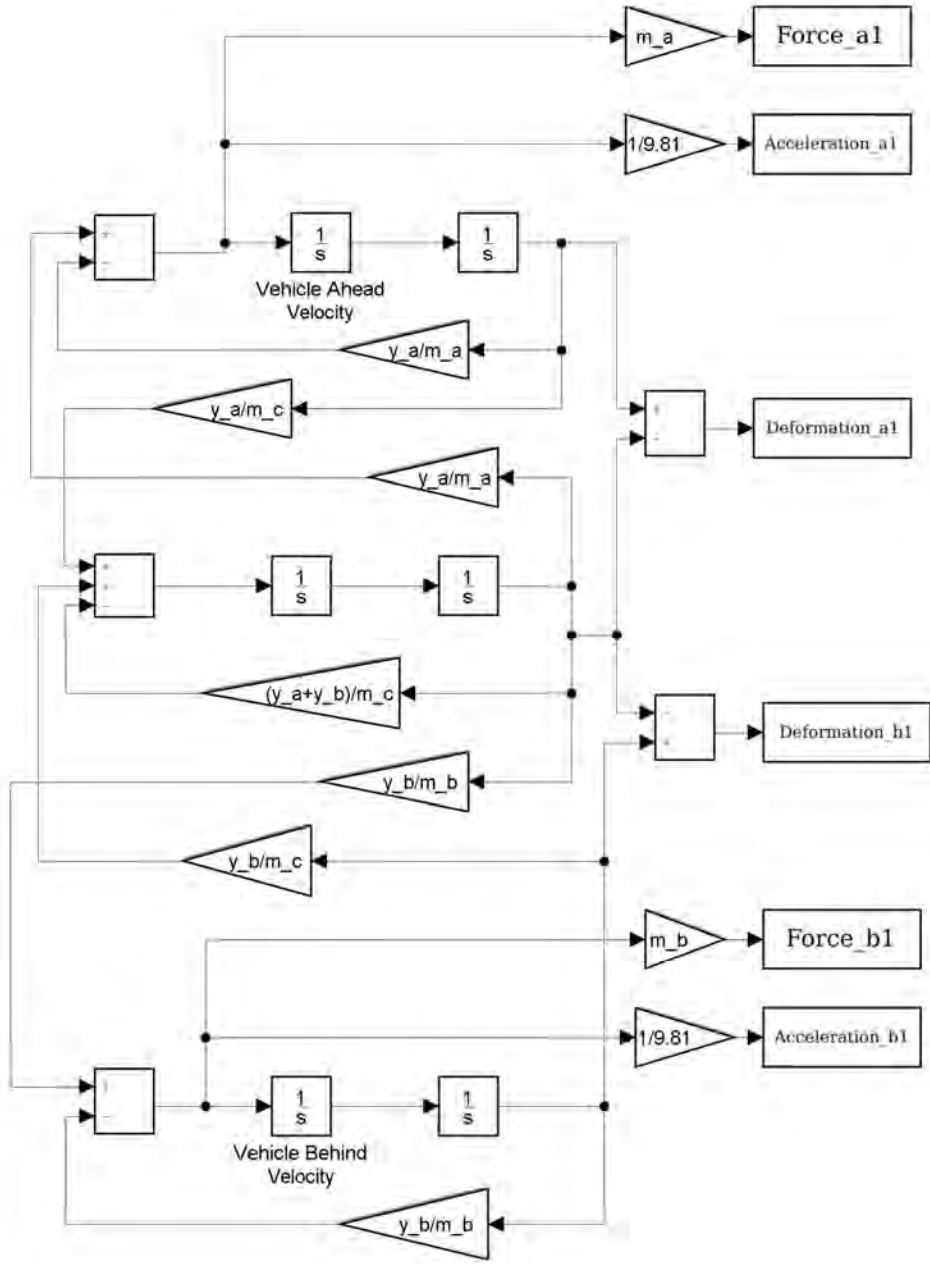
Figure 6-16 - Simulink Block Diagram Representing Linear Lumped Mass Modelling of Two Vehicle Collision

6.3.3.1 Validation of Model

For the simulation of the two-vehicle model developed in this Section, initially a full frontal impact collision scenario is set-up based on the US NCAP initial test conditions, i.e. two vehicles travelling in opposite directions at $35mph$ (i.e. $15.6464m/s$). This is initially undertaken to ensure the model's dynamics behave as would be expected, detailed in Section 6.3.2. The model tuning parameters as determined in Section 6.2.5 are used for the two-vehicle full-frontal collision (as identical vehicles are used) and the simulation of deformation was taken up to the first ¼ cycle (the corresponding time for peak deformation was used for all the graphical outputs).The same outputs as in the single vehicle case in Section 6.2 are of interest, i.e. peak deformation, peak acceleration and collision energy. The graphical outputs relating to these are given in Figure 6-17. It is visibly clear that the deformation and acceleration versus time graphical outputs of the two vehicles are identical, as would be expected when considering the physics, as detailed in Section 6.3.2. The peak values of the graphs are also identical to those presented in Table 6-3.
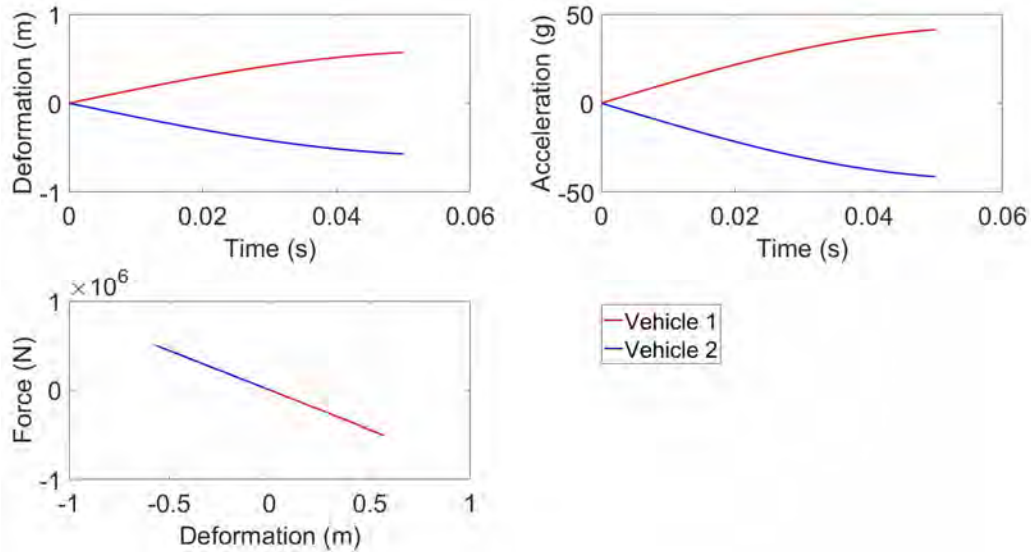
Figure 6-17 – Graphical Outputs from the Linear Two-Vehicle Full Frontal Impact with both Vehicles having Identical Properties

As a further verification check that the model operates as the physics suggests in Section 6.3.2, the mass and velocity of the second colliding vehicle is varied (with the first vehicles properties remaining as above, i.e. $1247kg$ and $15.6464m/s$). Figure 6-18 illustrates the case where the second colliding vehicle mass is increased by a factor of 1.5, i.e. 1.5 x $1247kg$ (with the velocities remaining the same). As would be expected, based on Section 6.3.2, the deformations and forces of the two colliding vehicles are equal and opposite, respectively, (due to the stiffness values of the vehicles being the same). However, the accelerations between the vehicles vary, with the lighter vehicle experiencing higher acceleration and the heavier vehicle experiencing lower acceleration, as would be expected. Figure 6-19 illustrates the case where the second colliding vehicle's velocity was increased from $15.6464m/s$ ($35mph$) to $22.3520m/s$ ($50mph$), with the first vehicle's properties remaining as above (with the vehicle masses being equal). Again, as would be expected, based on the collision physics in Section 6.3.1, the peak deformation, peak acceleration and collision energy are equal and opposite. It can be confirmed from these initial model verification checks that the developed two-vehicle full frontal collision scenarios are producing results as would be expected.
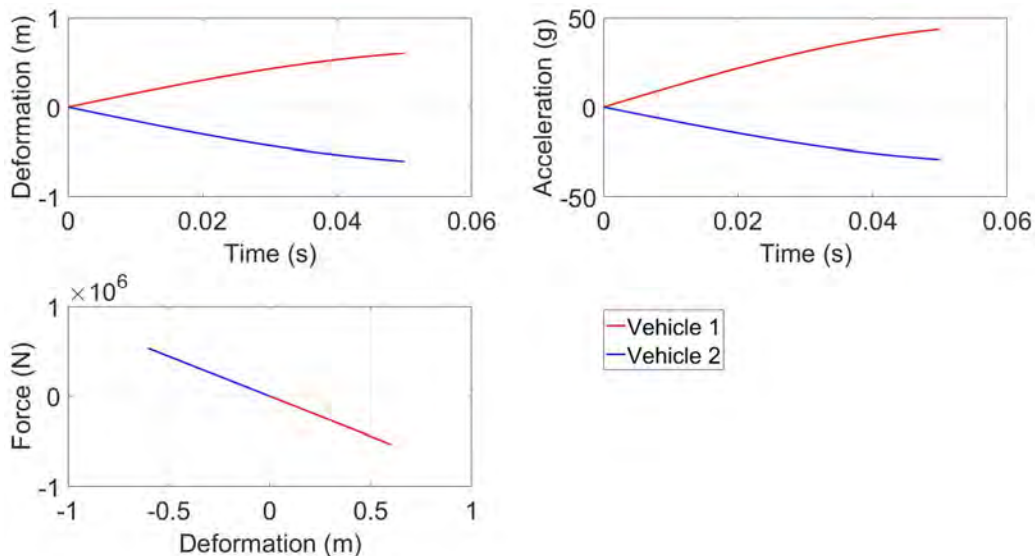
Figure 6-18 - Graphical Outputs from the Linear Two-Vehicle Full Frontal Impact with One Vehicle having a Higher Collision Mass
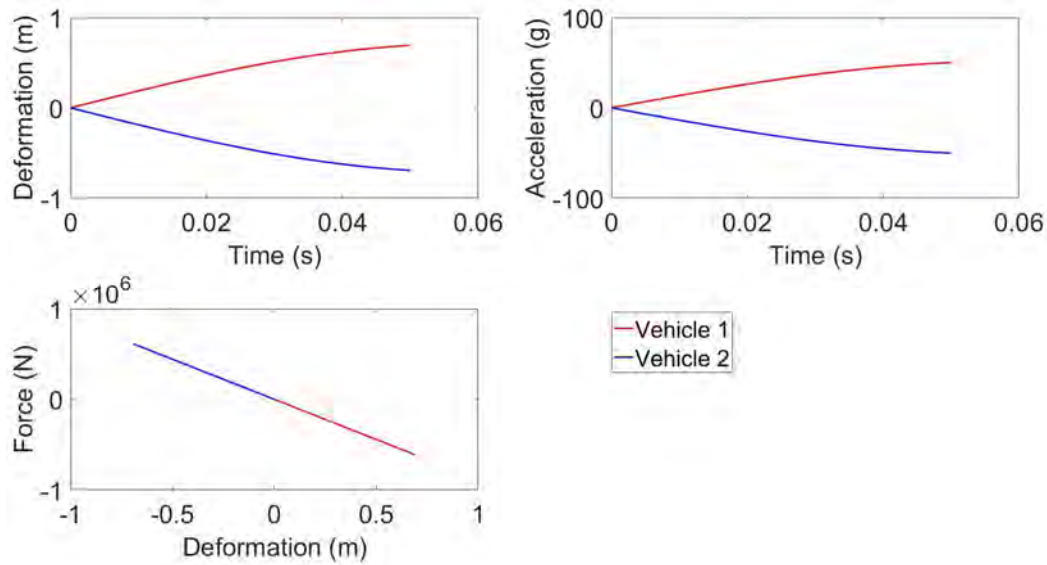
Figure 6-19 - Graphical Outputs from the Linear Two-Vehicle Full Frontal Impact with One Vehicle having a Higher Collision Velocity

6.3.4 Bilinear Lumped Mass Modelling and Simulation

Due to the inaccuracies of using a linear collision model, further attention is needed to develop a simulation model that can be used and relied upon for the collision modelling here. In Pickering et al. (2018) a bilinear model has been developed to simulate the accelerations and collision deformation energy of a full-frontal collision. Pickering et al. (2018) state that "*Bilinear system models are characterised by an input dependent dynamic and steady state behaviour.*" When considered independently, the models are described as linear for both the system state and control input, with the coupled terms which involve products of internal system state and control, and give rise to the bilinear properties as follows:

A second order dynamic bilinear system involving a bilinear function is formed with the state-dependent spring stiffness as:

$$M_n \ddot{x} + [K_n + \Lambda]x = 0 \tag{6-38}$$

where the bilinear function Λ is:

$$\Lambda = \begin{bmatrix} \eta_H f_H & & \\ & 0 & \\ & & \eta_a f_a \end{bmatrix} \tag{6-39}$$

with the coefficients of bilinear multiplicative terms of the single mass models given by η_H and η_a for the Host Vehicle and vehicle ahead respectively. The initial conditions generated from the mass and collision velocity generates the internal input forces f_H and f_a, again for the Host Vehicle and vehicle ahead respectively. $\overline{K}_{ab}$ denotes the normalised bilinear nodal stiffness matrix ($[K_n + \Lambda]$) represented by:

$$\overline{K}_{ab} = -\begin{bmatrix} \dfrac{k_{H_f}}{M_H} + \eta_H|\ddot{x}_H| & -\dfrac{k_{H_f}}{M_H} & 0 \\[2mm] -\dfrac{k_{H\_f}}{M_c} & \dfrac{(k_{V_H} + k_a)}{M_c} & -\dfrac{k_a}{M_c} \\[2mm] 0 & -\dfrac{k_a}{M_{V_a}} & \dfrac{k_a}{M_a} + \eta_a|\ddot{x}_a| \end{bmatrix} \tag{6-40}$$

Figure 6-20 shows the Simulink model of the bilinear two-vehicle collision. It is similar to Figure 6-16, except that the spring stiffness has a multiplication factor y and the feedback of the deformation goes through a gain n. The velocities of the vehicles at impact are input as the initial conditions in the first integrals, which are labelled Vehicle Ahead Velocity and Vehicle Behind Velocity. In Figure 6-20, subscript a denotes the vehicle ahead, c denotes the datum point, and the vehicle behind is denoted by subscript b. From Equations (6-38) and (6-40) the Host Vehicle is represented by the vehicle behind.

To ensure the model was performing subject to the collision physics in Section 6.3.2, the same scenarios were simulated in Section 6.3.3, i.e. in the linear case. Figure 6-21 highlights the case where the two colliding vehicles have identical properties, it can be seen that the collision outputs match that of the single vehicle into an immovable rigid barrier as given in Section 6.2.5, see Figure 6-10. Figure 6-22 illustrates the case where the second colliding vehicles mass was increased by a factor of 1.5, i.e. 1.5 x $1247kg$ (with the velocities equal). As would be expected based on Section 6.3.2, the deformations and forces of the two colliding vehicles are

equal and opposite (due to the stiffness's of the vehicles being the same). However, the accelerations between the vehicles differ, with the lighter vehicle experiencing higher accelerations and the heavier vehicle experiencing lower accelerations, as would be expected. Figure 6-23 illustrates the case where the second colliding vehicle's velocity was increased from $15.6464m/s$ ($35mph$) to $22.3520m/s$ ($50mph$), with the first vehicles properties remaining as above (with the vehicle masses equal). Again, as would be expected based on the collision physics in Section 6.3.1, the overall peak deformation, peak acceleration and collision energy values increase. All the properties are equal and opposite and in agreement with the laws of physics. The dynamics observed from the bilinear model match that of the linear model. It can be confirmed from these initial verification checks that the developed two-vehicle full frontal collision is doing as would be expected.
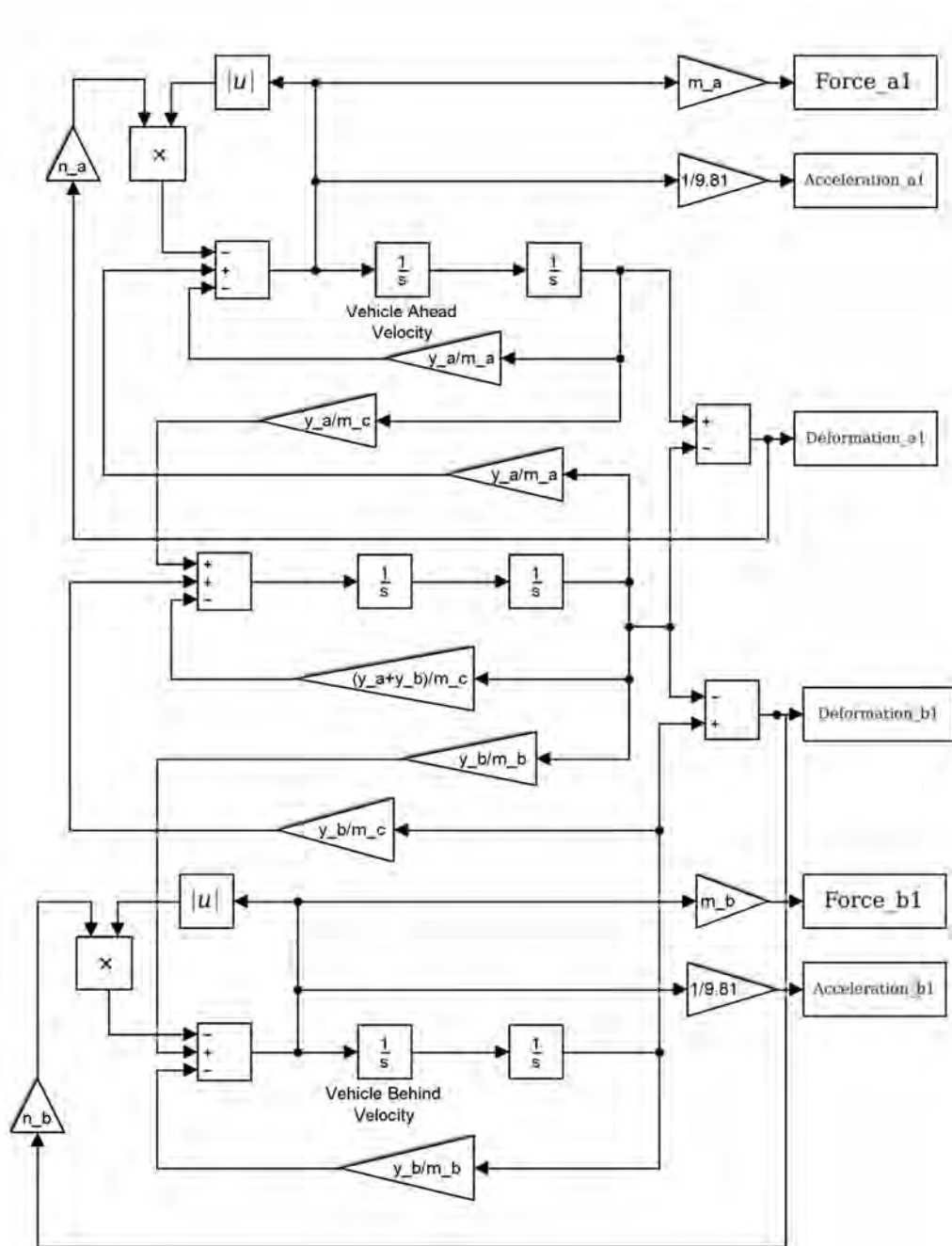
Figure 6-20 - Simulink Block Diagram Representing Bilinear Lumped Mass Modelling of Two Vehicle Collision
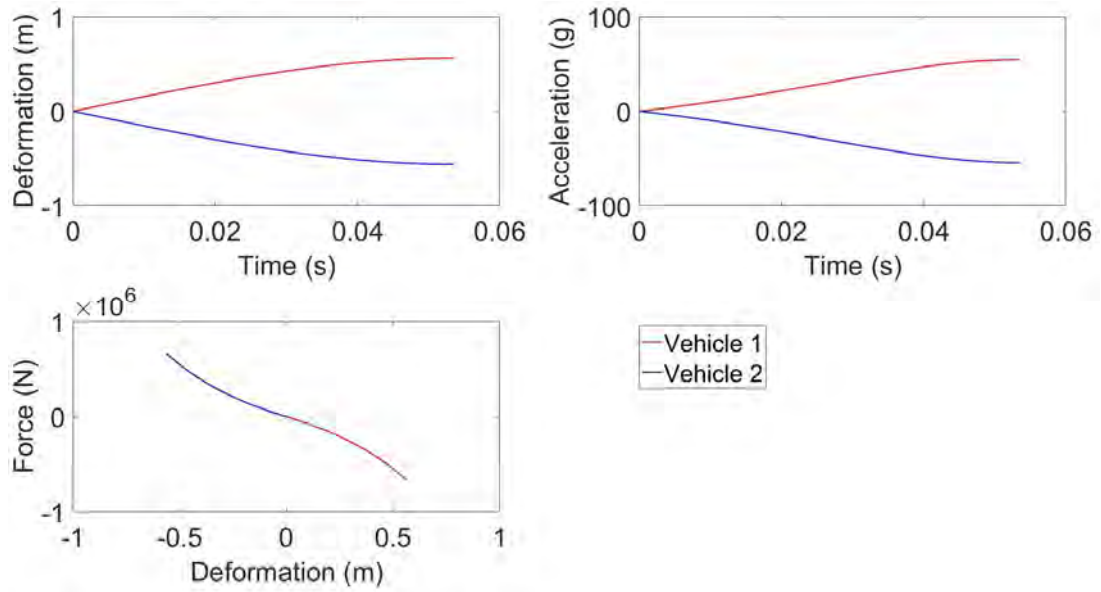
Figure 6-21 - Graphical Outputs from the Bilinear Two-Vehicle Full Frontal Impact with both Vehicles having Identical Properties
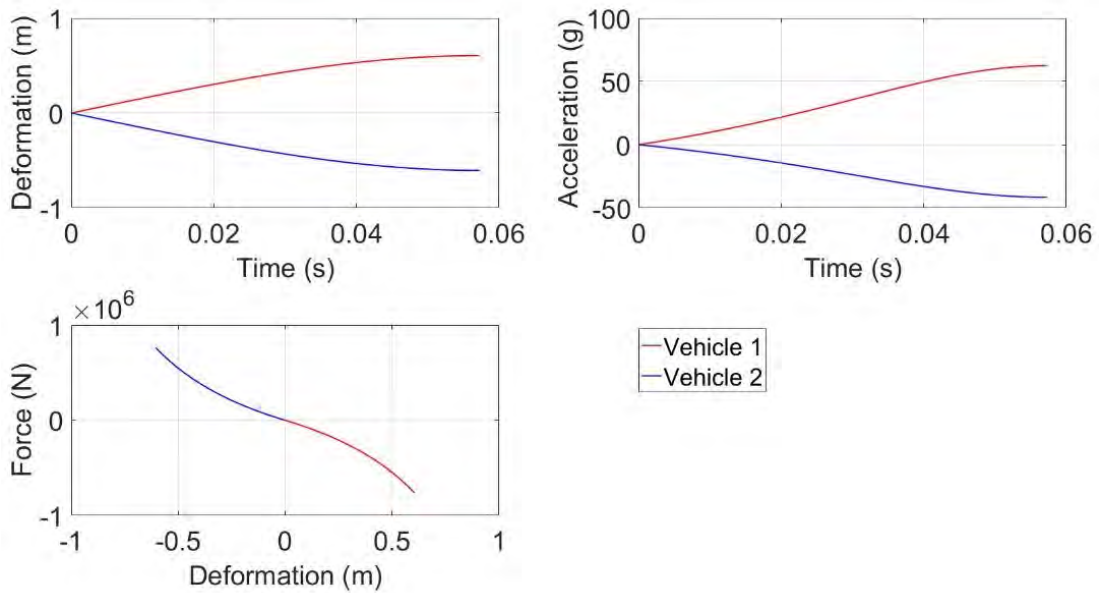
Figure 6-22 - Graphical Outputs from the Bilinear Two-Vehicle Full Frontal Impact with One Vehicle having a Higher Collision Mass
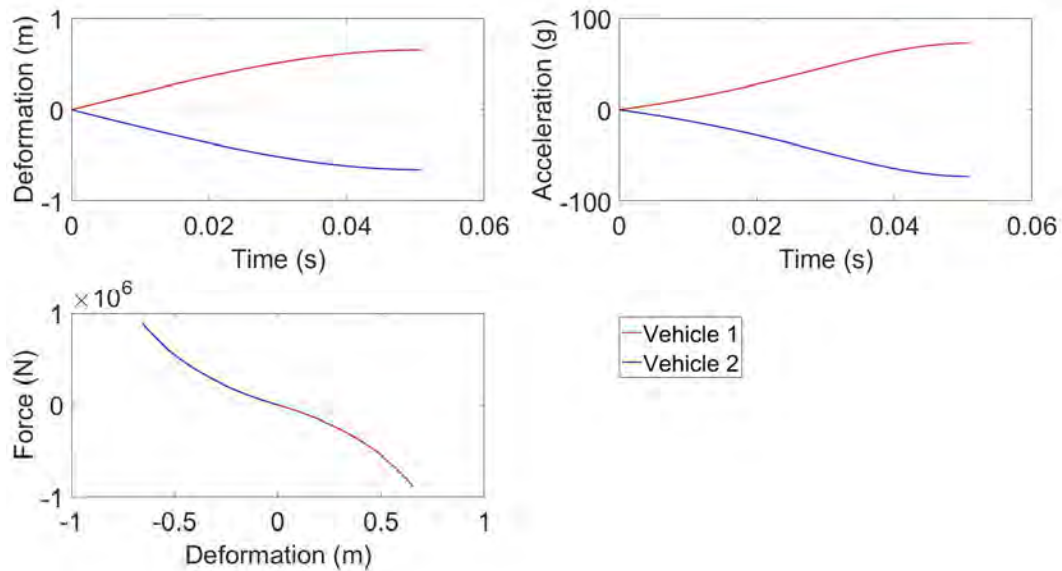
Figure 6-23 - Graphical Outputs from the Bilinear Two-Vehicle Full Frontal Impact with One Vehicle having a Higher Collision Velocity

6.3.5 Example Scenario

The two vehicle collision model developed in Section 6.2.4 is used to simulate the two-stage highway collision detailed in Section 6.3.1. The vehicle model in this case will involve the collision velocities acting in the same direction, i.e. convoying in the same direction. The rear-end spring stiffness of the vehicles in convoy on the highway simulations will assume to be equal, therefore, an assumption is made that a vehicles front end stiffness is identical to that of the rear. It is further assumed that all vehicles in the simulation have identical stiffness, i.e. collision structures. This modelling method has the potential to be used for vehicles with different crash structure stiffness values, this would require further FEA data to tune those models. This section serves to present the highway model working with an example scenario.

6.3.5.1 First Stage of the Highway Collision

This sub-section details the first stage of the highway collision scenario detailed in Section 6.3.1. For the rear-end collision simulations the vehicle ahead will be travelling at $22.3520m/s$ ($50mph$), whilst the vehicle behind impacts the vehicle ahead at a velocity of $31.2928m/s$ ($70mph$). The Toyota Yaris with mass of $1247kg$

will be the lightest vehicle (this being the laden vehicle mass), an increase to the mass will be known as the medium mass, given as $1500kg$ and the large mass vehicle will be $1750kg$, as detailed in Table 6-7. The full results are presented in Table 6-7 and an example graphical output from one of the scenarios is given in Figure 6-24. The scenario considered involves the $1750kg$ vehicle behind colliding into the vehicle ahead with a mass of $1247kg$. The model dynamics are as would be expected by the collision physics detailed in Section 6.3.2.

Table 6-7 – Highway Collision Simulation Results from the First Stage

Vehicle Behind		1247kg Vehicle		1500kg Vehicle		1750kg Vehicle	
		1247kg Vehicle	Vehicle Behind	1800kg Vehicle	Vehicle Behind	2400kg Vehicle	Vehicle Behind
1247kg Vehicle	Deformation (m)	0.1830	0.1830	0.1908	0.1908	0.1970	0.1970
	Acceleration (g)	11.7284	11.7284	10.2377	12.3147	9.1008	12.7829
	Energy (kJ)	12.466	12.466	1.3614	1.3614	15.637	15.637
	Combined Velocity after collision (m/s)	26.8201		26.4101		26.0712	
1500kg Vehicle	Deformation (m)	0.1909	0.1909	0.1998	0.1998	0.2069	0.2069
	Acceleration (g)	12.3147	10.2377	10.8031	10.8031	9.6514	11.2599
	Energy (kJ)	13.615	13.615	14.995	14.995	16.148	16.148
	Combined Velocity after collision (m/s)	27.2328		26.8262		26.4791	
1750kg Vehicle	Deformation (m)	0.1970	0.1970	0.2069	0.2069	0.2148	0.2148
	Acceleration (g)	12.7812	9.1075	11.2601	9.6515	10.0957	10.0957
	Energy (kJ)	14.556	14.556	16.148	16.148	17.495	17.495
	Combined Velocity after collision (m/s)	27.5734		27.1635		26.8225	
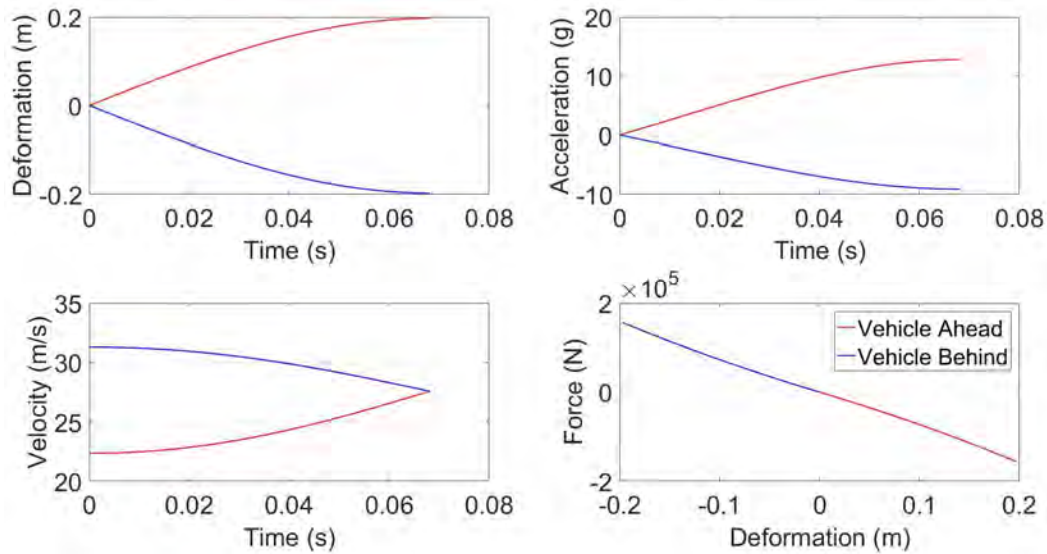
Figure 6-24 - Example Graphical Outputs from the Highway Collision Simulation Results from the First Stage

6.3.5.2   Second Stage of the Highway Collision

This sub-section details the first stage of the highway collision scenario detailed in Section 6.3.1. As in the first stage, the initial velocity of the vehicle behind colliding into the two combined vehicles ahead is travelling at a velocity of $31.2928m/s$ ($70mph$). The velocity of the two combined vehicles is captured from the first stage simulation, at the point whereby the two combined vehicles travel at a common velocity, as illustrated in Figure 6-24 for that example. The combined masses are as follows: $1247kg$ Vehicle and $1247kg$ Vehicle, $1247kg$ Vehicle and $1500kg$ Vehicle and $1247kg$ Vehicle and $1750kg$ Vehicle, as detailed in Table 6-8. The full results are presented in Table 6-8 and an example graphical output from one of the scenarios is given in Figure 6-25. The scenario considered involves the combined vehicle ahead being $1247kg$ Vehicle and $1750kg$ Vehicle and the vehicle behind being a mass of 1247kg. The model dynamics are as would be expected by the collision physics detailed in Section 6.3.2.

Table 6-8 - Highway Collision Simulation Results from the Second Stage

Vehicle Behind		1247kg Vehicle and 1247kg Vehicle		1247kg Vehicle and 1500kg Vehicle		1247kg Vehicle and 1750kg Vehicle	
		Vehicles Ahead	Vehicles Behind	Vehicles Ahead	Vehicle Behind	Vehicles Ahead	Vehicle Behind
1247kg Vehicle	Deformation (m)	0.2097	0.2097	0.2128	0.2128	0.2155	0.2155
	Acceleration (g)	6.8821	13.7642	6.3596	14.0095	5.9163	14.2191
	Energy (kJ)	16.618	16.618	17.149	17.149	17.607	17.607
1500kg Vehicle	Deformation (m)	0.2218	0.2218	0.2255	0.2255	0.2287	0.2287
	Acceleration (g)	7.3615	12.2396	6.8175	12.4851	6.3561	12.6994
	Energy (kJ)	18.728	18.725	19.396	19.396	19.987	19.987
1750kg Vehicle	Deformation (m)	0.2317	0.2317	0.2359	0.2359	0.2396	0.2396
	Acceleration (g)	7.7619	11.0618	7.2032	11.3069	6.7278	11.5219
	Energy (kJ)	20.561	20.561	21.368	21.368	22.085	22.085
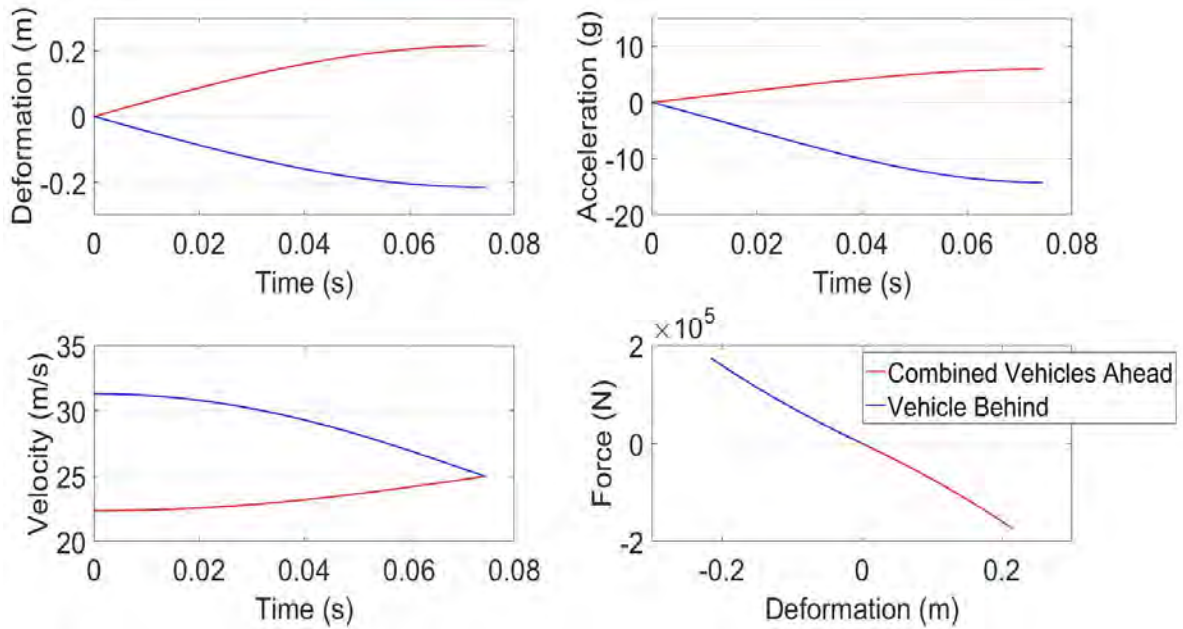
Figure 6-25 - Example Graphical Outputs from the Highway Collision Simulation Results from the Second Stage

6.4 Conclusions

A bilinear lumped mass model to simulate a multiple vehicle collision scenario is developed in this Chapter. The developed model comprises a nonlinear (bilinear) rear-end highway collision simulation initially between two vehicles. A Host Vehicle colliding into a vehicle ahead being the primary collision, and then when a vehicle behind collides into the primary collision, a secondary collision is simulated.

The bilinear model requires tuning, to obtain a closest representation of the FEA data. A Euclidean optimization process is proposed by the author of this thesis, which simulates a range of values for the bilinear term and a further tuning parameter. The simulated key properties of peak deformation, peak acceleration and collision energy are compared with the FEA data, and the minimum Euclidean metric norm indicates the most suitable model parameters. The Euclidean optimization also required refinement and tuning. It was found that initial values did not yield the most suitable model parameters. However, by narrowing the range of values in the search space the approach has been demonstrated to work effectively. Obtaining a set of model parameter values is clearly an area of further work.

Once tuned, it has been demonstrated that the bilinear model is able to simulate a multiple vehicle collision with acceptable accuracy, when considering the key collision properties. The results have been verified against the laws of physics to ensure that the simulated collision scenarios are justified.

The lumped mass modelling technique adapted and developed in this chapter provides a relatively fast and realistic simulation approach, which can be used to assess the severity of automotive collisions. It has been demonstrated that the modelling approach is able to simulate secondary collisions, implying that a multiple collision scenario involving any number of vehicles can, in principle, be evaluated, thus lending itself to assessing the potential impact in terms of the key properties.

Chapter 7

Motorway Simulation

7.1 Introduction

In the event of an unavoidable collision, an autonomous vehicle will need to make an informed decision on the best action to take with the aim of reducing the severity of a collision. For this purpose, a simulator of autonomous vehicles is developed that produces objective numerical outputs.

The simulator calculates metrics on possible collisions, for a 3-lane motorway situation. It must assess collisions if the Host Vehicle stays in its current lane, as well as to assess the outcomes should the Host Vehicle change the lane to avoid the hazard ahead. There also needs to be a consideration of secondary possible collisions, such as those that will occur if any vehicles behind collide with the Host Vehicle whilst it is trying to mitigate the initial collision ahead.

Once the required metrics are calculated, a decision on the best lane for the autonomous vehicle needs to be made. The decision method must guarantee that the selected output does not result in a more severe outcome than taking no action.

7.2 Definition of Motorway

First, the simulation requires a motorway to be modelled. Motorways (arterial roads) are considered as multiple high-speed lanes. Lanes are considered straight, so any directional control would be negligible. The important dimension is the width of each lane, which for simplicity will be assumed to be constant for each lane. Each lane width is set to $3.75m$, for a set number of lanes (n). This distance now better represents the lane width described by Leics.gov.uk (2016), as it is not just a steering manoeuvre but a three lane motorway which is simulated.

The current lane (CL) is the lane the host vehicle begins the simulation in. The number of lanes of the motorway is in fact irrelevant in this research. The host vehicle can be limited to a single lane change manoeuvre, so must not perform a lateral manoeuvre which exceeds this, as a large lateral manoeuvre has the potential of losing vehicle control by exceeding the maximum Yaw Rate. Decision control neglects all other lanes except those that fit the rule of +/- 1 lane from CL, and CL itself.

In the simulation, each lane is considered to have 2 vehicles, with velocity, headway distance and braking values. The headway of the vehicle ahead of the Host Vehicle in the current lane is specified as a function of time, in line with Adaptive Cruise Control (ACC). The deceleration value is set very high (e.g. $50m/s^2$) simulating a collision. The host vehicle velocity follows the vehicle ahead in the current lane.
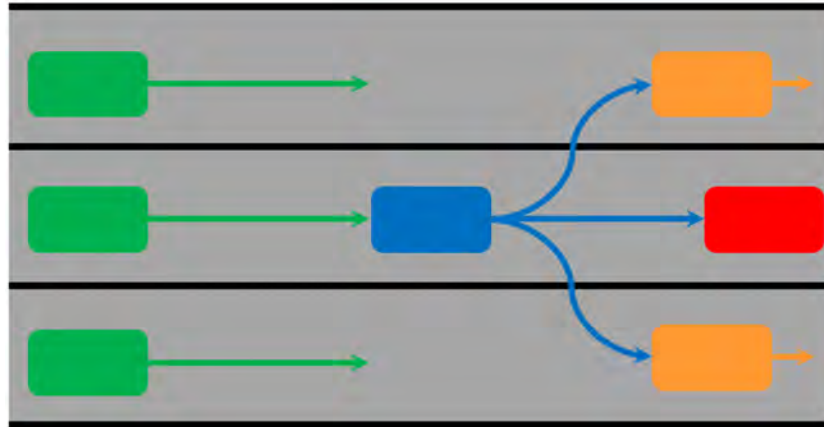
Figure 7-1 - Motorway Scenario

7.3 Linear Motorway Simulation

Chapter 7 will develop two motorway simulators which simulate the velocities and displacements of vehicles. One assumes V2V communication is not available and will require assumptions to simulate the behaviours of all vehicles. The second assumes that V2V communication will be available to provide the inputs for more accurate dynamic simulations. Assumptions that are relevant to both simulators are:

- The motorway is completely straight.
- All vehicles defined in the model are assumed to be in the centre of their lanes. This is just to calculate the required lateral distances, but in a real world application lateral distance could be calculated from the on-board sensor data.
- A no-deceleration scenario is assumed to determine if a lateral steering manoeuvre is possible. This is to avoid any possibility that the host vehicle can collide before the manoeuvre is completed, possibly resulting in a side-on collision.
- The steering manoeuvre for any direction is described by the longitudinal distance to vehicle ahead in the current lane. This ensures any steering manoeuvre is guaranteed to avoid any collision before completion.
- The simulation here uses inputted values for the calculations. For real-world applications these values would need to be acquired from on-board sensors, and confirmed to be accurate.

151

- All inputs required for the calculations are assumed to be available. Some parameters such as vehicle mass may only be available with V2V communication. It is assumed if a parameter is needed, it will be available.

The outputs from these simulators will be used to describe the severity of the potential collisions. The time to complete simulations is a concern, especially for the dynamic simulator, therefore simulation times will be compared to observe whether the simulator is impractical for implementation.

A motorway simulator is developed by starting with linear calculations of velocity and displacement relying on constant deceleration assumptions. The velocities and displacements of motorway and the Host Vehicle are simulated in discrete time steps. The time sampling rate is set to $0.001s$ for the simulations, which is used for all vehicles in the simulation, vehicles ahead, vehicles behind and Host Vehicle. The outputs of the simulation will provide a basis to describe the severity of the potential collisions in any of the simulated lanes. The velocity of all vehicles and moments of impact will inform the severity of the collision. The simulator must also determine whether a lane-change manoeuvre is safe to proceed, by assessing the manoeuvre capabilities of the host vehicle and whether collisions occur before a manoeuvre is complete. Collisions between the Host Vehicle and vehicles ahead and behind need to be evaluated.

Several methodologies are adapted from reviewing the simulators discussed in Section 2.5. Planning the steering trajectory cannot make the same assumptions as Hayashi et al. (2012) on full braking applied through the steering manoeuvre. The Cartesian coordinate system employed by Eidehall et al. (2007) is an effective method for plotting vehicle positions, which is used in this research. It is important to define the limitations of the host vehicle, as done by Anderson et al. (2010).

7.3.1 Motorway Vehicles Simulations

In order to determine the distance to impact and whether a collision into a vehicle ahead will occur before a manoeuvre is complete, the simulation will assume no-braking. This means the impact points of potential collisions with the vehicles ahead need to be calculated, and the host vehicle will be assumed to have no braking. This would result in the highest impact speed, and shortest distance to impact. It is this no-braking scenario that potential actions need to take into account. For the simulated lanes, the vehicle velocities and stopping distances are calculated. Based

on these a worst-case impact point is determined. This displacement is then assumed for the steering manoeuvre.

The SUVAT kinematic equations of motion given in Equation (5-14), and Equations (5-20) to (5-22) are used to simulate the position, velocity and deceleration of the simulated motorway vehicles. The SUVAT equations repeat the calculations for every discrete time step. The simulator calculates velocities and displacements in a given time step for all vehicles and compares them.

The vehicles ahead use a constant braking value assumed at the beginning of the simulation. This is the initial braking of the vehicle which may be determined by the Host Vehicle's sensors. However, there is an issue with the braking values of the vehicles behind. These will not have started braking, yet it is necessary to predict their actions to base a decision on. Without an assumed braking value, the simulation outputs are limited to a required braking value determined by the initial velocities and available braking distances. A braking value of the vehicles behind is assumed. For this, inspiration is taken from Driving Standards Agency for the Department for Transport (2007) which publishes the UK Highway Code as a set of rules and regulations for driving in the UK. Importantly, the Highway Code provides a generalised guide to car stopping distances. This is simply a guide according to which modern vehicles will certainly be able to achieve a greater deceleration. The stopping distances determine an assumed deceleration, which will be used for the vehicles where a deceleration value is not available, such as with the vehicles behind. Also, the Highway Code provides thinking distances, which is the distance the vehicle travels before braking is applied. This is a time delay applied to the velocities and displacements of the vehicles behind before they begin to decelerate. This is used in the simulator for assuming the velocities and displacements, giving potential impact velocities. Of course, this places strict assumptions in the simulator, but this allows impact velocities to be used for the later calculations.

The motorway is assumed to be perfectly straight, and the motorway vehicles do not change lanes. Therefore, directional factors do not need to be considered. It is only the longitudinal velocities and displacements that are being calculated.

7.3.2 Host Vehicle Braking

The constant deceleration assumption works well when the host vehicle stays in its current lane. However, the full braking that can be applied in this situation may not be possible when the host vehicle performs a lane-change manoeuvre into one of the adjacent lanes. Many parts of the steering controller as discussed in Chapter 5 are used to determine whether a steering manoeuvre is possible. Firstly, the Maximum available yaw rate is determined using Equation (5-5), for which Coefficient of Friction is required. Using the worst-case-scenario longitudinal distance, and known lateral distance, the steering trajectory to move into either the left or right lane is calculated. From this calculation the required yaw rate is found, and then it is determined if this exceeds the maximum available yaw rate. If it does, then the steering manoeuvres into the adjacent lanes are disqualified from the decision process.

Using the SUVAT equations the Host Vehicle's distance travelled with no braking is calculated. A point of impact for all vehicles under consideration is calculated, assuming no Host Vehicle braking (worst-case-scenario). From this worst-case-scenario collision, a required braking deceleration value is calculated. Of course, this value will not determine where an impact will occur, as a higher braking value would allow the vehicles ahead longer braking distances. But this value of deceleration of the Host Vehicle is used as a comparison for which lane would require the most braking effort of the Host Vehicle.

The longitudinal distance to the vehicle ahead in the same lane, is used for the steering trajectory. The yaw rate to complete the manoeuvre is calculated from this using Equations (5-6) to (5-8), which is used to determine the maximum available braking, using the 'g-g' diagram principle described in Section 5.8.1. This constant braking value produces new velocity and displacement values of the Host Vehicle. Using these values, and calculating a new impact point, the impact velocity and distance is found when the separation between the host vehicle and vehicles ahead reaches 0. In these calculations, distance travelled is simply the distance each vehicle travels for its given velocity. Displacement is the distance travelled plus the headway distance. Separation is the difference in displacement between the vehicles ahead on the simulated motorway and the host vehicle.

The lateral acceleration calculation follows the process described in Section 5.7.1, using Equations (5-14) to (5-21). Equation (5-22) gives the longitudinal

velocity, used for calculating the velocity of the Host Vehicle when it impacts the vehicles ahead and behind. For the simulation a unit circle 'g-g' diagram is assumed, utilising Equation (5-16), but the elliptical 'g-g' diagram could be applied if the Host Vehicle has different maximum longitudinal and lateral accelerations.

The no-braking scenario is assumed to ensure that any steering manoeuvre is allowed to be completed. A steering manoeuvre will only be allowed as a potential action if it can be guaranteed to be completed. If the Host Vehicle impacts or is impacted into before the manoeuvre is complete, this is considered to be an unacceptable scenario, as this is a different type of collision. The decisions based here must ensure a rear-end zero-lateral offset collision, for the safety of using the crash structures. Side-on collisions will effectively 'close' a lane, and that lane will be disqualified from the decision made.

7.3.2.1   Manoeuvre Acceleration

The decision to be made is based on metrics which describe the collision severity. It may also be beneficial to look at the severity of the manoeuvre itself, as this will describe if a steering or braking manoeuvre is severe for the vehicle occupants. The manoeuvre acceleration is calculated as the unit vector (a_v) of the longitudinal and lateral accelerations as follows:

$$a_v = \sqrt{a_x^2 + a_y^2} \qquad (7\text{-}1)$$

Lateral acceleration (a_y) is calculated using Equation (5-14). The longitudinal acceleration (a_x) is calculated from the SUVAT Equation (7-2), using the longitudinal velocity for v and u.

$$a_x = \frac{v_x - u_x}{t} \qquad (7\text{-}2)$$

7.3.2.2   Linear Vehicle Dynamics Limitations

The model developed has limiting factors that determine if a manoeuvre is possible, such as comparing the maximum manoeuvre yaw rate with the maximum allowable yaw rate as limited by friction. There are other factors, which can be considered to

make a quick decision on whether a manoeuvre is possible. These are the Skidding and Overturning speeds, given by Kett (1982).

$$Skidding\ Speed = \sqrt{\left\{ gr\left(\frac{\mu + \tan\theta}{1 - \mu\tan\theta} \right) \right\}} \qquad (7\text{-}3)$$

$$Overturning\ Speed = \sqrt{\left\{ gr\left(\frac{h\tan\theta + \frac{d}{2}}{h - \frac{d}{2}\tan\theta} \right) \right\}} \qquad (7\text{-}4)$$

where d is the vehicle track width, h is the height of the Centre of Mass (CoM), r is the radius of the turn (steady state) and θ is the bank angle of the road (assumed to be 0 for simulations).

The skidding speed describes the speed at which the coefficient of friction between the road surface and vehicle tyre will begin to skid for a given radius and velocity. The overturning speed describes the speed at which the height of the CoM will cause the inside wheels to have no vertical load forces.

These equations do assume steady-state conditions, which are not valid if braking velocity is taken into account. These equations are used as an indication of the skidding and overturning speeds, and are used as limiting factors. A quasi-state condition of a slowly changing deceleration best works with a dynamic simulator that can calculate the forces acting on the vehicle.

7.3.3 Linear Simulation Assumptions

The assumptions of this model and simulation are as follows:

- It must be noted that the velocity of a decelerating vehicle will likely not be linear, with aerodynamic and rolling resistances. However, the motorway simulation model needs to produce a numerical value with the available data, and resistance forces of all vehicles are not available. For simplicity, it is therefore assumed that all vehicles will maintain a constant rate of deceleration.
- For acquiring the relevant data including velocity and displacement, it is assumed that the closer the vehicle is to the hazard, the faster it can react. Therefore, by the time the Host Vehicle reacts, all vehicles ahead will have already started reacting, making all required data available. The same

therefore cannot be true of vehicles behind, which will not have started braking as they have not yet received the required information. As a result, the host vehicle may need to make assumptions on braking for the vehicles behind.

7.3.4 Linear Simulation Outputs

The outputs of the simulator which will inform the decision making are:

- Impact velocity with vehicle ahead (m/s)
- Required rate of deceleration for vehicles behind (m/s^2)
- Acceleration of Host Vehicle through manoeuvres (m/s^2). This describes the severity of the manoeuvre itself.
- Impact velocity with vehicle behind (m/s), using Highway Code assumed rates of deceleration.
- Lanes disqualified due to vehicle limitations or collisions occurring before manoeuvres are complete.

7.3.5 Linear Simulator Benchmark Parameters

The parameters that are inputted to the simulator will affect the outputted data for the decision making process. Each parameter will be tested on how it influences the decision made. First, a benchmark scenario is defined, where the Host Vehicle parameters are defined in Table 7-1, and the Motorway Vehicle parameters are defined in Table 7-2.

Table 7-1 - Host Vehicle Linear Simulator Benchmark Parameters

Parameter	Value
ACC Following Time	$1.4s$
Coefficient of Friction	0.7
Overall Manoeuvre acceleration	$8.83m/s^2$ ($0.9g$)
Maximum Host Vehicle Deceleration	$9m/s^2$
Height of CoM	$0.5m$
Track Width (front and rear)	$1.6m$

The following time is the time required for the autonomous vehicle to reach the rear of the vehicle ahead. The coefficient of friction is selected as 0.7 from Section 5.3.1, as this is more typical of a passenger vehicle on a dry road. Here, the motorway simulator is simulating a set scenario of a typical car on the road.

Table 7-2 - Motorway Vehicles Linear Simulator Benchmark Parameters

Parameter	Value
Mass of Vehicles Ahead	$2000kg$
Velocity of Vehicles Ahead	$70mph$
Headway Distance to Vehicles Ahead	$20m$
Braking Values of Vehicles Ahead	$7m/s^2$
Mass of Vehicles Behind	$2000kg$
Velocity of Vehicles Behind	$70mph$
Headway Distance of Vehicles Behind	$20m$

7.4 Dynamic Braking Simulation

The Linear Motorway Simulation of Section 7.3 is capable of producing useful outputs that inform a decision process to select the best lane for the host vehicle to drive into. However, the outputs can be made more accurate if the constant braking assumption is replaced by a dynamic braking simulator. This will rely more heavily on the capabilities of V2V to communicate the braking of other vehicles, but the assumption on V2V given in Section 7.3.3 is maintained.

7.4.1 Dynamic Braking Calculations

Rajamani (2011) gave the equation of motion for a vehicle:

$$M\ddot{x} = F_{xf} + F_{xr} - F_{aero} - R_{xf} - R_{xr} - Mgsin(\theta) \qquad (7\text{-}5)$$

where F_{xf} and F_{xr} are the longitudinal tyre forces at the front and rear respectively, F_{aero} is the aerodynamic drag force, M is vehicle mass, R_{xf} and R_{xr} are the Rolling Resistances at the front and rear respectively, $\ddot{x}$ is the second differential of

displacement (acceleration), and θ is the angle of incline. To simplify, the equation can be given as:

$$M\ddot{x} = F_{Long} - F_{Resistance} \qquad (7\text{-}6)$$

where F_{Long} is the forces acting from the vehicle to accelerate it, or decelerate by braking, and $F_{Resistance}$ is the total resistance forces of the aerodynamic drag, rolling resistance and gradient of incline. The motorway is assumed to be flat, meaning the gradient of incline is 0. Further on for simplicity, the forces of the front and rear axles will be calculated together, therefore $F_{Resistance}$ can be described as follows:

$$F_{Resistance} = F_{aero} + R_x + Mgsin(\theta) \qquad (7\text{-}7)$$

$$F_{aero} = \frac{1}{2}\rho C_d A_F (V_x + V_{wind})^2 \qquad (7\text{-}8)$$

where ρ is the density of air, C_d is the aerodynamic drag coefficient of the vehicle, A_F is the largest cross sectional area of the vehicle, V_x is the longitudinal speed, and V_{wind} is the headwind of the air the vehicle is driving through (assumed to be 0 for the simulation). A simplified equation for Rolling Resistance R_x is adapted from Yin and Jin (2013):

$$R_x = C_r Mg \qquad (7\text{-}9)$$

where C_r is the coefficient of rolling resistance.

Rolling Resistance can be modelled more accurately with tyre pressures, but for the purposes of this simulation, the static calculation is sufficient to display the effect mass has on vehicle acceleration.

To evaluate dynamic braking, two vehicles with identical parameters are simulated which are slowing to a complete stop. The only difference is each vehicle's mass. The parameters are given in Table 7-3. F_{Long} is the braking force applied by the vehicle, determined by $F_{Long} = Ma$, so a constant braking force for both vehicles is calculated by a desired rate of deceleration a.

Table 7-3 - Simulation Parameters

Parameter	Value
Initial Velocity	$30m/s$
Final Velocity	$0m/s$
A_F	$2.5m^3$
C_d	0.27
C_r	0.011
ρ	$1.225kg/m^3$
θ	$0degrees$
g	$9.81m/s^2$
a	$7m/s^2$

where A_F is the cross-sectional area of the vehicle, C_d is the aerodynamic drag coefficient, C_r is rolling resistance coefficient, ρ is the density of air, and θ is the gradient angle.

The values for parameters C_d and C_r are typical values given for an aerodynamic sports coupe vehicle driving on concrete or asphalt used by Bosch (2014). A_F is calculated by multiplying the maximum width and height of a Jaguar F-type, JAGUAR LAND ROVER LIMITED (2016), which is a representative of the aerodynamic coupe described by parameters C_d and C_r. The area calculated is rounded to the nearest $0.1m^2$ value. The only differing parameters are the masses of the two vehicles. Vehicle 1 has a mass of $1000kg$, while Vehicle 2 has a mass of $2500kg$.
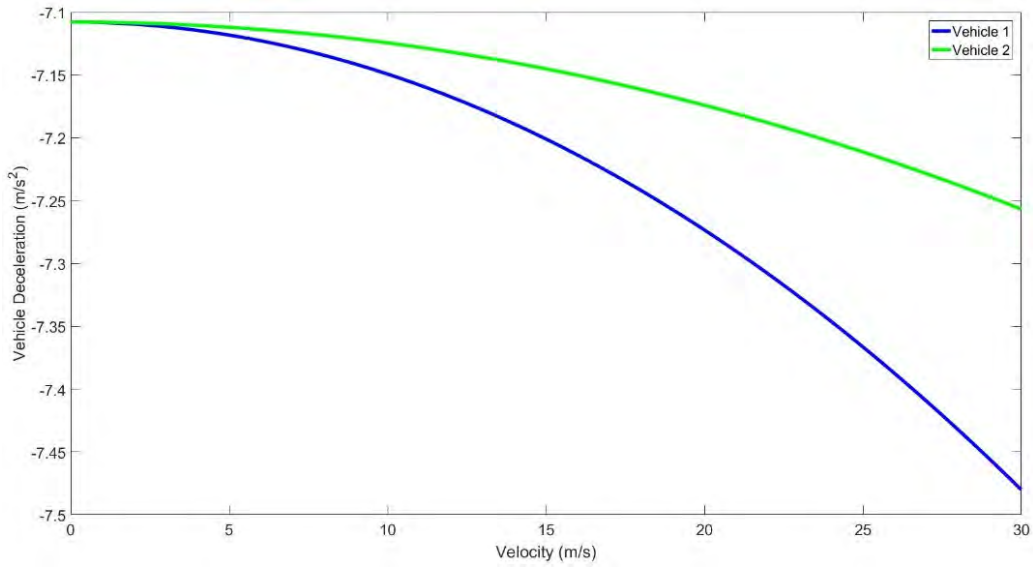
Figure 7-2 - Rates of Deceleration

Figure 7-2 shows that the lighter Vehicle 1 is able to achieve the higher maximum deceleration of -7.48m/s^2 , whilst vehicle 2 can only achieve -7.26m/s^2 at an initial speed of 30m/s. This is only a 0.22m/s^2 difference, but this will have an effect on the velocity and displacements of these two vehicles. As the vehicles reduce velocity, the difference in deceleration reduces, but it is clear that a lower mass allows the vehicle to reduce its speed more.
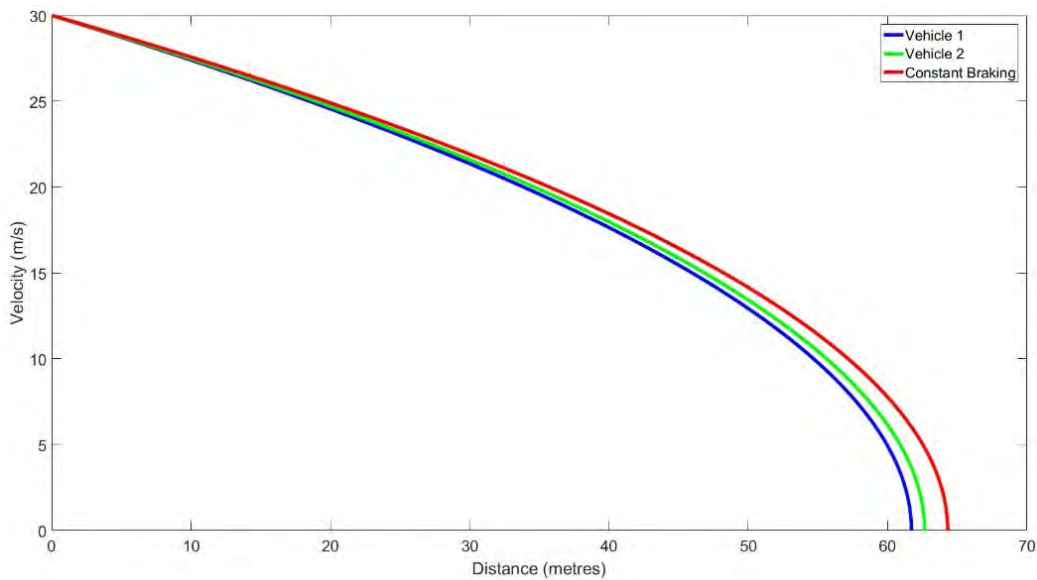
Figure 7-3 - Stopping Distances

Figure 7-3 shows the effect the different decelerations have on the stopping distances of the vehicles. The lighter vehicle 1 is able to come to a complete stop at $61.71m$, whilst vehicle 2 takes $62.66m$. This may not seem like a big difference ($0.95m$), but it does mean that the two vehicles will have different velocities and displacements at any given time, when only the mass parameter of the vehicles different.

Furthermore, this is compared to a constant braking scenario, which without the resistant forces calculated for the vehicle, takes $64.32m$ to stop. When developing the decision making process, it is important to consider that changing the mass of the vehicles, changes the velocities and displacements also. Therefore, by changing one parameter, mass, actually two outputs of the simulation, velocity and displacement. This will only affect scenarios when testing vehicles of different masses, but it must be noted that these vehicles will have different impact velocities.

Numerical Integration of Newton's 2nd Law is used to calculate the velocity and displacement of a dynamic moving object, as long as the force is a function of time. This method is used by Bathe and Baig (2005), and Savage, P. G. (1998). The implementation of this method in the dynamic braking simulator, is done by employing cumulative trapezoidal integration. Trapezoidal integration is used to integrate discrete data when the time of the samples is known, as it is in this simulator. Trapezoidal integration is also used by Bathe and Baig (2005).

$$v = \int a \, dt \qquad\qquad (7\text{-}10)$$

$$x = \int v \, dt \qquad\qquad (7\text{-}11)$$

7.4.2 Dynamic Tyre Force Vehicle Dynamics Modelling

In the dynamic braking simulator, it is necessary to perform a more detailed vehicle dynamics modelling in order to determine whether the vehicle will be able to perform the planned steering manoeuvre. In practise, a far more dedicated vehicle dynamics modelling would be employed to also assess tyre forces and vehicle roll. First, it is important to assess load distributions. Through the steering manoeuvre the load distributions will change due to the longitudinal and lateral accelerations. The load distribution can be described by the vertical load forces F_z acting on the wheels. A

162

non-linear model given by Doumiati et al. (2009) examines the longitudinal and lateral accelerations coupling.

$$F_{Z_{fl}} = \frac{1}{2}M\left(\frac{l_r}{l}g - \frac{h}{l}a_x\right) - M\left(\frac{l_r}{l}g - \frac{h}{l}a_x\right)\frac{h}{d_f g}a_y$$

$$F_{Z_{fr}} = \frac{1}{2}M\left(\frac{l_r}{l}g - \frac{h}{l}a_x\right) + M\left(\frac{l_r}{l}g - \frac{h}{l}a_x\right)\frac{h}{d_f g}a_y$$

$$F_{Z_{rl}} = \frac{1}{2}M\left(\frac{l_f}{l}g + \frac{h}{l}a_x\right) - M\left(\frac{l_f}{l}g + \frac{h}{l}a_x\right)\frac{h}{d_r g}a_y$$

$$F_{Z_{rr}} = \frac{1}{2}M\left(\frac{l_f}{l}g + \frac{h}{l}a_x\right) + M\left(\frac{l_f}{l}g + \frac{h}{l}a_x\right)\frac{h}{d_r g}a_y$$

(7-12)

where a_x and a_y are the longitudinal and lateral accelerations respectively, d_f and d_r are the track widths front and rear respectively, h is the height of the CoM, l is the total wheelbase length, l_f and l_r are the distances from the CoM to the front and rear axles respectively, and M is vehicle mass.

These equations build on from the simpler Overturning Speed calculation of Equation (7-4) and can calculate whether an individual wheel has no load. Therefore, whether a potential rollover may happen. This also considers the vehicle braking, as the a_x value will cause a longitudinal load distribution. A lane-change manoeuvre is to be disqualified if any of the F_Z loads have a value 0 at any point during the manoeuvre. It is worth mentioning that the limitations described in Section 7.3.2.2 are also used to disqualify a manoeuvre.
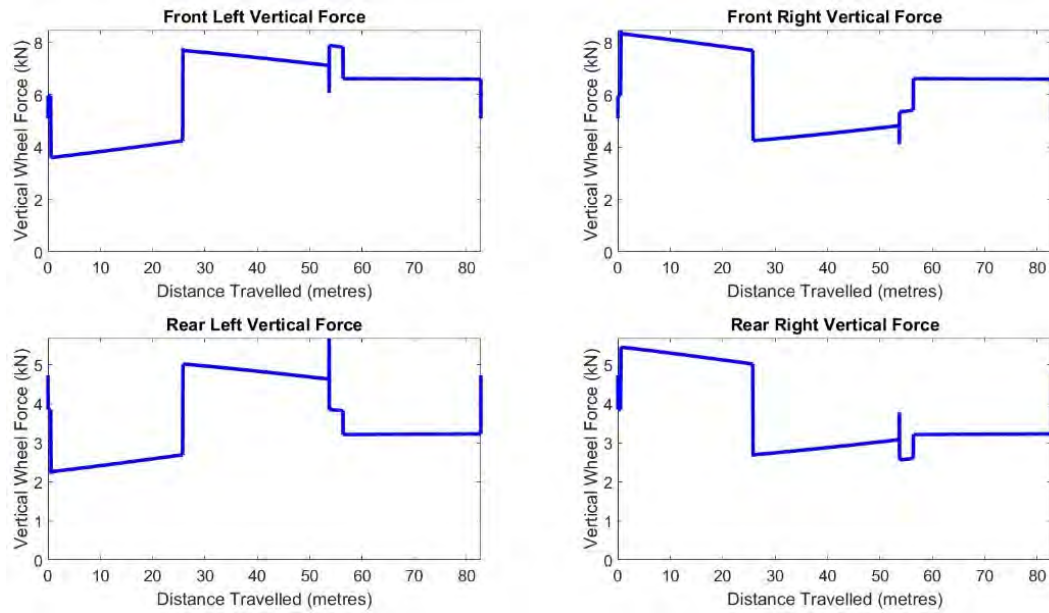
Figure 7-4 - Vertical Tyre Forces

Figure 7-4 demonstrates the vertical tyre forces acting on each wheel, as calculated in Equation (7-12). This example represents a manoeuvre from the centre lane into the adjacent left lane. Lateral weight transfer increases the vertical forces on the outside (right) wheels first, and conversely reduce the forces on the inside (left) wheels. When the manoeuvre requires a steering action to return the orientation to 0, a right turn is enacted and now the left wheels are the outside wheels and their vertical forces increase whilst the inner right wheels decrease vertical forces. It is also observed that the vertical forces on the front wheels are larger than the rear (on the same side of the vehicle). This is due to longitudinal weight transfer caused by the braking. At approximately $53m$ is when the steering manoeuvre ends, immediately afterwards a sudden decrease in vertical force is observed on the front wheels and increase on the rear wheels. At this brief time instant the vehicle applied no braking, which cause the front vertical forces to reduce, whilst increasing the rear forces. After this time instant, full longitudinal braking is applied, and the longitudinal weight transfer increases the vertical forces on the front wheels more than on the rear wheels. The left and right wheels of the same axles have equal vertical forces.

7.4.3 Dynamic Braking Simulation Assumptions

The assumptions listed in Section 7.3.3 remain true, except for the constant linear braking assumption. The additional assumptions are listed as:

- Whilst the braking is calculated to be dynamic, a constant applied braking force is assumed for the calculations. This is a braking force calculated by Newton's 2nd Law $F = Ma$, where the deceleration parameter a is simply a desired braking value.

- The dynamic braking calculations rely more heavily on the capabilities of V2V, so it is critical that this information can be communicated fully and quickly. This builds on a previous assumption, however, if it can be demonstrated that an input parameter is required then it may be made available.

- The vehicles behind will experience a time delay of $0.6711s$ before braking is applied. This is the same time delay as discussed in Section 7.3.1 from the Highway Code thinking distances.

7.4.4 Dynamic Braking Simulation Outputs

The dynamic braking simulator can provide the following outputs for the decision making:

- 4 vehicle impact velocities for the 2 collisions in each lane (m/s)
- Acceleration of Host Vehicle through manoeuvres (m/s^2), describing the severity of the manoeuvre itself.
- Time-To-Collision (s)
- Lanes disqualified due to vehicle limitations or collisions occurring before manoeuvres are complete.

7.5 Collision Severity

7.5.1 Kinetic Energy

Potential collisions are simulated for given impact velocities and required braking rates, and a decision needs to be made on which lane the Host Vehicle should drive into. Some decision making processes need more information than is already

available, so extra calculations are needed to provide this information, as described in the following sections. The discussion on kinetic energy from Section 6.3.2 is developed, to be used to generate a metric which could be used by a decision making process.

7.5.2 Severity of Collision Described by Kinetic Energy

A kinetic energy-based decision requires a number of calculations to be made. Firstly, all collisions are assumed to be inelastic, and using the conservation of linear momentum, a velocity of the vehicles can be calculated after the collision, as follows:

$$P = Mv \tag{7-13}$$

$$\sum P = M_1 v_1 + M_2 v_2 \tag{7-14}$$

$$P_{before} = P_{after} \tag{7-15}$$

$$v_3 = \frac{\sum P}{(M_1 + M_2)} \tag{7-16}$$

where M is Vehicle Mass, P is momentum, v is vehicle velocity, and subscripts 1 and 2 describe vehicles 1 and 2 respectively in the collision. v_3 is the velocity of Vehicles 1 and 2 after they have inelastically combined.

Now that a velocity after the impact has been calculated, kinetic energy values can be calculated for all vehicles in the collisions before and after the impact. Next, a difference in kinetic energy is calculated, which demonstrates how much of the kinetic energy before and after the collision is converted. This is an output that shows the severity of the collision, as energy will be transferred to deforming the vehicles, as well as sound and heat energy.

$$KE_i = \frac{1}{2} M_1 v_1^2 + \frac{1}{2} M_2 v_2^2 \tag{7-17}$$

$$KE_f = \frac{1}{2} (M_1 + M_2)(v_3^2) \tag{7-18}$$

$$\Delta KE = KE_f - KE_i \tag{7-19}$$

where KE denotes kinetic energy, and subscripts i and f denote the initial and final calculations respectively of the kinetic energy.

Equations (7-13) to (7-19) demonstrate a need for the input of Mass, and therefore it is assumed V2V communication from all simulated vehicles will communicate this parameter.

7.5.3 Kinetic Energy Decision Making Process

Assuming that there are 3 lanes available for the Host Vehicle manoeuvre (Current Lane, adjacent left, adjacent right), and there is 1 vehicle ahead in each lane and 1 vehicle behind in each lane, there are 6 vehicles for which ΔKE has to be calculated, as there are 6 potential collisions on which to base a decision. All collisions are considered to be independent of one another, meaning a collision with a vehicle behind in a lane does not affect the result for the collision with the vehicle ahead in the same lane. The parameters used in the benchmark simulation for kinetic energy are given in Table 7-4.

Table 7-4 – Kinetic Energy Simulation Benchmark Parameters

Parameter	Value
Mass of Vehicles Ahead	$2000kg$
Velocity of Vehicles Ahead	$70mph$
Headway Distance to Vehicles Ahead	$15m$
Braking Values of Vehicles Ahead	$7m/s^2$
Mass of Vehicles Behind	$2000kg$
Velocity of Vehicles Behind	$70mph$
Headway Distance of Vehicles Behind	$20m$

The parameters affecting the Host Vehicle's performance are adjusted also, given in Table 7-5.

Table 7-5 - Host Vehicle Kinetic Energy Benchmark Parameters

Parameter	Value
ACC Host Vehicle Following Time	1.4s
Coefficient of Friction with Road	0.7
Host Vehicle Maximum Lateral Acceleration	8.829m/s^2 (0.9g)
Host Vehicle Maximum Rate of Deceleration	9m/s^2

Using the Kinetic Energy Simulation Benchmark, 6 values for Kinetic Energy are produced, as given in Table 7-6. The current lane (CL) is referred to as Lane 2, adjacent left is Lane 1, and adjacent right is Lane 3.

Table 7-6 - Kinetic Energy Example Simulation Values

ΔKE_Ahead Lane 1 (*J*)	ΔKE_Ahead Lane 2 (*J*)	ΔKE_Ahead Lane 3 (*J*)
1.6653 * 1.0e^+4	0.7178 * 1.0e^+4	1.6653 * 1.0e^+4
ΔKE_Behind Lane 1 (*J*)	**ΔKE_Behind Lane 2 (*J*)**	**ΔKE_Behind Lane 3 (*J*)**
0	5.2360 * 1.0e^+4	0

where *J* denotes Joules.

Assuming all lanes are available for the selection, the lane is chosen using the method proposed. For each lane its maximum ΔKE is determined, as demonstrated in Table 7-7 – Maximum ΔKE Values.

Table 7-7 – Maximum ΔKE Values

ΔKE_Ahead Lane 1 (*J*)	ΔKE_Behind Lane 2 (*J*)	ΔKE_Ahead Lane 3 (*J*)
1.6653 * 1.0e^+4	5.236. * 1.0e^+4	1.6653 * 1.0e^+4

Afterwards, the minimum of these maximum ΔKE is selected. This will therefore select the lane by avoiding the lanes with the largest ΔKE value. Due to Lane 2 having the highest maximum ΔKE value, Lane 2 is disqualified from further selection. However, as the Kinetic Energy Benchmark simulation demonstrates, there are 2 ΔKE values in Table 7-7 which are identical.

Table 7-8 - Minimum ΔKE Values

ΔKE_Behind Lane 1 (*J*)	ΔKE_Ahead Lane 2 (*J*)	ΔKE_Behind Lane 3 (*J*)
0	0.7178 * 1.0e^+4	0

The minimum ΔKE values of Lanes 1 and 3 are then considered, and the minimum of these values is selected, making Table 7-8. However, again Lanes 1 and 3 have identical ΔKE values. So, the final decision process is to select Lane 1, because on a motorway this would be the lane closest to the emergency lane (Hard Shoulder), and most likely to have the slowest traffic.

7.5.3.1 Kinetic Energy and Vehicle Mass

Basing the decision to change lanes in the event of an emergency situation on a motorway on the difference in kinetic energy before and after the collision would appear to satisfy the requirement of selecting the lowest risk lane. However, the risk to the other vehicles involved in the collision needs to be considered also. The least severe collision must take into account the risk to the other vehicles, not just the Host Vehicle. Analyses of this issue is presented using the following scenario.

The Host Vehicle will be involved in an unavoidable collision and must select the lowest risk lane to drive into. There are 2 lanes to select from, and both have a vehicle ahead with which the Host Vehicle can collide. The two vehicles ahead are both stationary, $0 m/s$, and the host vehicle will collide with both at $10 m/s$. The only difference between the two vehicles ahead is their mass. The parameters for this scenario are given in Table 7-9.

Table 7-9 - Analysis Parameters

Parameter	Value
Host Vehicle Velocity at Impact	$10 m/s$
Vehicles Ahead Velocity at Impact	$0 m/s$
Host Vehicle Mass	$2000 kg$
Vehicle Ahead 1 Mass	$2500 kg$
Vehicle Ahead 2 Mass	$2100 kg$

Using Equations (7-17) to (7-19) ΔKE for the two collisions is calculated as given in Table 7-10.

Table 7-10 - Assessment Results

	Impact with Vehicle 1	Impact with Vehicle 2
ΔKE	5.5556e+04 J	4.2857e+04 J
Velocity of Vehicles Ahead after collision	4.4444 m/s	5.7143 m/s

Assessing the ΔKE values only would suggest selecting Vehicle 2 to collide with, because it leads to the least amount of kinetic energy to be converted in the collision. However, assessing the velocity of that vehicle after the inelastic collision shows that it accelerates to a higher velocity than Vehicle 1. Selecting a vehicle to collide with based solely on kinetic energy difference could be described as selfish as the higher acceleration indicates greater risk of injury to the vehicle occupants. There is also an issue of assuming an inelastic collision because car crashes exhibit both plastic and elastic behaviours. Coon and Reid (2006) modelled a car crash as a certain portion of the kinetic energy was lost to the system in the form of deformation. They derive the ratio of the velocities before and after the impact as the coefficient of restitution, e.

$$e = \frac{v_1' - v_2'}{v_2 - v_1} \qquad (7\text{-}20)$$

where v_1' and v_2' are the velocities of Vehicles 1 and 2 after the collision respectively. Brach and Brach (1998) gave equations of how the velocity of the vehicles involved in a collision has affected by the energy absorbed by the vehicle:

$$\Delta v_1 = \sqrt{\frac{2\gamma p_1 (E_1 + E_2)}{M_1(1 + \frac{\gamma p_1 M_1}{\gamma p_2 M_2})}} \qquad \Delta v_2 = \sqrt{\frac{2\gamma p_2 (E_1 + E_2)}{M_2(1 + \frac{\gamma p_2 M_2}{\gamma p_1 M_1})}} \qquad (7\text{-}21)$$

where E_1 and E_2 are the Energy absorbed by Vehicles 1 and 2 respectively, γp_1 and γp_2 are parameters calculated as:

$$\gamma p_i = \frac{kr_i^2}{kr_i^2 + h_i^2} \qquad (7\text{-}22)$$

where kr_i is the radii of gyration calculated by $I_i = M_i k_i^2$, and h_i is perpendicular distance to the CoM of the vehicle from the line of action of the principle direction of force. Calculating E_1 and E_2 is vital for determining accurate values of kinetic energy of a collision and the final velocities. However, calculating the energy absorbed requires further simulation. Whilst the ΔKE values are one indication of the severity of a collision, there are other values which need to be assessed. Therefore, more in-depth simulation of the vehicle's crash energy dissipation is needed to evaluate the severity of the simulated collisions.

7.5.4 Collision Modelling

Using Kinetic Energy does give an indication as to the severity of a collision. This process also has the benefit of producing an unbiased numerical value for the decision making process. However, the kinetic energy calculations do not take into account the performance of the vehicle's crash structure. Using the experience gained from the collision modelling in Chapter 6, the collision severity can be dynamically assessed.

For the collision modelling to be implemented in the motorway simulator and the decision making process a number of pessimistic assumptions are made. This is because the motorway simulation calculates the moment of impact and impact velocities for two separate collisions, including the collision between the Host Vehicle

171

and the vehicle ahead, and the collision between the Host Vehicle and the vehicle behind. Collisions between the Host Vehicle and vehicles in adjacent lanes with little or no headway distance will not be considered due to the collision occurring before a lane-change manoeuvre can be completed. This would result in that lane being disqualified from the decision making process. In reality, when one collision occurs, this will change the velocity and displacement of the second. There are also two possible orders that these collisions can occur, either:

1. The Host Vehicle impacts the vehicle ahead, and then the vehicle behind impacts the lumped Host vehicle and vehicle ahead, or
2. The vehicle behind impacts the Host Vehicle, then the lumped mass of the Host Vehicle and vehicle behind impacts the vehicle ahead.

The pessimistic assumptions will assume the maximum velocity differences, to calculate the worst collisions. In order 1, the velocity of the Host Vehicle and vehicle ahead will be assumed as the minimum velocity of both vehicles. The calculated velocity of the vehicle behind will still be used for the second impact. In order 2, the velocity of the lumped Host Vehicle and vehicle behind after the collision will be calculated, and this will be used as the impact velocity into the vehicle ahead. This assumes no additional braking after the first impact. It is assumed that the worst-case impact speeds will lead to the worst collision to be considered by the decision making process which will decide on which collisions to avoid. The motorway simulation will determine what order the vehicles collide in, based on the time of moments of collision.

Further assumptions that are made for the collision modelling to be combined with the dynamic braking simulator are:

- Vehicle Mass and Crash Structure Spring Stiffness will be available, through V2V. This has been discussed in the assumptions of Sections 7.3.3 and 7.4.3.
- The Bilinear terms discussed in Section 6.2.5 used to model the crash structure behaviour will be assumed equal in all simulation scenarios. A future consideration can be on how these crash structure properties will be determined/communicated, but in this research all vehicles will assume identical crash structures. Only the mass and stiffness will change. The collision modelling parameters used for all vehicles are given in Table 7-11.

Table 7-11 - Collision modelling Parameters

Parameter	Value
Bilinear Term	0.135
Stiffness	$886,009 N/m$
Multiple of Stiffness	3.167

Using the 4 vehicle impact velocities listed in Section 7.4.4 the collision modelling gives four vehicle accelerations. The vehicles ahead and vehicles behind in each lane, each have one acceleration value, and the Host Vehicle has two accelerations for each lane. Of course, one of these accelerations of the Host Vehicle will be shared with either a vehicle ahead or behind, depending on which collision occurs first. Along with the manoeuvre accelerations and times-to-collision these will be the inputs to the decision making process. This gives a total of 6 unbiased and uncorrelated criterion on which to base a decision.

7.6   Dynamic Braking Simulator Benchmark Parameters

With the collision modelling introduced to the dynamic braking simulator, a benchmark scenario is defined as follows. The parameters defining the Host Vehicle are given in Table 7-12, and the Motorway Vehicles parameters are given in Table 7-13.

Table 7-12 - Host Vehicle Dynamic Braking Simulator Benchmark Parameters

Parameter	Value
Mass	$2000kg$
ACC Following Time	$1.4s$
Maximum Longitudinal Deceleration (Braking)	$8m/s$
Maximum Lateral Acceleration (steering)	$8.5m/s$
Height of CoM	$0.5m$
Track Width Front Axle	$1.65m$
Track Width Rear Axle	$1.58m$
Longitudinal Distance from CoM to Front Axle	$1.3m$
Longitudinal Distance from CoM to Rear Axle	$1.4m$
Cross-Sectional-Area of Vehicle	$2.5m^2$
Aero Drag Coefficient	0.27
Rolling Resistance Coefficient	0.011
Coefficient of Friction between Tyre and Road	0.7

Table 7-13 - Motorway Vehicles Dynamic Braking Simulator Benchmark Parameters

Parameters	Vehicle Ahead	Vehicle Behind
Mass	$2000kg$	$2000kg$
Initial Velocity	$70mph$	$70mph$
Headway Distance from Host Vehicle	$12m$	$-20m$
Inputted Deceleration	$-7m/s^2$	$-5m/s^2$
Cross-Sectional-Area of Vehicle	$2.5m^2$	$2.5m^2$
Aero Drag Coefficient	0.27	0.27
Rolling Resistance Coefficient	0.011	0.011

7.7 Simulator Flowcharts

7.7.1 Flowchart of Linear Simulator

The Linear simulator begins by inputting all data about the motorway, the Host Vehicle, and the motorway vehicles. The simulator uses discretised time to synchronise all calculations, and therefore a simulation time Δ is defined. The time for the Host Vehicle to impact the vehicle ahead in the same lane is the first impact to calculate. Δ is set at twice this time period empirically, as testing has demonstrated that all collisions will have occurred within this Δ time sample. If a collision does not occur, then a collision avoidance can be observed.

Calculations for velocities and displacements for the vehicles ahead, and required braking distances for the vehicles behind are performed to determine the outputs of the simulator. Separation distances between the Host Vehicle and vehicles behind calculate when a collision will occur. The steering manoeuvre is also assessed for whether it can be completed before a collision occurs. This is used to determine any lanes that must be disqualified from the decision making process. The simulation ends once the outputs are defined. The simulator is represented in Figure 7-5, and the symbols are described in Table 7-14.

Table 7-14 - Flowchart Symbols

Symbol	Description
	Process – Action Performed
	Input – Incoming Data
	Output – Outgoing Data, may also be used in simulation for other calculations
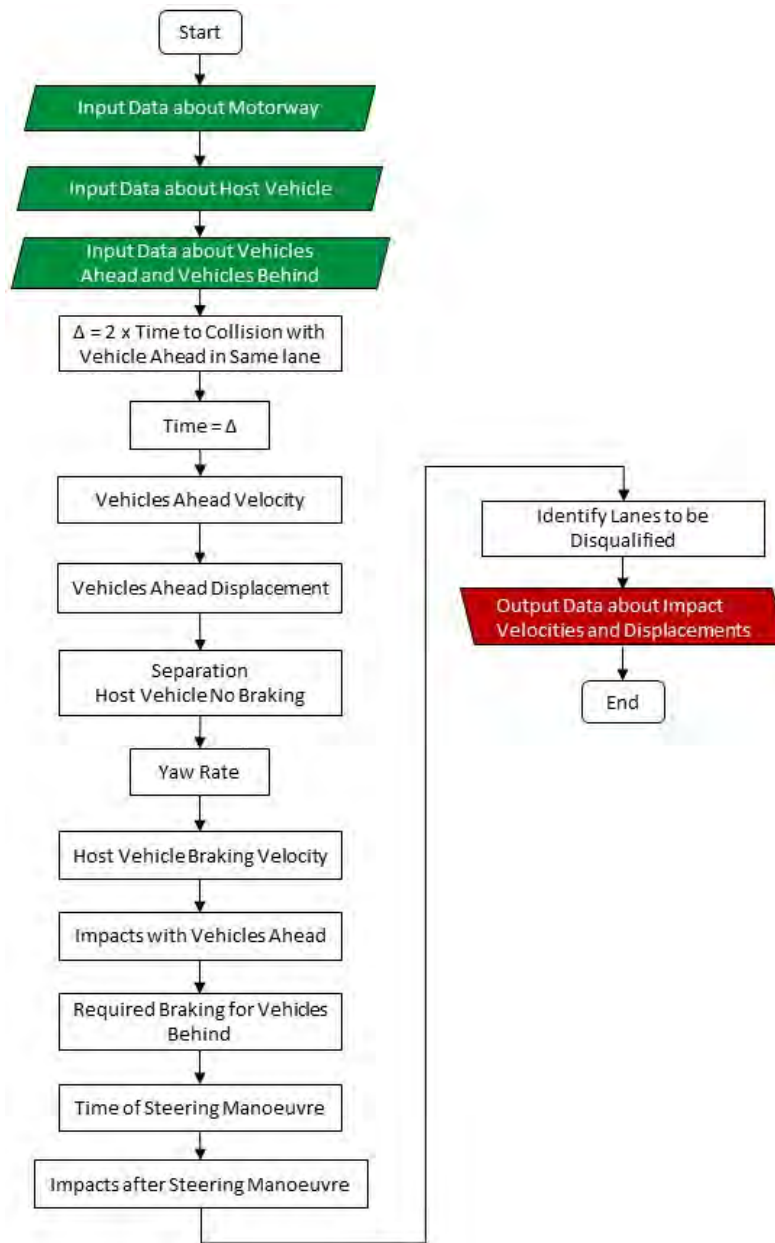
Figure 7-5 - Linear Simulator Flowchart

7.7.2 Flowchart of Dynamic Braking Simulator

Just as the linear simulator described in Section 7.7.1 defines the discretised time, the dynamic braking simulator also defines the same value for Δ. The calculations for velocity and displacement are performed for the vehicles ahead and behind, which are compared with the same calculations for the Host Vehicle to determine separation distances. The steering manoeuvre is assessed for completion before a collision, which allows for the evaluation of whether lanes should be disqualified from the decision process. The impact velocities are used as inputs to the collision modelling, and once the outputs of this are calculated the simulation ends. The simulator is represented in Figure 7-6, using the same symbols as represented in Table 7-14.
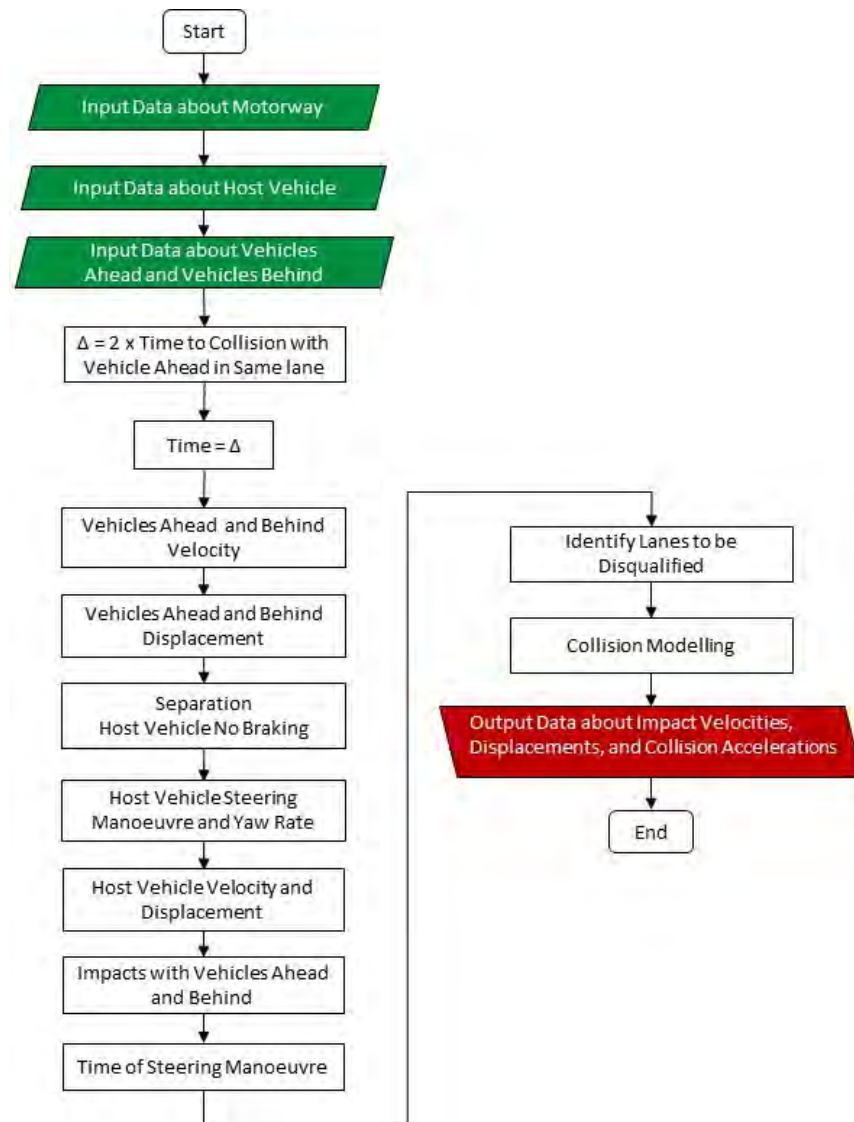
Figure 7-6 - Dynamic Braking Simulator Flowchart

7.8 Simulation Results

7.8.1 Linear Simulator Output Results

14 scenarios are simulated to demonstrate how the linear simulator produces its outputs, and how they can compare. Scenario 1 is the benchmark described in Section 7.3.5. Scenarios 2 to 6, and scenarios 8 to 10 only change parameters describing the vehicles in the adjacent Lane 3. Lane 1 will represent the benchmark scenario for scenarios 2 to 10. For scenarios 1 and 11 to 14, Lanes 1 and 3 will have identical outputs and therefore do not need to be presented. Scenario 7 describes a change to the vehicles in Lane 2. Scenarios 11 to 14 are parameters that affect the Host Vehicle's behaviour.

The results are presented in Table 7-15. Impact Velocity signifies the relative velocity difference between the Host Vehicle and vehicle ahead (m/s), Braking signifies the required braking of the vehicles behind to avoid an impact with the Host Vehicle (m/s^2), and Manoeuvre signifies the maximum acceleration experienced by the vehicle to perform its intended manoeuvre (m/s^2).

It is noted that in Scenario 5, when the initial velocity of the vehicle ahead in Lane 3 is reduced to $50 mph$, Lane 3 is disqualified as the collision occurs before the steering manoeuvre is complete. In Scenario 12, with a reduced CoF, Lanes 1 and 3 are disqualified as the required yaw rate to complete the manoeuvres exceeds the maximum allowable yaw rate due to friction.

Impact velocities are observed in Lane 3 when the headway distance ahead is reduced to $15 m$. This impact velocity actually reduces at headway distance $4 m$, and this is due to the vehicle ahead not having enough distance to brake sufficiently to reduce its velocity, therefore the relative velocity is lower with a lower initial headway. Impact velocities are also observed when the velocity ahead is reduced, or braking ahead is increased. If the headway behind is increased to $43 m$, this reduces the required braking of the vehicle behind in Lane 2 enough to be lower than the required braking of the vehicles behind in Lanes 1 and 3. Reducing the headway distance and increasing the velocity of the vehicle behind in Lane 3 causes the required braking to increase, whilst reducing the velocity reduces the required braking.

Table 7-15 - Linear Simulator Outputs

Scenario	Parameter Changed	Stay in Current Lane 2			Steer into Adjacent Lane 3		
		Impact Velocity (m/s)	Braking m/s^2	Manoeuvre m/s^2	Impact Velocity (m/s)	Braking m/s^2	Manoeuvre m/s^2
1	Benchmark Scenario	3.79	8.29	9.00	0.00	6.52	8.46
2	Headway Ahead 15m	3.79	8.29	9.00	5.77	6.52	8.46
3	Headway Ahead 4m	3.79	8.29	9.00	3.39	6.52	8.46
4	Velocity Ahead 68mph	3.79	8.29	9.00	4.64	6.52	8.46
5	Velocity Ahead 50mph	3.79	8.29	9.00	11.72	6.52	8.46
6	Braking Ahead 7.5m/s^2	3.79	8.29	9.00	5.44	6.52	8.46
7	Headway Behind Lane 2 43m	3.79	5.31	9.00	0.00	6.52	8.46
8	Headway Behind 17m	3.79	8.29	9.00	0.00	7.23	8.46
9	Velocity Behind 72mph	3.79	8.29	9.00	0.00	7.17	8.46
10	Velocity Behind 68mph	3.79	8.29	9.00	0.00	5.93	8.46
11	ACC Time 1.5s	0.52	8.12	8.63	0.00	6.52	7.95
12	CoF 0.6	3.79	8.29	9.00	0.00	7.10	9.16
13	Max Overall g - 0.8	3.79	8.29	9.00	11.30	5.40	7.44
14	Host Vehicle Braking 8m/s^2	11.02	7.82	8.00	0.00	6.52	8.46

Increasing the ACC following time improves all of the outputs for Lane 2, whilst also improving the manoeuvre acceleration for the adjacent lanes, but does increase the required braking of the vehicles behind in the adjacent lanes. This is due to the

increased time allowed to complete the steering manoeuvre, which reduces the available braking distance for the vehicles behind. Reducing the maximum overall g for the steering manoeuvres increases the impact velocity for the adjacent lanes, but reduces the required braking and manoeuvre acceleration. This result is due to the limited braking available when performing a steering manoeuvre as described by the tyre saturation. Reducing the maximum braking for the Host Vehicle does not directly affect the outputs for the adjacent lanes, as their braking values are determined by tyre saturation. The Host Vehicle's braking does increase the impact velocity in Lane 2, which is directly affected.

7.8.2 Dynamic Braking Output Results

The dynamic braking simulator produces more outputs which describe the severity of the collision. Therefore, only 5 scenarios will be demonstrated here which have a significant effect on the simulation results. The parameters for the vehicles in Lane 3 will be adjusted. The benchmark scenario described in Section 7.6 is simulated and presented in Table 7-16.

Table 7-16 - Dynamic Braking Simulator Benchmark Scenario Outputs

	Lane 1	Lane 2	Lane 3
Vehicle Ahead Velocity (m/s)	9.119	0	9.119
Host Vehicle Velocity Collision Ahead (m/s)	13.132	11.456	13.132
Host Vehicle Velocity Collision Behind (m/s)	3.692	10.358	3.692
Vehicle Behind Velocity (m/s)	12.689	21.425	12.689
Manoeuvre Acceleration (m/s^2)	8.776	8.310	8.776
Time-To-Collision (s)	3.080	2.417	3.080
Lanes Open	1	1	1

The benchmark has demonstrated that the results for Lanes 1 and 3 are identical. The velocities of Lane 2 are higher than those of Lanes 1 and 3, except for the vehicle ahead which is 0m/s. this describes that vehicle is at a full-stop. A collision occurs earlier if the Host Vehicle stays in Lane 2, and will have more time to

react if it moves into either Lane 1 or 3. All lanes demonstrate similar manoeuvre accelerations and all lanes are open, meaning that all lanes will be considered in the decision making process. The velocity outputs of Table 7-16 correspond to the following collision accelerations presented in Table 7-17.

Table 7-17 - Dynamic Braking Simulator Benchmark Scenario Collision Accelerations

	Lane 1	Lane 2	Lane 3
Collision Acceleration Vehicle Ahead (g)	3.974	12.683	3.974
Host Vehicle Collision with Vehicle Ahead (g)	3.974	12.683	3.974
Host Vehicle Collision with Vehicle Behind (g)	5.657	7.222	5.657
Collision Acceleration Vehicle Behind (g)	11.314	14.443	11.314

The collision acceleration results presented in Table 7-17 demonstrate that for all vehicle collisions, the highest accelerations are experienced in Lane 2. The highest acceleration is for the vehicle behind, which is in line with the results presented in Table 7-16. The vehicle behind in Lane 2 had the highest impact velocity, and this impact will occur with the mass of the Host Vehicle and the vehicle ahead, as that collision occurs before the collision behind.

The next scenario will change the initial headway distance of the vehicle ahead in Lane 3 from $12m$ to $7m$.

Table 7-18 - Dynamic Braking Simulator Outputs - Headway Ahead Distance 7m

	Lane 1	Lane 2	Lane 3
Vehicle Ahead Velocity (m/s)	9.119	0	16.935
Host Vehicle Velocity Collision Ahead (m/s)	13.132	11.456	21.929
Host Vehicle Velocity Collision Behind (m/s)	3.692	10.358	3.692
Vehicle Behind Velocity (m/s)	12.689	21.425	12.689
Manoeuvre Acceleration (m/s^2)	8.776	8.310	8.776
Time-To-Collision (s)	3.080	2.417	1.986
Lanes Open	1	1	0

There are only 3 differences between the outputs presented in the benchmark (Table 7-16) and the simulation of a reduced headway presented in Table 7-18. The impact velocities of the vehicle ahead, and the Host Vehicle into the vehicle ahead are higher, but the relative velocity between the two is approximately 5m/s which is still lower than the relative velocity of Lane 2. However, Lane 3 is described as disqualified due to the collision ahead occurring before the lane-change manoeuvre can be completed.

Table 7-19 - Dynamic Braking Simulator Collision Accelerations – Headway Ahead Distance 7m

	Lane 1	Lane 2	Lane 3
Collision Acceleration Vehicle Ahead (g)	3.974	12.683	5.018
Host Vehicle Collision with Vehicle Ahead (g)	3.974	12.683	5.018
Host Vehicle Collision with Vehicle Behind (g)	5.657	7.222	5.657
Collision Acceleration Vehicle Behind (g)	11.314	14.443	11.314

Table 7-19 demonstrates that although Lane 3 is disqualified, the collision accelerations of the vehicle ahead and Host Vehicle demonstrate the effect of the

relatively small impact velocity compared to their actual velocities at the moment of impact. Both accelerations are considerably lower than their counterparts in Lane 2.

The initial headway distance of the vehicle behind in Lane 3 is now reduced from 20m to 10m.

Table 7-20 - Dynamic Braking Simulator Outputs – Headway Behind Distance 10m

	Lane 1	Lane 2	Lane 3
Vehicle Ahead Velocity (m/s)	9.119	0	9.119
Host Vehicle Velocity Collision Ahead (m/s)	13.132	11.456	13.132
Host Vehicle Velocity Collision Behind (m/s)	3.692	10.358	15.602
Vehicle Behind Velocity (m/s)	12.689	21.425	20.255
Manoeuvre Acceleration (m/s^2)	8.776	8.310	8.776
Time-To-Collision (s)	3.080	2.417	2.868
Lanes Open	1	1	1

Table 7-20 shows that the collisions ahead are identical for Lanes 1 and 3, but as the headway distance behind is reduced, the impact velocities for the Host Vehicle and vehicle behind in Lane 3 are higher than those of Lane 1. All lanes are open, but one important difference is that in Lane 3 the collision behind occurs before the collision ahead.

Table 7-21 - Dynamic Braking Simulator Collision Accelerations – Headway Behind Distance 10m

	Lane 1	Lane 2	Lane 3
Collision Acceleration Vehicle Ahead (g)	3.974	12.683	11.044
Host Vehicle Collision with Vehicle Ahead (g)	3.974	12.683	5.522
Host Vehicle Collision with Vehicle Behind (g)	5.657	7.222	4.652
Collision Acceleration Vehicle Behind (g)	11.314	14.443	4.652

Table 7-21 demonstrates the effect of the collision behind occurring before the collision ahead in Lane 3 has affected the collision accelerations for all impacts. The combined mass of the Host Vehicle and vehicle behind impacting into the rear of the vehicle ahead has increased that vehicle's acceleration result. It has also reduced the acceleration values for the vehicle behind and the Host Vehicle's impact with the vehicle behind compared to Lane 1.

The mass of the vehicle ahead in Lane 3 is now reduced from $2000kg$, to $1000kg$.

Table 7-22 - Dynamic Braking Simulator Outputs – Vehicle Ahead Mass 1000kg

	Lane 1	Lane 2	Lane 3
Vehicle Ahead Velocity (m/s)	9.119	0	9.786
Host Vehicle Velocity Collision Ahead (m/s)	13.132	11.456	14.208
Host Vehicle Velocity Collision Behind (m/s)	3.692	10.358	3.692
Vehicle Behind Velocity (m/s)	12.689	21.425	12.689
Manoeuvre Acceleration (m/s^2)	8.776	8.310	8.776
Time-To-Collision (s)	3.080	2.417	2.948
Lanes Open	1	1	1

Reducing the mass of the vehicle ahead in Lane 3, as presented in Table 7-22, does not drastically change the simulator's outputs from the benchmark presented in Table 7-16. There is a small change to the impact velocities of the vehicle ahead and Host Vehicle, but this is to be expected as the lower mass will have affected the braking of the vehicle ahead, as described in Section 7.4.1.

Table 7-23 - Dynamic Braking Simulator Collision Accelerations – Vehicle Ahead Mass 1000kg

	Lane 1	Lane 2	Lane 3
Collision Acceleration Vehicle Ahead (g)	3.974	12.683	7.110
Host Vehicle Collision with Vehicle Ahead (g)	3.974	12.683	3.555
Host Vehicle Collision with Vehicle Behind (g)	5.657	7.222	7.097
Collision Acceleration Vehicle Behind (g)	11.314	14.443	10.646

Although only minor changes to the outputs of the simulator presented in Table 7-22 are observed, there are more considerable changes to the collision accelerations presented in Table 7-23. The lighter mass of the vehicle ahead in Lane 3 has nearly doubled the collision acceleration, compared to the same collision in Lane 1. This effect is also observed by the Host Vehicle and vehicle behind, which both have lighter masses to collide with. The acceleration for the Host Vehicle colliding with the vehicle behind has increased, as the overall mass of the Host Vehicle and vehicle ahead is now reduced.

The final scenario presented will increase the Host Vehicle's maximum lateral acceleration from $8.5 m/s^2$ to $10 m/s^2$. This will affect the tyre saturation braking for the steering manoeuvres.

Table 7-24 - Dynamic Braking Simulator Outputs – Host Vehicle Lateral Acceleration 10m/s²

	Lane 1	Lane 2	Lane 3
Vehicle Ahead Velocity (m/s)	0	0	0
Host Vehicle Velocity Collision Ahead (m/s)	0	11.456	0
Host Vehicle Velocity Collision Behind (m/s)	7.117	10.358	7.117
Vehicle Behind Velocity (m/s)	16.088	21.425	16.088
Manoeuvre Acceleration (m/s^2)	9.007	8.310	9.007
Time-To-Collision (s)	3.623	2.417	3.623
Lanes Open	1	1	1

The increased available lateral acceleration for the Host Vehicle has had a considerable effect of the simulator outputs presented in Table 7-24. The Host Vehicle collision with the vehicle ahead displays impact velocities of 0m/s for Lanes 1 and 3. This means that a collision avoidances has been achieved. However, compared to the benchmark presented in Table 7-16, the impact velocities with the vehicle behind have increased.

Table 7-25 - Dynamic Braking Simulator Collision Accelerations – Host Vehicle Lateral Acceleration 10m/s²

	Lane 1	Lane 2	Lane 3
Collision Acceleration Vehicle Ahead (g)	0	12.683	0
Host Vehicle Collision with Vehicle Ahead (g)	0	12.683	0
Host Vehicle Collision with Vehicle Behind (g)	9.562	7.222	9.562
Collision Acceleration Vehicle Behind (g)	9.562	14.443	9.562

This effect of the increased impact velocities for the collision behind is presented in Table 7-25. Compared to Table 7-17, the Host Vehicle's acceleration has increased, whilst the vehicle behind has reduced. The collision avoidance is also represented, which informs the acceleration results for the collision behind in Lanes 1 and 3. With no impact ahead, the vehicle behind only has the mass of the Host Vehicle to collide with. The Host Vehicle acceleration increase and vehicle behind acceleration decrease is consistent with this observation.

7.9 Simulator Performance

Two simulators are developed which can be employed to determine the outputs for a decision making process to decide on the best action for an autonomous vehicle to take when faced with an imminent collision. One simulator assumes constant braking described in Section 7.3, which is capable of performing its calculations without V2V to communicate vehicle parameters. The second simulator assumes dynamic braking featured in Section 7.4. The dynamic braking simulator is entirely dependent on the capabilities of V2V.

Both simulators are investigated for their advantages and disadvantages for application to a real autonomous vehicle. The usefulness of accuracy of the outputs is compared. The implementation issues and computational requirements of both simulators are also investigated.

7.9.1 Simulator Computational Time

It is stated that the dynamic braking simulator produces more comprehensive and useful output data, but this simulator is far more complex than its linear counterpart. In fact, the dynamic simulator is split into several simulators working together, which suggests a large computational effort needed compared to the linear simulator. Therefore, times to complete the calculations in the simulators will be compared.

It must be noted that these simulations are run using a PC. The simulations are run using MATLAB 2016a, on a $3.10GHz$ processor with $8GB$ RAM and 4 cores. Car ECUs are dedicated to performing a defined task, whereas PCs are adaptable to different programmes. It is taken into account that background applications are running on the PC, which will slow down the computational time. The times presented are intended only as a demonstration of the differences between the two simulators. The times presented vary, so each simulation is run 3 times, and an average is taken. The timing is using the internal wall-clock time. These times are used to compare the differences between the simulators, and presented in Table 7-26.

Table 7-26 - Total Simulation Times

	Simulation Runs (s)			Average (s)
	1	2	3	
Linear Braking Simulator	0.046	0.068	0.070	0.062
Dynamic Braking Simulator	5.767	5.784	5.801	5.784

There is a significant difference in simulation times between the linear braking (non-V2V) simulator and dynamic braking (V2V) simulator. The required outputs of the linear braking simulator are produced, on average, within $0.07s$, whilst the dynamic braking simulator takes an average of greater than $5.7s$. The dynamic

braking simulator does perform far more accurately, and it performs more complex calculations. However, this system is intended for use in an emergency situation and waiting 5.7s for the required outputs is impossible.

A closer look at the dynamic braking simulations demonstrates the complexity of this simulator as presented in Table 7-27. This simulator carries out three distinct simulations for the Host Vehicle and the Motorway Vehicles. It is clear that the most time consuming task is calculating the dynamic braking of the motorway vehicles, where in total 6 vehicles are simulated. Furthermore, calculating just the Host Vehicle's behaviour takes nearly 1s.

Table 7-27 - Dynamic Braking Simulator Times

	Simulation Runs (s)			Average (s)
	1	2	3	
Host Vehicle Simulation	0.984	0.984	0.981	0.983
Motorway Vehicles Simulation	4.783	4.800	4.820	4.801

The collision modelling that takes place after the dynamic braking simulations is more computationally heavy, as presented in Table 7-28.

Table 7-28 - Collision Modelling Simulator Times

	Simulation Runs (s)			Average (s)
	1	2	3	
Collision Modelling	45.307	45.864	45.813	45.661

The times presented in Table 7-28 are not practical for a real-world scenario where a decision must be made very quickly. The times presented represent 6 separate collision modelling simulations, 3 for the collisions ahead of the Host Vehicle, and 3 for the collisions behind the Host Vehicle.

7.9.2 Simulator Implication

It is clear that the dynamic braking calculations require significantly more computational effort than the linear simulator. The dynamic braking simulator relies on V2V, but this could be used to a simulator's advantage. The Host Vehicle calculates the velocities and displacements of all motorway vehicles, requiring parameters such as rolling resistance R_x and aerodynamic drag C_d to be communicated. Furthermore, it would be beneficial if each vehicle calculates its own velocities and displacements, and simply communicate those data sets. This means that the time required to do the motorway vehicle simulation can be improved. All vehicles would need to use the same time sampling rate, but again V2V would synchronise all vehicle's outputs together. This is in line with Kamali et al. (2017) who discussed the importance of vehicle-to-vehicle synchronisation, as well as the issues with its implication for highway platooning systems.

As autonomous vehicles will need to plan their velocities and displacements to perform any manoeuvre, it is reasonable to assume that these results of the Host Vehicle and Motorway Vehicles will already be available. The Host Vehicle simulation can be shortened to calculate the steering manoeuvre and its limitations, as well as the separation distances between all vehicles. A time-based synchronisation of V2V communication would be required. It is worth noting that this is required in the patent of Rubin and Betts-Lacroix (2016).

7.9.3 Future Considerations for Improvements

The time taken for the Host Vehicle simulation and collision modelling raised a concern, but the times presented in Section 7.9.1 are based on the computational ability of a PC. Autonomous vehicles will need significant computational power to perform all control activities. Hou et al. (2016) noted the required increase of communication and computational capability for autonomous vehicles and suggested vehicular clouds to be used as data centres and augmented processing resources. Computational tasks can be handled by parked vehicular clouds at company car parks, or communication resources can be shared, and messages be transmitted by collaborating vehicular clouds.

It is likely that the control systems for a single autonomous vehicle will require many cores to compute many calculations for many systems, not just a collision

avoidance/mitigation simulator. This is an issue that affects not only the implication of the simulators developed here, but all control systems on autonomous vehicles.

Due to the future developments of autonomous vehicle control architectures, it is assumed that the computational effort required to run the simulators and decision making processes will not be an issue, for both the linear and dynamic braking simulators.

7.10 Motorway Simulation Conclusions

Two simulators which can assess potential collisions between a Host Vehicle and simulated motorway vehicles ahead and behind are developed. The first simulator relies on constant braking assumptions and is intended for use when V2V communication is not available to provide data important for the calculation of dynamic braking and factors inputted for collision modelling. The SUVAT equations used to simulate velocity and displacement for all vehicle works significantly faster than the dynamic braking calculations, and so this simulator would be more easily introduced to a current autonomous vehicle, requiring sensors on board to determine the initial velocities, accelerations and displacements of the motorway vehicles. However, the outputs produced are limited in describing the severity of the collision.

To provide necessary inputs to the kinetic energy modelling, assumed braking values are required for the vehicles behind. However, the limitations of the kinetic energy modelling demonstrated the need for the collision modelling discussed in Chapter 6. The calculation of kinetic energy requires V2V to communicate mass of vehicles. However, if V2V is available then the more complex collision modelling to be included in the decision making on the least severe collision would be more appropriate. Without V2V, the linear braking simulator is limited in the outputs and in order to reduce the reliance on the assumptions, the impact velocities with the vehicles behind will no longer be used. The required braking of these vehicles will be used to describe the available braking distance and initial velocity of the vehicles behind for the decision making process.

The second simulator is a dynamic braking simulator developed which is based on input parameters that are assumed to be available by V2V. They are used to calculate dynamic braking which is combined with the collision modelling given in Chapter 6. This dynamic braking simulator produces outputs that better describe the

collision severity, and so would be preferable for the decision making process, but it cannot be guaranteed that V2V will be available all of the time from all vehicles. It is also significantly more computationally heavy, and so future developments on computational power of autonomous vehicles is needed.

Both the non-V2V and V2V simulators will continue to develop in this research, to decide on how a decision can be made from the available outputs. The simulators and their outputs are tested with the decision making process developed in Chapter 8. It is intended that the dynamic braking simulator working with V2V is the preferred simulator, but the non-V2V linear simulator is developed as a back-up when the ideal situation of fully V2V capable vehicles is not available.

Chapter 8

MADM Methods in Selection of the Lane for Collision

8.1 Introduction

The simulators developed in Chapter 7 produce outputs which describe the severity of potential collisions in three lanes of a motorway. A decision making process is required to assess the outputs from the simulator, and select the lane which will result in the least severe collisions. The Multi-Attribute Decision Making (MADM) methods discussed in Chapter 3 are appropriate.

The MADM methods are discussed in this chapter, and three methods are selected for further investigation. These three methods are the most appropriate for the research problem. The methods which are not investigated further are discussed for their disadvantages to the research problem. Each of the methods selected for further investigation are described for how they work, giving a practical demonstration of the steps to these processes. All methods use the linear braking benchmark scenario given in Chapter 7 to demonstrate the MADM processes.

8.2 MADM Terminology

Criterion – This is a metric by which the decision will be based upon.

Alternatives – These are the possible choices, which are available lanes. Each Lane will have a value for each criterion listed.

Goal – The Goal is to select the Alternative (Lane) which will result in the least severe outcome. The least severe results are the optimal values for each criterion.

Attribute Value – Refers to the value of each alternative for a given criterion.

Priority Vector – This is a normalized vector (unit vector) describing how each criterion is weighted, more important criteria will have a higher priority number.

Decision Matrix – A matrix of the attribute values for each alternative against each criterion.

It is important before employing any decision-making technique to define the Goal, Criteria and Alternatives. An important requirement of the criteria is that they cannot correlate. Correlating criteria can influence the decision process, as multiple criteria will bias the decision in favour of a certain alternative.

The three methods selected for further investigation are TOPSIS, AHP and ANP, and will be explained using the benchmark scenario defined in Section 7.3.5. This will illustrate the decision making process.

The following criteria are used:

Criteria 1. Impact velocity with vehicles ahead.

Criteria 2. Required braking of vehicles behind.

Criteria 3. Maximum manoeuvre acceleration.

The criteria presented describe the severity of the imminent collisions, whilst also having no correlation between other criteria. The criteria are calculated using the developed simulators in Chapter 7.

8.3 MADM Methods in Selection of the Lane for Collision

Thor, Ding, and Kamaruddin (2013) discussed the controlled consistency that AHP and ELECTRE featured, which SAW and TOPSIS did not. It is stated that TOPSIS was not an inferior method to AHP or ELECTRE, as TOPSIS employs a compromising idea in which the optimal solutions is obtained by the optimal attribute. No arguments arise regarding consistency due to each alternative being compared with the ideal solution. AHP is inferior to SAW, ELECTRE and TOPSIS regarding the structure of the problem, because when numerous criteria and alternative are concerned AHP cannot be employed. ELECTRE only provided partial pre-ordering, which makes it inferior to the other methods discussed regarding the final result. Further investigation of the results is required to obtain each alternative's final ranking. TOPSIS is described as being relatively simple to implement, whilst also being suitable for large-scale data. For these reasons, ELECTRE will not be investigated due to the requirement of further investigation due to the partial pre-ordering. SAW will also be discounted due to its lack of controlled consistency, which is important for ensuring all alternatives are assessed equally. This is mostly important with the assessment of subjective values, i.e. the criteria weights. Although the simulator outputs are all objective and the weighting methods for all MADM methods will be the same, the SAW method is also discounted due to its similarity with AHP. The AHP method has a similar process, by employing vector normalization as a standard principle to remove scale from the decision.

Thor, Ding, and Kamaruddin (2013) note the lack of controlled consistency for TOPSIS is not an issue due to the method which finds the ideal solution. And the

small number of alternatives and criteria which limits the performance of AHP is also not an issue, as there will be a limited number of alternatives and criterion for this decision-making algorithm.

Therefore, further investigation into TOPSIS and AHP will be conducted, see Sections 8.3.1 and 3.3.4. ANP method will also be investigated, which evolves on the AHP method, see Section 3.3.5.

The objective assessments from the simulators are objective, and so are considered to be consistent. The decision maker needs to process the objective data from the simulator effectively. In this case a normalization technique is used to format the results into a useful format for further processing. Saaty (2000) describes the benefit of employing vector normalization to remove scale from the decision process. Dominance numbers arise from an absolute scale which can be appropriately weighted by other numbers added.

8.3.1 TOPSIS Method

The TOPSIS method has been applied to a wide variety of decision making problems, and adapted to suit their individual needs. The application of TOPSIS follows the following steps:

Step 1. Define the weights of criteria, w_j. Each criterion is given a weight on a scale from 1 to 10. The weighting system is fairly simple, each criterion is ranked out of 10 for importance (10 is the highest importance, 1 is the lowest importance). This scale is determined by the designer of the decision-making problem. The weighted criteria are normalized and form a normalized Priority Vector, given in Table 8-1.

Table 8-1 - TOPSIS weighting of Criteria and Priority Vector

Criteria	1	2	3
Normalized Priority Vector	0.657	0.254	0.090

Step 2. Standardise the Decision Matrix given in Table 8-2. This is necessary so that each alternative can be assessed across criteria in a dimensionless format. The Alternatives for TOPSIS are standardised using the technique described by Yoon

and Hwang (1995), where the rating of each attribute value is calculated by Equation (3-1). The standardised decision matrix is given in Table 8-3.

Table 8-2 - Decision Matrix simulation values

	Criterion 1	Criterion 2	Criterion 3
Alternative Lane 1	0	42.537	7.289
Alternative Lane 2	14.355	68.752	8.257
Alternative Lane 3	0	42.537	7.289

Table 8-3 - Decision Matrix Standardised

	Criterion 1	Criterion 2	Criterion 3
Alternative Lane 1	0	0.526	0.565
Alternative Lane 2	1	0.669	0.601
Alternative Lane 3	0	0.526	0.565

Step 3. Calculate the weighted standardised decision matrix. The decision matrix which was standardised in Step 2 (Table 8-3) has each attribute value multiplied by its corresponding weight from the Priority Vector (Table 8-1).

$$t_{ij} = w_j r_{ij}, \quad i = 1, \ldots, m; \quad j = 1, \ldots, n \tag{8-1}$$

where w_j is the weight of the jth attribute of the criteria, r_{ij} is the standardised rank value of the attribute, and t_{ij} is the weighted standardised value of each attribute. The weighted decision matrix is given in Table 8-4.

Table 8-4 - TOPSIS Weighted Decision Matrix

	Criterion 1	Criterion 2	Criterion 3
Alternative Lane 1	0	0.133	0.051
Alternative Lane 2	0.657	0.170	0.054
Alternative Lane 3	0	0.133	0.051

Step 4. Determine the Ideal A^* and Negative Ideal A^- Solutions. These are the artificial alternatives determined from the weighted decision matrix (Step 3). The most desirable value for all criteria forms the Ideal solution, and the least desirable values form the Negative Ideal Solution. This is done depending on whether each

criterion is minimized or maximized for values of v_{ij}. For the linear braking simulator, all three criteria have to be minimized to form the Ideal solution.

The ideal and negative ideal solutions for each criterion are given in Table 8-5. It is noted for the Non-V2V benchmark scenario that Alternatives 1 and 3 are identical.

Table 8-5 - TOPSIS Ideal and Negative Ideal Solutions

	Criterion 1	Criterion 2	Criterion 3
Ideal Solution A^*	0	0.133	0.051
Negative Ideal Solution A^-	0.657	0.170	0.054

Step 5. Calculate the separation from the Ideal S^* and Negative Ideal S^- Solutions for each weighted attribute t_{ij}. The distance is calculated by Euclidean Distance. For a n criteria decision, the distance is calculated by Yoon and Hwang (1995):

$$S_i^* = \sqrt{\sum_{j=1}^{n}\left(t_{ij} - t_j^*\right)^2}, i = 1,\ldots,m. \tag{8-2}$$

$$S_i^- = \sqrt{\sum_{j=1}^{n}\left(t_{ij} - t_j^-\right)^2}, i = 1,\ldots,m. \tag{8-3}$$

where t_j^* is the ideal attribute value for criterion j, and t_j^- is the negative ideal attribute value for criterion j.

The ideal and negative ideal solutions are given in Table 8-6.

Table 8-6 - TOPSIS Ideal Solution Matrix

	S_i^*	S_i^-
Alternative Lane 1	0	0.658
Alternative Lane 2	0.658	0
Alternative Lane 3	0	0.658

Step 6. The Relative Closeness C_i^* of each alternative to the Ideal Solution is calculated by Yoon and Hwang (1995):

$$C_i^* = \frac{S_i^-}{\left(S_i^* + S_i^-\right)}, \quad i = 1,\ldots,m. \tag{8-4}$$

The relative closeness ranks for the presented example are given in Table 8-7.

Table 8-7 - TOPSIS Relative Closeness

	Closeness
Alternative Lane 1	1
Alternative Lane 2	0
Alternative Lane 3	1

Step 7. Select the optimal alternative by ranking the respective relative closeness, and select the alternative which is closest to 1. In the linear braking benchmark scenario Alternatives 1 and 3 result in the ideal ranks of 1. In this scenario the default decision is to select the lowest number alternative, as this represents the motorway lane closest to the emergency lane.

8.3.2 Analytical Hierarchy Process Method

The application of AHP follows these steps:

Step1. Define the weight of each pairwise criterion in the criteria weight matrix A. Each criterion is compared with each other criteria (Pairwise). The method for assessing pairwise comparisons uses values of 1 for equal weights, 2 to 9 where 2 represents a slightly more important criterion and 9 describes an extremely more important criterion, and the reciprocal of 2 to 9 to represent less important criterion, as described by Saaty and Vargas (2004). The pairwise rating of the criteria are given in Table 8-8.

Table 8-8 - AHP Criteria Pairwise Weighting

	Criterion 1	Criterion 2	Criterion 3
Criterion 1	1	1/4	1/6
Criterion 2	4	1	1/3
Criterion 3	6	3	1

The grey shaded boxes show that when one criteria is compared against itself, it must always have a value of 1. Criterion 1 of impact velocity is ranked as the most important. Criterion 3 of manoeuvre acceleration is ranked as the least

important. As criterion 2 of required braking of the vehicles behind relies on the assumption that the vehicles can achieve that braking value, it is considered less important than the impact velocity ahead, but more important than the manoeuvre acceleration.

Step 2. Normalize the weights of the criteria to create the Priority Vector (the normalized eigenvector of the matrix). Normalization is described by Saaty (1990) as the total dominance of the alternatives being compared to obtain the distribution of criterion priorities to each alternative corresponding to the relative dominance of the alternative. This process removes the scale of the attributes from influencing the decision. The normalized column sums technique to calculate the unit vector is given by Equation (3-2). The normalized priority vector is presented in Table 8-9.

Table 8-9 - AHP Priority Vector

Criteria	1	2	3
Normalized Vector (Priority Vector)	0.657	0.254	0.090

Step 3. Calculate the consistency of these subjectively assessed criterion weights. Consistency ensures that all subjective judgements have been assessed fairly. Saaty uses the eigenvector method to calculate consistency. In this example only the criteria weight matrix A is a judgement matrix. The Aw matrix is formed by multiplying each criteria attribute value by the priority vector calculated in step 2. Aw is used to determine the maximum eigenvalue λ_{max} by the following equation:

$$Aw = \lambda_{max}w \qquad (8\text{-}5)$$

The columns of the Aw matrix are summed and divided by the priority vector to give a numerical rank of each criterion. The newly calculated vector is then averaged to calculate the λ_{max}. This maximum eigenvalue is used to calculate the consistency index.

The consistency Index (CI) is calculated next using the formula from Saaty and Vargas (2004):

$$CI = \frac{(\lambda_{max} - n)}{(n - 1)} \qquad (8\text{-}6)$$

where n is the number of criteria.

The consistency ratio (CR) is calculated by dividing the consistency index by the corresponding Random Consistency Index number, given by Saaty and Vargas (2012) in Table 8-10. The value is a percentage indicating consistency of subjectively assessed values. The adjustment is small compared to the actual values of the eigenvector entries if there is an inconsistency of 10 percent or less.

A greater percentage will need the judgements of the priority vector to be reassessed, as this indicates that the subjective judgements are inconsistent.

Table 8-10 - AHP Random Consistency Index Numbers

n	1	2	3	4	5	6	7
Random Consistency Index Number	0	0	0.52	0.88	1.11	1.25	1.35

$$C.R. = \frac{C.I.}{R.I.} \qquad (8\text{-}7)$$

For the application of AHP here, only the priority vector weights are subjectively assessed, and so consistency of the decision matrix will not be required as this matrix is objectively determined from outputs produced by the simulators. The inconsistency of discrete data will always be zero. For the proposed example, the Consistency Ratio is calculated to be 7.57%, using Equations (8-5) to (8-7).

Step 4. The decision matrix with the objective attribute values from the simulator for each alternative against each criterion must be normalized, using Equation (3-2). The quantitative attributes allow for immediate vector normalization, without the need to pairwise compare or assess inconsistency, (Saaty and Vargas, 2012). The Decision Matrix given in Table 8-2 is normalized and presented in Table 8-11.

Table 8-11 - Vector Normalized Decision Matrix

	Criterion 1	Criterion 2	Criterion 3
Alternative Lane 1	0	0.306	0.326
Alternative Lane 2	1	0.389	0.347
Alternative Lane 3	0	0.306	0.326

Step 5. Multiply the normalized decision matrix by the priority vector normalized weights, as given in Table 8-12.

Table 8-12 - AHP Weighted Rank Matrix

	Criterion 1	Criterion 2	Criterion 3
Alternative Lane 1	0	0.078	0.029
Alternative Lane 2	0.658	0.099	0.031
Alternative Lane 3	0	0.078	0.029

Step 6. Calculate the weighted rank vector by summing all attributes for each alternative, as given in Table 8-13.

Table 8-13 - AHP Weighted Rank Vector

	Rank
Alternative Lane 1	0.107
Alternative Lane 2	0.786
Alternative Lane 3	0.107

Step 7. Select the optimal alternative by ranking the respective weighted rank vector. Note, for a minimizing optimization this will be the value closest to 0, for a maximizing optimization the value closest to 1 will be selected. In this case, Alternatives 1 and 3 are the optimal choice, and Lane 1 will be selected, as this is closest to the emergency lane.

8.3.3 Analytical Network Process Method

As ANP refers to a network it does not follow the hierarchical process of AHP. The criteria can affect the alternatives, but the alternatives can now affect the criteria as well. The nodes of this model need to be defined, as the feedback can influence nodes. The nodes are defined as the overall Goal, the Criteria and the Alternatives. The method is as follows:

Step 1. Calculate the Priority Vector of criteria weights, in the same way as for AHP Method (see Table 8-9).

Step 2. Use the Decision Matrix of normalized alternative attributes given in Table 8-11 to calculate the weighted ranks of the alternatives given in Table 8-12 by AHP Method. From this step, a rank of alternatives could be calculated, as with the AHP

method, but ANP introduces another consideration of the influence each alternative has on the decision made. This gives the ANP process a way to reassess the rank values produced, even change the rank order if criterion are assessed to be less important on the decision made.

Now the feedback of ANP is introduced with the Supermatrix as follows:

Step 3. Assess the influence of the attributes with respect to the criteria. For each criterion, determine which attribute best satisfies the goal. Normalize the alternative attributes, assessing how much of an influence each attribute has on satisfying the goal, as presented in Table 8-14 using Equation (3-2).

Table 8-14 - ANP Weighted Ranks of Alternatives

	Alternative Lane 1	Alternative Lane 2	Alternative Lane 3
Criteria 1	0	0.576	0
Criteria 2	0.484	0.224	0.484
Criteria 3	0.516	0.200	0.516

This matrix is transposed as represented in Table 8-14, to insert it into the Supermatrix in Table 8-15.

Step 4. Create the Supermatrix by starting with an Identity Matrix, which includes the nodes of goal, criteria, and alternatives. Input the Weighted Decision Matrix, the Normalized Alternative Values, and the Priority Vector. To aid with demonstrating how ANP is used, Table 8-15 shows how the matrices and vector are inputted into the Supermatrix.

Table 8-15 - Supermatrix of ANP Method

		1	2			3		
		Goal	Criteria 1	Criteria 2	Criteria 3	Alternative 1	Alternative 2	Alternative 3
1	Goal	1						
2	Criteria 1	0.657	1			0	0.576	0
	Criteria 2	0.254		1		0.484	0.224	0.484
	Criteria 3	0.090			1	0.516	0.200	0.516
3	Alternative 1		0	0.078	0.029	1		
	Alternative 2		0.657	0.099	0.031		1	
	Alternative 3		0	0.078	0.029			1

Table 8-15 demonstrates how the Supermatrix is formed as shown by Goepel (2011). The yellow boxes are the priority vector values calculated in Step 1. The orange boxes illustrate the decision matrix calculated in Step 2. The blue boxes illustrate the influence of attributes calculated in step 3, and it is these attribute values that will be used to tune the criteria for greater or lesser importance. The Grey boxes indicate a value of 1, as any Criteria or Alternative rated against itself has a value of 1. The red boxes will indicate the final normalized ranks of the alternatives.

Step 5. Calculate the Limit Supermatrix, by raising the Supermatrix' power to k+1. The value of k is the power to which the matrix converges in successive iterations (all values in each row are identical). The value of k is the power by which the Supermatrix is raised. It must be high enough, so the matrix fully converges. A loop calculation could find k exactly, but this would take greater computational effort. For simplicity, k should be set to a high value, which would mean only one calculation as represented in Equation (3-3). The limit Supermatrix is given in Table 8-16.

Note: the Supermatrix must be stochastic by columns, this is so when calculating the Limit Supermatrix it will converge when raising the matrix powers successively.

Table 8-16 – Limit Supermatrix of ANP Method

		1	2			3		
		Goal	Criteria 1	Criteria 2	Criteria 3	Alternative 1	Alternative 2	Alternative 3
1	Goal	0	0	0	0	0	0	0
2	Criteria 1	0.098	0.098	0.098	0.098	0.098	0.098	0.098
	Criteria 2	0.193	0.193	0.193	0.193	0.193	0.193	0.193
	Criteria 3	0.475	0.475	0.475	0.475	0.475	0.475	0.475
3	Alternative 1	0.049	0.049	0.049	0.049	0.049	0.049	0.049
	Alternative 2	0.135	0.135	0.135	0.135	0.135	0.135	0.135
	Alternative 3	0.049	0.049	0.049	0.049	0.049	0.049	0.049

Step 6. Normalize the clusters of nodes. A normalized value for criteria and for alternatives form the result of the Limit Supermatrix. The normalized alternatives are represented by the red boxes (Table 8-15). The normalized criteria will show the influence each criterion had on the decision due to the introduced feedback. The alternative ranks are normalized using Equation (3-2), and are given in Table 8-17.

Table 8-17 - ANP Normalized Alternative Ranks

	Rank
Alternative Lane 1	0.211
Alternative Lane 2	0.579
Alternative Lane 3	0.211

Step 7. Select the optimal alternative from the normalized values. For a minimizing objective, this will be the value closest to 0. Therefore, the normalized alternative ranks for Lanes 1 and 3 have the values closest to 0. Alternative Lane 1 is selected because of the default decision described in the TOPSIS Step 7 that when there are two or more identical rank values, it is the lowest lane number selected as this is the lane closest to the emergency lane.

8.4 MADM Conclusions

The simulators developed in Chapter 7 can be used to obtain values of a number of criteria by which to base a decision on the best lane the autonomous vehicle to be in regarding a potential collision. This data needs to be evaluated so a reliable decision can be made, instructing the autonomous vehicle to drive towards the best lane.

The MADM methods select the best choice from a discrete number of alternatives. In this research, the alternatives are lanes available for the Host Vehicle to select from. The decision is based on the criteria which are described by the outputs of the simulators presented in Chapter 7. There is also the added benefit of weighting the criteria, to give certain criteria greater influence on the decision made.

Several MADM methods are evaluated, and three methods have been selected for further investigation due to their suitability to the research problem. These methods are TOPSIS, AHP and ANP. These methods are selected due to the decision output that they provide. They are used to select the best choice lane without a further investigation of the results. They all employ normalizing or standardizing techniques to make an unbiased decision. The MADM methods are demonstrated using the linear braking benchmark scenario described in Chapter 7.

In this thesis AHP and ANP are investigated with a single structure of criteria. It is possible for these methods to structure the hierarchy with sub-criteria. This means that the problem can be decomposed into a hierarchy of interrelated elements, as described by Tzeng and Huang (2011). This gives the potential for further development into the structuring of hierarchy and including more criteria if this can be demonstrated to improve the performance of the MADM methods regarding the decisions made.

The three MADM methods selected can be employed with the developed simulators. The decisions made by these MADM methods will be investigated. All three methods will be tested with the Non-V2V Linear Braking Simulator and V2V Dynamic Braking Simulator described in Chapter 7, to observe whether the methods can determine the best lane for the Host Vehicle to drive into with the aim of avoiding or mitigating imminent collisions.

Chapter 9

Simulation Results

9.1 Introduction

The simulators and decision methods will be tested against several scenarios, which will assess how a specific parameter inputted to the simulator will affect the results calculated and then the decision made. The decision will recommend the safest lane for the Host Vehicle to drive into. The simulations will also evaluate any possible limitations of the simulators and decision processes, such as decision making processing time and when the simulator cannot calculate potential secondary collisions, stating implementation challenges and when the simulators and MADM decision processes cannot be used.

The scenarios are confined to the limitations of the simulator, which is set to calculate the behaviours of vehicles in a motorway setting. The simulators are limited to simulating motorway scenarios on a straight road. The Host Vehicle occupies the

middle lane of a three-lane motorway; there are also vehicles occupying all lanes of the motorway ahead and behind the position of the Host Vehicle. The simulators will calculate the severity of six potential collisions, between the Host Vehicle with the 3 vehicles ahead, and the 3 vehicles behind.

9.2 Motorway Simulation Scenarios

The MADM methods will be tested across different scenarios. The two simulator results (Non-V2V and V2V) will be used first with the benchmark scenarios defined for both simulators in Chapter 7. Further, in each simulation scenario only one parameter will change from the benchmark parameters. Each parameter change is evaluated with respect to how this affects the simulations results, and then the MADM output. The Non-V2V simulator and the outputs of the MADM methods will be assessed in Section 9.5, and the V2V simulator and the MADM method's outputs in Section 9.6.

The decision processes involve mathematical methods, so there needs to be a way to evaluate if the "correct" decision is made. For this reason, an Observer's decision is required. The Observer's decision is a human assessment of the available simulation results. The simulation values are used to make a human decision on what is thought to be the best lane choice. This Observer's choice is considered to be correct, and each MADM method has its lane selection choice compared with this human decision. Each MADM method is evaluated on how often it agrees with the Observer's decision, as a measure to determine the best MADM method for the applied simulators and scenarios.

9.3 Using Simulator Results in MADM Methods

9.3.1 Non-V2V Simulator

Without V2V communication, there is limited information available to the MADM methods, which cannot describe the severity of the collisions as well as when V2V is available. Impact velocity and required rate of deceleration (braking) are indications

of collision severity and will be used as the criterion for the MADM methods. Impact velocity is a parameter that is used for the calculation of collision severity by the collision modelling, and so it is relevant for assessing collision severity. In the case when V2V communication is not available, an assumed constant braking value is needed for the calculation of the vehicles ahead velocities and displacements. The Host Vehicle calculates the initial deceleration at time=0 for the vehicles ahead. This is an assumption, but needed to be made for a useful output of the decision process. For the vehicles behind that have not yet begun to communicate their deceleration rates, the required rates of deceleration are available, assuming a lower stopping distance and a higher initial velocity to result in a higher impact velocity meaning a more severe collision. The manoeuvre acceleration is the third criterion to describe the severity of the collision, as the manoeuvre itself could cause injury to vehicle occupants.

9.3.2 V2V Dynamic Braking Simulator

With V2V available to communicate vehicle parameters such as mass and crash structure stiffness for the collision modelling, the vehicle accelerations during the collisions can be calculated. V2V is also assumed to communicate the dynamic braking of all vehicles for calculating their velocities and displacements.

The velocities at impact of the vehicle ahead and the Host Vehicle produce one impact velocity. Similarly, the velocities of the Host Vehicle and vehicle behind produce another impact velocity. These calculations are repeated for each lane. They are used as criterion for the MADM, as well as the Time-To-Collision and Manoeuvre acceleration results from the dynamic braking simulator. In an ideal situation all vehicles would communicate the required information, because this method can only be used if this information is available.

9.4 MADM Criteria Weights

As there are two simulators with different criteria, two sets of criteria weights are defined. As the weighting method for AHP and ANP is limited to the Pairwise Comparison method of Saaty and Vargas (2004), and the TOPSIS weighting method

is less strict, all methods will use the same criteria weights. They form a Priority Vector for each of the simulators.

The criterion weighting for the Non-V2V simulator (Table 9-1) sets the most important criterion as the Impact Velocity with the vehicles ahead, as this will directly describe the severity of a collision. The Required Braking of the vehicles behind will indirectly describe the severity of the collision, as a lower braking value is desirable but will need the rate of deceleration of the vehicles behind to assess the true effect. The vehicles behind are further away from the initial hazard of the vehicle ahead coming to a sudden stop. Therefore, it is assumed that they will not react to the hazard as quickly as the Host Vehicle. Also, V2V communication can warn vehicles about the hazard, so they can then communicate a braking value, even before it is enacted. As the Non-V2V simulator does not have this feature available, a required braking value will need to suffice. The Manoeuvre Acceleration is the least important criterion, as it is the collisions that are the priority in making the decision. This is used as a criterion to describe the severity of the manoeuvre itself, as a sudden lane change or full braking could result in injury to the vehicle occupants if they are not fully restrained. The occupants could be injured by colliding with the interior of the car. The weights are set by the author of this thesis.

Table 9-1 - Non-V2V Criterion Pairwise Weighting

	Impact Velocity Ahead (m/s)	Required Braking of Vehicle Behind (m/s^2)	Manoeuvre Acceleration (m/s^2)
Impact Velocity Ahead (m/s)	1	1/4	1/6
Required Braking of Vehicles Behind (m/s^2)	4	1	1/3
Manoeuvre Acceleration (m/s^2)	6	3	1

The eigenvector analysis of the weights from Table 9-1, gives a consistency ratio of 7.57% from Step 3 of the AHP method, described in Section 8.3.2. As this is

a measure of inconsistency, and it must not exceed 10%, it can be concluded that the defined weights can be applied to the decision process. The resultant priority vector is given in Table 9-2, and is determined by Step 2 in Section 8.3.2.

Table 9-2 - Non-V2V Priority Vector

	Impact Velocity Ahead	Required Braking of Vehicles Behind	Manoeuvre Acceleration
Priority Vector	0.6567	0.2537	0.0896

The criterion weighting for the V2V simulator (Table 9-3) is set so that the relative impact velocities of the Host Vehicle impacting the vehicle ahead, and vehicle behind impacting the Host Vehicle are equal to each other. The impact velocities are more important criterion compared to the Manoeuvre Acceleration and Time-To-Collision. Manoeuvre Acceleration is more important than Time-To-Collision, as this will directly affect the comfort of the vehicle occupants. Time-To-Collision is the least important criterion, as this gives an indication to how much time the Host Vehicle has to react, but the other criteria describe the direct effect of the collisions and manoeuvres. Therefore, it has the lowest weight.

Table 9-3 - V2V Criterion Pairwise Weighting

	Collision Acceleration 1	Collision Acceleration 2	Collision Acceleration 3	Collision Acceleration 4	Manoeuvre Acceleration	Time-To-Collision
Collision Acceleration 1	1	1	1	1	1/3	1/7
Collision Acceleration 2	1	1	1	1	1/3	1/7
Collision Acceleration 3	1	1	1	1	1/3	1/7
Collision Acceleration 4	1	1	1	1	1/3	1/7
Manoeuvre Acceleration	3	3	3	3	1	1/5
Time-To-Collision	7	7	7	7	5	1

The pairwise comparison of Saaty and Vargas (2004) gives a structured method to give subjective ratings. This method also allows for slight inconsistency, as discussed in Section 3.3.4, for the assessment. The resultant priority vector is given in Table 9-4.

Table 9-4 - V2V Priority Vector

	Collision Acceleration 1	Collision Acceleration 2	Collision Acceleration 3	Collision Acceleration 4	Manoeuvre Acceleration	Time-To-Collision
Priority Vector	0.2150	0.2150	0.2150	0.2150	0.1126	0.0272

The priority vector is determined by Step 2 of Section 8.3.2. The consistency ratio for the defined weights of Table 9-4 is 2.47%, and so can be applied as a consistent priority vector to the decision process. The consistency ratio is calculated from Step 3 of the AHP method in Section 8.3.2.

Included in the simulation results is the Lanes Open criteria. This is not a criteria used in the MADM decision calculations, as this is a limit. 1 signifies an open lane, whereas 0 signifies a disqualified lane which will not be included in the available alternatives. Therefore, Lanes Open will not need a criteria weight.

9.5 Non-V2V Linear Braking Simulations

The non-V2V simulator are tested against the set parameters to see how each parameter will affect the results of the simulation and then the decision made. For the parameters that will change the behaviours of the motorway vehicles, the sensitivity analysis will aim to determine what values will influence a decision, i.e. a different lane to be selected. These parameters are examined in Sections 9.5.7 to 9.5.11. First, Sections 9.5.2 to 9.5.6 will analyse the Host Vehicle's performance, and the limits of the Host Vehicle to perform lane-change manoeuvres will be tested. Section 9.5.1 is the benchmark scenario from which the simulation results and MADM decisions will be compared.

9.5.1 Benchmark Simulation

The benchmark simulation will examine the decision made using the parameters set given in Table 7-1 and Table 7-2 in Section 7.3.5. The benchmark simulation results are presented in Table 9-5.

Table 9-5 - Benchmark Simulation Results

	Lane 1	Lane 2	Lane 3
Impact Velocity Ahead (m/s)	0	3.7888	0
Required Braking of Vehicles Behind (m/s^2)	6.522051	8.29168	6.522051
Manoeuvre Acceleration (m/s^2)	8.455976	9	8.455976
Lanes Open	1	1	1

Across all of the criteria, Lane 2 has the most severe criteria values. It demonstrates the highest Impact Velocity with the vehicle ahead, the highest required braking of the vehicles behind to avoid collision, and the highest acceleration for the manoeuvre. Lanes 1 and 3 have a value of 0 for the Impact Velocity Ahead, which signifies a collision avoidance as there is no impact velocity. Lanes 1 and 3 have identical values and so in this situation the decision will default to the lowest Lane number, as Lane 1 will be closer to the emergency lane should emergency vehicles be required. Therefore, the Observer's decision is to select Lane 1 as the benchmark decision. All lanes are 'open' as indicated by a number 1, therefore all are available and used in the decision process. The Lanes Open signifies that all lanes are open and therefore available as alternatives for the MADM decision.

Table 9-6 - Benchmark Simulation Decision

	Lane 1	Lane 2	Lane 3	Lane Select
TOPSIS	1	0	1	1
AHP	0.106786	0.786428	0.106786	1
ANP	0.210674	0.578653	0.210674	1

Table 9-6 demonstrates that all three MADM methods select Lane 1 as the best lane choice, agreeing with the Observer's decision. A closer look at how the methods rank each alternative shows that TOPSIS is fully supporting either Lane 1 or 3, as the

intention of TOPSIS is to select the rank closest to 1. For AHP and ANP the decision is to select the alternative closest to 0. Lane 1 is closer to 0 for AHP than ANP. It must be stressed that AHP and ANP vector normalize their ranks, so a value of 0 will likely never occur, while a value of 1 occurs in TOPSIS.

The ranks of Table 9-6 demonstrate that for the benchmark simulation, all three methods have performed in the same way, as expected, because Lane 1 has the lowest values of all the criteria, and agreed with the Observer's decision.

9.5.2 Host Vehicle ACC Following Time

Firstly, the ACC Following Time is set to $1.4s$. The lowest time this parameter can be set to is $1.35s$, as any lower value will cause Lanes 1 and 3 to be disqualified due to not having enough longitudinal distance for the steering manoeuvres to be completed before collision with vehicles ahead.

From a Host Vehicle ACC Following Time of $1.6s$ and greater, the longitudinal distance to complete the steering manoeuvre becomes so great that a collision occurs with vehicles behind before the steering manoeuvre is complete. This disqualifies Lanes 1 and 3 when the Host Vehicle ACC Following Time is $1.6s$ and greater. A $0.2s$ operating window from $1.35s$ to $1.55s$ does not seem desirable to use as a greater operating range would be preferred. However, one must be reminded that this is based on the benchmark scenario. If the headway distances for the vehicles behind were increased, then a different decision would have been available. For comparison, the ACC time is set to $2.0s$, and the rear Headway distance of Lane 3 is set to $34m$. In this scenario the decision is to select Lane 3, whilst Lane 1 is still disqualified, as represented in Table 9-7.

Table 9-7 - ACC Simulation Results

	Lane 1	Lane 2	Lane 3
Impact Velocity Ahead (m/s)	0	0.458931575	0
Required Braking (m/s^2)	6.516618076	7.187138264	4.760085184
Manoeuvre Acceleration (m/s^2)	6.553902773	6.76329643	6.553902773
Lanes Open	0	1	1

Immediately Lane 1 is disqualified, so the decision has to be made between Lanes 2 and 3. Lane 3 has 0m/s impact velocity and a lower required braking from the vehicle behind, so Lane 3 is the Observer's decision.

Table 9-8 - ACC Decision Ranks

	Lane 1	Lane 2	Lane 3	Lane Select
TOPSIS	DQ	0	1	3
AHP	DQ	0.85483474	0.14516526	3
ANP	DQ	0.703145238	0.296854762	3

All the MADM methods agree with the Observer's decision in Table 9-8, DQ denotes a disqualified lane from the decision making process. It is noted that between AHP and ANP, it is AHP that seems closer to 0 for the preferred alternative, which suggests that AHP is more confident in its decision. For ANP the feedback gives a greater weight to the Manoeuvre Acceleration, and reduces the weight of Impact Velocity Ahead.

9.5.3 Coefficient of Friction

The coefficient of friction CoF between the tyre and road is set to 0.7 in the benchmark. Lowering this to 0.65 causes disqualification for Lanes 1 and 3, due to the yaw rate $\dot{\psi}$ required to complete the manoeuvre exceeding the yaw rate limit $\dot{\psi}_{friction}$, and also because the skidding speed calculated in Equation (7-3) is exceeded by the vehicles speed during the manoeuvre. Both of these disqualifications are due to the high yaw rate required to complete the manoeuvre. In order for a manoeuvre to be completed at a lower CoF, the manoeuvre yaw rate needs to be reduced. This is done by increasing the longitudinal distance for the lane-change manoeuvre, which is done by increasing the ACC Following Time and Headway Distances for the vehicles ahead. Conversely, increasing the CoF to 0.8 allows for a minimum ACC Following Time of $1.25s$.

Table 9-9 - CoF Simulation Results

	Lane 1	Lane 2	Lane 3
Impact Velocity Ahead (m/s)	10.84549	9.9358	10.84549
Required Braking (m/s^2)	5.570096	8.29168	5.570096
Manoeuvre Acceleration (m/s^2)	8.691042	9	8.691042
Lanes Open	1	1	1

Lanes 1 and 3 do have slightly higher Impact Velocities than Lane 2, but there is a more considerable difference in the Required Braking of the vehicles behind, suggesting that the vehicle behind in Lane 2 will collide with greater severity. The Observer's Decision is to select Lane 1.

The closer alternative values given in Table 9-9 led to the closer ranks given in Table 9-10. However, all of the three MADM methods select Lane 1 as the best choice.

Table 9-10 - CoF Decision Ranks

	Lane 1	Lane 2	Lane 3	Lane Select
TOPSIS	0.648856	0.351144	0.648856	1
AHP	0.327435	0.345131	0.327435	1
ANP	0.319666	0.360668	0.319666	1

The testing of CoF does indicate one concern with the lateral acceleration. The Yaw Rate limit is used to calculate the maximum possible lateral acceleration, which then calculates the braking for the steering manoeuvre. The higher CoF actually reduces the steering manoeuvre braking. In reality, if the CoF were to increase then so would the overall manoeuvre acceleration, which calculates a braking value with tyre saturation. Simulation results support this; the benchmark steering manoeuvre's braking value is $5.5494m/s^2$, but if the CoF is increased to 0.8 and the overall manoeuvre acceleration to $1.0g$ then the lane-change braking value is $5.886m/s^2$. The velocity of the Host Vehicle through the lane-change manoeuvre will reduce more than the benchmark simulation lane-change manoeuvre. This

concludes that the higher the CoF, the greater the available braking for a lane-change manoeuvre which increases the rank preference to change lanes.

9.5.4 Maximum Host Vehicle Deceleration

The maximum deceleration of the Host Vehicle is applied when the Host Vehicle stays in the current lane and there is no steering manoeuvre to account for. The braking of the Host Vehicle through a steering manoeuvre is affected by the maximum braking value only when the maximum braking is less than the lane-change manoeuvre braking as determined by the tyre saturation in Equations (5-14) to (5-18). For the benchmark scenario, the tyre saturation calculation in Equation (5-18) determined the lane-change manoeuvre braking to be -5.5m/s^2.

The testing shows that increasing the maximum braking increases the required braking of the vehicle behind in the same lane, so effectively reducing the severity of one collision increases the severity of another. This is why an additional step has been added; the required braking for the Host Vehicle is to come to a full stop just before impacting the vehicle ahead is determined. For the benchmark scenario this is calculated as -9.13m/s^2. This ensures no impact with the vehicle ahead, but also aims to reduce the severity of a collision with the vehicle behind. In this case the required braking of the vehicle behind is -8.35m/s^2, which is higher than the values for Lanes 1 and 3, and so it does not change the decision to Lane 1. The rank values for this scenario are given in Table 9-11.

Table 9-11 - Host Vehicle Deceleration - Collision Avoidance Ahead

	Lane 1	Lane 2	Lane 3	Lane Select
TOPSIS	1	0	1	1
AHP	0.106786	0.786428	0.106786	1
ANP	0.210674	0.578653	0.210674	1

9.5.5 Host Vehicle Overall Manoeuvre Acceleration

Section 9.5.3 discusses the importance of overall manoeuvre acceleration for the lane-change manoeuvre braking value, which is influenced by the CoF. When the value of the overall acceleration is set to $0.7g$ and below, the resultant acceleration available for braking as determined by the tyre saturation in Equations (5-14) to (5-18) is 0. At $0.75g$ the resultant braking is $-2.64m/s^2$. As the overall acceleration increases, so does the resultant braking for the lane-change manoeuvres.

At $1g$, the rate of deceleration of the Host Vehicle is so high that it results in an impact with the vehicles behind before the manoeuvre is complete, therefore disqualifying Lanes 1 and 3. Increasing the initial headway distance of the vehicles behind does allow for those Lanes to remain open.
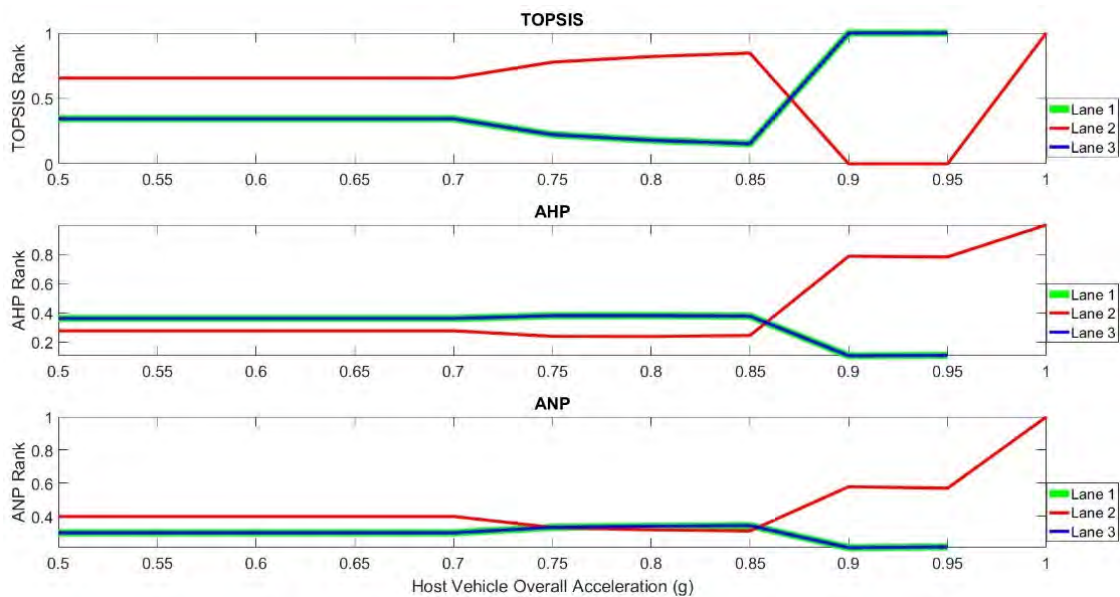
Figure 9-1 - Host Vehicle Overall Manoeuvre Acceleration Sensitivity Analysis

A sensitivity analysis is displayed graphically, plotting how the rank of each lane changes with the varying Host Vehicle Overall Manoeuvre Acceleration parameter. The three methods are plotted separately, but it must be remembered that for the TOPSIS graph the desired Lane is plotted higher up the graph (closer to 1), whereas for the AHP and ANP plots the desired lanes is plotted closer to 0. Figure 9-1 has identical rank values for Lanes 1 and 3, because these lanes have identical alternatives values.

Figure 9-1 demonstrates that for both TOPSIS and AHP from $0.5g$ to $0.85g$ the preferred choice is Lane 2, and then Lanes 1 and 3 are preferred from $0.9g$ to $0.95g$. At $1g$ Lanes 1 and 3 are disqualified, so Lane 2 is again the preferred choice. TOPSIS and AHP agree with the Observer's decision, but ANP gives preference to Lanes 1 and 3 from $0.5g$ to $0.7g$. From $0.75g$ to $0.85g$ the rank of ANP is very close between all three Lanes, but it is Lane 2 which is preferred. This is not a desirable result from ANP for accelerations below $0.7g$. The feedback has increased the weight of the least important criterion, and reduced the weight of the most important as set by the Priority Vector.

9.5.6 Host Vehicle CoM Height

The height of the Centre of Mass (CoM) determines if the Host Vehicle will overturn for the steering manoeuvre, as determined by Equation (7-4). The benchmark sets this height at $0.5m$. The highest that the CoM can be before the Overturning Speed limits a lane choice is $1.21m$ in the benchmark scenario. In order for the CoM to be raised, the track widths must also be increased to prevent the vehicle from overturning through the lane-change manoeuvres. The CoM height does not affect the results between Lanes 1 and 3, and so the decision is no different. It is only once the CoM height is high enough to result in the vehicle overturning that the decision changes, by disqualifying Lanes 1 and 3. The CoM height does not require further investigation, as this is a simple static calculation given in Equation (7-4) which determines if a manoeuvre can proceed without the vehicle rolling over.

9.5.7 Initial Velocity of Vehicles Ahead

The initial velocity of the vehicle ahead in Lane 3 is varied from $52.5mph$ to $75mph$. At initial velocities below $52.5mph$ a collision occurs before a steering manoeuvre is complete. It is also observed that from an initial velocity of $69mph$ and higher in Lanes 1 and 3, there is no collision ahead, therefore Lanes 1 and 3 will always have a collision avoidance. At the simulated initial velocities of $52.5mph$ to $75mph$, the collision avoidance of Lane 1 is the preferred choice lane for all three MADM methods. The decision process only looks at the potential impact speeds, so does not see a difference between initial velocities of $69mph$ to $75mph$ as they all result in collision avoidance, which is why from $69mph$ to $75mph$ the rank of Lane 3 is

identical to Lane 1. When ranks are equal the decision defaults to the lowest lane number, so Lane 1 is always selected for this analysis.
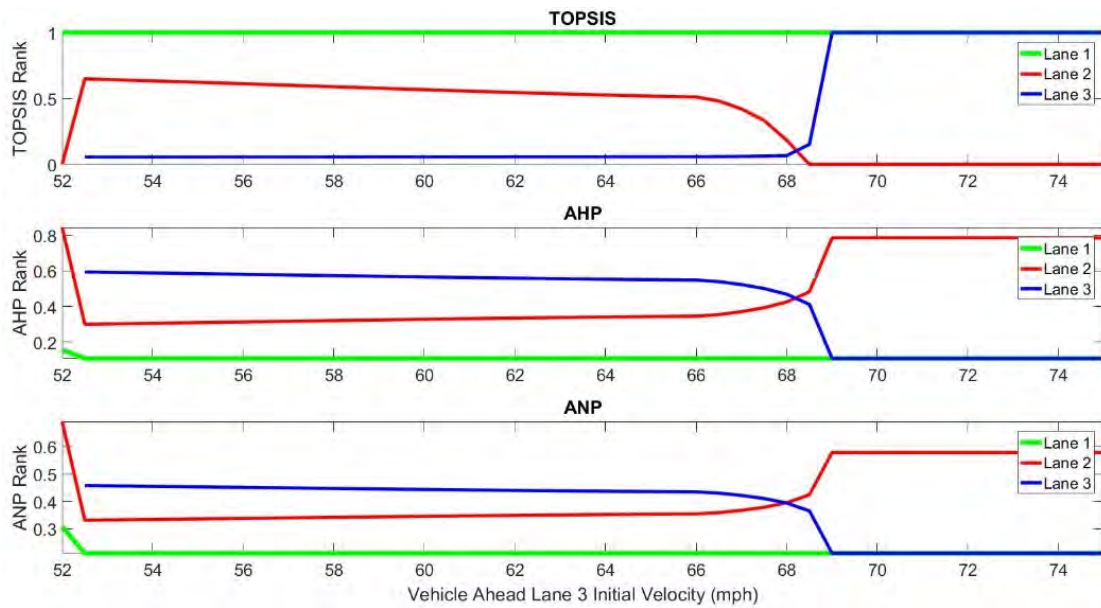
Figure 9-2 - Initial Velocity of Vehicle Ahead in Lane 3 Sensitivity Analysis

9.5.8 Initial Headway Distance to Vehicles Ahead

It is observed that the initial headway distance for the vehicle ahead in Lane 3 as low as $4m$ can still be enough to avoid a collision before the steering manoeuvre is complete. A headway distance of $18m$ and greater, results in no collision for Lanes 1 and 3.

Figure 9-3 demonstrates that Lane 1 is always the preferred choice with a collision avoidance, and for all of the MADM methods, Lane 3 has the same rank as Lane 1 from $18m$ onwards. The results of TOPSIS and AHP are similar, as Lane 2 has a better rank than Lane 3 from 6m to 16m. All of the three MADM methods selects Lane 1 even if Lane 3 has a greater initial headway distance, because in the decision process the impact velocity is 0 (collision avoidance) and this is the metric that informs the decision.
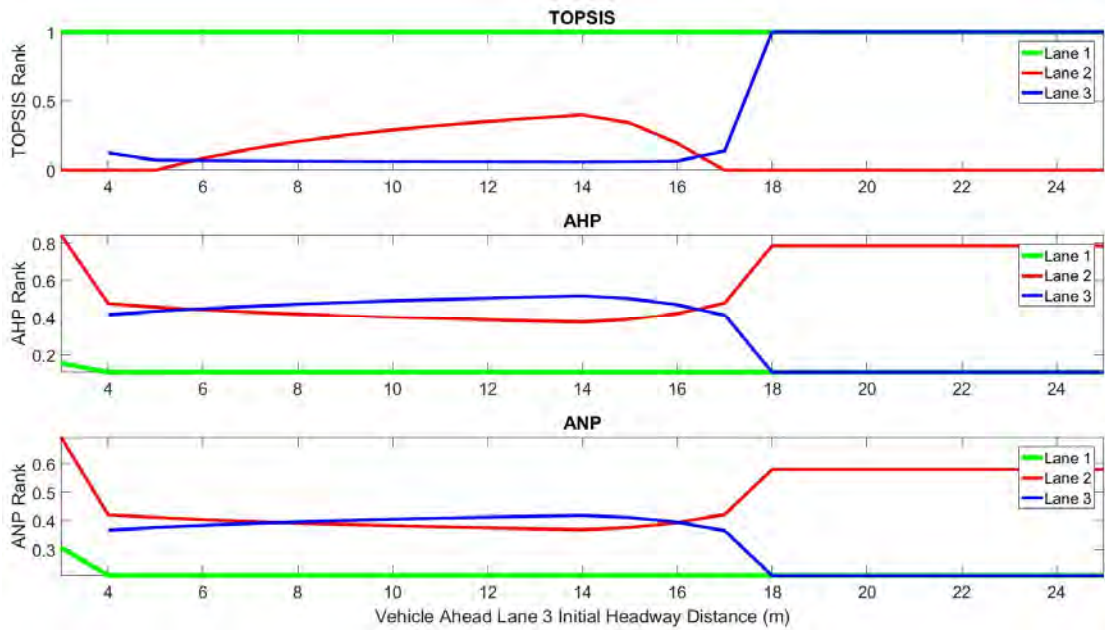
Figure 9-3 - Initial Headway Distance of Vehicle Ahead in Lane 3 Sensitivity Analysis

9.5.9 Braking Values of Vehicles Ahead

The deceleration of the vehicle ahead in Lane 3 will now be varied from $0 m/s^2$ to $-14.5 m/s^2$. With a rate of deceleration greater than $-14.5 m/s^2$, a collision occurs before the lane-change manoeuvre is complete.
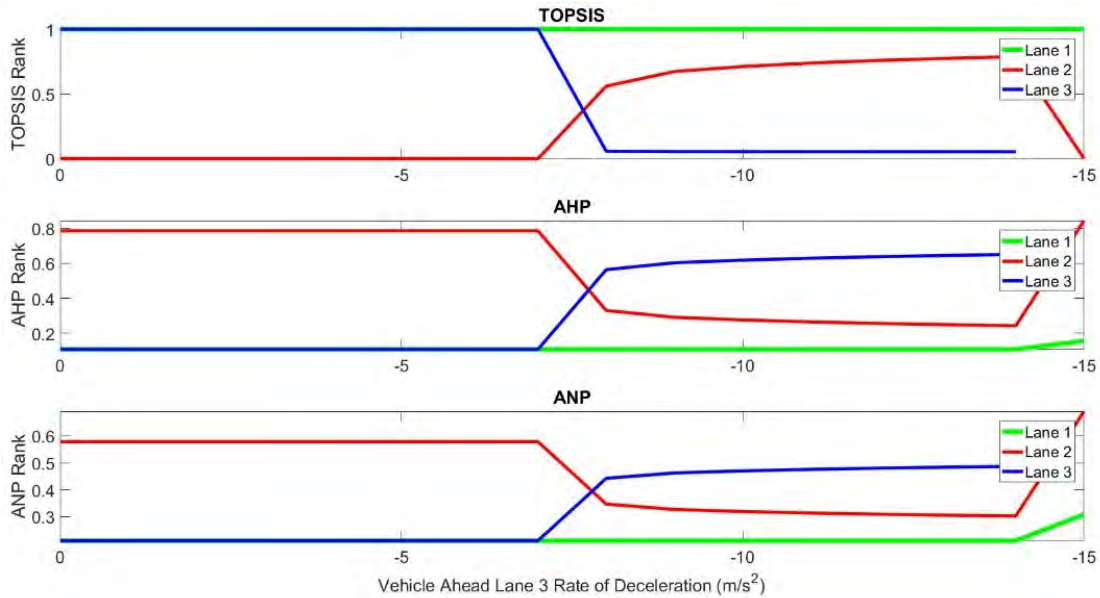
Figure 9-4 – Deceleration for Vehicle Ahead in Lane 3 Sensitivity Analysis

All of the three MADM methods preferred the collision avoidance in Lane 1. Lane 3 has an identical rank value up to -7m/s^2, because from -8m/s^2 and greater, a collision occurs in Lane 3. All of the MADM method decisions correlate from -9m/s^2 to prefer Lane 2 over Lane 3, due to the considerably larger impact velocities occurring in Lane 3 as a result of increasing the braking values of the vehicles ahead in this lane. Again, as there is no difference to the MADM methods regarding the collision avoidance, all of the MADM methods select Lane 1 for all of the deceleration values simulated.

9.5.10   Initial Velocity of Vehicles Behind

Testing the simulator demonstrated that the highest initial velocity of the vehicle behind in Lane 3 that will still allow a lane-change manoeuvre to be completed before impact is 73mph.
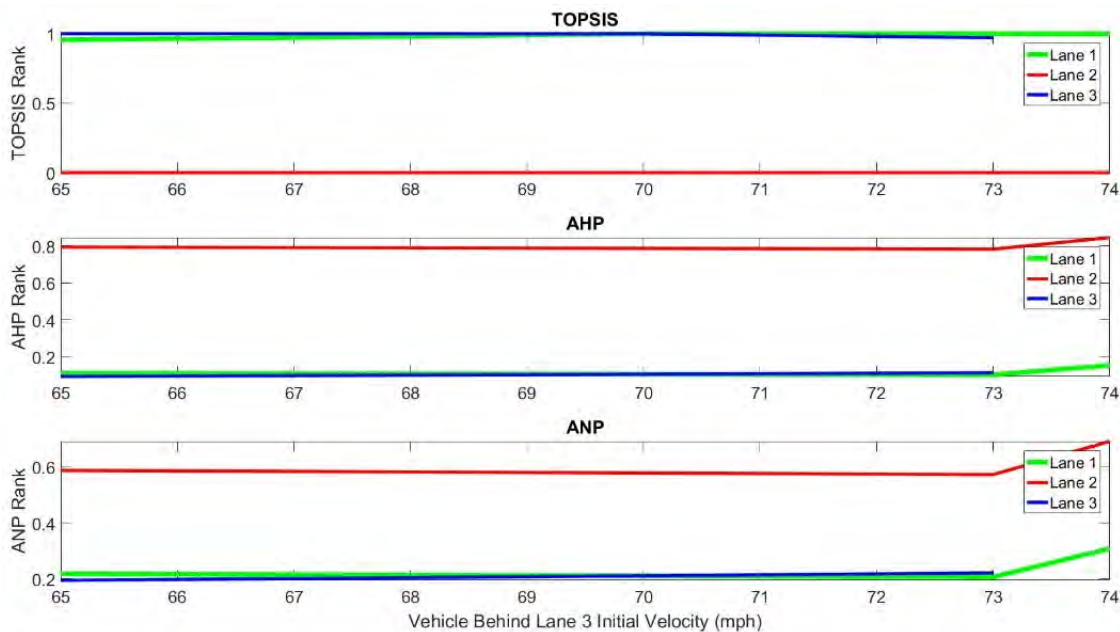
Figure 9-5 - Initial Velocity of Vehicle Behind in Lane 3 Sensitivity Analysis

Although the difference in rank is small, all of the three MADM methods agree with the observer's decision for each velocity simulated. From 65mph to 69mph the preferred choice is Lane 3, which has the lower initial velocity (see Figure 9-5). This means the vehicle in Lane 3 will have a lower impact velocity. From 70mph and

greater the preferred choice is now Lane 1, which remains at an initial velocity of $70mph$.

9.5.11   Initial Headway Distance to Vehicles Behind

The simulator shows that a lane will be disqualified if the initial headway distance of a vehicle behind in Lanes 1 or 3 is $16m$ or less. As Lane 2 is the same lane that the Host Vehicle is in, it will always remain open to the decision process. With the initial headway benchmark set at $20m$, the preferred choice is Lane 1. But as the distance in Lane 3 is increased further, all three MADM methods give a slight preference to Lane 3 over Lane 1, as in agreement with the Observer's decision in Section 9.5.1. At initial distances lower than $17m$, Lane 3 is disqualified due to a collision occurring before the lane-change manoeuvre is completed.
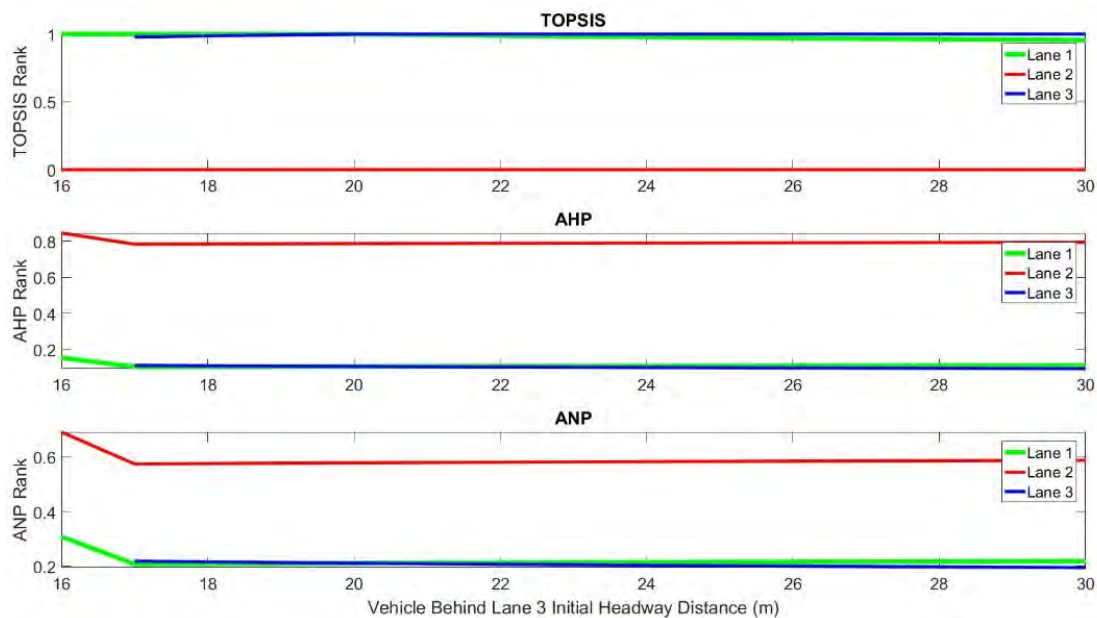
Figure 9-6 - Initial Headway Distance of Vehicle Behind in Lane 3 Sensitivity Analysis

9.5.12   Summary of Non-V2V Linear Braking MADM Results

The simulations demonstrated that TOPSIS and AHP both agreed with the Observer's decision on every simulation of the Non-V2V Linear Braking Simulator. ANP agreed all of the time, except for when testing different maximum overall

223

acceleration for the steering manoeuvres (Section 9.5.5). For the decision process a clear difference in the rank values is desired. Compared to AHP the rank values of different lanes are often close such as with the varying initial velocities and rates of deceleration for the vehicles ahead, in Section 9.5.7 and 9.5.9. One can conclude that with the Non-V2V Linear Braking Simulator the ANP has agreed with the Observer's decision less often than the TOPSIS and AHP methods.

9.6 V2V Dynamic Braking Simulations

With more parameters informing the dynamic braking simulator, there are more possible scenarios to test for both the Host Vehicle and Motorway Vehicles. There is also a number of parameters that will not be changed. These are the dynamic braking parameters of Cross-Sectional Area of Vehicles, Aerodynamic Drag Coefficients and Rolling Resistance Coefficients. Also, the Track widths and Longitudinal CoM positions for the Host Vehicle will remain unaltered. These parameters are being left unchanged to focus the evaluation on parameters that will have a greater influence on being able to change the decision. Changing the dynamic braking will alter the velocities and displacements of the vehicles, but this is better altered by the braking decelerations. The Host Vehicle Track Widths and CoM position will affect the Host Vehicle's turning ability, but this is better examined with CoF and CoM Height. The crash structure will be modelled using the same bilinear terms, described in Section 7.6, it is therefore assumed that all vehicle's crash structures will behave the same.

Section 9.6.1 is the benchmark scenario from which the simulation results and MADM decisions will be compared. Sections 9.6.2 to 9.6.6 present the parameters that describe the Host Vehicle, and so these will be investigated to see how they affect the possibility of a lane-change manoeuvre. For these parameters the simulated outputs for Lanes 1 and 3 will be identical, so there is no difference in the decision made between these lanes. Sections 9.6.7 to 9.6.14 will change the motorway vehicles, and so the simulated outputs will be different. A sensitivity analysis will assess the decision made for varying parameter values.

9.6.1 Benchmark Simulation

The Benchmark simulation will examine the decision made from the parameters set in Table 7-12 and Table 7-13 in Section 7.6.

9.6.2 Host Vehicle ACC Following Time

For the dynamic braking benchmark scenario, the available time range for the ACC is $1.35s$ to $1.91s$. For the times less than $1.35s$, there is not enough longitudinal distance for a lane-change manoeuvre to be completed before a collision occurs. For the times greater than $1.91s$, there is a collision avoidance ahead, and so Lane 2 becomes the preferred choice.

The simulations of the linear braking simulator for ACC Following Time given in Section 9.5.2 demonstrate a similar behaviour to these simulations when there is V2V communication, which is also influenced by the initial headway distances of the motorway vehicles. One of the adjacent lanes (Lanes 1 and 3) is disqualified when the ACC Time is set at $2.19s$ or greater. This disqualification is due to the large distance available to complete the lane-change manoeuvre, which results in a collision before the manoeuvre is complete.

9.6.3 Coefficient of Friction

The lowest CoF for the available longitudinal distance required to complete a lane-change manoeuvre in 0.7. This parameter's effect is the same as that on the linear braking simulator, discussed in Section 9.5.3.

9.6.4 Host Vehicle Maximum Longitudinal Deceleration (Braking)

The Maximum Longitudinal Deceleration is the braking the Host Vehicle will apply. With the dynamic braking, this value will actually be slightly higher with the resistance forces acting on the vehicle. However, for the steering manoeuvres this value cannot be exceeded otherwise a loss in tyre grip will occur.

Simulations reveal that a lane-change manoeuvre will be disqualified when this braking value is set at -1.2m/s^2 or lower due to an impact occurring before the lane-change manoeuvre is complete. However, Lane 2 will be selected when this value is set at -3.0m/s^2 or lower due to the low resultant braking value for the lane-change manoeuvre as the tyre saturation calculated a braking value of -1.77m/s^2.

The maximum rate of deceleration for this simulation scenario is -9.1m/s^2 before Lanes 1 and 3 are disqualified. This disqualification is due to the skidding speed, given in Equation (7-3), being lower than the Host Vehicle's initial speed. The skidding speed requires the coefficient of friction to be increased to complete the lane-change manoeuvre. Also increasing the available longitudinal distance to complete the lane-change manoeuvre would increase the skidding speed, as it is the low radius of curvature required to complete the manoeuvre. Therefore, Lanes 1 and 3 are disqualified based on skidding speed.

9.6.5 Host Vehicle Maximum Lateral Acceleration (Steering)

The benchmark Host Vehicle braking value for this scenario is -4.71m/s^2, as calculated from the tyre saturation. The lowest value the maximum lateral acceleration can be set to before Lanes 1 and 3 are disqualified due to a collision occurring before the lane-change manoeuvre is complete is 6.9m/s^2. This leads to a collision with the vehicles ahead, and the braking value for the lane-change manoeuvres at this maximum lateral acceleration is -0.78m/s^2.

A collision avoidance for the vehicles ahead in Lanes 1 and 3 is calculated when the maximum lateral acceleration is set at 12.3m/s^2 or higher. It is observed that the higher this value is set to, the more severe the collision accelerations are for the vehicles behind. As the Host Vehicle can decelerate quicker, the relative impact speeds between the Host and vehicles behind is greater. At lateral accelerations set at 7.2m/s^2 and lower, there is a collision avoidance in Lanes 1 and 3 for the vehicles behind.
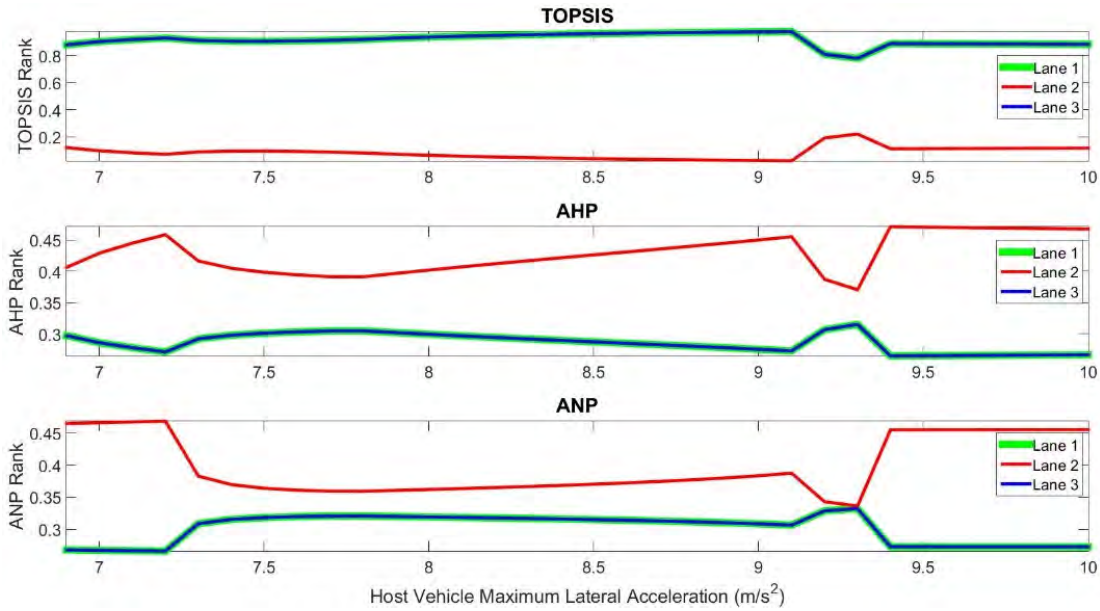
Figure 9-7 - Host Vehicle Lateral Manoeuvre Acceleration Sensitivity Analysis

Results of the sensitivity analysis displayed in Figure 9-7 show that Lanes 1 and 3 have identical rank values throughout, and they are preferred over Lane 2. With a maximum lateral acceleration of $6.9m/s^2$ to $9.1m/s^2$, the collision ahead in Lanes 1 and 3 occur before the collision behind. With lateral accelerations of $9.2m/s^2$ and greater, the available braking for the Host Vehicle is greater, and therefore the collision with the vehicles behind in Lanes 1 and 3 occur first. At $9.5m/s^2$ and greater lateral acceleration values, the Host Vehicle braking is sufficient to prevent a collision ahead. All MADM methods considered agreed with the Observer's Decision in every simulation scenario. The rank of Lane 2 for the ANP method does get very close to the ranks of Lanes 1 and 3 when the maximum lateral acceleration was set to $9.3m/s^2$. At this acceleration value, however, the lane preference is still Lane 1.

9.6.6 Host Vehicle CoM Height

The CoM height is used to determine if the Host Vehicle will rollover during the lane-change manoeuvre. This is a simple limitation, and the sensitivity analysis will determine if a rollover will occur, and disqualify the manoeuvre as a result if needed. It is observed that a rollover will result with a CoM height set at $1.21m$. However, when examining the vertical wheel loads with the height set just below the rollover height, at $1.20m$ it is clear that even though there is a vertical load pushing down on all wheels the Rear Left wheel reaches a minimum force of $0.016kN$ (Figure 9-8). Even the Front Left reaches a minimum value of $0.35kN$.
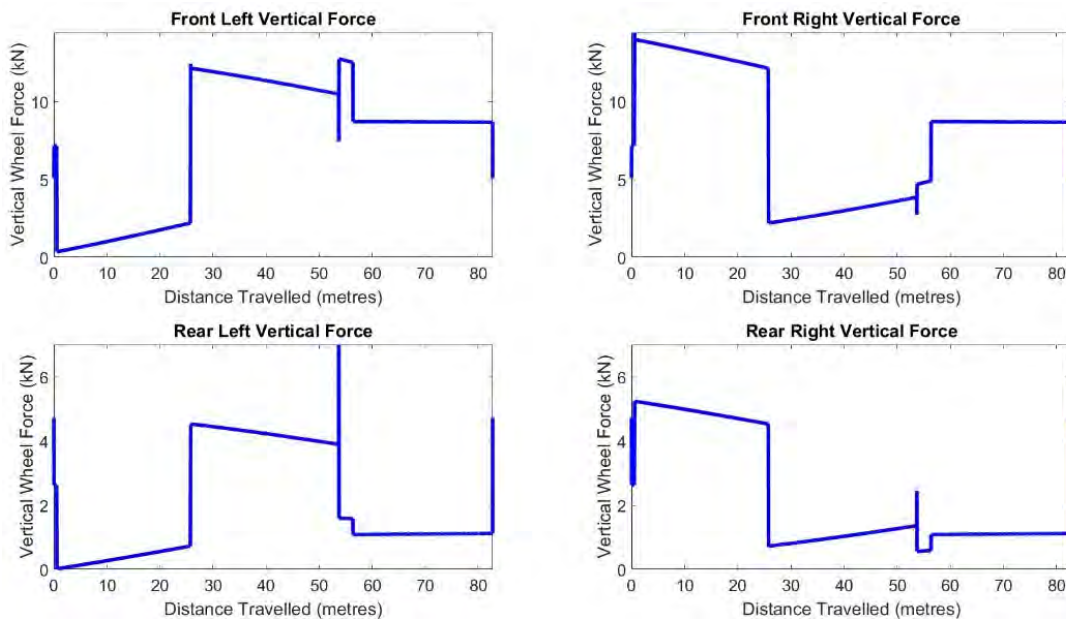
Figure 9-8 - Vertical Tyre Force approaching Rollover

Figure 9-8 suggests that perhaps the vertical wheel force limit should be set higher than $0kN$, as a safety factor. $0kN$ shows that there is no vertical force pushing the tyre down onto the road. This means that a value of $0kN$ mathematically represents a tyre lifting from the ground. This value would need to be determined by vehicle dynamics testing, but it is a simple matter of inserting this into the simulator instead of the limit set at $0kN$. At $53.61m$ the steering manoeuvre ends, and then the Host Vehicle can increase its braking from the value determined by the tyre saturation, given in Equations (5-14) to (5-18), to the maximum longitudinal braking defined in Table 7-12.

9.6.7 Vehicles Ahead Mass

The vehicle ahead in Lane 3 will vary its mass from $900kg$ to $3000kg$, while the benchmark is $2000kg$. Adjusting the mass will affect not only the collision acceleration results, but also the impact velocities as vehicle mass affects the dynamic braking. Figure 9-9 displays the sensitivity analysis for the mass of the vehicle ahead in Lane 3. All of the three MADM methods agreed with the Observer's Decision for every simulation. It is observed that the decisions made by the MADM methods are not to select the lighter vehicle. The collision accelerations demonstrated the dangers of a larger mass vehicle impacting with a smaller mass vehicle, and has taken all vehicles into account for the decision. From $900kg$ to $2000kg$, the preferred lane is Lane 1, to collide with the equal mass vehicle ahead of $2000kg$. From $2100kg$ to $3000kg$, the Host Vehicle selects the larger vehicle in Lane 3 to collide with.
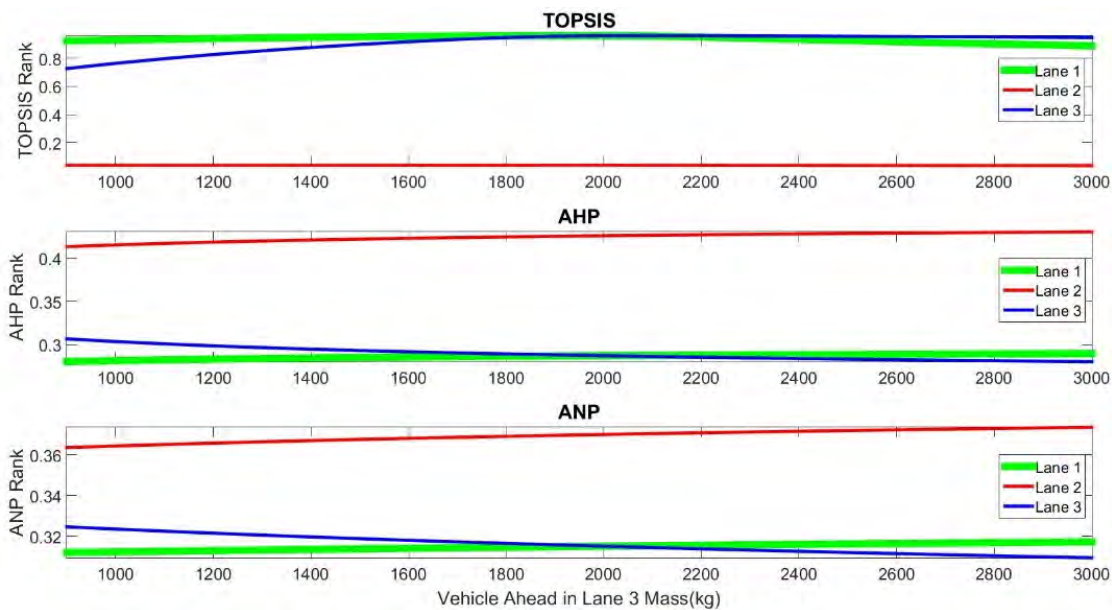
Figure 9-9 – Vehicle Ahead in Lane 3 Mass Sensitivity Analysis

Figure 9-9 represents the sensitiity analysis results. The rank values do not change drastically from $900kg$ to $3000kg$. A closer look at the simulation results reveals that for a mass of $900kg$, the vehicle ahead has a velocity at the moment of impact of $9.91m/s$, and the Host Vehicle has a velocity of $14.42m/s$. The simulation with a vehicle ahead mass of $3000kg$ reveals that the vehicle's ahead impact velocity is $8.86m/s$, and the Host Vehicle is travelling at $12.73m/s$. Whilst the mass of the

vehicle ahead influences the results, it does not change the results considerably. However, the larger mass vehicle does have an effective deceleration lower than the lighter mass vehicle. This allows for a greater stopping distance for the Host Vehicle, and so the Host Vehicle's preference is to select the collision with the larger mass vehicle.

9.6.8 Vehicles Behind Mass

The vehicles behind are examined using the same range of mass as with the vehicles ahead in Section 9.6.7.
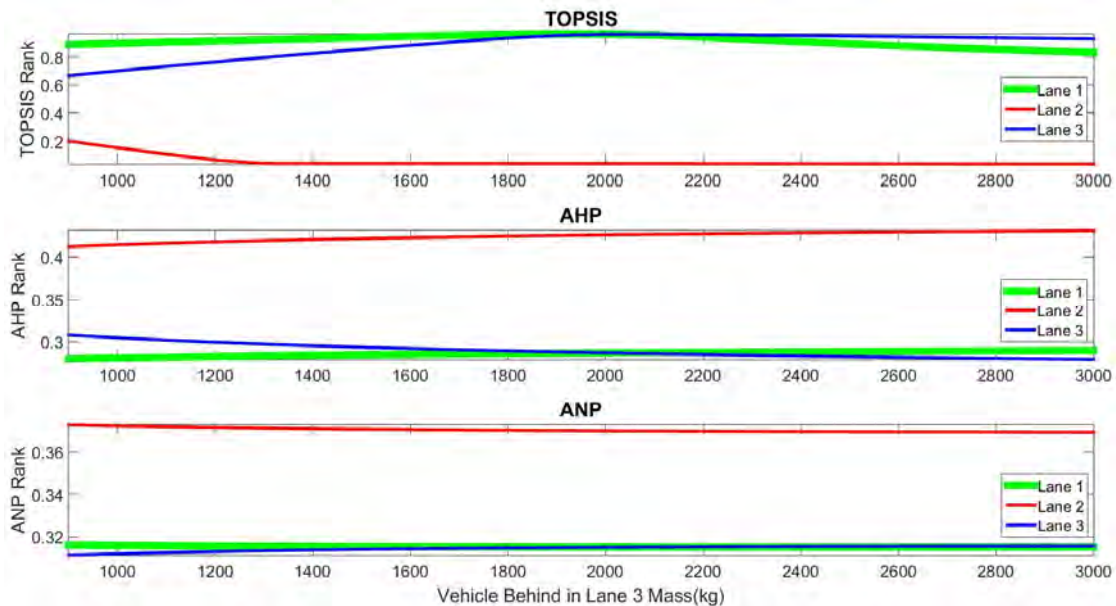
Figure 9-10 - Vehicle Behind in Lane 3 Mass Sensitivity Analysis

Figure 9-10 represents the sensitivity analysis of the mass of the vehicle behind in Lane 3. TOPSIS and AHP agreed with the Observer's Decision for every simulation, where Lane 1 is preferred due to the larger mass vehicle behind experiencing a lower collision acceleration from $900kg$ to $2000kg$. This preference for colliding with the higher mass vehicle is maintained when Lane 3 has the larger mass vehicle behind.

However, ANP disagreed with the Observer's Decision in every simulation scenario. It is observed that throughout the sensitivity analysis, the rank values of Lanes 1 and 3 are very close, but the ANP method has selected the lane with the

lower mass vehicle behind to collide with. The decision made by ANP does reflect the simulation results, as the lane with the lower mass vehicle behind does result in lower collision accelerations for the Host Vehicle, but not for the vehicle behind.

9.6.9 Vehicles Ahead Initial Velocity

The minimum initial velocity of a vehicle ahead in an adjacent lane is $65mph$, if it is lower than this, a collision occurs before the lane-change manoeuvre is complete. To lower this velocity further, the initial headway distance must be increased, as for these simulations the benchmark distance is only $12m$. To compare with the linear braking simulator, which had its benchmark headway distance set at $20m$, the minimum velocity for the dynamic braking simulator could be set to $56mp$h. A collision avoidance will occur if this initial velocity is set higher than $72mph$, as this is the highest speed at which a collision will still occur.
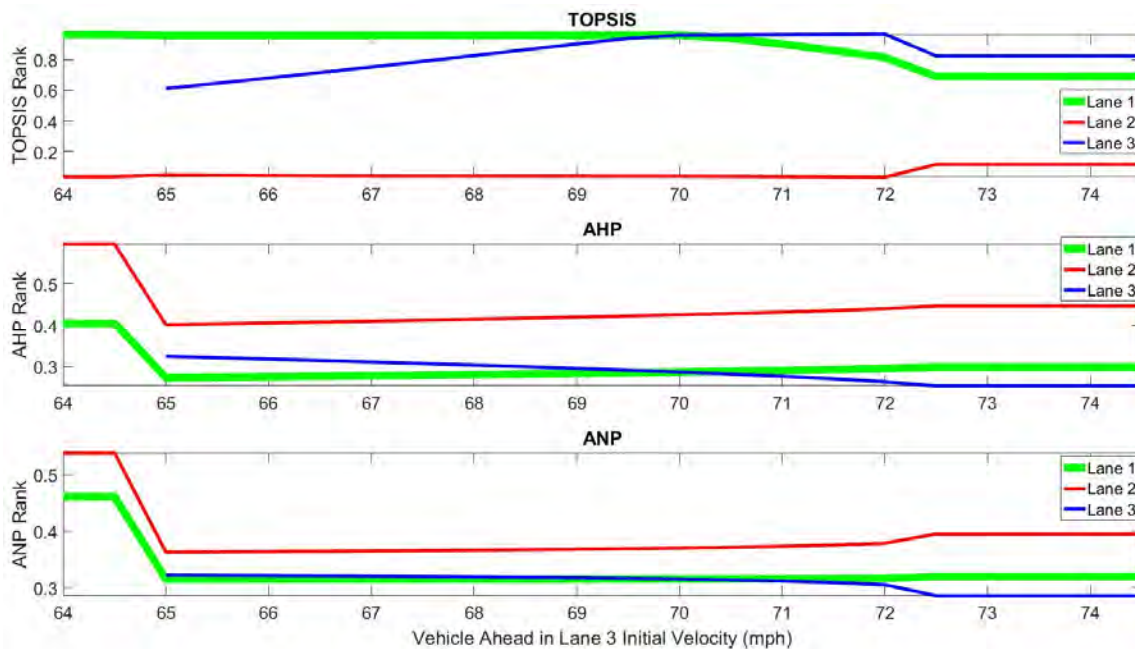
Figure 9-11 - Vehicle Ahead in Lane 3 Initial Velocity Sensitivity Analysis

Figure 9-11 shows the sensitivity analysis for varying the initial velocity of the vehicle ahead in Lane 3. The benchmark velocity is $70mph$, and the MADM rank values show that a starting velocity lower than this is not the ideal choice. Lane 3 is the preferred choice when the initial velocity of the vehicle ahead in Lane 3 is higher

than the Host Vehicle's 70mph, and Lane 1 is the preferred choice when the initial velocity is 70mph or lower. All MADM methods agree with the Observer's Decision for every simulation. At 72.5mph a collision avoidance is achieved ahead in Lane 3, and this lane is selected as the preferred choice.

9.6.10   Vehicles Behind Initial Velocity

The minimum velocity of a vehicle behind in an adjacent lane for a collision to still occur is 65mph. The highest initial velocity of a vehicle behind before an adjacent lane is disqualified due to a collision occurring before the lane-change manoeuvre is complete is 84mph. These limits are of course dependent on the initial headway distances.
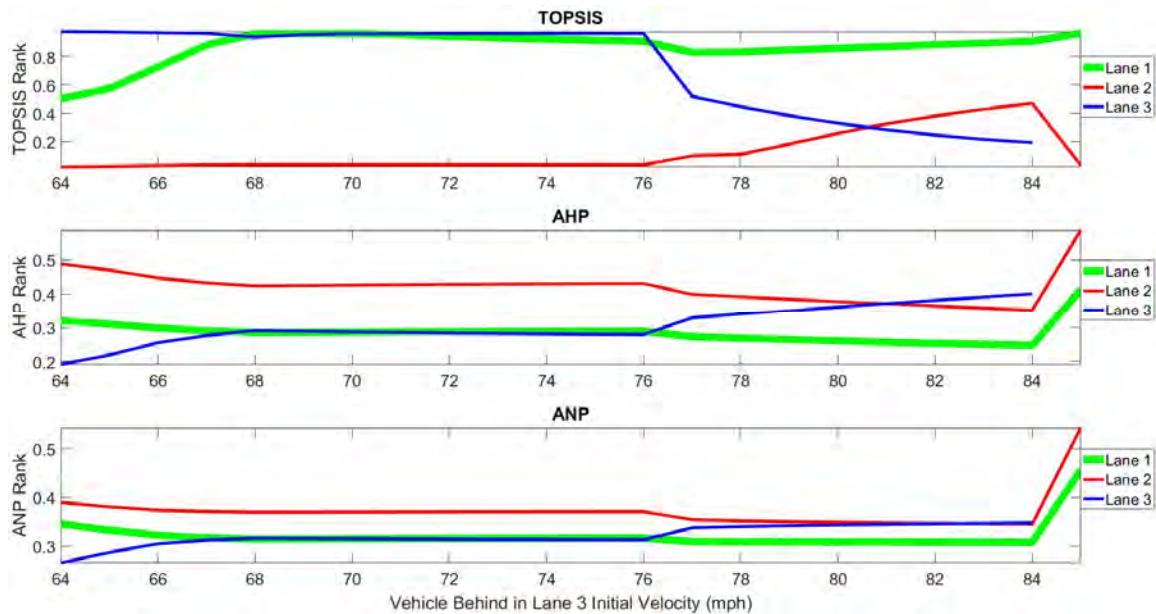
Figure 9-12 - Vehicle Behind in Lane 3 Initial Velocity Sensitivity Analysis

For all velocities simulated, all MADM methods agreed with the Observer's Decision. Figure 9-12 shows that for the vehicle behind, a lower initial velocity is preferred to the Host Vehicle's initial 70mphh. This lower initial velocity means the impact velocity between the two vehicles is also lower, therefore lowering the collision acceleration and increasing the time-to-collision. From 68mph to 76mph, the rank values for all MADM methods are very similar.

Interestingly, the preferred choice is not as obvious as a lower velocity is better. From $64mph$ to $67mph$ the preferred choice is Lane 3, which has the lower initial velocity for the vehicle behind. But from $68mph$ to $70mph$ the preferred choice is Lane 1. This is due to the relative velocity of the impact in Lane 3 is greater. Lane 3 is then preferred from $71mph$ to $76mph$, but at $77mph$ it is the collision behind the Host Vehicle that occurs first. At $77mph$, the impact velocity creates a high collision acceleration for the Host Vehicle and vehicle behind, which the combined mass of these two vehicles then impacts the vehicle ahead in Lane 3. When the collision behind occurs first, it is Lane 1 that is preferred.

9.6.11   Headway Distance to Vehicles Ahead

The minimum initial headway distance for a vehicle ahead in an adjacent lane is $7.5m$. At distances less than this, a lane-change manoeuvre cannot be completed before impact. A greater headway distance is always desirable, giving the Host Vehicle more distance to decelerate, and a collision avoidance will occur when this initial headway distance is set to $17m$ or greater.
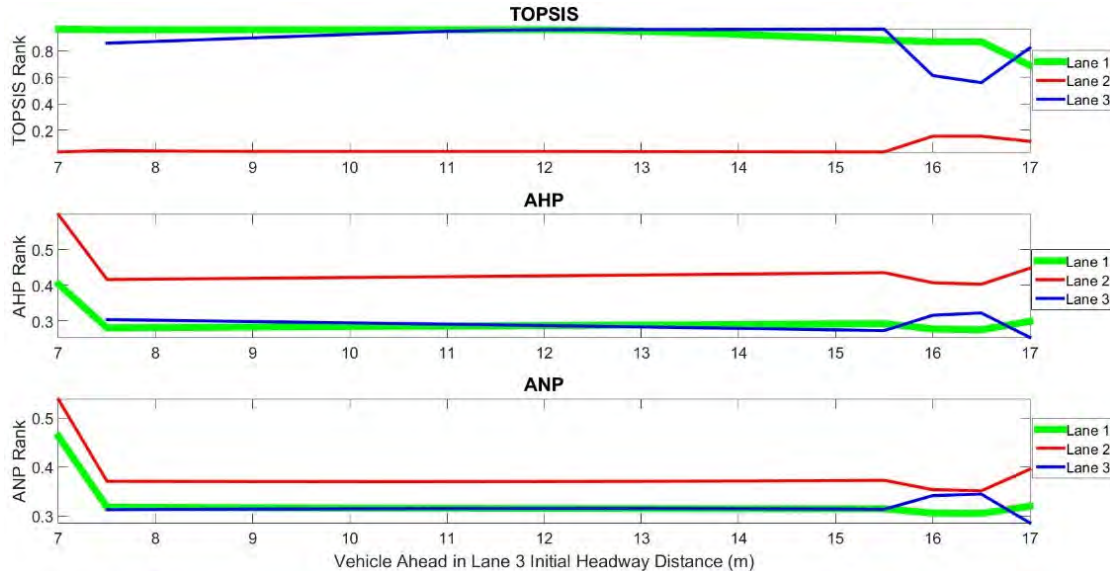
Figure 9-13 - Vehicle Ahead in Lane 3 Initial Headway Distance Sensitivity Analysis

For all of the simulations, TOPSIS and AHP agreed with the Observer's Decision in every simulation scenario. But from $7.5m$ to $14.0m$, ANP did not agree. The rank values for ANP show that Lanes 1 and 3 almost identical for this headway

distance range. At $16m$, the collision behind the Host Vehicle occurs first, and as a result all MADM methods prefer Lane 1 over the higher distance in Lane 3. At $17m$ a collision avoidance is calculated for Lane 3, and so the collision accelerations of $0m/s^2$ for the vehicle ahead and Host Vehicle dominates the decision.

However, although a collision avoidance was calculated for a headway distance of $17m$ in Lane 3, a closer look at the impact velocities of the vehicle behind, and the Host Vehicle for the rear collision gives an insight into a limitation of the simulator. The impact velocities for the vehicle ahead and Host Vehicle colliding with the vehicle ahead are $0m/s$, but the impact velocities for the vehicle behind and Host Vehicle colliding with the vehicle behind is not $0m/s$. The distance between the Host Vehicle and vehicle ahead for this simulation is only $0.23m$. The impact with the vehicle behind will push the Host Vehicle forwards, and if this distance is greater than $0.23m$, it will collide with the vehicle ahead. The simulator does not calculate this, as it has determined the collision avoidance to be final. In order to determine the collision accelerations of the vehicle ahead in this situation, further modelling will need to use the velocity of the Host Vehicle after being impacted by the vehicle behind.

9.6.12   Headway Distance to Vehicles Behind

For the vehicles behind a greater headway distance is also desirable as this gives those vehicles more distance to decelerate, reducing the impact velocity with the Host Vehicle. The minimum distance this can be set at before an impact occurs before the lane-change manoeuvre is complete is $8m$. A collision avoidance will occur if this distance is set to 35m and greater.

Much like the headway distance of the vehicles ahead in Section 9.6.11, the preferred lane is not as obvious as the larger available braking distance. Figure 9-14 shows the sensitivity analysis as the preferred lane changes between Lanes 1 and 3 for each MADM method. From $7m$ to $10m$, the Observer's Decision is Lane 1, as Lane 3 has a lower available braking distance for the vehicle behind. From $7m$ to $11m$, it is the collision behind which occurs first. From $11m$ to $19m$ the Observer's Decision is to select Lane 3. Although lane 3 has higher available braking distance for vehicle behind at $20m$, it is not yet enough to reduce the relative velocity of Host and vehicle behind, and so the lane preference is Lane 1. At headway distance $25m$, the Host Vehicle manages to come to a full stop. However, the lane preference is still

Lane 1. As this distance increases, the relative velocity between the Host Vehicle and vehicle behind will reduce, as the Host Vehicle's impact velocity cannot drop below $0 m/s$. The effect of this is seen at $27m$, when the Observer's Decision is to select Lane 3, and this is agreed with the MADM methods. TOPSIS and AHP agreed with the Observer's Decision in every simulation scenario.

At $8m$ and $9m$, ANP disagrees with the Observer's Decision and selects Lane 3. The preferred choice of Lane 3 is due to the limited headway distance actually results in smaller relative impact velocities, as the Host Vehicle cannot decelerate considerably compared to the vehicle behind.

Figure 9-14 - Vehicle Behind in Lane 3 Initial Headway Distance Sensitivity Analysis

9.6.13   Vehicles Ahead Inputted Deceleration

Much like the deceleration considered in Section 9.6.4, the actual rate of deceleration will be greater than the inputted value due to dynamic resistance forces acting on the vehicle. However, the most effective stopping force is from the brakes, and the inputted deceleration determines the braking force. A lane is disqualified due to a collision occurring before the lane-change manoeuvre is complete, if this braking value is set at -9.4m/s^2 or greater. A collision avoidance will occur if this rate of deceleration is set to -6.5m/s^2 or lower.
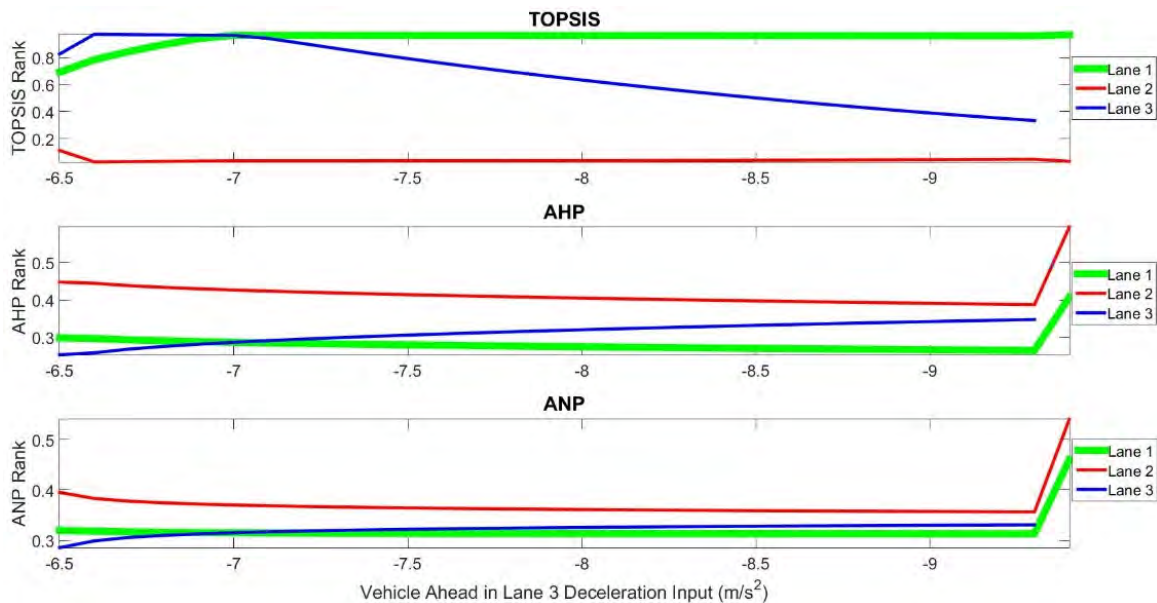
Figure 9-15 - Vehicle Ahead in Lane 3 Inputted Deceleration Sensitivity Analysis

The sensitivity analysis results presented in Figure 9-15 demonstrate a clear conclusion. The deceleration of the vehicle ahead is preferred to be lower. From -6.5m/s^2 to -6.9m/s^2 the preferred lane is Lane 3 for all of the MADM methods. From the benchmark of -7m/s^2 the preferred choice is Lane 1, which will have the lower collision accelerations due to the lower impact velocities. All of the MADM methods agreed with the Observer's Decision for every simulation in this sensitivity analysis.

9.6.14   Vehicles Behind Inputted Deceleration

For the benchmark parameters of the dynamic braking simulator, there is a sufficient initial headway distance for the vehicles behind not to brake, and all of the lanes are available for decision as no collision occurs before the Host Vehicle's lane-change manoeuvre is complete. A collision avoidance will occur if this rate of deceleration is set to -6.0m/s^2 or greater.
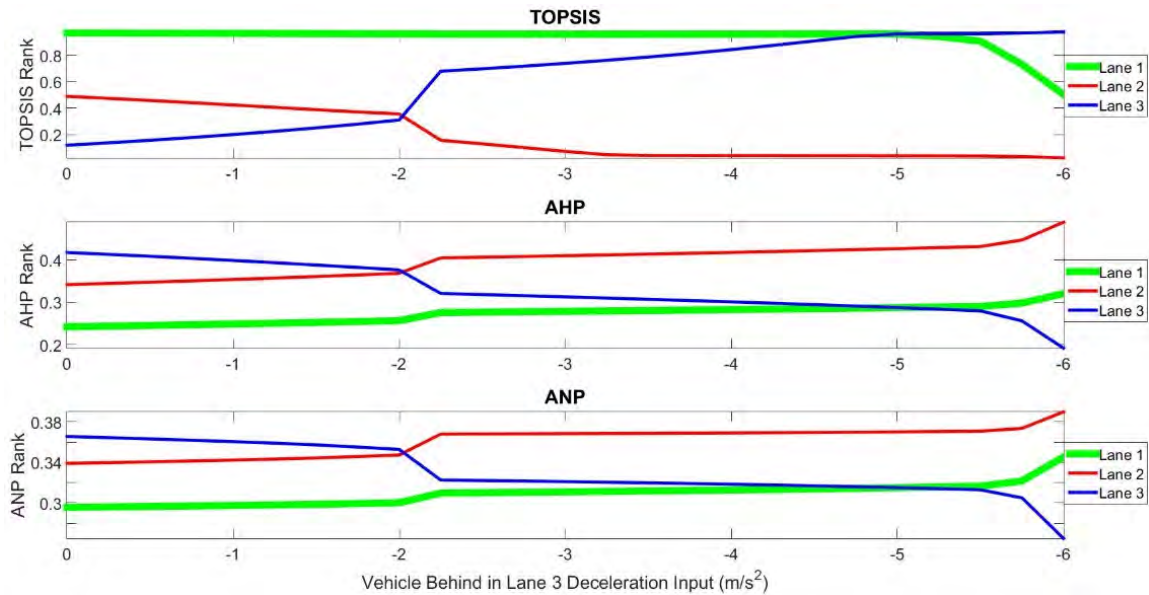
Figure 9-16 - Vehicle Behind in Lane 3 Inputted Deceleration Sensitivity Analysis

The sensitivity analysis results are presented in Figure 9-16. All of the MADM methods agreed with the Observer's Decision for every simulation. For deceleration values of $0m/s^2$ to the benchmark deceleration of -5m/s^2, the preferred lane is Lane 1. It is the vehicle behind in Lane 3 that has its braking varied, and so the lower the deceleration, the higher the impact velocity. For all deceleration values greater than -5m/s^2, it is Lane 3 that is preferred. However, for all of the MADM methods plotted in Figure 9-16 there is a noticeable change in some of the rank values at -2.25m/s^2. This is because from $0m/s^2$ to -2m/s^2, it is the collision behind that occurs before the collision ahead. From -2.25m/s^2 to greater deceleration values, it is the collision ahead that occurs first.

9.6.15   Summary of V2V Dynamic Braking MADM Results

The simulations showed that TOPSIS and AHP agreed with the Observer's Decision on every simulation of the V2V Dynamic Braking Simulator. There are 3 sensitivity analyses presented where ANP disagreed with the Observer's Decision (Sections 9.6.8, 9.6.11, and 9.6.12). The rank values of ANP were often closer than the equivalent AHP values, similar to the observations of Section 9.5.12.

The reason for the close ranking of the ANP, providing at times a decision that disagreed with the Observer's Decision, is due to the feedback which is calculated from the normalized alternative values. The feedback is beneficial in re-assessing the importance of each criteria, but this is not necessarily required for this application. The proposed simulators and decision making processes must make an unbiased decision to result in the best outcome for all vehicles involved in the potential collisions. The AHP and TOPSIS methods assess the situation, and do not re-evaluate the decision made. The result of the feedback is that it may give a greater weight to a criteria which originally was determined to be less important. This is the intended purpose of the feedback, but may not be useful if that criterion should remain less important. In the simulations presented, this did not always occur as criterion occasionally had their weights reduced when they were not intended or desired to be reduced.

The simulation of headway distance for the vehicles ahead did present a limitation of the dynamic braking simulator. This can happen when a collision avoidance is calculated ahead, but the collision behind could still push the Host Vehicle into the vehicle ahead. This would require further modelling of the Host Vehicle's longitudinal velocity and displacement from the modelling of the collision behind, and then another collision modelling simulation.

9.7   MADM Processing Time

Section 7.9.1 discusses the computational times of the simulators. A decision still needs to be made after these simulators' results are used by the MADM methods. The Non-V2V and V2V simulators both use the same decision processes, the difference being that the V2V Dynamic Braking Simulator has 6 criteria to assess,

whilst the Non-V2V simulator only assesses 3. The V2V Dynamic Braking decision process times are evaluated to assess the MADM process. The times of the benchmark simulation for the V2V Dynamic Braking Simulator used by the MADM methods are presented in Table 9-12.

Table 9-12 - MADM Processing Times for Benchmark Simulations

	Simulation Runs (s)			Average (s)
	1	2	3	
TOPSIS	0.0141	0.0073	0.0067	0.0094
AHP	0.0016	0.0016	0.0011	0.0014
ANP	0.0032	0.0029	0.0022	0.0028

Table 9-12 demonstrates that there are differences in the processing times of the considered MADM methods, but overall it is noted that the largest time presented is still less than $0.015s$. AHP is consistently the fastest method, and so based on speed alone this method would be the preferred choice. However, compared to the simulation times presented in Table 7-27, the processing times of all methods are considerably faster. The MADM methods are far simpler calculations, and therefore faster to compute than those used to simulate the Host Vehicle, vehicles ahead and vehicles behind. The times presented means that the implementation of these methods combined with the simulators is not a concern. The discussion of future computational capabilities of autonomous vehicles in Section 7.9.3 to speed up the simulation times would also allow for the decision process times to reduce.

9.8 Simulation and MADM Conclusions

The two simulators developed in Chapter 7 are used with the decision making processes described in Chapter 8. Using the benchmark scenarios defined in Chapter 7 as a reference, the decision made by the MADM processes are evaluated. Individual parameters are adjusted to observe its effect on the outputs of the simulation, but more critically the decision made. The developed trajectory planner

from Chapter 5 and collision modelling from Chapter 6 are used for critical parts of the simulators as well.

Sensitivity analyses are performed for the scenarios involving fine adjustments of the parameters describing the scenario, and it is analysed for how the parameter value can change the decision made. For some scenarios it is a simple task of determining an operating window, and observe at what point a potential lane may need to be disqualified. One limitation of the V2V Dynamic Braking Simulator is observed which will need to be addressed in the future developments, regarding the calculation of possible secondary collisions with the vehicle ahead, even if an original collision has been avoided.

Out of the three MADM methods that were developed for use with the simulators, TOPSIS and AHP were the best performing, as determined by their agreement with the Observer's Decision. ANP was less satisfactory for both the Non-V2V Linear Braking Simulator, and the V2V Dynamic Braking Simulator. It is concluded that feedback needs a different method of assessing the influence of the alternatives on the criteria. In other examples of ANP, discussed in Chapter 3, the feedback is assessed subjectively by human participants. This is not possible for this research problem.

The Non-V2V Linear Braking Simulator is computationally faster and so at this stage of development more appropriate for application with a real vehicle. However, the V2V Dynamic Braking Simulator produces results which describe the collision severity in more useful results. This is because the collision severity is directly described by the collision accelerations, as opposed to the impact velocity and required braking of the Non-V2V Linear Braking Simulator.

Generally, it is observed that decisions on changing lanes are made by the MADM methods, as informed by the simulators. The proposed method of combining simulation results and MADM methods for an autonomous vehicle to avoid or mitigate collisions on a motorway, based on what can be calculated to be the least-severe outcome, has therefore achieved the main aim of this thesis. Of course, the proposed simulators and decision processes require further development before such a system could be employed by a real vehicle, but this proposed concept demonstrates encouraging findings.

Chapter 10

Conclusions

10.1 Research Problem

This thesis addresses the problem of what an autonomous vehicle is to do when facing imminent collisions. Any action the vehicle takes may result in collision. This research is focused on high-speed motorway driving, where the available choice the autonomous vehicle can make is the lane in which it should be. The autonomous vehicle is driving in the middle lane of a three lane motorway, and with a single lane-change manoeuvre possible, there are three lanes available for the decision. The autonomous vehicle must select one lane to drive into, as to prevent further collisions in multiple lanes.

10.2 Summary of Findings

In Chapter 2, a literature review was compiled, giving an overview of the existing research and technologies that are relevant to collisions avoidance. Existing collision avoidance systems are included in the review, and the limitations of such existing technologies is discussed from which the developments of this thesis are inspired. The literature review also includes the relevant information on vehicle dynamics and automotive collision research, which greatly informs developments in the following chapters. Here, the first objective of evaluating the current problems is addressed.

Chapter 3 is a literature review of MADM methods, which will be used in a later stage of the thesis. A broad view of several techniques is covered, and examples of these methods being employed is also included.

Chapter 4 demonstrated that an autonomous vehicle can have a collision when driving in an automated highway platoon. This results in the platoon becoming unstable as acceleration inputs to the vehicles begin to oscillate. The system fails when a collision is created. Multiple platooning models are tested and stressed, which served the intended purpose of demonstrating that it is possible for autonomous driving systems to crash. The second objective of evaluating whether an autonomous vehicle can still have a collision is achieved, by evaluating how factors such as platoon size, speed and time delays can cause a platoon to become unstable.

One limitation is concerning the highway platooning. At first, it was considered whether the steering manoeuvre to avoid collision could be implemented in a highway platooning system. If for example, a vehicle ahead stops suddenly, can a vehicle behind move into an adjacent lane to avoid impact? The answer is no. The steering manoeuvre to move into the adjacent lane requires a longitudinal distance much greater than the 5m tested with the highway platooning simulations.

Chapter 5 presents the developments of the collision avoidance/mitigation system. If an autonomous vehicle is to avoid a collision, then a possible lane-change manoeuvre must be planned. Autonomous vehicle research carried out at universities and research groups have already developed steering controllers, with examples discussed in the literature review, but the lane-change manoeuvre proposed in this thesis is specific to the research problem considered. A fully dynamic steering controller with dynamic cornering stiffness would most likely provide the greatest accuracy, but Chapter 5 demonstrates that the sinusoidal

trajectory planner can be implemented with a steering controller. This approach can even be used to calculate a safe braking value for the vehicle without over-saturating the tyres and potentially losing control of the vehicle.

In Chapter 6, the behaviour of the vehicle in a crash is examined. This is done by creating lumped-mass models to simulate collisions. The models must be tuned to best represent the available FEA data, and a Euclidean optimization process is demonstrated using the simulated key properties of peak acceleration, peak deformation, collision energy and collision time results. The Euclidean optimization finds the bilinear term and multiple of stiffness which best reproduces the key properties compared to the FEA data. The third objective of evaluating the impact of a collision is, in part achieved here, as the collision modelling gives a method for assessing the severity of collisions.

Chapter 7 developed the simulators which calculate the potential impact speeds of the imminent collisions. Two simulators are developed, one for when V2V communication is available, and one for when V2V is not available. Chapter 7 does address one of the main concerns that autonomous vehicle research faces, which is V2V communication. If V2V is available, and all of the parameters described in this thesis are communicated, then the collision avoidance/mitigation system developed here will be able to make complex calculations which can simulate the potential collisions, and make a decision based on these results. However, without V2V these calculations are limited in their capability. For this reason, two simulators were developed. It is intended that the simulator with V2V available would be the preferred method, but the non-V2V simulator is available if V2V is not. The simulators also assess the feasibility of steering manoeuvres by assessing the yaw rates, and the vehicle dynamics considerations of tyre loads and overturning speeds. The simulators also disqualify a manoeuvre based on whether a collision occurs before the manoeuvre is complete.

The proposed simulators are run using MATLAB 2016a. The outputs of the Non-V2V simulator include the velocities of the Host Vehicle and vehicle ahead at the moment of impact, which determines the relative impact velocity. This simulator also calculates the required braking of the vehicles behind, as to prevent a collision with the Host Vehicle. The manoeuvres are assessed for acceleration to describe the severity of a lane-change manoeuvre or full braking manoeuvre as this too could cause injury to the vehicle occupants. The V2V simulator also calculates manoeuvre acceleration, but instead of just the impact velocities ahead, also calculates the

velocities for the vehicles behind. With this a Time-To-Collision is also calculated. The velocities of all vehicles at the moment of impact are used as the inputs to the collision modelling. The collision modelling calculates the peak accelerations of the vehicles during the collisions.

Chapter 8 demonstrated how MADM methods can be applied for the research problem. The Non-V2V simulator's benchmark scenario from Section 7.3.5 is used to demonstrate how the three selected methods of TOPSIS, AHP, and ANP use the simulation results to determine the rank values for the lanes. This benchmark scenario is used because it has fewer criteria than the V2V simulator and Lanes 1 and 3 will have identical rank values. This means that a final default decision is made based on which lane is closer to the emergency lane. TOPSIS, AHP, and ANP are selected for development with the simulators as these are popular methods which have been applied to many varying situations. The alternative available are the 3 motorway lanes and the criteria for the Non-V2V simulator are impact velocity ahead, required braking of the vehicles behind, and a maximum acceleration. The V2V simulator uses collision accelerations of all vehicles for the impacts, manoeuvre acceleration and Time-To-Collision (TTC).

Chapter 9 presents the results of the two simulators developed in Chapter 7, with the decision making processes described in Chapter 8. The limits of the simulators are presented and discussed, and a sensitivity analysis is performed for the parameters which show a varying rank preference generated by the MADM methods. The varying parameters include the Host Vehicle's lateral acceleration, the initial velocity of the motorway vehicles, initial headway distance of the motorway vehicles and braking value of the motorway vehicles. The V2V simulator also includes the mass of the motorway vehicles as a varying parameter for a sensitivity analysis. These sensitivity analyses are compared to Observer's Decisions. The Observer is the author of this thesis, assessing the simulator outputs for a human preference on which is the best lane. The general conclusion to these simulations are that TOPSIS and AHP performed well compared to the Observer's Decision, but ANP does not agree as often. This is due to the feedback that ANP introduces. ANP could be further developed to improve its performance, but it would require a new method of calculating the feedback, and the superior performances of TOPSIS and AHP make it hard to justify the extra complication required by ANP. The simulators perform well, although a limitation is demonstrated, when the dynamic braking V2V simulator calculated an avoidance ahead, but does not take into account the collision behind forcing a second collision ahead.

Overall, it is demonstrated that the simulators and decision processes can be used by the Host Vehicle to select a lane to drive into to avoid the most severe collision. The Host Vehicle can autonomously select the safest lane, taking all collision partners into account, and also assessed the safety of the manoeuvres themselves.

This thesis proposes a method to simulate potential collisions, simulate lane-change manoeuvres and make a decision on what actions should be taken by the autonomously driven Host Vehicle. The range of disciplines required to achieve this aim has been larger than first thought when beginning this thesis. Using lumped-mass models to simulate collisions and provide information describing the severity of a collision was not at first considered. MADM was also not an initial consideration, but proved to be critically useful for the applied problem.

10.3 Recommendations for Further Research

The research presented in this thesis is encouraging, but limitations discussed in the chapters demonstrates the need for further research. The proposed collision avoidance/mitigation system is a concept, and as such the presented simulations only represent a limited range of scenarios and assume that all data is readily available. AHP has performed very well in the simulations and it can be further developed by adding sub-criteria to the criteria hierarchy. This has the potential to improve the performance even further.

The accuracy and computational effort required for a fully dynamic steering controller are discussed, but in order to enact the decisions from the decision making process, the vehicle will need to steer itself into the desired lane. A steering controller will need to perform as intended, in a wide range of driving scenarios in order for the proposed collision avoidance/mitigation system to be employed. A steering controller which uses the recommend lane choice, made by the simulator and MADM decision process, to perform the required lane-change manoeuvre is required for the collision mitigation system to work with a real vehicle.

The collision modelling used for describing the accelerations and deformations of collisions with a useable accuracy is relatively simple. It is applied to one situation of a zero-lateral offset collision only. This is also an encouraging research area. Modelling offset collisions have not been addressed, or even side

impacts. It also only considers cars, and no other vehicles such as vans or lorries. If these impacts could be modelled accurately and quickly, other collision situations would be considered. It also opens the scope to situations other than motorway rear-end collisions, perhaps even side impacts in urban environments.

The collision modelling itself could further investigate the severity of collisions by performing in-depth sensitivity analyses to observe the accelerations and deformations of one vehicle colliding with a range of other vehicles. This could determine limits to crash compatibility, meaning some vehicle types could be considered too dangerous to collide with given certain factors such as impact speed and vehicle mass. This would require extensive collision data, which is why in this thesis the collision modelling is limited to the available data. The lumped mass modelling gives outputs of peak acceleration and deformation, as well as force versus deformation which is used to calculate the energy of the collision. FEA modelling and real vehicle collision testing would give greater detailed analysis of the crash structure deformation, but the lumped mass modelling is an effective method of simulating the key properties accurately and fast. A sensitivity analysis focusing on these outputs can provide useful results about collision performance. This could be used to better inform the development of vehicle crash structures for use with more in-depth FEA modelling.

The simulators developed are proved to be useful, but the limitation discussed would need to be addressed before the proposed system would be tested with a real vehicle. The limitation of the collision avoidance ahead assuming that no second collision will occur became clear after the simulations, and so further simulations would better define areas of improvements and how to solve this. The simulators work well with the MADM methods, and so this would need to be tested with a real vehicle. Real vehicle testing would require considerable simulation testing before physical testing, with the development of more capable simulators as more limitations may be discovered. The physical testing would require test track simulations of scenarios, starting with simpler scenarios of only 2 potential collision partners, and building up to multiple collision scenarios across multiple lanes.

Other concerns raised in the thesis include computational speed of the on-board vehicle computers, and the availability of V2V communications. Throughout this thesis, these have been assumed to be problems that will be addressed in the future. However, in order for the developed collision avoidance/mitigation system to be implemented in real vehicles, these concerns must be addressed. The required

information must be available, and this thesis demonstrates that such information as vehicle mass and braking rates are required for a safety system. Therefore, if it can be demonstrated that such information will be used to reduce the risk to life, it could be recommended that such information be compulsory for all vehicles to make available. The computational speed of autonomous vehicles is a concern which requires a multi-disciplinary approach addressed by the automotive industry, so this will likely be addressed. It is still intended that the developed collision mitigation decision making system could be used in real-time with future vehicles, but the speed of the simulation must be considerably increased.

Another research problem could be raised by the findings of this thesis. One of the limitations of this thesis is that the proposed system would not work with highway platooning. However, the collision modelling could be used to determine the best order of the vehicles in the platoon, should a collision occur. The collision modelling could simulate all vehicles colliding into one another, if the lead vehicle stops suddenly, and then the accelerations of the vehicles could use a MADM method to suggest an order for the vehicles to be in. It could also take maximum braking available to the vehicles into account.

10.4 Concluding Remarks

The system developed in this thesis could be used as an autonomous driving safety system for motorway driving, alongside existing technologies such as Adaptive Cruise Control, and Automatic Emergency Braking. The system aims to reduce the risk to life, by selecting the best collision situation for the Host Vehicle. This system has the potential to save lives, and limit serious injuries. The high speeds involved with motorway collisions make them more likely to result in fatality or serious injury, and so the benefits of this thesis are evident. The system simulates a motorway; many countries around the world have extensive motorway networks, which transport millions of people daily. The potential benefit is far-reaching.

This thesis also raises further concerns regarding autonomous vehicle ethics. Although not everybody is interested in automotive engineering, everybody who lives in developed areas will have some exposure of some degree to autonomous vehicles, as the technology becomes more capable and available. Even if a person will never drive a car in their life, only taking public transport, that public transport will likely be exposed to autonomous vehicle safety systems and autonomous decision

being made regarding their safety. This thesis presents a decision making method, which could be adapted beyond the scope of this research problem. It may be necessary for the safest collision to be assessed by more than cars on a motorway, such as in urban environments where there are other hazards such as pedestrians and cyclists. Other vehicle types such as buses could also be considered with many people on-board.

This thesis proposes a concept of a collision avoidance/mitigation system. The concept simulates lane-change manoeuvres as potential actions for an autonomously driven Host Vehicle to make. Potential collisions are simulated using the accelerations of the collisions as metrics to describe the severity of the collisions. Motorway simulators calculate the impact speeds that will happen, given the braking rates of all vehicles on a three-lane motorway, and assess the feasibility of lane-change manoeuvres. The Host Vehicle is simulated in scenarios where it is following a vehicle which has a high and sudden deceleration. MADM is used to make an unbiased decision for which lane the Host Vehicle should drive into. The simulations are presented and discussed.

Although, this system is a concept, the simulation results are encouraging. This research can be split into different areas, such as collision modelling and vehicle dynamics, and so with further attention from researchers with expertise in these fields could become a very desirable new technology for emerging autonomous vehicles to implement. The potential impact is that the proposed system could save lives and reduce the risk of serious injury, which will always be the focus of automotive safety.

Chapter 11

Papers and Presentations

The following papers are publications by the author of this thesis which have contributed to the progression of this research programme:

Gilbert, A., Petrovic, D., Warwick, K., and Serghi, V. (2018) *VEHITS 2018: 4th International Conference on Vehicle Technology and Intelligent Transport Systems*. 'Autonomous Vehicle Simulation Model to Assess Potential Collisions to Reduce Severity of Impacts'. held 16-18 March at Funchal, Madeira, Portugal. Portugal: INSTICC

Pickering, J., E., Ashman, P., Gilbert, A., Petrovic, D., Warwick, K., and Burnham, K. (2018) *The 12th International UKACC Conference on Control*. 'Model-to-Decision Aproach for Autonomous Vehicle Convoy Collision Ethics'. held 5th-7th September at Sheffield, UK: IEEEXplore

The following presentations by the author of this thesis have contributed to the progression of this research programme:

March 2018	Research Seminar of Institute for Future Transport and Cities at Coventry University, UK
Dec 2016	Poster presentation for Jaguar Land Rover ltd. PhD and EngDoc conference at the British Motor Museum and Conference Centre at Gaydon, Warwickshire, UK
March 2016	Mini-Symposium of Control Engineering Projects at Wolverhampton University, UK
Nov 2015	Poster presentation for Jaguar Land Rover ltd. PhD and EngDoc conference at the International Manufacturing Centre at the University of Warwick, UK
Sept 2015	International Conference of Systems Engineering at Coventry University, UK
June 2015	Polish British Workshop at Wroclaw University, Poland

List of References

Abe, M. (1999) 'Vehicle Dynamics and Control for Improving Handling and Active Safety: From Four-Wheel Steering to Direct Yaw Moment Control'. Proceedings of the Institution of Mechanical Engineers, Part K: Journal of Multi-Body Dynamics 213 (2), 87-101

Abe, M. (2009) Vehicle Handling Dynamics. 1st edn. Oxford, UK: Butterworth-Heinemann

Afshari, A. R., Yusuff, R., and Derayatifar, A. R. (2012) *Innovation Management and Technology Research (ICIMTR), 2012 International Conference on*. 'Project Manager Selection by using Fuzzy Simple Additive Weighting Method'. held 21-22 May at Malacca, Malaysia: IEEE

Ahmed, M. and Yüksel, M. (2013) *2013 World Congress on Multimedia and Computer Science*. 'Design and Implementation of a Path Tracking Steering Controller for EO Smart Connecting Car'. held 4-6 October 2013 at Hammamet, Tunisia: ACEEE

Ammoun, S. and Nashashibi, F. (2009) Intelligent Computer Communication and Processing, 2009. ICCP 2009. IEEE 5th International Conference on Intelligent Computer Communication and Processing. 'Real Time Trajectory Prediction for Collision Risk Estimation between Vehicles'. held 27-29 August at Cluj Napoca, Romania: IEEE

Anderson, S. J., Peters, S. C., Pilutti, T. E., and Iagnemma, K. (2010) 'An Optimal-Control-Based Framework for Trajectory Planning, Threat Assessment, and Semi-Autonomous Control of Passenger Vehicles in Hazard Avoidance Scenarios'. International Journal of Vehicle Autonomous Systems 8 (2-4), 190-216

Asif, S. and Webb, P. (2015) 'Networked Control System - an Overview'. *International Journal of Computer Applications* 115 (6), 26-30

Bastien, C., Blundell, M., Neal-Sturgess, C., Hoffmann, J., Diederich, A., Van Der Made, R., and Freisinger, M. (eds.) (2013) *Proceedings of the 23rd International Conference on the Enhanced Safety of Vehicles Conference*. 'Safety Assessment of Autonomous Emergency Braking Systems on Unbelted Occupants using a Fully Active Human Model'. held 27-30 May at Seoul, Republic of Korea: NHTSA

Bathe, K. and Baig, M. M. I. (2005) 'On a Composite Implicit Time Integration Procedure for Nonlinear Dynamics'. *Computers & Structures* 83 (31-32), 2513-2524

Batista, M., 2005. A Note on Linear Force Model in Car Accident Reconstruction. *arXiv preprint physics/0511127*.

Behzadian, M., Otaghsara, S. K., Yazdani, M., and Ignatius, J. (2012) 'A State-of the-Art Survey of TOPSIS Applications'. Expert Systems with Applications 39 (17), 13051-13069

Bergenhem, C., Shladover, S., Coelingh, E., Englund, C., and Tsugawa, S. (2012) *Proceedings of the 19th ITS World Congress*. 'Overview of Platooning Systems'. held 22-26 October at Vienna, Austria

Bertocci, G. E., Pierce, M. C., Deemer, E., Aguel, F., Janosky, J. E., and Vogeley, E. (2003) 'Using Test Dummy Experiments to Investigate Pediatric Injury Risk in Simulated Short-Distance Falls'. *Archives of Pediatrics & Adolescent Medicine* 157 (5), 480-486

Best, M. C. (2012) 'Optimisation of High-Speed Crash Avoidance in Autonomous Vehicles'. International Journal of Vehicle Autonomous Systems 10 (4), 337-354

Bianchi, D., Borri, A., Di Benedetto, M. D., Di Gennaro, S., and Burgio, G. (2010) 'Adaptive Integrated Vehicle Control using Active Front Steering and Rear Torque Vectoring'. International Journal of Vehicle Autonomous Systems 8 (2-4), 85-105

Bleske-Rechek, A., Nelson, L. A., Baker, J. P., Remiker, M. W., and Brandt, S. J. (2010) 'Evolution and the Trolley Problem: People Save Five Over One Unless the One is Young, Genetically Related, Or a Romantic Partner.'. *Journal of Social, Evolutionary, and Cultural Psychology* 4 (3), 115

Blundell, M. and Harty, D. (2004) The Multibody Systems Approach to Vehicle Dynamics. 1st edn. Oxford: Elsevier

Bosch (2014) *Automotive Handbook*. 9th edn. trans. by Star Deutschland GmbH. Karlsruhe: Robert Bosch GmbH

Box, G. E. and Draper, N. R. (1987) *Empirical Model-Building and Response Surfaces.* 1st edn. New York, USA: John Wiley & Sons

Brach, R. M. and Brach, R. M. (1998) Crush Energy and Planar Impact Mechanics for Accident Reconstruction: SAE Technical Paper 980025

Bruni, C., Dipillo, G., and Koch, G. (1974) 'Bilinear Systems: An Appealing Class of "nearly Linear" Systems in Theory and Applications'. *IEEE Transactions on Automatic Control* 19 (4), 334-348

Burnham, K. (1991) *Self-Tuning Control for Bilinear Systems*. [online] PhD thesis or dissertation. Coventry, UK: Coventry Polytechnic

CarAndDriver.com (Aug 2008) *The Power to Stop* [online] available from <http://www.caranddriver.com/features/the-power-to-stop-performance-cars-page-4> [December 14 2016]

Carlucci, D. (2010) 'Evaluating and Selecting Key Performance Indicators: An ANP-Based Model'. Measuring Business Excellence 14 (2), 66-76

Cars.McLaren.com (2015) Innovative Technology. Unmatched Performance. [online] [06 January 2015]

Centre for Collision Safety and Analysis (2017) *Centre for Collision Safety and Analysis - 2010 Toyota Yaris* [online] available from <https://www.ccsa.gmu.edu/models/2010-toyota-yaris/> [12 June 2018]

Chamblás, O. and Pradenas, L. (2018) 'Multi-Criteria Optimization for Seawater Desalination.'. Tecnología y Ciencias Del Agua 9 (3), 193-213

Cheng, E. W. and Li, H. (2005) 'Analytic Network Process Applied to Project Selection'. Journal of Construction Engineering and Management 131 (4), 459-466

Cheva, W., Yasuki, T., Gupta, V., and Mendis, K. (1996) *Vehicle Development for frontal/offset Crash using Lumped Parameter Modeling*. Warrendale, USA: SAE Technical Paper

Comaniţă, E., Ghinea, C., Hlihor, R. M., Simion, I. M., Smaranda, C., Favier, L., Roşca, M., Gostin, I., and Gavrilescu, M. (2015) 'Challenges and Opportunities in Green Plastics: An Assessment using the ELECTRE Decision-Aid Method'. Environmental Engineering and Management Journal 14 (3), 689-702

Compere, M. (2016) *Simple 2D Kinematic Vehicle Steering Model and Animation* [online] available from <http://uk.mathworks.com/matlabcentral/fileexchange/54852-simple-2d-kinematic-vehicle-steering-model-and-animation> [05 October 2016]

Consumer Reports News (2013) SUVs are Safer than Cars in Front Crashes, but there is More to the Story [online] available from <http://www.consumerreports.org/cro/news/2013/05/suvs-are-safer-than-cars-in-front-crashes-but-there-is-more-to-the-story/index.htm> [21 March 2016]

Cook, P. (2007) 'Stable Control of Vehicle Convoys For Safety and Comfort'. *IEEE Transactions on Automatic Control* 52 (3), 526 – 531

Cook, P. and Sudin, S. (2003) 'Convoy dynamics with bidirectional flow of control information'. In Tsugawa, S. and Aoki, M. (ed.) *10Th IFAC Symp. Control*

Transportation Systems, 'Control in Transportation Systems'. held 4-6 August 2003 at Tokyo, Japan. Oxford: Elsevier IFAC Publications, 433 – 438

Coon, B. A. and Reid, J. D. (2006) 'Reconstruction Techniques for Energy-Absorbing Guardrail End Terminals'*. Accident Analysis & Prevention* 38 (1), 1-13

Deb, A. and Srinivas, K. (2008) 'Development of a New Lumped-Parameter Model for Vehicle Side-Impact Safety Simulation'*. Proceedings of the Institution of Mechanical Engineers, Part D: Journal of Automobile Engineering* 222 (10), 1793-1811

Department for Transport (2014) Reported Road Casualties in Great Britain: Quarterly Provisional Estimates Q2 2014 [online] available from <https://www.gov.uk/government/uploads/system/uploads/attachment_data/file/370826/quarterly-estimates-apr-to-jun-2014.pdf> [28 May 2015]

Department for Transport (2015) Reported Road Casualties in Great Britain: Main Results 2014 [online] available from <https://www.gov.uk/government/uploads/system/uploads/attachment_data/file/438040/reported-road-casualties-in-great-britain-main-results-2014-release.pdf> [26 June 2015]

Doumiati, M., Victorino, A., Charara, A., and Lechner, D. (2009) 'Lateral Load Transfer and Normal Forces Estimation for Vehicle Safety: Experimental Test'*. Vehicle System Dynamics* 47 (12), 1511-1533

Driving Standards Agency for the Department for Transport (2007) The Official Highway Code. 15th edn. Norwich: Crown Copyright

Du, H., Zhang, N., and Dong, G. (2010) 'Stabilizing Vehicle Lateral Dynamics with Considerations of Parameter Uncertainties and Control Saturation through Robust Yaw Control'. IEEE Transactions on Vehicular Technology 59 (5), 2593-2597

Eidehall, A., Pohl, J., Gustafsson, F., and Ekmark, J. (2007) 'Toward Autonomous Collision Avoidance by Steering'. IEEE Transactions on Intelligent Transportation Systems 8 (1), 84-94

Ekman, M. (2005) *Modelling and Control of Bilinear Systems: Applications to the Activated Sludge Process*. [online] PhD thesis or dissertation. Sweden: Uppsala University

Elmarkbi, A. M. and Zu, J. W. (2004) 'Dynamic Modeling and Analysis of Vehicle Smart Structures for Frontal Collision Improvement'. *International Journal of Automotive Technology* 5 (4), 247-255

EURO NCAP (2017) *Full Width Rigid Barrier* [online] available from <https://www.euroncap.com/en/vehicle-safety/the-ratings-explained/adult-occupant-protection/full-width-rigid-barrier/> [17 July 2018]

Hwang, C. and Yoon, K. (1981) 'Methods for Multiple Attribute Decision Making'. in *Multiple Attribute Decision Making*. Springer, 58-191

Falcone, P., Eric Tseng, H., Borrelli, F., Asgari, J., and Hrovat, D. (2008) 'MPC-Based Yaw and Lateral Stabilisation Via Active Front Steering and Braking'. *Vehicle System Dynamics* 46 (1), 611-628

Falcone, P., Tufo, M., Borrelli, F., Asgari, J., Tseng, H. E., and Hrovat, D. (2007) *46th IEEE Conference on Decision and Control*. 'Predictive Active Steering Control for Autonomous Vehicle Systems'. held 12-14 December at New Orleans, LA, USA: IEEE

Gasser, T. M. and Westhoff, D. (2012) UNECE -Workshop: German Federal Highway Research Institute Towards a New Transportation Culture: Technology Innovations for Safe, Efficient and Sustainable Mobility. 'BASt-Study: Definitions of Automation and Legal Issues in Germany'. held 17-18 November 2014 at Brussels: BASt

GCDC.net (2016) *GCDC 2016 Looks Back on a Successful Event* [online] available from <http://www.gcdc.net/en/> [20 July 2018]

Gencer, C. and Gürpinar, D. (2007) 'Analytic Network Process in Supplier Selection: A Case Study in an Electronic Firm'. Applied Mathematical Modelling 31 (11), 2475-2486

Gillespie, T. D. (1992) *Fundamentals of Vehicle Dynamics*. 1st edn. Warrendale, PA, USA: Society of Automotive Engineers

Goepel, K. D. (2011) Analytical Network Process (ANP) [Online Lecture] BPMSG available from <https://bpmsg.com/wordpress/wp-content/uploads/2011/11/ANP-03.02.11-HD.Pdf> [04 August 2017].

Gov.UK (2013) THINK! Road Safety Survey. UK: Gov.UK

Hämäläinen, R. P. and Seppäläinen, T. O. (1986) 'The Analytic Network Process in Energy Policy Planning'. *Socio-Economic Planning Sciences* 20 (6), 399-405

Handfield, R., Walton, S. V., Sroufe, R., and Melnyk, S. A. (2002) 'Applying Environmental Criteria to Supplier Assessment: A Study in the Application of the Analytical Hierarchy Process'. *European Journal of Operational Research* 141 (1), 70-87

Haney, P. (2003) The Racing & High-Performance Tire. 1st edn. Warrendale, Pa: TV MOTORSPORTS AND SAE

Harker, P. T. (1989) 'The Art and Science of Decision Making: The Analytic Hierarchy Process'. in The Analytic Hierarchy Process. Berlin, Heidelberg: Springer, 3-36

Hayashi, R., Isogai, J., Raksincharoensak, P., and Nagai, M. (2012) 'Autonomous Collision Avoidance System by Combined Control of Steering and Braking using Geometrically Optimised Vehicular Trajectory'. Vehicle System Dynamics 50 (sup1), 151-168

Hou, X., Li, Y., Chen, M., Wu, D., Jin, D., and Chen, S. (2016) 'Vehicular Fog Computing: A Viewpoint of Vehicles as the Infrastructures'. *IEEE Transactions on Vehicular Technology* 65 (6), 3860-3873

Houenou, A., Bonnifait, P., Cherfaoui, V., and Yao, W. (2013) *2013 IEEE/RSJ International Conference on Intelligent Robots and Systems*. 'Vehicle Trajectory Prediction Based on Motion Model and Maneuver Recognition'. held 3-7 Nov. 2013 at Tokyo, Japan: IEEE

House of Commons Library (2013) Reported Road Accident Statistics [online] available from <http://www.parliament.uk/briefing-papers/sn02198.pdf> [26 June 2015]

Huang, S. and Dong, J. (2015) Transportation Information and Safety (ICTIS), 2015 International Conference on. 'Optimization Study of Vehicle Crashworthiness Based on Two Types of Frontal Impacts'. held 25 - 28 June at Wuhan, P. R. China: IEEE

Hwang, C. and Yoon, K. (1981) 'Methods for Multiple Attribute Decision Making'. in *Lecture Notes in Economics and Mathematical Systems*. ed. by Beckmann, M. and Künzi, H. P.: Springer, 58-191

IIHS.org (2016) General Statistics [online] available from
<http://www.iihs.org/iihs/topics/t/general-statistics/fatalityfacts/passenger-vehicles> [October 05 2017]

IIHS.org (2017) IIHS Safety Awards [online] available from
<http://www.iihs.org/iihs/ratings> [February 02 2017]

JAGUAR LAND ROVER LIMITED (2016) F-Type Coupe Specifications [online]
available from <https://www.jaguar.com/jaguar-range/f-type/specifications/index.html> [January 26 2018]

Jansson, J. (2005) Collision Avoidance Theory: With Application to Automotive
Collision Mitigation. Unpublished PhD thesis or dissertation. Linköping:
Linköping University

Jansson, J. and Gustafsson, F. (2008) 'A Framework and Automotive Application of
Collision Avoidance Decision Making'. Automatica 44 (9), 2347-2351

Jones, E., R. and Childers, R., L. (2001) *Contemporary College Physics*. 3rd edn.
USA: McGraw-Hill Publishing Co.

Jula, H., Kosmatopoulos, E. B., and Ioannou, P. A. (2000) 'Collision Avoidance
Analysis for Lane Changing and Merging'. IEEE Transactions on Vehicular
Technology 49 (6), 2295-2308

Kahraman, C. (2008) Fuzzy Multi-Criteria Decision Making: Theory and Applications
with Recent Developments. 1st edn. New York, USA: Springer Science &
Business Media

Kamali, M., Dennis, L. A., McAree, O., Fisher, M., and Veres, S. M. (2017) 'Formal
Verification of Autonomous Vehicle Platooning'. *Science of Computer
Programming* 148, 88-106

Kentley, T. D. (2017) Independent Steering, Power Torque Control and Transfer in
Autonomous Vehicles. US20170120753A1

Kett, P. (1982) *Motor Vehicle Science Part 2*. 1st edn. Netherlands: Springer

Kim, C. H. and Arora, J. S. (2003) 'Nonlinear Dynamic System Identification for
Automotive Crash using Optimization: A Review'. *Structural and
Multidisciplinary Optimization* 25 (1), 2-18

Klausen, A., Tørdal, S. S., Karimi, H. R., Robbersmyr, K. G., Jecmenica, M., and
Melteig, O. (2014) 'Firefly Optimization and Mathematical Modeling of a

Vehicle Crash Test Based on Single-Mass'. *Journal of Applied Mathematics* 2014 (ID 150319)

Kong, J., Pfeiffer, M., Schildbach, G., and Borrelli, F. (2015) *Intelligent Vehicles Symposium (IV), 2015 IEEE*. 'Kinematic and Dynamic Vehicle Models for Autonomous Driving Control Design'. held 28th June - 1st July 2015 at Seoul, South Korea: IEEE

Kritayakirana, K. and Gerdes, J. C. (2012) 'Autonomous Vehicle Control at the Limits of Handling'. *International Journal of Vehicle Autonomous Systems* 10 (4), 271-296

Lee, S., Son, Y., Kang, C. M., and Chung, C. C. (2013) *IFAC Intelligent Autonomous Vehicles Symposium*. 'Slip Angle Estimation: Development and Experimental Evaluation'. held 26-28 June at Gold Coast, Australia: Elsevier

Leics.gov.uk (2016) *Part 3 Design Guidance* [online] available from <http://www.leics.gov.uk/index/htd/highway_req_development_part3.htm> [December 14 2016]

Lim, J. (2015) 'A Consideration on the Offset Frontal Impact Modeling using Spring-Mass Model'. *International Journal of Mechanical, Aerospace, Industrial, Mechatronic and Manufacturing Engineering* 9 (8), 1392-1397

Lim, J. M. (2017) 'Lumped Mass-Spring Model Construction for Crash Analysis using Full Frontal Impact Test Data'. *International Journal of Automotive Technology* 18 (3), 463-472

Liu, S., Tang, J., Zhang, Z., and Gaudiot, J. (2017) *CAAD: Computer Architecture for Autonomous Driving*. arXiv preprint: arXiv: 1702.01894

Marzbanrad, J. and Ebrahimi, M. R. (2011) 'Multi-Objective Optimization of Aluminum Hollow Tubes for Vehicle Crash Energy Absorption using a Genetic Algorithm and Neural Networks'. *Thin-Walled Structures* 49 (12), 1605-1615

Marzougui, D., Samaha, R. R., Cui, C., Kan, C., and Opiela, K. S. (2012) *Extended Validation of the Finite Element Model for the 2010 Toyota Yaris Passenger Sedan*. Washington, DC, USA: National Crash Analysis Centre, George Washington University

Mathworld.Wolfram.com (2016) *Radius of Curvature* [online] available from <http://mathworld.wolfram.com/RadiusofCurvature.html> [December 14 2016]

Michael, J. B., Godbole, D. N., Lygeros, J., and Sengupta, R. (1998) 'Capacity Analysis of Traffic Flow Over a Single-Lane Automated Highway System'. *Journal of Intelligent Transportation System* 4 (1-2), 49-80

Milliken, W. F. and Milliken, D. L. (1995) *Race Car Vehicle Dynamics*. 1st edn. Warrendale, PA, USA: SAE International, 128

Mohler, R. R. (1973) *Bilinear Control Processes: With Applications to Engineering, Ecology and Medicine*. Orlando, FL, USA: Academic Press, Inc.

Mohler, R. R. and Kolodziej, W. (1980) 'An Overview of Bilinear System Theory and Applications'. *IEEE Transactions on Systems, Man and Cybernetics* 10 (10), 683-688

Moon, S., Moon, I., and Yi, K. (2009) 'Design, Tuning, and Evaluation of a Full-Range Adaptive Cruise Control System with Collision Avoidance'. Control Engineering Practice 17 (4), 442-455

Nam, K., Oh, S., Fujimoto, H., and Hori, Y. (2013) 'Estimation of Sideslip and Roll Angles of Electric Vehicles using Lateral Tire Force Sensors through RLS and Kalman Filter Approaches'. *IEEE Transactions on Industrial Electronics* 60 (3), 988-1000

National Transportation Safety Board (2015) The use of Forward Collision Avoidance Systems to Prevent and Mitigate Rear-End Crashes. Alexandria, VA, USA: National Technical Information Service

Nyholm, S. and Smids, J. (2016) 'The Ethics of Accident-Algorithms for Self-Driving Cars: An Applied Trolley Problem?'. *Ethical Theory and Moral Practice* 19 (5), 1275-1289

Omasa, T., Kishimoto, M., Kawase, M., and Yagi, K. (2004) 'An Attempt at Decision Making in Tissue Engineering: Reactor Evaluation using the Analytic Hierarchy Process (AHP)'. Biochemical Engineering Journal 20 (2-3), 173-179

Pickering, J., E., Ashman, P., Gilbert, A., Petrovic, D., Warwick, K., and Burnham, K. (eds.) (2018) *The 12th International UKACC Conference on Control*. 'Model-to-Decision Approach for Autonomous Vehicle Convoy Collision Ethics'. held 5th-7th September at Sheffield, UK: IEEEXplore

Pilutti, T., Ulsoy, G., and Hrovat, D. (1995) 'Vehicle Steering Intervention through Differential Braking'. *Journal of Dynamic Systems, Measurement, and Control* 120 (3), 314-321

Pinto, L., Aldworth, S., Franco-Jorge, M. D. M., and Watkinson, M. J. (2015a) Yaw Motion Control of a Vehicle. EP2576298A1

Pinto, L., Aldworth, S., Franco-Jorge, M. D. M., and Watkinson, M. J. (2015b) Yaw Motion Control of a Vehicle. US9008876B2

Porsche.com (2018) Rear-Axle Steering [online] available from <https://www.porsche.com/international/models/911/911-turbo-models/911-turbo/chassis/rear-axles-steering/> [May 11 2018]

Pörtner, R., Nagel-Heyer, S., Goepfert, C., Adamietz, P., and Meenen, N. M. (2005) 'Bioreactor Design for Tissue Engineering'. Journal of Bioscience and Bioengineering 100 (3), 235-245

Rajamani, R. (2011) Vehicle Dynamics and Control. 2nd edn. New York, NY, USA: Springer

Rubin, K. T. and Betts-Lacroix, J. (2016) *Device for Synchronizing a Time Base for V2V Communication*. US 9,300,423 B2

Saaty, T. L. (1980) 'The Analytical Hierarchy Process, Planning, Priority'. *Resource Allocation. RWS Publications, USA*

Saaty, T. L. (1990) 'How to make a Decision: The Analytic Hierarchy Process'. European Journal of Operational Research 48 (1), 9-26

Saaty, T. L. (1996) The Analytic Network Process: Decision Making with Dependence and Feedback; the Organization and Prioritization of Complexity. Pittsburgh, PA, USA: RWS Publications

Saaty, T. L. (ed.) (2000) Proceedings of the Fifteenth International Conference on Multiple Criteria Decision Making (MCDM). 'The Seven Pillars of the Analytic Hierarchy Process'. held 10-14 July at Ankara, Turkey. Berlin, Heidelberg: Springer

Saaty, T. L. and Vargas, L. G. (2004) Decision making—the Analytic Hierarchy and Network Processes (AHP/ANP). 2nd edn. New York, NY, USA: Springer

Saaty, T. L. and Vargas, L. G. (2012) Models, Methods, Concepts & Applications of the Analytic Hierarchy Process. 2nd edn. New York, NY, USA: Springer Science & Business Media

Safety.TRW.com (2013) What's a Small Overlap Frontal Crash Test? [online] available from <http://safety.trw.com/whats-a-small-overlap-frontal-crash-test/1007/> [22 March 2016]

Sartre-project.eu (2012) The SARTRE Project [online] available from <http://www.sartre-project.eu/en/Sidor/default.aspx> [08 May 2015]

Savage, P. G. (1998) 'Strapdown Inertial Navigation Integration Algorithm Design Part 2: Velocity and Position Algorithms'. Journal of Guidance, Control, and Dynamics 21 (2), 208-221

Schramm, D., Bardini, R., and Hiller, M. (2014) Vehicle Dynamics Modelling and Simulation. 1st edn. Berlin, Heidelberg: Springer

Shah, J., Best, M., Benmimoun, A., and Ayat, M. L. (2015) 'Autonomous Rear-End Collision Avoidance using an Electric Power Steering System'. Proceedings of the Institution of Mechanical Engineers, Part D: Journal of Automobile Engineering 229 (12), 1638-1655

Shanian, A. and Savadogo, O. (2006) 'A Material Selection Model Based on the Concept of Multiple Attribute Decision Making'. Materials & Design 27 (4), 329-337

Sierra, C., Tseng, E., Jain, A., and Peng, H. (2006) 'Cornering Stiffness Estimation Based on Vehicle Lateral Dynamics'. Vehicle System Dynamics 44 (sup1), 24-38

Snider, J. M. (2009) Automatic Steering Methods for Autonomous Automobile Path Tracking. Pittsburgh, Pennsylvania: Robotics Institute, Carnegie Mellon University

Song, J. (2012) 'Integrated Control of Brake Pressure and Rear-Wheel Steering to Improve Lateral Stability with Fuzzy Logic'. International Journal of Automotive Technology 13 (4), 563-570

Spentzas, K., Alkhazali, I., and Demic, M. (2001) 'Kinematics of Four-Wheel-Steering Vehicles'. Forschung Im Ingenieurwesen 66 (5), 211-216

Stanbrough, J. L. (2006) Inelastic Collisions in Two Dimensions [online] available from
<http://www.batesville.k12.in.us/Physics/APPhyNet/Dynamics/Collisions/inelastic_2d.htm> [September 27 2017]

Stigson, H., Kullgren, A., and Rosen, E. (2012) 'Injury Risk Functions in Frontal Impacts using Data from Crash Pulse Recorders'. Annals of Advances in Automotive Medicine. Association for the Advancement of Automotive Medicine/Annual Scientific Conference 56, 267-276

Supercars.net (2010) 2010 McLaren mp4-12c [online] available from
<http://www.supercars.net/cars/4584.html> [06 January 2015]

Takacs, D. and Stepan, G. (2013) 'Contact Patch Memory of Tyres Leading to Lateral Vibrations of Four-Wheeled Vehicles'. *Philosophical Transactions. Series A, Mathematical, Physical, and Engineering Sciences* 371 (1993), 20120427

Thor, J., Ding, S., and Kamaruddin, S. (2013) 'Comparison of Multi Criteria Decision Making Methods from the Maintenance Alternative Selection Perspective'. The International Journal of Engineering and Science 2 (6), 27-34

Trackpedia (2010) Data Collection and Analysis [online] available from
<http://www.trackpedia.com/wiki/Data_Collection_and_Analysis> [17 October 2014]

Triantaphyllou, E. and Mann, S. H. (1995) 'Using the Analytic Hierarchy Process for Decision Making in Engineering Applications: Some Challenges'. International Journal of Industrial Engineering: Applications and Practice 2 (1), 35-44

Tsugawa, S., Kato, S., and Aoki, K. (2011) *IEEE/RSJ International Conference on Intelligent Robots and Systems (IROS)*. 'An Automated Truck Platoon for Energy Saving'. held 25-30 September at San Francisco, USA: IEEE

Tzeng, G. and Huang, J. (2011) Multiple Attribute Decision Making: Methods and Applications. 1st edn. New York, USA: Chapman and Hall/CRC

U.S. Department of Transportation - Federal Highway Administration (2014) *Lane Width* [online] available from
<http://safety.fhwa.dot.gov/geometric/pubs/mitigationstrategies/chapter3/3_lanewidth.cfm> [December 14 2016]

US NCAP (2017) *Ratings* [online] available from <https://www.nhtsa.gov/ratings> [26 July 2018]

Wang, L., Huang, W., Liu, X., and Tian, Y. (2012) Intelligent Control and Information Processing (ICICIP), 2012 Third International Conference on. 'Vehicle Collision Avoidance Algorithm Based on State Estimation in the Roundabout'. held 15-17 July 2012 at Dalian, China: IEEE

Wang, T. and Chang, T. (2007) 'Application of TOPSIS in Evaluating Initial Training Aircraft Under a Fuzzy Environment'. Expert Systems with Applications 33 (4), 870-880

Wang, X. and Triantaphyllou, E. (2008) 'Ranking Irregularities when Evaluating Alternatives by using some ELECTRE Methods'. *Omega* 36 (1), 45-63

Watson, G. S. (1967) 'Linear Least Squares Regression'. *The Annals of Mathematical Statistics* 38 (6), 1679-1699

Xu, T., Li, Y., Li, Q., Hao, L., and Song, W. (2010) Computational Science and Optimization (CSO), 2010 Third International Joint Conference on. 'Crashworthiness Design of Frontal Rail using Strain-Energy-Density and Topology Optimization Approach': IEEE

Yang, T. and Kuo, C. (2003) 'A Hierarchical AHP/DEA Methodology for the Facilities Layout Design Problem'. *European Journal of Operational Research* 147 (1), 128-136

Yin, G. and Jin, X. (2013) *Cooperative Control of Regenerative Braking and Antilock Braking for a Hybrid Electric Vehicle*. http://web.b.ebscohost.com/ehost/pdfviewer/pdfviewer?vid=0&sid=1 caff81e-ebff-4626-920e-0d203aab4121%40pdc-v-sessmgr01 edn: Hindawi Publishing Corporation

Yoon, K. P. and Hwang, C. (1995) Multiple Attribute Decision Making: An Introduction. Thousand Oaks, CA, USA: Sage Publications

Zhang, L., Gao, L., Shao, X., Wen, L., and Zhi, J. (2010) 'A PSO-Fuzzy Group Decision-Making Support System in Vehicle Performance Evaluation'. Mathematical and Computer Modelling 52 (11-12), 1921-1931

Zhang, Z., Zhai, Y., Su, Y., Wang, X., Qiao, L., Liu, H., Li, S., and Du, Y. (2016) 'Research on Lamp Auto-Control System Based on Infrared Image

Processing'. *Optik-International Journal for Light and Electron Optics* 127 (3), 1144-1147

Appendices

Appendix A – IIHS Collision Data

A - Small Overlap Crash Test Results

Data acquired from IIHS.org (2017).

"The small overlap front rating is based on a 40 mph crash test in which 25 percent of the vehicle's width strikes a rigid barrier."

Table A.1 - Small Overlap Collision IIHS Test Ratings

Small Overlap Collision	2017 Audi Q7 3.0T Premium Plus 4-door 4wd	2015 Subaru Legacy 2.5i Premium 4-door 4wd	2014 Mini Cooper 2-door
Vehicle Class	Large SUV	Midsize car	Minicar
Weight (approx. kg)	2300.17	1565.8	1212.91
Wheelbase Length (approx. mm)	2997.2	2743.2	2489.2
Length (approx. mm)	5080	4800.6	3835.4
Width (approx. mm)	1955.8	1828.8	1727.2
Lower Occupant Compartment			
Lower hinge Pillar max (cm)	4	9	7
Footrest (cm)	5	7	7
Left toepan (cm)	4	3	2
Brake pedal (cm)	4	6	5
Rocker panel lateral average (cm)	0	1	1
Upper Occupant compartment			
Steering column (cm)	0	1	3

Upper hinge pillar max (cm)	3	5	5
Upper dash (cm)	3	6	5
Lower instrument panel (cm)	2	6	4
Driver Injury Measures			
Head			
HIC-15	225	120	167
Peak gs at hard contact	no contact	no contact	no contact
Neck			
Tension (kN)	1.3	1.2	1.1
Extension bending moment (Nm)	8	4	13
Maximum Nij	0.3	0.22	0.2
Chest maximum compression (mm)	30	25	24
Femur (kN)			
Left	5.5	1.7	0.8
Right	0.1	0.1	0
Knee Displacement (mm)			
Left	5	4	1
Right	0	1	2
Knee-thigh-hip injury risk (%)			
Left	4	0	0
Right	0	0	0
Maximum tibia index			
Left	0.57	0.53	0.64

Right	0.7	0.36	0.28
Tibia axial force (kN)			
Left	4.2	1.5	2.2
Right	0.3	0.1	0.4
Foot Acceleration (g)			
Left	121	65	93
Right	127	43	52

A – Moderate Overlap Crash Test Results

"The moderate overlap front rating is based on a 40 mph crash test in which 40 percent of the vehicle's width strikes a deformable barrier."

Table A.2 - Moderate Overlap Collision IIHS Test Ratings

Moderate Overlap Collision	2017 Audi Q7 3.0T Premium Plus 4-door 4wd	2015 Subaru Legacy 2.5i Premium 4-door 4wd	2014 Mini Cooper 2-door
Vehicle Class	Large SUV	Midsize car	Minicar
Weight (approx. kg)	2300.17	1565.8	1212.91
Wheelbase Length (approx. mm)	2997.2	2743.2	2489.2
Length (approx. mm)	5080	4800.6	3835.4
Width (approx. mm)	1955.8	1828.8	1727.2
Footwell Intrusion			
Footrest (cm)	1	2	4
Left (cm)	0	3	8

Centre (cm)	1	4	8
Right (cm)	1	4	8
Brake Pedal (cm)	1	6	4
Instrument panel rearward movement			
Left (cm)	0	0	2
Right (cm)	0	0	2
Steering Column Movement			
Upward (cm)	0	-3	-1
Rearward (cm)	-7	-6	-5
A-pillar rearward movement (cm)	0	0	2
Driver Injury Measures			
Head			
HIC-15	174	117	138
Peak gs at hard contact	no contact	no contact	no contact
Neck			
Tension (kN)	1.1	1.2	1.2
Extension bending moment (Nm)	11	20	6
Maximum Nij	0.23	0.27	0.23
Chest maximum compression (mm)	31	32	35
Legs			
Femur Force - Left (kN)	0.5	0.4	0.7
Femur Force - Right (kN)	0.3	0.6	1
Knee Displacement - left (mm)	7	1	1

Knee Displacement - right (mm)	0	1	1
maximum tibia Index - Left	0.57	0.48	0.39
maximum tibia Index - Right	0.6	0.55	0.43
Tibia Axial Force - left (kN)	1.9	2.7	2.3
Tibia Axial Force - right (kN)	1.5	2.4	2.5
Foot Acceleration (g)			
Left	64	67	97
Right	43	57	92

Appendix B – Non-V2V Linear Simulator Results

B - Section 9.5.5 Host Vehicle Overall Manoeuvre Acceleration

Table B.1 - Section 9.5.5 Simulation Results

Parameter Value (m/s²)	Lane 1 Impact Velocity (m/s)	Lane 1 Required Braking (m/s²)	Lane 1 Manoeuvre Acceleration (m/s²)	Lane 1 Lane Open	Lane 2 Impact Velocity (m/s)	Lane 2 Required Braking (m/s²)	Lane 2 Manoeuvre Acceleration (m/s²)	Lane 2 Lane Open	Lane 3 Impact Velocity (m/s)	Lane 3 Required Braking (m/s²)	Lane 3 Manoeuvre Acceleration (m/s²)	Lane 3 Lane Open
0.5	16.737	1.913	6.443	1	3.789	8.292	9	1	16.737	1.913	6.443	1
0.55	16.737	1.913	6.443	1	3.789	8.292	9	1	16.737	1.913	6.443	1
0.6	16.737	1.913	6.443	1	3.789	8.292	9	1	16.737	1.913	6.443	1
0.65	16.737	1.913	6.443	1	3.789	8.292	9	1	16.737	1.913	6.443	1
0.7	16.737	1.913	6.443	1	3.789	8.292	9	1	16.737	1.913	6.443	1
0.75	13.193	4.500	6.932	1	3.789	8.292	9	1	13.193	4.500	6.932	1
0.8	11.296	5.397	7.440	1	3.789	8.292	9	1	11.296	5.397	7.440	1
0.85	9.497	6.022	7.948	1	3.789	8.292	9	1	9.497	6.022	7.948	1
0.9	0	6.522	8.456	1	3.789	8.292	9	1	0	6.522	8.456	1
0.95	0	6.948	8.963	1	3.789	8.292	9	1	0	6.948	8.963	1
1	0	7.329	9.468	0	3.789	8.292	9	1	0	7.329	9.468	0

Table B.2 - Section 9.5.5 MADM Results

Parameter Value (m/s²)	Observer's Decision	TOPSIS				AHP				ANP			
		Lane 1	Lane 2	Lane 3	Decision	Lane 1	Lane 2	Lane 3	Decision	Lane 1	Lane 2	Lane 3	Decision
0.5	2	0.3445	0.6555	0.3445	2	0.3614	0.2772	0.3614	2	0.3005	0.3991	0.3005	1
0.55	2	0.3445	0.6555	0.3445	2	0.3614	0.2772	0.3614	2	0.3005	0.3991	0.3005	1
0.6	2	0.3445	0.6555	0.3445	2	0.3614	0.2772	0.3614	2	0.3005	0.3991	0.3005	1
0.65	2	0.3445	0.6555	0.3445	2	0.3614	0.2772	0.3614	2	0.3005	0.3991	0.3005	1
0.7	2	0.3445	0.6555	0.3445	2	0.3614	0.2772	0.3614	2	0.3005	0.3991	0.3005	1
0.75	2	0.2230	0.7770	0.2230	2	0.3803	0.2394	0.3803	2	0.3335	0.3329	0.3335	2
0.8	2	0.1801	0.8199	0.1801	2	0.3808	0.2383	0.3808	2	0.3408	0.3183	0.3408	2
0.85	2	0.1539	0.8461	0.1539	2	0.3775	0.2450	0.3775	2	0.3441	0.3118	0.3441	2
0.9	1	1	0	1	1	0.1068	0.7864	0.1068	1	0.2107	0.5787	0.2107	1
0.95	1	1	0	1	1	0.1093	0.7815	0.1093	1	0.2153	0.5693	0.2153	1
1	2	NaN	1	NaN	2	NaN	1	NaN	2	NaN	1	NaN	2

B - Section 9.5.7 Initial Velocity of Vehicles Ahead

Table B.3 - Section 9.5.7 Simulation Results

Parameter Value (mph)	Lane 1				Lane 2				Lane 3			
	Impact Velocity (m/s)	Required Braking (m/s²)	Manoeuvre Acceleration (m/s²)	Lane Open	Impact Velocity (m/s)	Required Braking (m/s²)	Manoeuvre Acceleration (m/s²)	Lane Open	Impact Velocity (m/s)	Required Braking (m/s²)	Manoeuvre Acceleration (m/s²)	Lane Open
52	0	6.522	8.456	1	3.789	8.292	9	1	11.048	6.522	8.456	0
52.5	0	6.522	8.456	1	3.789	8.292	9	1	10.886	6.522	8.456	1
53	0	6.522	8.456	1	3.789	8.292	9	1	10.727	6.522	8.456	1
53.5	0	6.522	8.456	1	3.789	8.292	9	1	10.569	6.522	8.456	1
54	0	6.522	8.456	1	3.789	8.292	9	1	10.414	6.522	8.456	1
54.5	0	6.522	8.456	1	3.789	8.292	9	1	10.262	6.522	8.456	1
55	0	6.522	8.456	1	3.789	8.292	9	1	10.113	6.522	8.456	1
55.5	0	6.522	8.456	1	3.789	8.292	9	1	9.966	6.522	8.456	1
56	0	6.522	8.456	1	3.789	8.292	9	1	9.822	6.522	8.456	1
56.5	0	6.522	8.456	1	3.789	8.292	9	1	9.681	6.522	8.456	1
57	0	6.522	8.456	1	3.789	8.292	9	1	9.543	6.522	8.456	1
57.5	0	6.522	8.456	1	3.789	8.292	9	1	9.408	6.522	8.456	1
58	0	6.522	8.456	1	3.789	8.292	9	1	9.278	6.522	8.456	1
58.5	0	6.522	8.456	1	3.789	8.292	9	1	9.150	6.522	8.456	1
59	0	6.522	8.456	1	3.789	8.292	9	1	9.027	6.522	8.456	1
59.5	0	6.522	8.456	1	3.789	8.292	9	1	8.907	6.522	8.456	1
60	0	6.522	8.456	1	3.789	8.292	9	1	8.792	6.522	8.456	1
60.5	0	6.522	8.456	1	3.789	8.292	9	1	8.680	6.522	8.456	1
61	0	6.522	8.456	1	3.789	8.292	9	1	8.573	6.522	8.456	1
61.5	0	6.522	8.456	1	3.789	8.292	9	1	8.470	6.522	8.456	1
62	0	6.522	8.456	1	3.789	8.292	9	1	8.372	6.522	8.456	1
62.5	0	6.522	8.456	1	3.789	8.292	9	1	8.279	6.522	8.456	1
63	0	6.522	8.456	1	3.789	8.292	9	1	8.192	6.522	8.456	1
63.5	0	6.522	8.456	1	3.789	8.292	9	1	8.108	6.522	8.456	1
64	0	6.522	8.456	1	3.789	8.292	9	1	8.031	6.522	8.456	1
64.5	0	6.522	8.456	1	3.789	8.292	9	1	7.959	6.522	8.456	1
65	0	6.522	8.456	1	3.789	8.292	9	1	7.893	6.522	8.456	1
65.5	0	6.522	8.456	1	3.789	8.292	9	1	7.833	6.522	8.456	1
66	0	6.522	8.456	1	3.789	8.292	9	1	7.779	6.522	8.456	1
66.5	0	6.522	8.456	1	3.789	8.292	9	1	7.319	6.522	8.456	1
67	0	6.522	8.456	1	3.789	8.292	9	1	6.556	6.522	8.456	1
67.5	0	6.522	8.456	1	3.789	8.292	9	1	5.682	6.522	8.456	1
68	0	6.522	8.456	1	3.789	8.292	9	1	4.641	6.522	8.456	1
68.5	0	6.522	8.456	1	3.789	8.292	9	1	3.271	6.522	8.456	1
69	0	6.522	8.456	1	3.789	8.292	9	1	0	6.522	8.456	1
69.5	0	6.522	8.456	1	3.789	8.292	9	1	0	6.522	8.456	1
70	0	6.522	8.456	1	3.789	8.292	9	1	0	6.522	8.456	1
70.5	0	6.522	8.456	1	3.789	8.292	9	1	0	6.522	8.456	1
71	0	6.522	8.456	1	3.789	8.292	9	1	0	6.522	8.456	1
71.5	0	6.522	8.456	1	3.789	8.292	9	1	0	6.522	8.456	1
72	0	6.522	8.456	1	3.789	8.292	9	1	0	6.522	8.456	1
72.5	0	6.522	8.456	1	3.789	8.292	9	1	0	6.522	8.456	1
73	0	6.522	8.456	1	3.789	8.292	9	1	0	6.522	8.456	1
73.5	0	6.522	8.456	1	3.789	8.292	9	1	0	6.522	8.456	1
74	0	6.522	8.456	1	3.789	8.292	9	1	0	6.522	8.456	1
74.5	0	6.522	8.456	1	3.789	8.292	9	1	0	6.522	8.456	1
75	0	6.522	8.456	1	3.789	8.292	9	1	0	6.522	8.456	1

Table B.4 - Section 9.5.7 MADM Results

Parameter Value (mph)	Observer's Decision	TOPSIS				AHP				ANP			
		Lane 1	Lane 2	Lane 3	Decision	Lane 1	Lane 2	Lane 3	Decision	Lane 1	Lane 2	Lane 3	Decision
52	1	1	0	NaN	1	0.1551	0.8449	NaN	1	0.3082	0.6918	NaN	1
52.5	1	1	0.6488	0.0554	1	0.1068	0.2993	0.5939	1	0.2107	0.3314	0.4579	1
53	1	1	0.6437	0.0554	1	0.1068	0.3011	0.5921	1	0.2107	0.3323	0.4570	1
53.5	1	1	0.6385	0.0555	1	0.1068	0.3030	0.5902	1	0.2107	0.3333	0.4560	1
54	1	1	0.6332	0.0556	1	0.1068	0.3049	0.5883	1	0.2107	0.3342	0.4551	1
54.5	1	1	0.6279	0.0557	1	0.1068	0.3068	0.5864	1	0.2107	0.3352	0.4541	1
55	1	1	0.6225	0.0558	1	0.1068	0.3087	0.5845	1	0.2107	0.3362	0.4532	1
55.5	1	1	0.6170	0.0559	1	0.1068	0.3106	0.5826	1	0.2107	0.3371	0.4522	1
56	1	1	0.6115	0.0560	1	0.1068	0.3125	0.5807	1	0.2107	0.3381	0.4512	1
56.5	1	1	0.6059	0.0561	1	0.1068	0.3144	0.5788	1	0.2107	0.3391	0.4502	1
57	1	1	0.6003	0.0562	1	0.1068	0.3163	0.5769	1	0.2107	0.3400	0.4493	1
57.5	1	1	0.5947	0.0563	1	0.1068	0.3182	0.5750	1	0.2107	0.3410	0.4483	1
58	1	1	0.5891	0.0564	1	0.1068	0.3201	0.5731	1	0.2107	0.3420	0.4474	1
58.5	1	1	0.5834	0.0565	1	0.1068	0.3220	0.5712	1	0.2107	0.3429	0.4464	1
59	1	1	0.5778	0.0566	1	0.1068	0.3239	0.5694	1	0.2107	0.3439	0.4455	1
59.5	1	1	0.5722	0.0567	1	0.1068	0.3257	0.5675	1	0.2107	0.3448	0.4445	1
60	1	1	0.5667	0.0568	1	0.1068	0.3275	0.5657	1	0.2107	0.3457	0.4436	1
60.5	1	1	0.5612	0.0570	1	0.1068	0.3293	0.5640	1	0.2107	0.3466	0.4427	1
61	1	1	0.5558	0.0571	1	0.1068	0.3310	0.5622	1	0.2107	0.3475	0.4418	1
61.5	1	1	0.5504	0.0572	1	0.1068	0.3327	0.5605	1	0.2107	0.3483	0.4410	1
62	1	1	0.5452	0.0573	1	0.1068	0.3343	0.5589	1	0.2107	0.3492	0.4402	1
62.5	1	1	0.5402	0.0574	1	0.1068	0.3359	0.5573	1	0.2107	0.3500	0.4394	1
63	1	1	0.5353	0.0575	1	0.1068	0.3374	0.5558	1	0.2107	0.3507	0.4386	1
63.5	1	1	0.5306	0.0576	1	0.1068	0.3389	0.5544	1	0.2107	0.3515	0.4379	1
64	1	1	0.5261	0.0577	1	0.1068	0.3402	0.5530	1	0.2107	0.3522	0.4372	1
64.5	1	1	0.5219	0.0578	1	0.1068	0.3415	0.5517	1	0.2107	0.3528	0.4365	1
65	1	1	0.5180	0.0578	1	0.1068	0.3427	0.5505	1	0.2107	0.3534	0.4359	1
65.5	1	1	0.5143	0.0579	1	0.1068	0.3438	0.5494	1	0.2107	0.3540	0.4353	1
66	1	1	0.5109	0.0580	1	0.1068	0.3448	0.5484	1	0.2107	0.3545	0.4348	1
66.5	1	1	0.4805	0.0587	1	0.1068	0.3537	0.5395	1	0.2107	0.3590	0.4303	1
67	1	1	0.4206	0.0601	1	0.1068	0.3702	0.5230	1	0.2107	0.3674	0.4219	1
67.5	1	1	0.3321	0.0624	1	0.1068	0.3924	0.5008	1	0.2107	0.3787	0.4107	1
68	1	1	0.1830	0.0667	1	0.1068	0.4249	0.4683	1	0.2107	0.3951	0.3942	1
68.5	1	1	0	0.1521	1	0.1068	0.4821	0.4111	1	0.2107	0.4242	0.3651	1
69	1	1	0	1	1	0.1068	0.7864	0.1068	1	0.2107	0.5787	0.2107	1
69.5	1	1	0	1	1	0.1068	0.7864	0.1068	1	0.2107	0.5787	0.2107	1
70	1	1	0	1	1	0.1068	0.7864	0.1068	1	0.2107	0.5787	0.2107	1
70.5	3	1	0	1	1	0.1068	0.7864	0.1068	1	0.2107	0.5787	0.2107	1
71	3	1	0	1	1	0.1068	0.7864	0.1068	1	0.2107	0.5787	0.2107	1
71.5	3	1	0	1	1	0.1068	0.7864	0.1068	1	0.2107	0.5787	0.2107	1
72	3	1	0	1	1	0.1068	0.7864	0.1068	1	0.2107	0.5787	0.2107	1
72.5	3	1	0	1	1	0.1068	0.7864	0.1068	1	0.2107	0.5787	0.2107	1
73	3	1	0	1	1	0.1068	0.7864	0.1068	1	0.2107	0.5787	0.2107	1
73.5	3	1	0	1	1	0.1068	0.7864	0.1068	1	0.2107	0.5787	0.2107	1
74	3	1	0	1	1	0.1068	0.7864	0.1068	1	0.2107	0.5787	0.2107	1
74.5	3	1	0	1	1	0.1068	0.7864	0.1068	1	0.2107	0.5787	0.2107	1
75	3	1	0	1	1	0.1068	0.7864	0.1068	1	0.2107	0.5787	0.2107	1

B - Section 9.5.8 Initial Headway Distance to Vehicles Ahead

Table B.5 - Section 9.5.8 Simulation Results

Parameter Value (m)	Lane 1				Lane 2				Lane 3			
	Impact Velocity (m/s)	Required Braking (m/s²)	Manoeuvre Acceleration (m/s²)	Lane Open	Impact Velocity (m/s)	Required Braking (m/s²)	Manoeuvre Acceleration (m/s²)	Lane Open	Impact Velocity (m/s)	Required Braking (m/s²)	Manoeuvre Acceleration (m/s²)	Lane Open
3	0	6.522	8.456	1	3.789	8.292	9	1	2.932	6.522	8.456	0
4	0	6.522	8.456	1	3.789	8.292	9	1	3.386	6.522	8.456	1
5	0	6.522	8.456	1	3.789	8.292	9	1	3.786	6.522	8.456	1
6	0	6.522	8.456	1	3.789	8.292	9	1	4.147	6.522	8.456	1
7	0	6.522	8.456	1	3.789	8.292	9	1	4.479	6.522	8.456	1
8	0	6.522	8.456	1	3.789	8.292	9	1	4.789	6.522	8.456	1
9	0	6.522	8.456	1	3.789	8.292	9	1	5.078	6.522	8.456	1
10	0	6.522	8.456	1	3.789	8.292	9	1	5.353	6.522	8.456	1
11	0	6.522	8.456	1	3.789	8.292	9	1	5.614	6.522	8.456	1
12	0	6.522	8.456	1	3.789	8.292	9	1	5.864	6.522	8.456	1
13	0	6.522	8.456	1	3.789	8.292	9	1	6.104	6.522	8.456	1
14	0	6.522	8.456	1	3.789	8.292	9	1	6.334	6.522	8.456	1
15	0	6.522	8.456	1	3.789	8.292	9	1	5.771	6.522	8.456	1
16	0	6.522	8.456	1	3.789	8.292	9	1	4.713	6.522	8.456	1
17	0	6.522	8.456	1	3.789	8.292	9	1	3.327	6.522	8.456	1
18	0	6.522	8.456	1	3.789	8.292	9	1	0	6.522	8.456	1
19	0	6.522	8.456	1	3.789	8.292	9	1	0	6.522	8.456	1
20	0	6.522	8.456	1	3.789	8.292	9	1	0	6.522	8.456	1
21	0	6.522	8.456	1	3.789	8.292	9	1	0	6.522	8.456	1
22	0	6.522	8.456	1	3.789	8.292	9	1	0	6.522	8.456	1
23	0	6.522	8.456	1	3.789	8.292	9	1	0	6.522	8.456	1
24	0	6.522	8.456	1	3.789	8.292	9	1	0	6.522	8.456	1
25	0	6.522	8.456	1	3.789	8.292	9	1	0	6.522	8.456	1

Table B.6 - Section 9.5.8 MADM Results

Parameter Value (m)	Observer's Decision	TOPSIS				AHP				ANP			
		Lane 1	Lane 2	Lane 3	Decision	Lane 1	Lane 2	Lane 3	Decision	Lane 1	Lane 2	Lane 3	Decision
3	1	1	0	NaN	1	0.1551	0.8449	NaN	1	0.3082	0.6918	NaN	1
4	1	1	0	0.1266	1	0.1068	0.4765	0.4167	1	0.2107	0.4213	0.3680	1
5	1	1	0	0.0726	1	0.1068	0.4582	0.4350	1	0.2107	0.4120	0.3773	1
6	1	1	0.0861	0.0697	1	0.1068	0.4433	0.4500	1	0.2107	0.4045	0.3849	1
7	1	1	0.1537	0.0676	1	0.1068	0.4306	0.4626	1	0.2107	0.3981	0.3913	1
8	1	1	0.2081	0.0659	1	0.1068	0.4198	0.4734	1	0.2107	0.3926	0.3968	1
9	1	1	0.2531	0.0646	1	0.1068	0.4103	0.4829	1	0.2107	0.3878	0.4016	1
10	1	1	0.2913	0.0635	1	0.1068	0.4019	0.4913	1	0.2107	0.3835	0.4059	1
11	1	1	0.3240	0.0626	1	0.1068	0.3943	0.4989	1	0.2107	0.3796	0.4097	1
12	1	1	0.3528	0.0618	1	0.1068	0.3875	0.5057	1	0.2107	0.3761	0.4132	1
13	1	1	0.3780	0.0612	1	0.1068	0.3812	0.5120	1	0.2107	0.3730	0.4163	1
14	1	1	0.4005	0.0606	1	0.1068	0.3755	0.5177	1	0.2107	0.3701	0.4192	1
15	1	1	0.3424	0.0621	1	0.1068	0.3900	0.5032	1	0.2107	0.3774	0.4119	1
16	1	1	0.1955	0.0663	1	0.1068	0.4224	0.4708	1	0.2107	0.3939	0.3955	1
17	1	1	0	0.1396	1	0.1068	0.4794	0.4138	1	0.2107	0.4228	0.3665	1
18	1	1	0	1	1	0.1068	0.7864	0.1068	1	0.2107	0.5787	0.2107	1
19	1	1	0	1	1	0.1068	0.7864	0.1068	1	0.2107	0.5787	0.2107	1
20	1	1	0	1	1	0.1068	0.7864	0.1068	1	0.2107	0.5787	0.2107	1
21	3	1	0	1	1	0.1068	0.7864	0.1068	1	0.2107	0.5787	0.2107	1
22	3	1	0	1	1	0.1068	0.7864	0.1068	1	0.2107	0.5787	0.2107	1
23	3	1	0	1	1	0.1068	0.7864	0.1068	1	0.2107	0.5787	0.2107	1
24	3	1	0	1	1	0.1068	0.7864	0.1068	1	0.2107	0.5787	0.2107	1
25	3	1	0	1	1	0.1068	0.7864	0.1068	1	0.2107	0.5787	0.2107	1

B - Section 9.5.9 Braking Values of Vehicles Ahead

Table B.7 - Section 9.5.9 Simulation Results

Parameter Value (m/s²)	Lane 1				Lane 2				Lane 3			
	Impact Velocity (m/s)	Required Braking (m/s²)	Manoeuvre Acceleration (m/s²)	Lane Open	Impact Velocity (m/s)	Required Braking (m/s²)	Manoeuvre Acceleration (m/s²)	Lane Open	Impact Velocity (m/s)	Required Braking (m/s²)	Manoeuvre Acceleration (m/s²)	Lane Open
0	0	6.522	8.456	1	3.789	8.292	9	1	0	6.522	8.456	1
1	0	6.522	8.456	1	3.789	8.292	9	1	0	6.522	8.456	1
2	0	6.522	8.456	1	3.789	8.292	9	1	0	6.522	8.456	1
3	0	6.522	8.456	1	3.789	8.292	9	1	0	6.522	8.456	1
4	0	6.522	8.456	1	3.789	8.292	9	1	0	6.522	8.456	1
5	0	6.522	8.456	1	3.789	8.292	9	1	0	6.522	8.456	1
6	0	6.522	8.456	1	3.789	8.292	9	1	0	6.522	8.456	1
7	0	6.522	8.456	1	3.789	8.292	9	1	0	6.522	8.456	1
8	0	6.522	8.456	1	3.789	8.292	9	1	8.661	6.522	8.456	1
9	0	6.522	8.456	1	3.789	8.292	9	1	11.718	6.522	8.456	1
10	0	6.522	8.456	1	3.789	8.292	9	1	13.320	6.522	8.456	1
11	0	6.522	8.456	1	3.789	8.292	9	1	14.744	6.522	8.456	1
12	0	6.522	8.456	1	3.789	8.292	9	1	16.043	6.522	8.456	1
13	0	6.522	8.456	1	3.789	8.292	9	1	17.243	6.522	8.456	1
14	0	6.522	8.456	1	3.789	8.292	9	1	18.366	6.522	8.456	1
15	0	6.522	8.456	1	3.789	8.292	9	1	19.431	6.522	8.456	0

Table B.8 - Section 9.5.9 MADM Results

Parameter Value (m/s²)	Observer's Decision	TOPSIS				AHP				ANP			
		Lane 1	Lane 2	Lane 3	Decision	Lane 1	Lane 2	Lane 3	Decision	Lane 1	Lane 2	Lane 3	Decision
0	3	1	0	1	1	0.1068	0.7864	0.1068	1	0.2107	0.5787	0.2107	1
1	3	1	0	1	1	0.1068	0.7864	0.1068	1	0.2107	0.5787	0.2107	1
2	3	1	0	1	1	0.1068	0.7864	0.1068	1	0.2107	0.5787	0.2107	1
3	3	1	0	1	1	0.1068	0.7864	0.1068	1	0.2107	0.5787	0.2107	1
4	3	1	0	1	1	0.1068	0.7864	0.1068	1	0.2107	0.5787	0.2107	1
5	3	1	0	1	1	0.1068	0.7864	0.1068	1	0.2107	0.5787	0.2107	1
6	3	1	0	1	1	0.1068	0.7864	0.1068	1	0.2107	0.5787	0.2107	1
7	1	1	0	1	1	0.1068	0.7864	0.1068	1	0.2107	0.5787	0.2107	1
8	1	1	0.5602	0.0570	1	0.1068	0.3296	0.5636	1	0.2107	0.3468	0.4426	1
9	1	1	0.6732	0.0550	1	0.1068	0.2902	0.6030	1	0.2107	0.3268	0.4626	1
10	1	1	0.7114	0.0544	1	0.1068	0.2751	0.6181	1	0.2107	0.3191	0.4702	1
11	1	1	0.7384	0.0541	1	0.1068	0.2640	0.6292	1	0.2107	0.3135	0.4759	1
12	1	1	0.7587	0.0538	1	0.1068	0.2552	0.6380	1	0.2107	0.3090	0.4803	1
13	1	1	0.7747	0.0536	1	0.1068	0.2480	0.6452	1	0.2107	0.3054	0.4840	1
14	1	1	0.7877	0.0535	1	0.1068	0.2420	0.6512	1	0.2107	0.3023	0.4870	1
15	1	1	0.0000	NaN	1	0.1551	0.8449	NaN	1	0.3082	0.6918	NaN	1

B - Section 9.5.10 Initial Velocity of Vehicles Behind

Table B.9 - Section 9.5.10 Simulation Results

Parameter Value (mph)	Lane 1				Lane 2				Lane 3			
	Impact Velocity (m/s)	Required Braking (m/s²)	Manoeuvre Acceleration (m/s²)	Lane Open	Impact Velocity (m/s)	Required Braking (m/s²)	Manoeuvre Acceleration (m/s²)	Lane Open	Impact Velocity (m/s)	Required Braking (m/s²)	Manoeuvre Acceleration (m/s²)	Lane Open
65	0	6.522	8.456	1	3.789	8.292	9	1	0	5.127	8.456	1
66	0	6.522	8.456	1	3.789	8.292	9	1	0	5.380	8.456	1
67	0	6.522	8.456	1	3.789	8.292	9	1	0	5.647	8.456	1
68	0	6.522	8.456	1	3.789	8.292	9	1	0	5.926	8.456	1
69	0	6.522	8.456	1	3.789	8.292	9	1	0	6.216	8.456	1
70	0	6.522	8.456	1	3.789	8.292	9	1	0	6.522	8.456	1
71	0	6.522	8.456	1	3.789	8.292	9	1	0	6.840	8.456	1
72	0	6.522	8.456	1	3.789	8.292	9	1	0	7.172	8.456	1
73	0	6.522	8.456	1	3.789	8.292	9	1	0	7.519	8.456	1
74	0	6.522	8.456	1	3.789	8.292	9	1	0	7.880	8.456	0

Table B.10 - Section 9.5.10 MADM Results

Parameter Value (mph)	Observer's Decision	TOPSIS				AHP				ANP			
		Lane 1	Lane 2	Lane 3	Decision	Lane 1	Lane 2	Lane 3	Decision	Lane 1	Lane 2	Lane 3	Decision
65	3	0.9561	0	1	3	0.1122	0.7933	0.0945	3	0.2178	0.5877	0.1945	3
66	3	0.9641	0	1	3	0.1112	0.7920	0.0968	3	0.2164	0.5860	0.1976	3
67	3	0.9726	0	1	3	0.1101	0.7906	0.0993	3	0.2150	0.5842	0.2008	3
68	3	0.9813	0	1	3	0.1090	0.7893	0.1017	3	0.2136	0.5824	0.2040	3
69	3	0.9905	0	1	3	0.1079	0.7879	0.1042	3	0.2122	0.5805	0.2073	3
70	1	1	0	1	1	0.1068	0.7864	0.1068	1	0.2107	0.5787	0.2107	1
71	1	1	0	0.9903	1	0.1056	0.7850	0.1094	1	0.2092	0.5767	0.2141	1
72	1	1	0	0.9807	1	0.1045	0.7835	0.1120	1	0.2077	0.5748	0.2175	1
73	1	1	0	0.9711	1	0.1033	0.7820	0.1147	1	0.2061	0.5729	0.2210	1
74	1	1	0	NaN	1	0.1551	0.8449	NaN	1	0.3082	0.6918	NaN	1

B - Section 9.5.11 Initial Headway Distance to Vehicles Behind

Table B.11 - Section 9.5.11 - Simulation Results

Parameter Value (m)	Lane 1				Lane 2				Lane 3			
	Impact Velocity (m/s)	Required Braking (m/s²)	Manoeuvre Acceleration (m/s²)	Lane Open	Impact Velocity (m/s)	Required Braking (m/s²)	Manoeuvre Acceleration (m/s²)	Lane Open	Impact Velocity (m/s)	Required Braking (m/s²)	Manoeuvre Acceleration (m/s²)	Lane Open
16	0	6.522	8.456	1	3.789	8.292	9	1	0	7.530	8.456	0
17	0	6.522	8.456	1	3.789	8.292	9	1	0	7.234	8.456	1
18	0	6.522	8.456	1	3.789	8.292	9	1	0	6.973	8.456	1
19	0	6.522	8.456	1	3.789	8.292	9	1	0	6.735	8.456	1
20	0	6.522	8.456	1	3.789	8.292	9	1	0	6.522	8.456	1
21	0	6.522	8.456	1	3.789	8.292	9	1	0	6.327	8.456	1
22	0	6.522	8.456	1	3.789	8.292	9	1	0	6.150	8.456	1
23	0	6.522	8.456	1	3.789	8.292	9	1	0	5.986	8.456	1
24	0	6.522	8.456	1	3.789	8.292	9	1	0	5.834	8.456	1
25	0	6.522	8.456	1	3.789	8.292	9	1	0	5.694	8.456	1
26	0	6.522	8.456	1	3.789	8.292	9	1	0	5.562	8.456	1
27	0	6.522	8.456	1	3.789	8.292	9	1	0	5.440	8.456	1
28	0	6.522	8.456	1	3.789	8.292	9	1	0	5.326	8.456	1
29	0	6.522	8.456	1	3.789	8.292	9	1	0	5.219	8.456	1
30	0	6.522	8.456	1	3.789	8.292	9	1	0	5.117	8.456	1

Table B.12 - Section 9.5.11 MADM Results

Parameter Value (m)	Observer's Decision	TOPSIS				AHP				ANP			
		Lane 1	Lane 2	Lane 3	Decision	Lane 1	Lane 2	Lane 3	Decision	Lane 1	Lane 2	Lane 3	Decision
16	1	1	0	NaN	1	0.1551	0.8449	NaN	1	0.3082	0.6918	NaN	1
17	1	1	0	0.9790	1	0.1043	0.7832	0.1125	1	0.2074	0.5745	0.2181	1
18	1	1	0	0.9864	1	0.1052	0.7844	0.1104	1	0.2086	0.5760	0.2155	1
19	1	1	0	0.9935	1	0.1060	0.7855	0.1085	1	0.2097	0.5774	0.2130	1
20	1	1	0	1	1	0.1068	0.7864	0.1068	1	0.2107	0.5787	0.2107	1
21	3	0.9939	0	1	3	0.1075	0.7873	0.1052	3	0.2116	0.5798	0.2085	3
22	3	0.9884	0	1	3	0.1082	0.7882	0.1037	3	0.2125	0.5809	0.2066	3
23	3	0.9832	0	1	3	0.1088	0.7890	0.1022	3	0.2133	0.5820	0.2047	3
24	3	0.9785	0	1	3	0.1094	0.7897	0.1009	3	0.2141	0.5830	0.2030	3
25	3	0.9740	0	1	3	0.1099	0.7904	0.0997	3	0.2148	0.5839	0.2013	3
26	3	0.9699	0	1	3	0.1104	0.7911	0.0985	3	0.2155	0.5848	0.1998	3
27	3	0.9660	0	1	3	0.1109	0.7917	0.0974	3	0.2161	0.5856	0.1983	3
28	3	0.9624	0	1	3	0.1114	0.7923	0.0963	3	0.2167	0.5863	0.1969	3
29	3	0.9590	0	1	3	0.1118	0.7928	0.0953	3	0.2173	0.5871	0.1956	3
30	3	0.9558	0	1	3	0.1123	0.7934	0.0944	3	0.2179	0.5878	0.1944	3

Appendix C –V2V Dynamic Simulator Results

C - Section 9.6.5 Host Vehicle Manoeuvre Lateral Acceleration (Steering)

Table C.1 - Section 9.6.5 Simulation Results

Lane 1

Parameter Value (m/s²)	Impact Velocity VA (m/s)	Impact Velocity HV1 (m/s)	Impact Velocity HV2 (m/s)	Impact Velocity VB (m/s)	Manoeuvre Acceleration (m/s²)	TTC (s)	Lane Open
6.9	13.5702	29.9007	0	0	10.1696	1.738	1
7	17.7306	27.8636	0	0	9.8512	1.875	1
7.1	17.0924	26.4408	0	0	9.6627	1.964	1
7.2	16.5263	25.2463	0	0	9.5223	2.043	1
7.3	15.9819	24.1608	0	4.2905	9.4096	2.119	1
7.4	15.4593	23.1581	0	6.0189	9.3153	2.192	1
7.5	14.9370	22.1960	0	7.2111	9.2348	2.265	1
7.6	14.4220	21.2821	0	8.1225	9.1639	2.337	1
7.7	13.8929	20.3746	0	8.8807	9.1019	2.411	1
7.8	13.3641	19.4941	0.1751	9.5162	9.0461	2.485	1
7.9	12.8312	18.6157	0.8211	10.0854	8.9961	2.561	1
8	12.2642	17.7368	1.4090	10.6387	8.9510	2.639	1
8.1	11.6861	16.8510	1.9488	11.0911	8.9097	2.72	1
8.2	11.0868	15.9523	2.4427	11.5378	8.8722	2.804	1
8.3	10.4663	15.0432	2.8932	11.9487	8.8375	2.891	1
8.4	9.8104	14.1023	3.3034	12.3290	8.8059	2.983	1
8.5	9.1191	13.1322	3.6921	12.6888	8.7765	3.08	1
8.6	8.3825	12.1320	4.0419	13.0179	8.7491	3.182	1
8.7	7.6092	11.0730	4.3732	13.3316	8.7239	3.292	1
8.8	6.7521	9.9499	4.5804	13.6249	8.7003	3.411	1
8.9	5.8512	8.7620	4.9628	13.8977	8.6781	3.539	1
9	4.8268	7.4489	5.2331	14.1603	8.6578	3.683	1
9.1	3.6247	5.9971	5.4777	14.4024	8.6385	3.845	1
9.2	2.3452	4.3493	5.7123	14.6342	8.6718	3.886	1
9.3	0.7387	2.3916	5.5283	14.8506	8.7194	3.847	1
9.4	0	0	6.1308	15.0568	8.7653	3.809	1
9.5	0	0	6.3167	15.2475	8.8094	3.773	1
9.6	0	0	6.4967	15.4331	8.8520	3.74	1
9.7	0	0	6.6649	15.6085	8.8930	3.708	1
9.8	0	0	6.8259	15.7788	8.9325	3.678	1
9.9	0	0	6.9791	15.9387	8.9706	3.65	1
10	0	0	7.1155	16.0884	9.0074	3.623	1

Lane 2

Parameter Value (m/s²)	Impact Velocity VA (m/s)	Impact Velocity HV1 (m/s)	Impact Velocity HV2 (m/s)	Impact Velocity VB (m/s)	Manoeuvre Acceleration (m/s²)	TTC (s)	Lane Open
6.9	0	11.4561	10.3582	21.4249	8.3103	2.417	1
7	0	11.4561	10.3582	21.4249	8.3103	2.417	1
7.1	0	11.4561	10.3582	21.4249	8.3103	2.417	1
7.2	0	11.4561	10.3582	21.4249	8.3103	2.417	1
7.3	0	11.4561	10.3582	21.4249	8.3103	2.417	1
7.4	0	11.4561	10.3582	21.4249	8.3103	2.417	1
7.5	0	11.4561	10.3582	21.4249	8.3103	2.417	1
7.6	0	11.4561	10.3582	21.4249	8.3103	2.417	1
7.7	0	11.4561	10.3582	21.4249	8.3103	2.417	1
7.8	0	11.4561	10.3582	21.4249	8.3103	2.417	1
7.9	0	11.4561	10.3582	21.4249	8.3103	2.417	1
8	0	11.4561	10.3582	21.4249	8.3103	2.417	1
8.1	0	11.4561	10.3582	21.4249	8.3103	2.417	1
8.2	0	11.4561	10.3582	21.4249	8.3103	2.417	1
8.3	0	11.4561	10.3582	21.4249	8.3103	2.417	1
8.4	0	11.4561	10.3582	21.4249	8.3103	2.417	1
8.5	0	11.4561	10.3582	21.4249	8.3103	2.417	1
8.6	0	11.4561	10.3582	21.4249	8.3103	2.417	1
8.7	0	11.4561	10.3582	21.4249	8.3103	2.417	1
8.8	0	11.4561	10.3582	21.4249	8.3103	2.417	1
8.9	0	11.4561	10.3582	21.4249	8.3103	2.417	1
9	0	11.4561	10.3582	21.4249	8.3103	2.417	1
9.1	0	11.4561	10.3582	21.4249	8.3103	2.417	1
9.2	0	11.4561	10.3582	21.4249	8.3103	2.417	1
9.3	0	11.4561	10.3582	21.4249	8.3103	2.417	1
9.4	0	11.4561	10.3582	21.4249	8.3103	2.417	1
9.5	0	11.4561	10.3582	21.4249	8.3103	2.417	1
9.6	0	11.4561	10.3582	21.4249	8.3103	2.417	1
9.7	0	11.4561	10.3582	21.4249	8.3103	2.417	1
9.8	0	11.4561	10.3582	21.4249	8.3103	2.417	1
9.9	0	11.4561	10.3582	21.4249	8.3103	2.417	1
10	0	11.4561	10.3582	21.4249	8.3103	2.417	1

Lane 3

Parameter Value (m/s²)	Impact Velocity V1 (m/s)	Impact Velocity HV1 (m/s)	Impact Velocity HV2 (m/s)	Impact Velocity V8 (m/s)	Manoeuvre Acceleration (m/s²)	TTC (s)	Lane Open
6.9	18.5702	29.9007	0	0	10.1696	1.738	1
7	17.7306	27.8636	0	0	9.8512	1.875	1
7.1	17.0924	26.4408	0	0	9.6627	1.964	1
7.2	16.5263	25.2463	0	0	9.5223	2.043	1
7.3	15.9819	24.1608	0	4.2905	9.4096	2.119	1
7.4	15.4593	23.1581	0	6.0189	9.3153	2.192	1
7.5	14.9370	22.1960	0	7.2111	9.2348	2.265	1
7.6	14.4220	21.2821	0	8.1225	9.1639	2.337	1
7.7	13.8929	20.3746	0	8.8807	9.1019	2.411	1
7.8	13.3641	19.4941	0.1751	9.5162	9.0461	2.485	1
7.9	12.8212	18.6157	0.8211	10.0854	8.9961	2.561	1
8	12.2642	17.7368	1.4090	10.6387	8.9510	2.639	1
8.1	11.6861	16.8510	1.9488	11.0911	8.9097	2.72	1
8.2	11.0868	15.9523	2.4427	11.5378	8.8722	2.804	1
8.3	10.4663	15.0432	2.8932	11.9487	8.8375	2.891	1
8.4	9.8104	14.1023	3.3034	12.3290	8.8059	2.983	1
8.5	9.1192	13.1322	3.6921	12.6888	8.7765	3.08	1
8.6	8.3925	12.1320	4.0419	13.0179	8.7491	3.182	1
8.7	7.5092	11.0730	4.3732	13.3316	8.7239	3.292	1
8.8	6.7621	9.9499	4.5804	13.6249	8.7003	3.411	1
8.9	5.8512	8.7620	4.9628	13.8977	8.6781	3.539	1
9	4.8258	7.4489	5.2331	14.1603	8.6578	3.683	1
9.1	3.5747	5.9971	5.4777	14.4024	8.6385	3.845	1
9.2	2.3452	4.3493	5.7123	14.6342	8.6718	3.886	1
9.3	0.7387	2.3916	5.9283	14.8506	8.7194	3.847	1
9.4	0	0	6.1308	15.0568	8.7653	3.809	1
9.5	0	0	6.3167	15.2475	8.8094	3.773	1
9.6	0	0	6.4967	15.4331	8.8520	3.74	1
9.7	0	0	6.6649	15.6085	8.8950	3.708	1
9.8	0	0	6.8269	15.7788	8.9325	3.676	1
9.9	0	0	6.9791	15.9387	8.9706	3.65	1
10	0	0	7.1165	16.0884	9.0074	3.623	1

Table C.2 - Section 9.6.5 Collision Modelling Results

Parameter Value (m/s²)	Lane 1						Lane 2						Lane 3					
	Collision Acceleration VA (g)	Collision Acceleration HV1 (g)	Collision Acceleration HV2 (g)	Collision Acceleration VB (g)	Manoeuvre Acceleration (m/s²)	TTC (s)	Collision Acceleration VA (g)	Collision Acceleration HV1 (g)	Collision Acceleration HV2 (g)	Collision Acceleration VB (g)	Manoeuvre Acceleration (m/s²)	TTC (s)	Collision Acceleration VA (g)	Collision Acceleration HV1 (g)	Collision Acceleration HV2 (g)	Collision Acceleration VB (g)	Manoeuvre Acceleration (m/s²)	TTC (s)
6.9	12.5192	12.5192	0	0	10.1696	1.758	12.6826	12.6826	7.2208	14.4416	8.3103	2.417	12.5192	12.5192	0	0	10.1696	1.758
7	10.9915	10.9915	0	0	9.8512	1.875	12.6826	12.6826	7.2208	14.4416	8.3103	2.417	10.9915	10.9915	0	0	9.8512	1.875
7.1	10.0197	10.0197	0	0	9.6627	1.964	12.6826	12.6826	7.2208	14.4416	8.3103	2.417	10.0197	10.0197	0	0	9.6627	1.964
7.2	9.2576	9.2576	0	0	9.5223	2.043	12.6826	12.6826	7.2208	14.4416	8.3103	2.417	9.2576	9.2576	0	0	9.5223	2.043
7.3	8.6126	8.6126	2.4867	4.9734	9.4096	2.119	12.6826	12.6826	7.2208	14.4416	8.3103	2.417	8.6126	8.6126	2.4867	4.9734	9.4096	2.119
7.4	8.0488	8.0488	3.5926	7.1852	9.3153	2.192	12.6826	12.6826	7.2208	14.4416	8.3103	2.417	8.0488	8.0488	3.5926	7.1852	9.3153	2.192
7.5	7.5394	7.5394	4.3939	8.7877	9.2348	2.265	12.6826	12.6826	7.2208	14.4416	8.3103	2.417	7.5394	7.5394	4.3939	8.7877	9.2348	2.265
7.6	7.0828	7.0828	5.0286	10.0573	9.1639	2.337	12.6826	12.6826	7.2208	14.4416	8.3103	2.417	7.0828	7.0828	5.0286	10.0573	9.1639	2.337
7.7	6.6546	6.6546	5.5720	11.1440	9.1019	2.411	12.6826	12.6826	7.2208	14.4416	8.3103	2.417	6.6546	6.6546	5.5720	11.1440	9.1019	2.411
7.8	6.2609	6.2609	5.9090	11.8180	9.0461	2.485	12.6826	12.6826	7.2208	14.4416	8.3103	2.417	6.2609	6.2609	5.9090	11.8180	9.0461	2.485
7.9	5.8891	5.8891	5.8524	11.7049	8.9961	2.561	12.6826	12.6826	7.2208	14.4416	8.3103	2.417	5.8891	5.8891	5.8524	11.7049	8.9961	2.561
8	5.5356	5.5356	5.8049	11.6099	8.9510	2.639	12.6826	12.6826	7.2208	14.4416	8.3103	2.417	5.5356	5.5356	5.8049	11.6099	8.9510	2.639
8.1	5.2009	5.2009	5.7629	11.5257	8.9097	2.72	12.6826	12.6826	7.2208	14.4416	8.3103	2.417	5.2009	5.2009	5.7629	11.5257	8.9097	2.72
8.2	4.8780	4.8780	5.7283	11.4565	8.8722	2.804	12.6826	12.6826	7.2208	14.4416	8.3103	2.417	4.8780	4.8780	5.7283	11.4565	8.8722	2.804
8.3	4.5694	4.5694	5.6993	11.3986	8.8375	2.891	12.6826	12.6826	7.2208	14.4416	8.3103	2.417	4.5694	4.5694	5.6993	11.3986	8.8375	2.891
8.4	4.2671	4.2671	5.6775	11.3549	8.8059	2.983	12.6826	12.6826	7.2208	14.4416	8.3103	2.417	4.2671	4.2671	5.6775	11.3549	8.8059	2.983
8.5	3.9738	3.9738	5.6564	11.3129	8.7765	3.08	12.6826	12.6826	7.2208	14.4416	8.3103	2.417	3.9738	3.9738	5.6564	11.3129	8.7765	3.08
8.6	3.6882	3.6882	5.6413	11.2826	8.7491	3.182	12.6826	12.6826	7.2208	14.4416	8.3103	2.417	3.6882	3.6882	5.6413	11.2826	8.7491	3.182
8.7	3.4028	3.4028	5.6286	11.2572	8.7239	3.292	12.6826	12.6826	7.2208	14.4416	8.3103	2.417	3.4028	3.4028	5.6286	11.2572	8.7239	3.292
8.8	3.1192	3.1192	5.6185	11.2369	8.7003	3.411	12.6826	12.6826	7.2208	14.4416	8.3103	2.417	3.1192	3.1192	5.6185	11.2369	8.7003	3.411
8.9	2.8368	2.8368	5.6114	11.2229	8.6781	3.539	12.6826	12.6826	7.2208	14.4416	8.3103	2.417	2.8368	2.8368	5.6114	11.2229	8.6781	3.539
9	2.5449	2.5449	5.6058	11.2116	8.6578	3.683	12.6826	12.6826	7.2208	14.4416	8.3103	2.417	2.5449	2.5449	5.6058	11.2116	8.6578	3.683
9.1	2.2443	2.2443	5.6040	11.2079	8.6385	3.845	12.6826	12.6826	7.2208	14.4416	8.3103	2.417	2.2443	2.2443	5.6040	11.2079	8.6385	3.845
9.2	9.6431	4.8216	5.5009	9.5009	8.6718	3.886	12.6826	12.6826	7.2208	14.4416	8.3103	2.417	9.6431	4.8216	5.5009	9.5009	8.6718	3.886
9.3	12.2776	6.1388	9.5014	9.5014	8.7194	3.847	12.6826	12.6826	7.2208	14.4416	8.3103	2.417	12.2776	6.1388	9.5014	9.5014	8.7194	3.847
9.4	0	0	9.5058	9.5058	8.7653	3.809	12.6826	12.6826	7.2208	14.4416	8.3103	2.417	0	0	9.5058	9.5058	8.7653	3.809
9.5	0	0	9.5117	9.5117	8.8094	3.773	12.6826	12.6826	7.2208	14.4416	8.3103	2.417	0	0	9.5117	9.5117	8.8094	3.773
9.6	0	0	9.5185	9.5185	8.8520	3.74	12.6826	12.6826	7.2208	14.4416	8.3103	2.417	0	0	9.5185	9.5185	8.8520	3.74
9.7	0	0	9.5271	9.5271	8.8930	3.708	12.6826	12.6826	7.2208	14.4416	8.3103	2.417	0	0	9.5271	9.5271	8.8930	3.708
9.8	0	0	9.5372	9.5372	8.9325	3.678	12.6826	12.6826	7.2208	14.4416	8.3103	2.417	0	0	9.5372	9.5372	8.9325	3.678
9.9	0	0	9.5466	9.5466	8.9706	3.65	12.6826	12.6826	7.2208	14.4416	8.3103	2.417	0	0	9.5466	9.5466	8.9706	3.65
10	0	0	9.5614	9.5614	9.0074	3.623	12.6826	12.6826	7.2208	14.4416	8.3103	2.417	0	0	9.5614	9.5614	9.0074	3.623

Table C.3 - Section 9.6.5 MADM Results

Parameter Value (m/s²)	Observer's Decision	TOPSIS				AHP				ANP			
		Lane 1	Lane 2	Lane 3	Decision	Lane 1	Lane 2	Lane 3	Decision	Lane 1	Lane 2	Lane 3	Decision
6.9	1	0.8799	0.1201	0.8799	1	0.2970	0.4060	0.2970	1	0.2679	0.4642	0.2679	1
7	1	0.9037	0.0963	0.9037	1	0.2856	0.4287	0.2856	1	0.2671	0.4657	0.2671	1
7.1	1	0.9184	0.0816	0.9184	1	0.2776	0.4447	0.2776	1	0.2666	0.4669	0.2666	1
7.2	1	0.9295	0.0705	0.9295	1	0.2709	0.4582	0.2709	1	0.2660	0.4680	0.2660	1
7.3	1	0.9118	0.0882	0.9118	1	0.2919	0.4162	0.2919	1	0.3087	0.3825	0.3087	1
7.4	1	0.9064	0.0936	0.9064	1	0.2977	0.4046	0.2977	1	0.3153	0.3694	0.3153	1
7.5	1	0.9058	0.0942	0.9058	1	0.3009	0.3981	0.3009	1	0.3182	0.3636	0.3182	1
7.6	1	0.9085	0.0915	0.9085	1	0.3030	0.3940	0.3030	1	0.3197	0.3607	0.3197	1
7.7	1	0.9130	0.0870	0.9130	1	0.3044	0.3911	0.3044	1	0.3204	0.3592	0.3204	1
7.8	1	0.9197	0.0803	0.9197	1	0.3045	0.3909	0.3045	1	0.3204	0.3591	0.3204	1
7.9	1	0.9290	0.0710	0.9290	1	0.3018	0.3964	0.3018	1	0.3198	0.3604	0.3198	1
8	1	0.9367	0.0633	0.9367	1	0.2992	0.4017	0.2992	1	0.3191	0.3618	0.3191	1
8.1	1	0.9433	0.0567	0.9433	1	0.2966	0.4068	0.2966	1	0.3184	0.3632	0.3184	1
8.2	1	0.9490	0.0510	0.9490	1	0.2941	0.4118	0.2941	1	0.3176	0.3648	0.3176	1
8.3	1	0.9539	0.0461	0.9539	1	0.2917	0.4166	0.2917	1	0.3168	0.3664	0.3168	1
8.4	1	0.9581	0.0419	0.9581	1	0.2893	0.4213	0.2893	1	0.3159	0.3681	0.3159	1
8.5	1	0.9619	0.0381	0.9619	1	0.2870	0.4260	0.2870	1	0.3150	0.3700	0.3150	1
8.6	1	0.9652	0.0348	0.9652	1	0.2847	0.4306	0.2847	1	0.3140	0.3720	0.3140	1
8.7	1	0.9682	0.0318	0.9682	1	0.2824	0.4353	0.2824	1	0.3128	0.3743	0.3128	1
8.8	1	0.9708	0.0292	0.9708	1	0.2800	0.4400	0.2800	1	0.3116	0.3769	0.3116	1
8.9	1	0.9732	0.0268	0.9732	1	0.2776	0.4448	0.2776	1	0.3101	0.3798	0.3101	1
9	1	0.9754	0.0246	0.9754	1	0.2751	0.4498	0.2751	1	0.3084	0.3832	0.3084	1
9.1	1	0.9774	0.0226	0.9774	1	0.2725	0.4550	0.2725	1	0.3064	0.3872	0.3064	1
9.2	1	0.8089	0.1911	0.8089	1	0.3065	0.3870	0.3065	1	0.3286	0.3427	0.3286	1
9.3	1	0.7797	0.2203	0.7797	1	0.3149	0.3702	0.3149	1	0.3320	0.3361	0.3320	1
9.4	1	0.8885	0.1115	0.8885	1	0.2645	0.4709	0.2645	1	0.2727	0.4546	0.2727	1
9.5	1	0.8878	0.1122	0.8878	1	0.2649	0.4703	0.2649	1	0.2727	0.4546	0.2727	1
9.6	1	0.8871	0.1129	0.8871	1	0.2652	0.4697	0.2652	1	0.2727	0.4547	0.2727	1
9.7	1	0.8863	0.1137	0.8863	1	0.2655	0.4691	0.2655	1	0.2726	0.4547	0.2726	1
9.8	1	0.8854	0.1146	0.8854	1	0.2658	0.4684	0.2658	1	0.2726	0.4548	0.2726	1
9.9	1	0.8845	0.1155	0.8845	1	0.2661	0.4679	0.2661	1	0.2726	0.4548	0.2726	1
10	1	0.8835	0.1165	0.8835	1	0.2664	0.4672	0.2664	1	0.2726	0.4549	0.2726	1

C - Section 9.6.7 Vehicles Ahead Mass

Table C.4 - Section 9.6.7 Simulation Results

Parameter Value (kg)	Lane 1							Lane 2							Lane 3						
	Impact Velocity VA (m/s)	Impact Velocity HV1 (m/s)	Impact Velocity HV2 (m/s)	Impact Velocity VB (m/s)	Manoeuvre Acceleration (m/s²)	TTC (s)	Lane Open	Impact Velocity VA (m/s)	Impact Velocity HV1 (m/s)	Impact Velocity HV2 (m/s)	Impact Velocity VB (m/s)	Manoeuvre Acceleration (m/s²)	TTC (s)	Lane Open	Impact Velocity VA (m/s)	Impact Velocity HV1 (m/s)	Impact Velocity HV2 (m/s)	Impact Velocity VB (m/s)	Manoeuvre Acceleration (m/s²)	TTC (s)	Lane Open
900	9.1192	13.1322	3.6921	12.6888	8.7765	3.08	1	0	11.4561	10.3582	21.4249	8.3103	2.417	1	9.9116	14.4195	3.6921	12.6888	8.7765	2.922	1
1000	9.1192	13.1322	3.6921	12.6888	8.7765	3.08	1	0	11.4561	10.3582	21.4249	8.3103	2.417	1	9.7856	14.2076	3.6921	12.6888	8.7765	2.948	1
1100	9.1192	13.1322	3.6921	12.6888	8.7765	3.08	1	0	11.4561	10.3582	21.4249	8.3103	2.417	1	9.6777	14.0283	3.6921	12.6888	8.7765	2.97	1
1200	9.1192	13.1322	3.6921	12.6888	8.7765	3.08	1	0	11.4561	10.3582	21.4249	8.3103	2.417	1	9.5752	13.8653	3.6921	12.6888	8.7765	2.99	1
1300	9.1192	13.1322	3.6921	12.6888	8.7765	3.08	1	0	11.4561	10.3582	21.4249	8.3103	2.417	1	9.4972	13.7350	3.6921	12.6888	8.7765	3.006	1
1400	9.1192	13.1322	3.6921	12.6888	8.7765	3.08	1	0	11.4561	10.3582	21.4249	8.3103	2.417	1	9.4276	13.6209	3.6921	12.6888	8.7765	3.02	1
1500	9.1192	13.1322	3.6921	12.6888	8.7765	3.08	1	0	11.4561	10.3582	21.4249	8.3103	2.417	1	9.3612	13.5150	3.6921	12.6888	8.7765	3.033	1
1600	9.1192	13.1322	3.6921	12.6888	8.7765	3.08	1	0	11.4561	10.3582	21.4249	8.3103	2.417	1	9.2988	13.4173	3.6921	12.6888	8.7765	3.045	1
1700	9.1192	13.1322	3.6921	12.6888	8.7765	3.08	1	0	11.4561	10.3582	21.4249	8.3103	2.417	1	9.2480	13.3358	3.6921	12.6888	8.7765	3.055	1
1800	9.1192	13.1322	3.6921	12.6888	8.7765	3.08	1	0	11.4561	10.3582	21.4249	8.3103	2.417	1	9.2021	13.2625	3.6921	12.6888	8.7765	3.064	1
1900	9.1192	13.1322	3.6921	12.6888	8.7765	3.08	1	0	11.4561	10.3582	21.4249	8.3103	2.417	1	9.1614	13.1974	3.6921	12.6888	8.7765	3.072	1
2000	9.1192	13.1322	3.6921	12.6888	8.7765	3.08	1	0	11.4561	10.3582	21.4249	8.3103	2.417	1	9.1192	13.1322	3.6921	12.6888	8.7765	3.08	1
2100	9.1192	13.1322	3.6921	12.6888	8.7765	3.08	1	0	11.4561	10.3582	21.4249	8.3103	2.417	1	9.0827	13.0752	3.6921	12.6888	8.7765	3.087	1
2200	9.1192	13.1322	3.6921	12.6888	8.7765	3.08	1	0	11.4561	10.3582	21.4249	8.3103	2.417	1	9.0521	13.0254	3.6921	12.6888	8.7765	3.093	1
2300	9.1192	13.1322	3.6921	12.6888	8.7765	3.08	1	0	11.4561	10.3582	21.4249	8.3103	2.417	1	9.0205	12.9775	3.6921	12.6888	8.7765	3.099	1
2400	9.1192	13.1322	3.6921	12.6888	8.7765	3.08	1	0	11.4561	10.3582	21.4249	8.3103	2.417	1	8.9951	12.9368	3.6921	12.6888	8.7765	3.104	1
2500	9.1192	13.1322	3.6921	12.6888	8.7765	3.08	1	0	11.4561	10.3582	21.4249	8.3103	2.417	1	8.9689	12.8951	3.6921	12.6888	8.7765	3.109	1
2600	9.1192	13.1322	3.6921	12.6888	8.7765	3.08	1	0	11.4561	10.3582	21.4249	8.3103	2.417	1	8.9420	12.8554	3.6921	12.6888	8.7765	3.114	1
2700	9.1192	13.1322	3.6921	12.6888	8.7765	3.08	1	0	11.4561	10.3582	21.4249	8.3103	2.417	1	8.9216	12.8228	3.6921	12.6888	8.7765	3.118	1
2800	9.1192	13.1322	3.6921	12.6888	8.7765	3.08	1	0	11.4561	10.3582	21.4249	8.3103	2.417	1	8.9006	12.7902	3.6921	12.6888	8.7765	3.122	1
2900	9.1192	13.1322	3.6921	12.6888	8.7765	3.08	1	0	11.4561	10.3582	21.4249	8.3103	2.417	1	8.8791	12.7577	3.6921	12.6888	8.7765	3.126	1
3000	9.1192	13.1322	3.6921	12.6888	8.7765	3.08	1	0	11.4561	10.3582	21.4249	8.3103	2.417	1	8.8643	12.7333	3.6921	12.6888	8.7765	3.129	1

Table C.5 - Section 9.6.7 Collision Modelling Results

Parameter Value (kg)	Lane 1						Lane 2						Lane 3					
	Collision Acceleration VA (g)	Collision Acceleration HV1 (g)	Collision Acceleration HV2 (g)	Collision Acceleration VB (g)	Manoeuvre Acceleration (m/s²)	TTC (s)	Collision Acceleration VA (g)	Collision Acceleration HV1 (g)	Collision Acceleration HV2 (g)	Collision Acceleration VB (g)	Manoeuvre Acceleration (m/s²)	TTC (s)	Collision Acceleration VA (g)	Collision Acceleration HV1 (g)	Collision Acceleration HV2 (g)	Collision Acceleration VB (g)	Manoeuvre Acceleration (m/s²)	TTC (s)
900	3.9738	3.9738	5.6564	11.3129	8.7765	3.08	12.5826	12.5826	7.2208	14.4416	8.3103	2.417	7.7629	3.4933	7.2839	10.5616	8.7765	2.922
1000	3.9738	3.9738	5.6564	11.3129	8.7765	3.08	12.5826	12.5826	7.2208	14.4416	8.3103	2.417	7.1089	3.5545	7.0967	10.6451	8.7765	2.948
1100	3.9738	3.9738	5.6564	11.3129	8.7765	3.08	12.5826	12.5826	7.2208	14.4416	8.3103	2.417	6.5653	3.6109	5.9193	10.7250	8.7765	2.97
1200	3.9738	3.9738	5.6564	11.3129	8.7765	3.08	12.5826	12.5826	7.2208	14.4416	8.3103	2.417	6.1037	3.6622	5.7509	10.8014	8.7765	2.99
1300	3.9738	3.9738	5.6564	11.3129	8.7765	3.08	12.5826	12.5826	7.2208	14.4416	8.3103	2.417	5.7095	3.7112	5.5907	10.8747	8.7765	3.006
1400	3.9738	3.9738	5.6564	11.3129	8.7765	3.08	12.5826	12.5826	7.2208	14.4416	8.3103	2.417	5.3659	3.7558	5.4382	10.9449	8.7765	3.02
1500	3.9738	3.9738	5.6564	11.3129	8.7765	3.08	12.5826	12.5826	7.2208	14.4416	8.3103	2.417	5.0651	3.7988	5.2928	11.0124	8.7765	3.033
1600	3.9738	3.9738	5.6564	11.3129	8.7765	3.08	12.5826	12.5826	7.2208	14.4416	8.3103	2.417	4.7971	3.8377	5.1540	11.0772	8.7765	3.045
1700	3.9738	3.9738	5.6564	11.3129	8.7765	3.08	12.5826	12.5826	7.2208	14.4416	8.3103	2.417	4.5588	3.8750	5.0214	11.1395	8.7765	3.055
1800	3.9738	3.9738	5.6564	11.3129	8.7765	3.08	12.5826	12.5826	7.2208	14.4416	8.3103	2.417	4.3445	3.9100	5.8945	11.1995	8.7765	3.064
1900	3.9738	3.9738	5.6564	11.3129	8.7765	3.08	12.5826	12.5826	7.2208	14.4416	8.3103	2.417	4.1508	3.9432	5.7729	11.2572	8.7765	3.072
2000	3.9738	3.9738	5.6564	11.3129	8.7765	3.08	12.5826	12.5826	7.2208	14.4416	8.3103	2.417	3.9738	3.9738	5.6554	11.3129	8.7765	3.08
2100	3.9738	3.9738	5.6564	11.3129	8.7765	3.08	12.5826	12.5826	7.2208	14.4416	8.3103	2.417	3.8124	4.0030	5.5447	11.3666	8.7765	3.087
2200	3.9738	3.9738	5.6564	11.3129	8.7765	3.08	12.5826	12.5826	7.2208	14.4416	8.3103	2.417	3.6647	4.0312	5.4373	11.4184	8.7765	3.093
2300	3.9738	3.9738	5.6564	11.3129	8.7765	3.08	12.5826	12.5826	7.2208	14.4416	8.3103	2.417	3.5281	4.0573	5.3341	11.4684	8.7765	3.099
2400	3.9738	3.9738	5.6564	11.3129	8.7765	3.08	12.5826	12.5826	7.2208	14.4416	8.3103	2.417	3.4023	4.0828	5.2349	11.5167	8.7765	3.104
2500	3.9738	3.9738	5.6564	11.3129	8.7765	3.08	12.5826	12.5826	7.2208	14.4416	8.3103	2.417	3.2853	4.1056	5.1393	11.5635	8.7765	3.109
2600	3.9738	3.9738	5.6564	11.3129	8.7765	3.08	12.5826	12.5826	7.2208	14.4416	8.3103	2.417	3.1750	4.1288	5.0473	11.6087	8.7765	3.114
2700	3.9738	3.9738	5.6564	11.3129	8.7765	3.08	12.5826	12.5826	7.2208	14.4416	8.3103	2.417	3.0747	4.1508	4.9585	11.6525	8.7765	3.118
2800	3.9738	3.9738	5.6564	11.3129	8.7765	3.08	12.5826	12.5826	7.2208	14.4416	8.3103	2.417	2.9796	4.1715	4.8729	11.6949	8.7765	3.122
2900	3.9738	3.9738	5.6564	11.3129	8.7765	3.08	12.5826	12.5826	7.2208	14.4416	8.3103	2.417	2.8903	4.1909	4.7902	11.7359	8.7765	3.126
3000	3.9738	3.9738	5.6564	11.3129	8.7765	3.08	12.5826	12.5826	7.2208	14.4416	8.3103	2.417	2.8070	4.2104	4.7103	11.7758	8.7765	3.129

Table C.6 - Section 9.6.7 MADM Results

Parameter Value (kg)	Observer's Decision	TOPSIS				AHP				ANP			
		Lane 1	Lane 2	Lane 3	Decision	Lane 1	Lane 2	Lane 3	Decision	Lane 1	Lane 2	Lane 3	Decision
900	1	0.9255	0.0378	0.7280	1	0.2802	0.4133	0.3065	1	0.3119	0.3636	0.3245	1
1000	1	0.9315	0.0375	0.7649	1	0.2813	0.4154	0.3034	1	0.3122	0.3643	0.3234	1
1100	1	0.9370	0.0375	0.7979	1	0.2822	0.4171	0.3007	1	0.3125	0.3651	0.3224	1
1200	1	0.9420	0.0376	0.8276	1	0.2830	0.4186	0.2984	1	0.3128	0.3657	0.3214	1
1300	1	0.9466	0.0376	0.8542	1	0.2837	0.4199	0.2964	1	0.3131	0.3664	0.3205	1
1400	1	0.9506	0.0377	0.8782	1	0.2843	0.4211	0.2946	1	0.3134	0.3670	0.3196	1
1500	1	0.9540	0.0378	0.8998	1	0.2849	0.4221	0.2930	1	0.3137	0.3676	0.3187	1
1600	1	0.9568	0.0378	0.9191	1	0.2854	0.4231	0.2915	1	0.3140	0.3681	0.3179	1
1700	1	0.9591	0.0379	0.9358	1	0.2859	0.4239	0.2903	1	0.3142	0.3686	0.3172	1
1800	1	0.9606	0.0380	0.9493	1	0.2863	0.4247	0.2891	1	0.3145	0.3691	0.3164	1
1900	1	0.9616	0.0381	0.9585	1	0.2866	0.4254	0.2880	1	0.3148	0.3695	0.3157	1
2000	1	0.9619	0.0381	0.9619	1	0.2870	0.4260	0.2870	1	0.3150	0.3700	0.3150	1
2100	3	0.9592	0.0378	0.9619	3	0.2873	0.4266	0.2861	3	0.3152	0.3704	0.3143	3
2200	3	0.9529	0.0374	0.9614	3	0.2876	0.4272	0.2852	3	0.3155	0.3708	0.3137	3
2300	3	0.9448	0.0371	0.9605	3	0.2879	0.4277	0.2844	3	0.3157	0.3712	0.3131	3
2400	3	0.9362	0.0368	0.9593	3	0.2882	0.4282	0.2837	3	0.3159	0.3716	0.3125	3
2500	3	0.9276	0.0366	0.9579	3	0.2884	0.4286	0.2830	3	0.3161	0.3719	0.3119	3
2600	3	0.9193	0.0363	0.9563	3	0.2886	0.4290	0.2823	3	0.3164	0.3723	0.3114	3
2700	3	0.9114	0.0361	0.9546	3	0.2888	0.4294	0.2817	3	0.3166	0.3726	0.3108	3
2800	3	0.9038	0.0359	0.9528	3	0.2890	0.4298	0.2811	3	0.3168	0.3729	0.3103	3
2900	3	0.8966	0.0357	0.9510	3	0.2892	0.4302	0.2806	3	0.3170	0.3732	0.3098	3
3000	3	0.8899	0.0355	0.9491	3	0.2894	0.4305	0.2801	3	0.3172	0.3735	0.3093	3

C - Section 9.6.8 Vehicles Behind Mass

Table C.7 - Section 9.6.8 Simulation Results

Parameter Value (kg)	Lane 1							Lane 2							Lane 3						
	Impact Velocity VA (m/s)	Impact Velocity HV1 (m/s)	Impact Velocity HV2 (m/s)	Impact Velocity VB (m/s)	Manoeuvre Acceleration (m/s²)	TTC (s)	Lane Open	Impact Velocity VA (m/s)	Impact Velocity HV1 (m/s)	Impact Velocity HV2 (m/s)	Impact Velocity VB (m/s)	Manoeuvre Acceleration (m/s²)	TTC (s)	Lane Open	Impact Velocity VA (m/s)	Impact Velocity HV1 (m/s)	Impact Velocity HV2 (m/s)	Impact Velocity VB (m/s)	Manoeuvre Acceleration (m/s²)	TTC (s)	Lane Open
900	9.1192	13.1322	3.6921	12.5888	8.7765	3.08	1	0	11.4561	10.3582	21.4249	8.3103	2.417	1	9.1192	13.1322	2.7513	11.6466	8.7765	3.08	1
1000	9.1192	13.1322	3.6921	12.5888	8.7765	3.08	1	0	11.4561	10.3582	21.4249	8.3103	2.417	1	9.1192	13.1322	2.9216	11.8347	8.7765	3.08	1
1100	9.1192	13.1322	3.6921	12.5888	8.7765	3.08	1	0	11.4561	10.3582	21.4249	8.3103	2.417	1	9.1192	13.1322	3.0676	11.9931	8.7765	3.08	1
1200	9.1192	13.1322	3.6921	12.5888	8.7765	3.08	1	0	11.4561	10.3582	21.4249	8.3103	2.417	1	9.1192	13.1322	3.1811	12.1202	8.7765	3.08	1
1300	9.1192	13.1322	3.6921	12.5888	8.7765	3.08	1	0	11.4561	10.3582	21.4249	8.3103	2.417	1	9.1192	13.1322	3.2784	12.2287	8.7765	3.08	1
1400	9.1192	13.1322	3.6921	12.5888	8.7765	3.08	1	0	11.4561	10.3582	21.4249	8.3103	2.417	1	9.1192	13.1322	3.3676	12.3254	8.7765	3.08	1
1500	9.1192	13.1322	3.6921	12.5888	8.7765	3.08	1	0	11.4561	10.3582	21.4249	8.3103	2.417	1	9.1192	13.1322	3.4406	12.4066	8.7765	3.08	1
1600	9.1192	13.1322	3.6921	12.5888	8.7765	3.08	1	0	11.4561	10.3582	21.4249	8.3103	2.417	1	9.1192	13.1322	3.4974	12.4732	8.7765	3.08	1
1700	9.1192	13.1322	3.6921	12.5888	8.7765	3.08	1	0	11.4561	10.3582	21.4249	8.3103	2.417	1	9.1192	13.1322	3.5542	12.5363	8.7765	3.08	1
1800	9.1192	13.1322	3.6921	12.5888	8.7765	3.08	1	0	11.4561	10.3582	21.4249	8.3103	2.417	1	9.1192	13.1322	3.6028	12.5912	8.7765	3.08	1
1900	9.1192	13.1322	3.6921	12.5888	8.7765	3.08	1	0	11.4561	10.3582	21.4249	8.3103	2.417	1	9.1192	13.1322	3.6515	12.6436	8.7765	3.08	1
2000	9.1192	13.1322	3.6921	12.5888	8.7765	3.08	1	0	11.4561	10.3582	21.4249	8.3103	2.417	1	9.1192	13.1322	3.6921	12.6888	8.7765	3.08	1
2100	9.1192	13.1322	3.6921	12.5888	8.7765	3.08	1	0	11.4561	10.3582	21.4249	8.3103	2.417	1	9.1192	13.1322	3.7245	12.7269	8.7765	3.08	1
2200	9.1192	13.1322	3.6921	12.5888	8.7765	3.08	1	0	11.4561	10.3582	21.4249	8.3103	2.417	1	9.1192	13.1322	3.7569	12.7635	8.7765	3.08	1
2300	9.1192	13.1322	3.6921	12.5888	8.7765	3.08	1	0	11.4561	10.3582	21.4249	8.3103	2.417	1	9.1192	13.1322	3.7894	12.7987	8.7765	3.08	1
2400	9.1192	13.1322	3.6921	12.5888	8.7765	3.08	1	0	11.4561	10.3582	21.4249	8.3103	2.417	1	9.1192	13.1322	3.8137	12.8276	8.7765	3.08	1
2500	9.1192	13.1322	3.6921	12.5888	8.7765	3.08	1	0	11.4561	10.3582	21.4249	8.3103	2.417	1	9.1192	13.1322	3.8381	12.8554	8.7765	3.08	1
2600	9.1192	13.1322	3.6921	12.5888	8.7765	3.08	1	0	11.4561	10.3582	21.4249	8.3103	2.417	1	9.1192	13.1322	3.8624	12.8823	8.7765	3.08	1
2700	9.1192	13.1322	3.6921	12.5888	8.7765	3.08	1	0	11.4561	10.3582	21.4249	8.3103	2.417	1	9.1192	13.1322	3.8867	12.9083	8.7765	3.08	1
2800	9.1192	13.1322	3.6921	12.5888	8.7765	3.08	1	0	11.4561	10.3582	21.4249	8.3103	2.417	1	9.1192	13.1322	3.9029	12.9284	8.7765	3.08	1
2900	9.1192	13.1322	3.6921	12.5888	8.7765	3.08	1	0	11.4561	10.3582	21.4249	8.3103	2.417	1	9.1192	13.1322	3.9273	12.9530	8.7765	3.08	1
3000	9.1192	13.1322	3.6921	12.5888	8.7765	3.08	1	0	11.4561	10.3582	21.4249	8.3103	2.417	1	9.1192	13.1322	3.9435	12.9718	8.7765	3.08	1

Table C.8 - Section 9.6.8 Collision Modelling Results

Parameter Value (kg)	Lane 1						Lane 2						Lane 3					
	Collision Acceleration VA (g)	Collision Acceleration HV1 (g)	Collision Acceleration HV2 (g)	Collision Acceleration VB (g)	Manoeuvre Acceleration (m/s²)	TTC (s)	Collision Acceleration VA (g)	Collision Acceleration HV1 (g)	Collision Acceleration HV2 (g)	Collision Acceleration VB (g)	Manoeuvre Acceleration (m/s²)	TTC (s)	Collision Acceleration VA (g)	Collision Acceleration HV1 (g)	Collision Acceleration HV2 (g)	Collision Acceleration VB (g)	Manoeuvre Acceleration (m/s²)	TTC (s)
900	3.9738	3.9738	5.6564	11.3129	8.7765	3.08	12.5826	12.6826	7.2208	14.4416	8.3103	2.417	3.9738	3.9738	3.9812	17.6941	8.7765	3.08
1000	3.9738	3.9738	5.6564	11.3129	8.7765	3.08	12.5826	12.6826	7.2208	14.4416	8.3103	2.417	3.9738	3.9738	4.1844	16.7376	8.7765	3.08
1100	3.9738	3.9738	5.6564	11.3129	8.7765	3.08	12.5826	12.6826	7.2208	14.4416	8.3103	2.417	3.9738	3.9738	4.3723	15.8994	8.7765	3.08
1200	3.9738	3.9738	5.6564	11.3129	8.7765	3.08	12.5826	12.6826	7.2208	14.4416	8.3103	2.417	3.9738	3.9738	4.5499	15.1663	8.7765	3.08
1300	3.9738	3.9738	5.6564	11.3129	8.7765	3.08	12.5826	12.6826	7.2208	14.4416	8.3103	2.417	3.9738	3.9738	4.7164	14.5118	8.7765	3.08
1400	3.9738	3.9738	5.6564	11.3129	8.7765	3.08	12.5826	12.6826	7.2208	14.4416	8.3103	2.417	3.9738	3.9738	4.8719	13.9196	8.7765	3.08
1500	3.9738	3.9738	5.6564	11.3129	8.7765	3.08	12.5826	12.6826	7.2208	14.4416	8.3103	2.417	3.9738	3.9738	5.0198	13.3862	8.7765	3.08
1600	3.9738	3.9738	5.6564	11.3129	8.7765	3.08	12.5826	12.6826	7.2208	14.4416	8.3103	2.417	3.9738	3.9738	5.1617	12.9043	8.7765	3.08
1700	3.9738	3.9738	5.6564	11.3129	8.7765	3.08	12.5826	12.6826	7.2208	14.4416	8.3103	2.417	3.9738	3.9738	5.2947	12.4581	8.7765	3.08
1800	3.9738	3.9738	5.6564	11.3129	8.7765	3.08	12.5826	12.6826	7.2208	14.4416	8.3103	2.417	3.9738	3.9738	5.4217	12.0482	8.7765	3.08
1900	3.9738	3.9738	5.6564	11.3129	8.7765	3.08	12.5826	12.6826	7.2208	14.4416	8.3103	2.417	3.9738	3.9738	5.5413	11.6660	8.7765	3.08
2000	3.9738	3.9738	5.6564	11.3129	8.7765	3.08	12.5826	12.6826	7.2208	14.4416	8.3103	2.417	3.9738	3.9738	5.5564	11.3129	8.7765	3.08
2100	3.9738	3.9738	5.6564	11.3129	8.7765	3.08	12.5826	12.6826	7.2208	14.4416	8.3103	2.417	3.9738	3.9738	5.7676	10.9860	8.7765	3.08
2200	3.9738	3.9738	5.6564	11.3129	8.7765	3.08	12.5826	12.6826	7.2208	14.4416	8.3103	2.417	3.9738	3.9738	5.8732	10.6786	8.7765	3.08
2300	3.9738	3.9738	5.6564	11.3129	8.7765	3.08	12.5826	12.6826	7.2208	14.4416	8.3103	2.417	3.9738	3.9738	5.9736	10.3889	8.7765	3.08
2400	3.9738	3.9738	5.6564	11.3129	8.7765	3.08	12.5826	12.6826	7.2208	14.4416	8.3103	2.417	3.9738	3.9738	6.0716	10.1193	8.7765	3.08
2500	3.9738	3.9738	5.6564	11.3129	8.7765	3.08	12.5826	12.6826	7.2208	14.4416	8.3103	2.417	3.9738	3.9738	6.1651	9.8641	8.7765	3.08
2600	3.9738	3.9738	5.6564	11.3129	8.7765	3.08	12.5826	12.6826	7.2208	14.4416	8.3103	2.417	3.9738	3.9738	6.2544	9.6222	8.7765	3.08
2700	3.9738	3.9738	5.6564	11.3129	8.7765	3.08	12.5826	12.6826	7.2208	14.4416	8.3103	2.417	3.9738	3.9738	6.3399	9.3924	8.7765	3.08
2800	3.9738	3.9738	5.6564	11.3129	8.7765	3.08	12.5826	12.6826	7.2208	14.4416	8.3103	2.417	3.9738	3.9738	6.4242	9.1774	8.7765	3.08
2900	3.9738	3.9738	5.6564	11.3129	8.7765	3.08	12.5826	12.6826	7.2208	14.4416	8.3103	2.417	3.9738	3.9738	6.5026	8.9691	8.7765	3.08
3000	3.9738	3.9738	5.6564	11.3129	8.7765	3.08	12.5826	12.6826	7.2208	14.4416	8.3103	2.417	3.9738	3.9738	6.5799	8.7733	8.7765	3.08

Table C.9 - Section 9.6.8 MADM Results

Parameter Value (kg)	Observer's Decision	TOPSIS				AHP				ANP			
		Lane 1	Lane 2	Lane 3	Decision	Lane 1	Lane 2	Lane 3	Decision	Lane 1	Lane 2	Lane 3	Decision
900	1	0.8879	0.2008	0.6656	1	0.2798	0.4124	0.3078	1	0.3160	0.3728	0.3112	3
1000	1	0.8963	0.1528	0.6996	1	0.2809	0.4145	0.3046	1	0.3158	0.3723	0.3119	3
1100	1	0.9049	0.1065	0.7326	1	0.2819	0.4163	0.3018	1	0.3156	0.3719	0.3124	3
1200	1	0.9138	0.0647	0.7643	1	0.2827	0.4179	0.2994	1	0.3155	0.3716	0.3129	3
1300	1	0.9225	0.0394	0.7951	1	0.2834	0.4193	0.2973	1	0.3154	0.3713	0.3134	3
1400	1	0.9315	0.0389	0.8253	1	0.2841	0.4206	0.2953	1	0.3153	0.3710	0.3137	3
1500	1	0.9397	0.0387	0.8546	1	0.2847	0.4217	0.2936	1	0.3152	0.3708	0.3140	3
1600	1	0.9471	0.0386	0.8827	1	0.2852	0.4227	0.2920	1	0.3151	0.3706	0.3143	3
1700	1	0.9532	0.0384	0.9096	1	0.2857	0.4237	0.2906	1	0.3151	0.3704	0.3145	3
1800	1	0.9579	0.0383	0.9340	1	0.2862	0.4245	0.2893	1	0.3151	0.3702	0.3147	3
1900	1	0.9608	0.0382	0.9536	1	0.2866	0.4253	0.2881	1	0.3150	0.3701	0.3149	3
2000	1	0.9619	0.0381	0.9619	1	0.2870	0.4260	0.2870	1	0.3150	0.3700	0.3150	3
2100	3	0.9551	0.0378	0.9613	3	0.2873	0.4267	0.2860	3	0.3150	0.3699	0.3151	1
2200	3	0.9405	0.0374	0.9593	3	0.2877	0.4273	0.2850	3	0.3150	0.3698	0.3152	1
2300	3	0.9241	0.0371	0.9563	3	0.2880	0.4279	0.2842	3	0.3150	0.3697	0.3153	1
2400	3	0.9082	0.0368	0.9526	3	0.2883	0.4284	0.2833	3	0.3150	0.3696	0.3154	1
2500	3	0.8931	0.0365	0.9486	3	0.2885	0.4289	0.2826	3	0.3150	0.3696	0.3155	1
2600	3	0.8790	0.0362	0.9445	3	0.2888	0.4294	0.2819	3	0.3150	0.3695	0.3155	1
2700	3	0.8659	0.0359	0.9404	3	0.2890	0.4298	0.2812	3	0.3150	0.3695	0.3155	1
2800	3	0.8539	0.0356	0.9362	3	0.2892	0.4302	0.2805	3	0.3150	0.3694	0.3156	1
2900	3	0.8425	0.0354	0.9322	3	0.2894	0.4306	0.2799	3	0.3150	0.3694	0.3156	1
3000	3	0.8320	0.0351	0.9283	3	0.2896	0.4310	0.2794	3	0.3151	0.3694	0.3156	1

C - Section 9.6.9 Vehicles Ahead Initial Velocity

Table C.10 - Section 9.6.9 Simulation Results

Parameter Value (mph)	Lane 1							Lane 2							Lane 3						
	Impact Velocity VA (m/s)	Impact Velocity HV1 (m/s)	Impact Velocity HV2 (m/s)	Impact Velocity VB (m/s)	Manoeuvre Acceleration (m/s²)	TTC (s)	Lane Open	Impact Velocity VA (m/s)	Impact Velocity HV1 (m/s)	Impact Velocity HV2 (m/s)	Impact Velocity VB (m/s)	Manoeuvre Acceleration (m/s²)	TTC (s)	Lane Open	Impact Velocity VA (m/s)	Impact Velocity HV1 (m/s)	Impact Velocity HV2 (m/s)	Impact Velocity VB (m/s)	Manoeuvre Acceleration (m/s²)	TTC (s)	Lane Open
64	9.1192	13.1322	3.6921	12.6888	8.7765	3.08	1	0	11.4561	10.3582	21.4249	8.3103	2.417	1	14.5596	22.0986	3.6921	12.6888	8.7765	1.95	0
64.5	9.1192	13.1322	3.6921	12.6888	8.7765	3.08	1	0	11.4561	10.3582	21.4249	8.3103	2.417	1	14.3573	21.8204	3.6921	12.6888	8.7765	2.009	0
65	9.1192	13.1322	3.6921	12.6888	8.7765	3.08	1	0	11.4561	10.3582	21.4249	8.3103	2.417	1	14.1406	21.3846	3.6921	12.6888	8.7765	2.07	1
65.5	9.1192	13.1322	3.6921	12.6888	8.7765	3.08	1	0	11.4561	10.3582	21.4249	8.3103	2.417	1	13.8953	20.8516	3.6921	12.6888	8.7765	2.135	1
66	9.1192	13.1322	3.6921	12.6888	8.7765	3.08	1	0	11.4561	10.3582	21.4249	8.3103	2.417	1	13.6071	20.2697	3.6921	12.6888	8.7765	2.206	1
66.5	9.1192	13.1322	3.6921	12.6888	8.7765	3.08	1	0	11.4561	10.3582	21.4249	8.3103	2.417	1	13.2832	19.6472	3.6921	12.6888	8.7765	2.282	1
67	9.1192	13.1322	3.6921	12.6888	8.7765	3.08	1	0	11.4561	10.3582	21.4249	8.3103	2.417	1	12.9093	18.9679	3.6921	12.6888	8.7765	2.365	1
67.5	9.1192	13.1322	3.6921	12.6888	8.7765	3.08	1	0	11.4561	10.3582	21.4249	8.3103	2.417	1	12.4854	18.2317	3.6921	12.6888	8.7765	2.455	1
68	9.1192	13.1322	3.6921	12.6888	8.7765	3.08	1	0	11.4561	10.3582	21.4249	8.3103	2.417	1	11.9973	17.4226	3.6921	12.6888	8.7765	2.554	1
68.5	9.1192	13.1322	3.6921	12.6888	8.7765	3.08	1	0	11.4561	10.3582	21.4249	8.3103	2.417	1	11.4379	16.5323	3.6921	12.6888	8.7765	2.663	1
69	9.1192	13.1322	3.6921	12.6888	8.7765	3.08	1	0	11.4561	10.3582	21.4249	8.3103	2.417	1	10.7860	15.5366	3.6921	12.6888	8.7765	2.785	1
69.5	9.1192	13.1322	3.6921	12.6888	8.7765	3.08	1	0	11.4561	10.3582	21.4249	8.3103	2.417	1	10.0201	14.4113	3.6921	12.6888	8.7765	2.923	1
70	9.1192	13.1322	3.6921	12.6888	8.7765	3.08	1	0	11.4561	10.3582	21.4249	8.3103	2.417	1	9.1192	13.1322	3.6921	12.6888	8.7765	3.08	1
70.5	9.1192	13.1322	3.6921	12.6888	8.7765	3.08	1	0	11.4561	10.3582	21.4249	8.3103	2.417	1	8.0334	11.6427	3.6921	12.6888	8.7765	3.263	1
71	9.1192	13.1322	3.6921	12.6888	8.7765	3.08	1	0	11.4561	10.3582	21.4249	8.3103	2.417	1	6.5918	9.8618	3.6921	12.6888	8.7765	3.482	1
71.5	9.1192	13.1322	3.6921	12.6888	8.7765	3.08	1	0	11.4561	10.3582	21.4249	8.3103	2.417	1	4.9810	7.6602	3.6921	12.6888	8.7765	3.753	1
72	9.1192	13.1322	3.6921	12.6888	8.7765	3.08	1	0	11.4561	10.3582	21.4249	8.3103	2.417	1	2.5310	4.7303	3.6921	12.6888	8.7765	4.114	1
72.5	9.1192	13.1322	3.6921	12.6888	8.7765	3.08	1	0	11.4561	10.3582	21.4249	8.3103	2.417	1	0	0	3.6921	12.6888	8.7765	4.248	1
73	9.1192	13.1322	3.6921	12.6888	8.7765	3.08	1	0	11.4561	10.3582	21.4249	8.3103	2.417	1	0	0	3.6921	12.6888	8.7765	4.248	1
73.5	9.1192	13.1322	3.6921	12.6888	8.7765	3.08	1	0	11.4561	10.3582	21.4249	8.3103	2.417	1	0	0	3.6921	12.6888	8.7765	4.248	1
74	9.1192	13.1322	3.6921	12.6888	8.7765	3.08	1	0	11.4561	10.3582	21.4249	8.3103	2.417	1	0	0	3.6921	12.6888	8.7765	4.248	1
74.5	9.1192	13.1322	3.6921	12.6888	8.7765	3.08	1	0	11.4561	10.3582	21.4249	8.3103	2.417	1	0	0	3.6921	12.6888	8.7765	4.248	1

Table C.11 - Section 9.6.9 Collision Modelling Results

Parameter Value (mph)	Lane 1						Lane 2						Lane 3					
	Collision Acceleration VA (g)	Collision Acceleration HV1 (g)	Collision Acceleration HV2 (g)	Collision Acceleration VB (g)	Manoeuvre Acceleration (m/s²)	TTC (s)	Collision Acceleration VA (g)	Collision Acceleration HV1 (g)	Collision Acceleration HV2 (g)	Collision Acceleration VB (g)	Manoeuvre Acceleration (m/s²)	TTC (s)	Collision Acceleration VA (g)	Collision Acceleration HV1 (g)	Collision Acceleration HV2 (g)	Collision Acceleration VB (g)	Manoeuvre Acceleration (m/s²)	TTC (s)
64	3.9738	3.9738	5.6564	11.3129	8.7765	3.08	12.6826	12.6825	7.2208	14.4416	8.3103	2.417	7.8629	7.8529	5.6564	11.3129	8.7765	1.95
64.5	3.9738	3.9738	5.6564	11.3129	8.7765	3.08	12.6826	12.6825	7.2208	14.4416	8.3103	2.417	7.7750	7.7250	5.6564	11.3129	8.7765	2.009
65	3.9738	3.9738	5.6564	11.3129	8.7765	3.08	12.6826	12.6825	7.2208	14.4416	8.3103	2.417	7.5220	7.5220	5.6564	11.3129	8.7765	2.07
65.5	3.9738	3.9738	5.6564	11.3129	8.7765	3.08	12.6826	12.6825	7.2208	14.4416	8.3103	2.417	7.1923	7.1923	5.6564	11.3129	8.7765	2.135
66	3.9738	3.9738	5.6564	11.3129	8.7765	3.08	12.6826	12.6825	7.2208	14.4416	8.3103	2.417	6.8587	6.8587	5.6564	11.3129	8.7765	2.206
66.5	3.9738	3.9738	5.6564	11.3129	8.7765	3.08	12.6826	12.6825	7.2208	14.4416	8.3103	2.417	6.5225	6.5225	5.6564	11.3129	8.7765	2.282
67	3.9738	3.9738	5.6564	11.3129	8.7765	3.08	12.6826	12.6825	7.2208	14.4416	8.3103	2.417	6.1815	6.1815	5.6564	11.3129	8.7765	2.365
67.5	3.9738	3.9738	5.6564	11.3129	8.7765	3.08	12.6826	12.6825	7.2208	14.4416	8.3103	2.417	5.8360	5.8360	5.6564	11.3129	8.7765	2.455
68	3.9738	3.9738	5.6564	11.3129	8.7765	3.08	12.6826	12.6825	7.2208	14.4416	8.3103	2.417	5.4839	5.4839	5.6564	11.3129	8.7765	2.554
68.5	3.9738	3.9738	5.6564	11.3129	8.7765	3.08	12.6826	12.6825	7.2208	14.4416	8.3103	2.417	5.1245	5.1245	5.6564	11.3129	8.7765	2.663
69	3.9738	3.9738	5.6564	11.3129	8.7765	3.08	12.6826	12.6825	7.2208	14.4416	8.3103	2.417	4.7549	4.7549	5.6564	11.3129	8.7765	2.785
69.5	3.9738	3.9738	5.6564	11.3129	8.7765	3.08	12.6826	12.6825	7.2208	14.4416	8.3103	2.417	4.3722	4.3722	5.6564	11.3129	8.7765	2.923
70	3.9738	3.9738	5.6564	11.3129	8.7765	3.08	12.6826	12.6825	7.2208	14.4416	8.3103	2.417	3.9738	3.9738	5.6564	11.3129	8.7765	3.08
70.5	3.9738	3.9738	5.6564	11.3129	8.7765	3.08	12.6826	12.6825	7.2208	14.4416	8.3103	2.417	3.5531	3.5531	5.6564	11.3129	8.7765	3.263
71	3.9738	3.9738	5.6564	11.3129	8.7765	3.08	12.6826	12.6825	7.2208	14.4416	8.3103	2.417	3.1010	3.1010	5.6564	11.3129	8.7765	3.482
71.5	3.9738	3.9738	5.6564	11.3129	8.7765	3.08	12.6826	12.6825	7.2208	14.4416	8.3103	2.417	2.6025	2.6025	5.6564	11.3129	8.7765	3.753
72	3.9738	3.9738	5.6564	11.3129	8.7765	3.08	12.6826	12.6825	7.2208	14.4416	8.3103	2.417	2.0224	2.0224	5.6564	11.3129	8.7765	4.114
72.5	3.9738	3.9738	5.6564	11.3129	8.7765	3.08	12.6826	12.6825	7.2208	14.4416	8.3103	2.417	0	0	5.6564	9.5915	8.7765	4.248
73	3.9738	3.9738	5.6564	11.3129	8.7765	3.08	12.6826	12.6825	7.2208	14.4416	8.3103	2.417	0	0	5.6564	9.5915	8.7765	4.248
73.5	3.9738	3.9738	5.6564	11.3129	8.7765	3.08	12.6826	12.6825	7.2208	14.4416	8.3103	2.417	0	0	5.6564	9.5915	8.7765	4.248
74	3.9738	3.9738	5.6564	11.3129	8.7765	3.08	12.6826	12.6825	7.2208	14.4416	8.3103	2.417	0	0	5.6564	9.5915	8.7765	4.248
74.5	3.9738	3.9738	5.6564	11.3129	8.7765	3.08	12.6826	12.6825	7.2208	14.4416	8.3103	2.417	0	0	5.6564	9.5915	8.7765	4.248

Table C.12 - Section 9.6.9 MADM Results

Parameter Value (mph)	Observer's Decision	TOPSIS				AHP				ANP			
		Lane 1	Lane 2	Lane 3	Decision	Lane 1	Lane 2	Lane 3	Decision	Lane 1	Lane 2	Lane 3	Decision
64	1	0.9657	0.0343	NaN	1	0.4049	0.5951	NaN	1	0.4611	0.5389	NaN	1
64.5	1	0.9657	0.0343	NaN	1	0.4048	0.5952	NaN	1	0.4611	0.5389	NaN	1
65	1	0.9604	0.0460	0.6120	1	0.2733	0.4021	0.3246	1	0.3148	0.3627	0.3224	1
65.5	1	0.9606	0.0437	0.6462	1	0.2745	0.4041	0.3214	1	0.3148	0.3632	0.3220	1
66	1	0.9607	0.0417	0.6812	1	0.2757	0.4063	0.3180	1	0.3148	0.3637	0.3215	1
66.5	1	0.9609	0.0401	0.7167	1	0.2769	0.4084	0.3146	1	0.3148	0.3642	0.3210	1
67	1	0.9610	0.0391	0.7530	1	0.2782	0.4107	0.3111	1	0.3148	0.3648	0.3205	1
67.5	1	0.9612	0.0388	0.7899	1	0.2795	0.4130	0.3075	1	0.3148	0.3654	0.3198	1
68	1	0.9613	0.0387	0.8276	1	0.2809	0.4154	0.3038	1	0.3148	0.3661	0.3191	1
68.5	1	0.9615	0.0385	0.8659	1	0.2823	0.4178	0.2999	1	0.3148	0.3669	0.3183	1
69	1	0.9616	0.0384	0.9044	1	0.2838	0.4204	0.2958	1	0.3148	0.3678	0.3174	1
69.5	1	0.9617	0.0383	0.9409	1	0.2853	0.4231	0.2915	1	0.3149	0.3688	0.3163	1
70	1	0.9619	0.0381	0.9619	1	0.2870	0.4260	0.2870	1	0.3150	0.3700	0.3150	1
70.5	3	0.9417	0.0364	0.9636	3	0.2888	0.4291	0.2821	3	0.3152	0.3714	0.3134	3
71	3	0.9036	0.0348	0.9652	3	0.2907	0.4325	0.2768	3	0.3154	0.3732	0.3114	3
71.5	3	0.8614	0.0331	0.9669	3	0.2929	0.4363	0.2708	3	0.3158	0.3754	0.3088	3
72	3	0.8158	0.0313	0.9687	3	0.2955	0.4408	0.2637	3	0.3164	0.3786	0.3050	3
72.5	3	0.6910	0.1148	0.8244	3	0.2989	0.4473	0.2538	3	0.3195	0.3951	0.2854	3
73	3	0.6910	0.1148	0.8244	3	0.2989	0.4473	0.2538	3	0.3195	0.3951	0.2854	3
73.5	3	0.6910	0.1148	0.8244	3	0.2989	0.4473	0.2538	3	0.3195	0.3951	0.2854	3
74	3	0.6910	0.1148	0.8244	3	0.2989	0.4473	0.2538	3	0.3195	0.3951	0.2854	3
74.5	3	0.6910	0.1148	0.8244	3	0.2989	0.4473	0.2538	3	0.3195	0.3951	0.2854	3

C - Section 9.6.10 Vehicles Behind Initial Velocity

Table C.13 - Section 9.6.10 Simulation Results

Parameter Value (mph)	Lane 1							Lane 2							Lane 3						
	Impact Velocity VA (m/s)	Impact Velocity HV1 (m/s)	Impact Velocity HV2 (m/s)	Impact Velocity VB (m/s)	Manoeuvre Acceleration (m/s²)	TTC (s)	Lane Open	Impact Velocity VA (m/s)	Impact Velocity HV1 (m/s)	Impact Velocity HV2 (m/s)	Impact Velocity VB (m/s)	Manoeuvre Acceleration (m/s²)	TTC (s)	Lane Open	Impact Velocity VA (m/s)	Impact Velocity HV1 (m/s)	Impact Velocity HV2 (m/s)	Impact Velocity VB (m/s)	Manoeuvre Acceleration (m/s²)	TTC (s)	Lane Open
64	9.1192	13.1322	3.6921	12.6888	8.7765	3.08	1	0	11.4561	10.3582	21.4249	8.3103	2.417	1	9.1192	13.1322	0	0	8.7765	3.08	1
65	9.1192	13.1322	3.6921	12.6888	8.7765	3.08	1	0	11.4561	10.3582	21.4249	8.3103	2.417	1	9.1192	13.1322	0	2.5375	8.7765	3.08	1
66	9.1192	13.1322	3.6921	12.6888	8.7765	3.08	1	0	11.4561	10.3582	21.4249	8.3103	2.417	1	9.1192	13.1322	0	5.8989	8.7765	3.08	1
67	9.1192	13.1322	3.6921	12.6888	8.7765	3.08	1	0	11.4561	10.3582	21.4249	8.3103	2.417	1	9.1192	13.1322	0	7.9742	8.7765	3.08	1
68	9.1192	13.1322	3.6921	12.6888	8.7765	3.08	1	0	11.4561	10.3582	21.4249	8.3103	2.417	1	9.1192	13.1322	0.2377	9.6355	8.7765	3.08	1
69	9.1192	13.1322	3.6921	12.6888	8.7765	3.08	1	0	11.4561	10.3582	21.4249	8.3103	2.417	1	9.1192	13.1322	1.9809	11.1721	8.7765	3.08	1
70	9.1192	13.1322	3.6921	12.6888	8.7765	3.08	1	0	11.4561	10.3582	21.4249	8.3103	2.417	1	9.1192	13.1322	3.6921	12.5888	8.7765	3.08	1
71	9.1192	13.1322	3.6921	12.6888	8.7765	3.08	1	0	11.4561	10.3582	21.4249	8.3103	2.417	1	9.1192	13.1322	5.3469	14.1713	8.7765	3.08	1
72	9.1192	13.1322	3.6921	12.6888	8.7765	3.08	1	0	11.4561	10.3582	21.4249	8.3103	2.417	1	9.1192	13.1322	6.9520	15.5501	8.7765	3.08	1
73	9.1192	13.1322	3.6921	12.6888	8.7765	3.08	1	0	11.4561	10.3582	21.4249	8.3103	2.417	1	9.1192	13.1322	8.5211	17.0548	8.7765	3.08	1
74	9.1192	13.1322	3.6921	12.6888	8.7765	3.08	1	0	11.4561	10.3582	21.4249	8.3103	2.417	1	9.1192	13.1322	10.0244	18.4457	8.7765	3.08	1
75	9.1192	13.1322	3.6921	12.6888	8.7765	3.08	1	0	11.4561	10.3582	21.4249	8.3103	2.417	1	9.1192	13.1322	11.4637	19.7973	8.7765	3.08	1
76	9.1192	13.1322	3.6921	12.6888	8.7765	3.08	1	0	11.4561	10.3582	21.4249	8.3103	2.417	1	9.1192	13.1322	12.8554	21.1201	8.7765	3.08	1
77	9.1192	13.1322	3.6921	12.6888	8.7765	3.08	1	0	11.4561	10.3582	21.4249	8.3103	2.417	1	9.1192	13.1322	14.1750	22.3685	8.7765	2.98	1
78	9.1192	13.1322	3.6921	12.6888	8.7765	3.08	1	0	11.4561	10.3582	21.4249	8.3103	2.417	1	9.1192	13.1322	15.4387	23.5427	8.7765	2.85	1
79	9.1192	13.1322	3.6921	12.6888	8.7765	3.08	1	0	11.4561	10.3582	21.4249	8.3103	2.417	1	9.1192	13.1322	16.6384	24.8474	8.7765	2.708	1
80	9.1192	13.1322	3.6921	12.6888	8.7765	3.08	1	0	11.4561	10.3582	21.4249	8.3103	2.417	1	9.1192	13.1322	17.7739	25.0124	8.7765	2.574	1
81	9.1192	13.1322	3.6921	12.6888	8.7765	3.08	1	0	11.4561	10.3582	21.4249	8.3103	2.417	1	9.1192	13.1322	18.8452	27.1376	8.7765	2.446	1
82	9.1192	13.1322	3.6921	12.6888	8.7765	3.08	1	0	11.4561	10.3582	21.4249	8.3103	2.417	1	9.1192	13.1322	19.8520	28.2227	8.7765	2.326	1
83	9.1192	13.1322	3.6921	12.6888	8.7765	3.08	1	0	11.4561	10.3582	21.4249	8.3103	2.417	1	9.1192	13.1322	20.8024	29.2730	8.7765	2.213	1
84	9.1192	13.1322	3.6921	12.6888	8.7765	3.08	1	0	11.4561	10.3582	21.4249	8.3103	2.417	1	9.1192	13.1322	21.6963	30.2881	8.7765	2.107	1
85	9.1192	13.1322	3.6921	12.6888	8.7765	3.08	1	0	11.4561	10.3582	21.4249	8.3103	2.417	1	9.1192	13.1322	22.1834	31.2573	8.7765	2.008	0

Table C.14 - Section 9.6.10 Collision Modelling Results

Parameter Value (mph)	Lane 1						Lane 2						Lane 3					
	Collision Acceleration VA (g)	Collision Acceleration HV1 (g)	Collision Acceleration HV2 (g)	Collision Acceleration VB (g)	Manoeuvre Acceleration (m/s²)	TTC (s)	Collision Acceleration VA (g)	Collision Acceleration HV1 (g)	Collision Acceleration HV2 (g)	Collision Acceleration VB (g)	Manoeuvre Acceleration (m/s²)	TTC (s)	Collision Acceleration VA (g)	Collision Acceleration HV1 (g)	Collision Acceleration HV2 (g)	Collision Acceleration VB (g)	Manoeuvre Acceleration (m/s²)	TTC (s)
64	3.9738	3.9738	5.6564	11.3129	8.7765	3.08	12.5826	12.6826	7.2208	14.4415	8.3103	2.417	3.9738	3.9738	0	0	8.7765	3.08
65	3.9738	3.9738	5.6564	11.3129	8.7765	3.08	12.5826	12.6826	7.2208	14.4415	8.3103	2.417	3.9738	3.9738	1.4282	2.8564	8.7765	3.08
66	3.9738	3.9738	5.6564	11.3129	8.7765	3.08	12.5826	12.6826	7.2208	14.4415	8.3103	2.417	3.9738	3.9738	3.5137	7.0275	8.7765	3.08
67	3.9738	3.9738	5.6564	11.3129	8.7765	3.08	12.5826	12.6826	7.2208	14.4415	8.3103	2.417	3.9738	3.9738	4.9240	9.8480	8.7765	3.08
68	3.9738	3.9738	5.6564	11.3129	8.7765	3.08	12.5826	12.6826	7.2208	14.4415	8.3103	2.417	3.9738	3.9738	5.9516	11.9032	8.7765	3.08
69	3.9738	3.9738	5.6564	11.3129	8.7765	3.08	12.5826	12.6826	7.2208	14.4415	8.3103	2.417	3.9738	3.9738	5.7987	11.5973	8.7765	3.08
70	3.9738	3.9738	5.6564	11.3129	8.7765	3.08	12.5826	12.6826	7.2208	14.4415	8.3103	2.417	3.9738	3.9738	5.6564	11.3129	8.7765	3.08
71	3.9738	3.9738	5.6564	11.3129	8.7765	3.08	12.5826	12.6826	7.2208	14.4415	8.3103	2.417	3.9738	3.9738	5.5312	11.0623	8.7765	3.08
72	3.9738	3.9738	5.6564	11.3129	8.7765	3.08	12.5826	12.6826	7.2208	14.4415	8.3103	2.417	3.9738	3.9738	5.4182	10.8365	8.7765	3.08
73	3.9738	3.9738	5.6564	11.3129	8.7765	3.08	12.5826	12.6826	7.2208	14.4415	8.3103	2.417	3.9738	3.9738	5.3216	10.6433	8.7765	3.08
74	3.9738	3.9738	5.6564	11.3129	8.7765	3.08	12.5826	12.6826	7.2208	14.4415	8.3103	2.417	3.9738	3.9738	5.2411	10.4822	8.7765	3.08
75	3.9738	3.9738	5.6564	11.3129	8.7765	3.08	12.5826	12.6826	7.2208	14.4415	8.3103	2.417	3.9738	3.9738	5.1285	10.3571	8.7765	3.08
76	3.9738	3.9738	5.6564	11.3129	8.7765	3.08	12.5826	12.6826	7.2208	14.4415	8.3103	2.417	3.9738	3.9738	5.1295	10.2591	8.7765	3.08
77	3.9738	3.9738	5.6564	11.3129	8.7765	3.08	12.5826	12.6826	7.2208	14.4415	8.3103	2.417	11.5613	5.7806	8.6554	8.6654	8.7765	2.98
78	3.9738	3.9738	5.6564	11.3129	8.7765	3.08	12.5826	12.6826	7.2208	14.4415	8.3103	2.417	13.4420	6.7210	8.6422	8.6422	8.7765	2.85
79	3.9738	3.9738	5.6564	11.3129	8.7765	3.08	12.5826	12.6826	7.2208	14.4415	8.3103	2.417	15.3235	7.6618	8.6481	8.6481	8.7765	2.708
80	3.9738	3.9738	5.6564	11.3129	8.7765	3.08	12.5826	12.6826	7.2208	14.4415	8.3103	2.417	17.1965	8.5982	8.6831	8.6831	8.7765	2.574
81	3.9738	3.9738	5.6564	11.3129	8.7765	3.08	12.5826	12.6826	7.2208	14.4415	8.3103	2.417	19.0608	9.5304	8.7471	8.7471	8.7765	2.446
82	3.9738	3.9738	5.6564	11.3129	8.7765	3.08	12.5826	12.6826	7.2208	14.4415	8.3103	2.417	20.8958	10.4479	8.8402	8.8402	8.7765	2.326
83	3.9738	3.9738	5.6564	11.3129	8.7765	3.08	12.5826	12.6826	7.2208	14.4415	8.3103	2.417	22.7324	11.3662	8.9590	8.9590	8.7765	2.213
84	3.9738	3.9738	5.6564	11.3129	8.7765	3.08	12.5826	12.6826	7.2208	14.4415	8.3103	2.417	24.5429	12.2714	9.1038	9.1038	8.7765	2.107
85	3.9738	3.9738	5.6564	11.3129	8.7765	3.08	12.5826	12.6826	7.2208	14.4415	8.3103	2.417	25.9666	12.9833	9.6851	9.6851	8.7765	2.008

Table C.15 - Section 9.6.10 MADM Results

Parameter Value (mph)	Observer's Decision	TOPSIS				AHP				ANP			
		Lane 1	Lane 2	Lane 3	Decision	Lane 1	Lane 2	Lane 3	Decision	Lane 1	Lane 2	Lane 3	Decision
64	3	0.5031	0.0223	0.9777	3	0.3201	0.4885	0.1914	3	0.3453	0.3898	0.2649	3
65	3	0.5751	0.0255	0.9745	3	0.3105	0.4703	0.2192	3	0.3326	0.3805	0.2869	3
66	3	0.7268	0.0314	0.9686	3	0.2981	0.4469	0.2550	3	0.3218	0.3735	0.3047	3
67	3	0.8822	0.0359	0.9641	3	0.2906	0.4328	0.2765	3	0.3170	0.3710	0.3120	3
68	1	0.9615	0.0385	0.9380	1	0.2856	0.4233	0.2911	1	0.3143	0.3697	0.3161	1
69	1	0.9617	0.0383	0.9549	1	0.2863	0.4247	0.2890	1	0.3146	0.3698	0.3155	1
70	1	0.9619	0.0381	0.9619	1	0.2870	0.4260	0.2870	1	0.3150	0.3700	0.3150	1
71	3	0.9568	0.0378	0.9622	3	0.2876	0.4272	0.2852	3	0.3153	0.3701	0.3145	3
72	3	0.9458	0.0374	0.9626	3	0.2882	0.4282	0.2836	3	0.3156	0.3703	0.3141	3
73	3	0.9342	0.0372	0.9628	3	0.2886	0.4291	0.2823	3	0.3159	0.3704	0.3137	3
74	3	0.9239	0.0369	0.9631	3	0.2890	0.4298	0.2811	3	0.3161	0.3705	0.3134	3
75	3	0.9157	0.0367	0.9633	3	0.2893	0.4304	0.2802	3	0.3163	0.3706	0.3131	3
76	3	0.9092	0.0366	0.9634	3	0.2896	0.4309	0.2795	3	0.3164	0.3707	0.3129	3
77	1	0.8287	0.1012	0.5202	1	0.2725	0.3988	0.3287	1	0.3087	0.3539	0.3374	1
78	1	0.8328	0.1105	0.4466	1	0.2686	0.3916	0.3398	1	0.3084	0.3517	0.3400	1
79	1	0.8459	0.1822	0.3837	1	0.2647	0.3845	0.3508	1	0.3082	0.3500	0.3419	1
80	1	0.8591	0.2587	0.3298	1	0.2610	0.3777	0.3613	1	0.3080	0.3486	0.3434	1
81	1	0.8721	0.3251	0.2842	1	0.2573	0.3711	0.3716	1	0.3079	0.3475	0.3446	1
82	1	0.8846	0.3810	0.2466	1	0.2538	0.3647	0.3815	1	0.3078	0.3466	0.3456	1
83	1	0.8967	0.4293	0.2160	1	0.2504	0.3585	0.3911	1	0.3076	0.3458	0.3466	1
84	1	0.9082	0.4706	0.1923	1	0.2471	0.3526	0.4003	1	0.3075	0.3451	0.3474	1
85	1	0.9657	0.0343	NaN	1	0.4130	0.5870	NaN	1	0.4565	0.5435	NaN	1

C - Section 9.6.11 Headway Distance to Vehicles Ahead

Table C.16 - Section 9.6.11 Simulation Results

Parameter Value (m)	Lane 1							Lane 2							Lane 3						
	Impact Velocity VA (m/s)	Impact Velocity HV1 (m/s)	Impact Velocity HV2 (m/s)	Impact Velocity VB (m/s)	Manoeuvre Acceleration (m/s²)	TTC (s)	Lane Open	Impact Velocity VA (m/s)	Impact Velocity HV1 (m/s)	Impact Velocity HV2 (m/s)	Impact Velocity VB (m/s)	Manoeuvre Acceleration (m/s²)	TTC (s)	Lane Open	Impact Velocity VA (m/s)	Impact Velocity HV1 (m/s)	Impact Velocity HV2 (m/s)	Impact Velocity VB (m/s)	Manoeuvre Acceleration (m/s²)	TTC (s)	Lane Open
7	9.1192	13.1322	3.6921	12.6888	8.7765	3.08	1	0	11.4561	10.3582	21.4249	8.3103	2.417	1	16.9347	21.9238	3.6921	12.6888	8.7765	1.986	0
7.5	9.1192	13.1322	3.6921	12.6888	8.7765	3.08	1	0	11.4561	10.3582	21.4249	8.3103	2.417	1	16.2254	21.2616	3.6921	12.6888	8.7765	2.085	1
8	9.1192	13.1322	3.6921	12.6888	8.7765	3.08	1	0	11.4561	10.3582	21.4249	8.3103	2.417	1	15.5094	20.4418	3.6921	12.6888	8.7765	2.185	1
8.5	9.1192	13.1322	3.6921	12.6888	8.7765	3.08	1	0	11.4561	10.3582	21.4249	8.3103	2.417	1	14.7724	19.5981	3.6921	12.6888	8.7765	2.288	1
9	9.1192	13.1322	3.6921	12.6888	8.7765	3.08	1	0	11.4561	10.3582	21.4249	8.3103	2.417	1	14.0216	18.7388	3.6921	12.6888	8.7765	2.393	1
9.5	9.1192	13.1322	3.6921	12.6888	8.7765	3.08	1	0	11.4561	10.3582	21.4249	8.3103	2.417	1	13.2599	17.8639	3.6921	12.6888	8.7765	2.5	1
10	9.1192	13.1322	3.6921	12.6888	8.7765	3.08	1	0	11.4561	10.3582	21.4249	8.3103	2.417	1	12.4713	16.5651	3.6921	12.6888	8.7765	2.61	1
10.5	9.1192	13.1322	3.6921	12.6888	8.7765	3.08	1	0	11.4561	10.3582	21.4249	8.3103	2.417	1	11.6718	16.0507	3.6921	12.6888	8.7765	2.722	1
11	9.1192	13.1322	3.6921	12.6888	8.7765	3.08	1	0	11.4561	10.3582	21.4249	8.3103	2.417	1	10.8443	15.1043	3.6921	12.6888	8.7765	2.838	1
11.5	9.1192	13.1322	3.6921	12.6888	8.7765	3.08	1	0	11.4561	10.3582	21.4249	8.3103	2.417	1	9.9958	14.1342	3.6921	12.6888	8.7765	2.957	1
12	9.1192	13.1322	3.6921	12.6888	8.7765	3.08	1	0	11.4561	10.3582	21.4249	8.3103	2.417	1	9.1192	13.1322	3.6921	12.6888	8.7765	3.08	1
12.5	9.1192	13.1322	3.6921	12.6888	8.7765	3.08	1	0	11.4561	10.3582	21.4249	8.3103	2.417	1	8.2216	12.1065	3.6921	12.6888	8.7765	3.206	1
13	9.1192	13.1322	3.6921	12.6888	8.7765	3.08	1	0	11.4561	10.3582	21.4249	8.3103	2.417	1	7.2888	11.0407	3.6921	12.6888	8.7765	3.337	1
13.5	9.1192	13.1322	3.6921	12.6888	8.7765	3.08	1	0	11.4561	10.3582	21.4249	8.3103	2.417	1	6.3208	9.9349	3.6921	12.6888	8.7765	3.473	1
14	9.1192	13.1322	3.6921	12.6888	8.7765	3.08	1	0	11.4561	10.3582	21.4249	8.3103	2.417	1	5.3176	8.7892	3.6921	12.6888	8.7765	3.614	1
14.5	9.1192	13.1322	3.6921	12.6888	8.7765	3.08	1	0	11.4561	10.3582	21.4249	8.3103	2.417	1	4.2721	7.5953	3.6921	12.6888	8.7765	3.761	1
15	9.1192	13.1322	3.6921	12.6888	8.7765	3.08	1	0	11.4561	10.3582	21.4249	8.3103	2.417	1	3.1770	6.3451	3.6921	12.6888	8.7765	3.915	1
15.5	9.1192	13.1322	3.6921	12.6888	8.7765	3.08	1	0	11.4561	10.3582	21.4249	8.3103	2.417	1	2.0253	5.0305	3.6921	12.6888	8.7765	4.077	1
16	9.1192	13.1322	3.6921	12.6888	8.7765	3.08	1	0	11.4561	10.3582	21.4249	8.3103	2.417	1	0.8027	3.6353	3.6921	12.6888	8.7765	4.229	1
16.5	9.1192	13.1322	3.6921	12.6888	8.7765	3.08	1	0	11.4561	10.3582	21.4249	8.3103	2.417	1	0	2.0945	3.6921	12.6888	8.7765	4.248	1
17	9.1192	13.1322	3.6921	12.6888	8.7765	3.08	1	0	11.4561	10.3582	21.4249	8.3103	2.417	1	0	0	3.6921	12.6888	8.7765	4.248	1

Table C.17 - Section 9.6.11 Collision modelling Results

Parameter Value (m)	Lane 1						Lane 2						Lane 3					
	Collision Acceleration VA (g)	Collision Acceleration HV1 (g)	Collision Acceleration HV2 (g)	Collision Acceleration VB (g)	Manoeuvre Acceleration (m/s²)	TTC (s)	Collision Acceleration VA (g)	Collision Acceleration HV1 (g)	Collision Acceleration HV2 (g)	Collision Acceleration VB (g)	Manoeuvre Acceleration (m/s²)	TTC (s)	Collision Acceleration VA (g)	Collision Acceleration HV1 (g)	Collision Acceleration HV2 (g)	Collision Acceleration VB (g)	Manoeuvre Acceleration (m/s²)	TTC (s)
7	3.9738	3.9738	5.6564	11.3129	8.7765	3.08	12.6826	12.6826	7.2208	14.4416	8.3103	2.417	5.0163	5.0163	5.6564	11.3129	8.7765	1.986
7.5	3.9738	3.9738	5.6564	11.3129	8.7765	3.08	12.6826	12.6826	7.2208	14.4416	8.3103	2.417	5.0517	5.0517	5.6564	11.3129	8.7765	2.085
8	3.9738	3.9738	5.6564	11.3129	8.7765	3.08	12.6826	12.6826	7.2208	14.4416	8.3103	2.417	4.9498	4.9498	5.6564	11.3129	8.7765	2.185
8.5	3.9738	3.9738	5.6564	11.3129	8.7765	3.08	12.6826	12.6826	7.2208	14.4416	8.3103	2.417	4.8353	4.8353	5.6564	11.3129	8.7765	2.288
9	3.9738	3.9738	5.6564	11.3129	8.7765	3.08	12.6826	12.6826	7.2208	14.4416	8.3103	2.417	4.7191	4.7191	5.6564	11.3129	8.7765	2.393
9.5	3.9738	3.9738	5.6564	11.3129	8.7765	3.08	12.6826	12.6826	7.2208	14.4416	8.3103	2.417	4.6014	4.6014	5.6564	11.3129	8.7765	2.5
10	3.9738	3.9738	5.6564	11.3129	8.7765	3.08	12.6826	12.6826	7.2208	14.4416	8.3103	2.417	4.4810	4.4810	5.6564	11.3129	8.7765	2.61
10.5	3.9738	3.9738	5.6564	11.3129	8.7765	3.08	12.6826	12.6826	7.2208	14.4416	8.3103	2.417	4.3591	4.3591	5.6564	11.3129	8.7765	2.722
11	3.9738	3.9738	5.6564	11.3129	8.7765	3.08	12.6826	12.6826	7.2208	14.4416	8.3103	2.417	4.2335	4.2335	5.6564	11.3129	8.7765	2.838
11.5	3.9738	3.9738	5.6564	11.3129	8.7765	3.08	12.6826	12.6826	7.2208	14.4416	8.3103	2.417	4.1054	4.1054	5.6564	11.3129	8.7765	2.957
12	3.9738	3.9738	5.6564	11.3129	8.7765	3.08	12.6826	12.6826	7.2208	14.4416	8.3103	2.417	3.9738	3.9738	5.6564	11.3129	8.7765	3.08
12.5	3.9738	3.9738	5.6564	11.3129	8.7765	3.08	12.6826	12.6826	7.2208	14.4416	8.3103	2.417	3.8397	3.8397	5.6564	11.3129	8.7765	3.206
13	3.9738	3.9738	5.6564	11.3129	8.7765	3.08	12.6826	12.6826	7.2208	14.4416	8.3103	2.417	3.7011	3.7011	5.6564	11.3129	8.7765	3.337
13.5	3.9738	3.9738	5.6564	11.3129	8.7765	3.08	12.6826	12.6826	7.2208	14.4416	8.3103	2.417	3.5581	3.5581	5.6564	11.3129	8.7765	3.473
14	3.9738	3.9738	5.6564	11.3129	8.7765	3.08	12.6826	12.6826	7.2208	14.4416	8.3103	2.417	3.4107	3.4107	5.6564	11.3129	8.7765	3.614
14.5	3.9738	3.9738	5.6564	11.3129	8.7765	3.08	12.6826	12.6826	7.2208	14.4416	8.3103	2.417	3.2580	3.2580	5.6564	11.3129	8.7765	3.751
15	3.9738	3.9738	5.6564	11.3129	8.7765	3.08	12.6826	12.6826	7.2208	14.4416	8.3103	2.417	3.0990	3.0990	5.6564	11.3129	8.7765	3.915
15.5	3.9738	3.9738	5.6564	11.3129	8.7765	3.08	12.6826	12.6826	7.2208	14.4416	8.3103	2.417	2.9328	2.9328	5.6564	11.3129	8.7765	4.077
16	3.9738	3.9738	5.6564	11.3129	8.7765	3.08	12.6826	12.6826	7.2208	14.4416	8.3103	2.417	9.0306	4.5153	5.6564	9.5915	8.7765	4.229
16.5	3.9738	3.9738	5.6564	11.3129	8.7765	3.08	12.6826	12.6826	7.2208	14.4416	8.3103	2.417	10.1534	5.0267	5.6564	9.5915	8.7765	4.248
17	3.9738	3.9738	5.6564	11.3129	8.7765	3.08	12.6826	12.6826	7.2208	14.4416	8.3103	2.417	0	0	9.5915	9.5915	8.7765	4.248

Table C.18 - Section 9.6.11 MADM Results

Parameter Value (m)	Observer's Decision	TOPSIS				AHP				ANP			
		Lane 1	Lane 2	Lane 3	Decision	Lane 1	Lane 2	Lane 3	Decision	Lane 1	Lane 2	Lane 3	Decision
7	1	0.9657	0.0343	NaN	1	0.4029	0.5971	NaN	1	0.4623	0.5377	NaN	1
7.5	1	0.9616	0.0442	0.8596	1	0.2806	0.4158	0.3037	1	0.3173	0.3704	0.3123	3
8	1	0.9616	0.0413	0.8729	1	0.2813	0.4169	0.3018	1	0.3170	0.3702	0.3128	3
8.5	1	0.9616	0.0393	0.8864	1	0.2820	0.4180	0.3000	1	0.3167	0.3701	0.3133	3
9	1	0.9616	0.0384	0.8998	1	0.2827	0.4191	0.2981	1	0.3164	0.3700	0.3137	3
9.5	1	0.9617	0.0383	0.9131	1	0.2835	0.4203	0.2963	1	0.3161	0.3699	0.3140	3
10	1	0.9617	0.0383	0.9263	1	0.2842	0.4214	0.2944	1	0.3158	0.3698	0.3144	3
10.5	1	0.9617	0.0383	0.9387	1	0.2849	0.4225	0.2926	1	0.3156	0.3698	0.3146	3
11	1	0.9618	0.0382	0.9498	1	0.2856	0.4237	0.2907	1	0.3154	0.3698	0.3148	3
11.5	1	0.9618	0.0382	0.9582	1	0.2863	0.4248	0.2889	1	0.3152	0.3699	0.3149	3
12	1	0.9619	0.0381	0.9619	1	0.2870	0.4260	0.2870	1	0.3150	0.3700	0.3150	3
12.5	3	0.9588	0.0376	0.9624	3	0.2877	0.4272	0.2851	3	0.3148	0.3702	0.3150	1
13	3	0.9506	0.0370	0.9630	3	0.2884	0.4284	0.2832	3	0.3147	0.3704	0.3149	1
13.5	3	0.9392	0.0364	0.9636	3	0.2892	0.4296	0.2812	3	0.3146	0.3706	0.3148	1
14	3	0.9261	0.0359	0.9641	3	0.2899	0.4309	0.2792	3	0.3145	0.3710	0.3145	1
14.5	3	0.9122	0.0353	0.9647	3	0.2907	0.4322	0.2771	3	0.3144	0.3714	0.3142	3
15	3	0.8977	0.0347	0.9653	3	0.2915	0.4335	0.2750	3	0.3144	0.3718	0.3138	3
15.5	3	0.8828	0.0341	0.9659	3	0.2923	0.4349	0.2728	3	0.3144	0.3724	0.3132	3
16	1	0.8705	0.1536	0.6139	1	0.2775	0.4068	0.3158	1	0.3054	0.3534	0.3412	1
16.5	1	0.8699	0.1536	0.5602	1	0.2752	0.4025	0.3223	1	0.3047	0.3509	0.3444	1
17	3	0.6910	0.1148	0.8244	3	0.2989	0.4473	0.2538	3	0.3195	0.3951	0.2854	3

C - Section 9.6.12 Headway Distance to Vehicles Behind

Table C.19 - Section 9.6.12 Simulation Results

Parameter Value (m)	Lane 1							Lane 2							Lane 3						
	Impact Velocity VA (m/s)	Impact Velocity HV1 (m/s)	Impact Velocity HV2 (m/s)	Impact Velocity VB (m/s)	Manoeuvre Acceleration (m/s²)	TTC (s)	Lane Open	Impact Velocity VA (m/s)	Impact Velocity HV1 (m/s)	Impact Velocity HV2 (m/s)	Impact Velocity VB (m/s)	Manoeuvre Acceleration (m/s²)	TTC (s)	Lane Open	Impact Velocity VA (m/s)	Impact Velocity HV1 (m/s)	Impact Velocity HV2 (m/s)	Impact Velocity VB (m/s)	Manoeuvre Acceleration (m/s²)	TTC (s)	Lane Open
7	9.1192	13.1322	3.6921	12.6688	8.7765	3.08	1	0	11.4561	10.3582	21.4249	8.3103	2.417	1	9.1192	13.1322	22.4003	24.9008	8.7755	1.214	0
8	9.1192	13.1322	3.6921	12.6688	8.7765	3.08	1	0	11.4561	10.3582	21.4249	8.3103	2.417	1	9.1192	13.1322	19.8110	22.9357	8.7755	2.429	1
9	9.1192	13.1322	3.6921	12.6688	8.7765	3.08	1	0	11.4561	10.3582	21.4249	8.3103	2.417	1	9.1192	13.1322	17.5043	21.4666	8.7755	2.664	1
10	9.1192	13.1322	3.6921	12.6688	8.7765	3.08	1	0	11.4561	10.3582	21.4249	8.3103	2.417	1	9.1192	13.1322	15.6019	20.2554	8.7755	2.868	1
11	9.1192	13.1322	3.6921	12.6688	8.7765	3.08	1	0	11.4561	10.3582	21.4249	8.3103	2.417	1	9.1192	13.1322	13.9550	19.2074	8.7755	2.96	1
12	9.1192	13.1322	3.6921	12.6688	8.7765	3.08	1	0	11.4561	10.3582	21.4249	8.3103	2.417	1	9.1192	13.1322	12.4809	18.2697	8.7755	3.08	1
13	9.1192	13.1322	3.6921	12.6688	8.7765	3.08	1	0	11.4561	10.3582	21.4249	8.3103	2.417	1	9.1192	13.1322	11.1302	17.4109	8.7755	3.08	1
14	9.1192	13.1322	3.6921	12.6688	8.7765	3.08	1	0	11.4561	10.3582	21.4249	8.3103	2.417	1	9.1192	13.1322	9.8862	16.6202	8.7755	3.08	1
15	9.1192	13.1322	3.6921	12.6688	8.7765	3.08	1	0	11.4561	10.3582	21.4249	8.3103	2.417	1	9.1192	13.1322	8.7161	15.8768	8.7755	3.08	1
16	9.1192	13.1322	3.6921	12.6688	8.7765	3.08	1	0	11.4561	10.3582	21.4249	8.3103	2.417	1	9.1192	13.1322	7.6115	15.1753	8.7755	3.08	1
17	9.1192	13.1322	3.6921	12.6688	8.7765	3.08	1	0	11.4561	10.3582	21.4249	8.3103	2.417	1	9.1192	13.1322	6.5642	14.5105	8.7755	3.08	1
18	9.1192	13.1322	3.6921	12.6688	8.7765	3.08	1	0	11.4561	10.3582	21.4249	8.3103	2.417	1	9.1192	13.1322	5.5660	13.8871	8.7755	3.08	1
19	9.1192	13.1322	3.6921	12.6688	8.7765	3.08	1	0	11.4561	10.3582	21.4249	8.3103	2.417	1	9.1192	13.1322	4.6087	13.2699	8.7755	3.08	1
20	9.1192	13.1322	3.6921	12.6688	8.7765	3.08	1	0	11.4561	10.3582	21.4249	8.3103	2.417	1	9.1192	13.1322	6.5642	14.5105	8.7755	3.08	1
21	9.1192	13.1322	3.6921	12.6688	8.7765	3.08	1	0	11.4561	10.3582	21.4249	8.3103	2.417	1	9.1192	13.1322	2.8081	12.1285	8.7755	3.08	1
22	9.1192	13.1322	3.6921	12.6688	8.7765	3.08	1	0	11.4561	10.3582	21.4249	8.3103	2.417	1	9.1192	13.1322	1.9485	11.5860	8.7755	3.08	1
23	9.1192	13.1322	3.6921	12.6688	8.7765	3.08	1	0	11.4561	10.3582	21.4249	8.3103	2.417	1	9.1192	13.1322	1.1214	11.0603	8.7755	3.08	1
24	9.1192	13.1322	3.6921	12.6688	8.7765	3.08	1	0	11.4561	10.3582	21.4249	8.3103	2.417	1	9.1192	13.1322	0.3187	10.5522	8.7755	3.08	1
25	9.1192	13.1322	3.6921	12.6688	8.7765	3.08	1	0	11.4561	10.3582	21.4249	8.3103	2.417	1	9.1192	13.1322	0	10.0495	8.7755	3.08	1
26	9.1192	13.1322	3.6921	12.6688	8.7765	3.08	1	0	11.4561	10.3582	21.4249	8.3103	2.417	1	9.1192	13.1322	0	9.5265	8.7755	3.08	1
27	9.1192	13.1322	3.6921	12.6688	8.7765	3.08	1	0	11.4561	10.3582	21.4249	8.3103	2.417	1	9.1192	13.1322	0	8.9929	8.7755	3.08	1
28	9.1192	13.1322	3.6921	12.6688	8.7765	3.08	1	0	11.4561	10.3582	21.4249	8.3103	2.417	1	9.1192	13.1322	0	8.3837	8.7755	3.08	1
29	9.1192	13.1322	3.6921	12.6688	8.7765	3.08	1	0	11.4561	10.3582	21.4249	8.3103	2.417	1	9.1192	13.1322	0	7.7487	8.7755	3.08	1
30	9.1192	13.1322	3.6921	12.6688	8.7765	3.08	1	0	11.4561	10.3582	21.4249	8.3103	2.417	1	9.1192	13.1322	0	7.0576	8.7755	3.08	1
31	9.1192	13.1322	3.6921	12.6688	8.7765	3.08	1	0	11.4561	10.3582	21.4249	8.3103	2.417	1	9.1192	13.1322	0	6.2900	8.7755	3.08	1
32	9.1192	13.1322	3.6921	12.6688	8.7765	3.08	1	0	11.4561	10.3582	21.4249	8.3103	2.417	1	9.1192	13.1322	0	5.4155	8.7755	3.08	1
33	9.1192	13.1322	3.6921	12.6688	8.7765	3.08	1	0	11.4561	10.3582	21.4249	8.3103	2.417	1	9.1192	13.1322	0	4.3723	8.7755	3.08	1
34	9.1192	13.1322	3.6921	12.6688	8.7765	3.08	1	0	11.4561	10.3582	21.4249	8.3103	2.417	1	9.1192	13.1322	0	2.9322	8.7755	3.08	1
35	9.1192	13.1322	3.6921	12.6688	8.7765	3.08	1	0	11.4561	10.3582	21.4249	8.3103	2.417	1	9.1192	13.1322	0	0	8.7755	3.08	1

Table C.20 - Section 9.6.12 Collision Modelling Results

Parameter Value (m)	Lane 1						Lane 2						Lane 3					
	Collision Acceleration VA (g)	Collision Acceleration HV1 (g)	Collision Acceleration HV2 (g)	Collision Acceleration VB (g)	Manoeuvre Acceleration (m/s²)	TTC (s)	Collision Acceleration VA (g)	Collision Acceleration HV1 (g)	Collision Acceleration HV2 (g)	Collision Acceleration VB (g)	Manoeuvre Acceleration (m/s²)	TTC (s)	Collision Acceleration VA (g)	Collision Acceleration HV1 (g)	Collision Acceleration HV2 (g)	Collision Acceleration VB (g)	Manoeuvre Acceleration (m/s²)	TTC (s)
7	3.9738	3.9738	5.6564	11.3129	8.7765	3.08	12.6826	12.6826	7.2208	14.4416	8.3103	2.417	20.2152	10.1076	2.4227	2.4227	8.7765	1.214
8	3.9738	3.9738	5.6564	11.3129	8.7765	3.08	12.6826	12.6826	7.2208	14.4416	8.3103	2.417	16.3413	8.1706	5.0547	3.0547	8.7765	2.429
9	3.9738	3.9738	5.6564	11.3129	8.7765	3.08	12.6826	12.6826	7.2208	14.4416	8.3103	2.417	13.3574	6.5787	3.9206	3.9206	8.7765	2.664
10	3.9738	3.9738	5.6564	11.3129	8.7765	3.08	12.6826	12.6826	7.2208	14.4416	8.3103	2.417	11.0413	5.5206	4.5511	4.5511	8.7765	2.858
11	3.9738	3.9738	5.6564	11.3129	8.7765	3.08	12.6826	12.6826	7.2208	14.4416	8.3103	2.417	9.1333	4.5667	5.2958	5.2958	8.7765	2.98
12	3.9738	3.9738	5.6564	11.3129	8.7765	3.08	12.6826	12.6826	7.2208	14.4416	8.3103	2.417	3.9738	3.9738	3.4417	6.8833	8.7765	3.08
13	3.9738	3.9738	5.6564	11.3129	8.7765	3.08	12.6826	12.6826	7.2208	14.4416	8.3103	2.417	3.9738	3.9738	3.7658	7.5316	8.7765	3.08
14	3.9738	3.9738	5.6564	11.3129	8.7765	3.08	12.6826	12.6826	7.2208	14.4416	8.3103	2.417	3.9738	3.9738	4.0693	8.1387	8.7765	3.08
15	3.9738	3.9738	5.6564	11.3129	8.7765	3.08	12.6826	12.6826	7.2208	14.4416	8.3103	2.417	3.9738	3.9738	4.3593	8.7187	8.7765	3.08
16	3.9738	3.9738	5.6564	11.3129	8.7765	3.08	12.6826	12.6826	7.2208	14.4416	8.3103	2.417	3.9738	3.9738	4.6372	9.2744	8.7765	3.08
17	3.9738	3.9738	5.6564	11.3129	8.7765	3.08	12.6826	12.6826	7.2208	14.4416	8.3103	2.417	3.9738	3.9738	4.9044	9.8088	8.7765	3.08
18	3.9738	3.9738	5.6564	11.3129	8.7765	3.08	12.6826	12.6826	7.2208	14.4416	8.3103	2.417	3.9738	3.9738	5.1625	10.3250	8.7765	3.08
19	3.9738	3.9738	5.6564	11.3129	8.7765	3.08	12.6826	12.6826	7.2208	14.4416	8.3103	2.417	3.9738	3.9738	5.4133	10.8266	8.7765	3.08
20	3.9738	3.9738	5.6564	11.3129	8.7765	3.08	12.6826	12.6826	7.2208	14.4416	8.3103	2.417	3.9738	3.9738	5.6564	11.3129	8.7765	3.08
21	3.9738	3.9738	5.6564	11.3129	8.7765	3.08	12.6826	12.6826	7.2208	14.4416	8.3103	2.417	3.9738	3.9738	5.8938	11.7876	8.7765	3.08
22	3.9738	3.9738	5.6564	11.3129	8.7765	3.08	12.6826	12.6826	7.2208	14.4416	8.3103	2.417	3.9738	3.9738	6.1273	12.2546	8.7765	3.08
23	3.9738	3.9738	5.6564	11.3129	8.7765	3.08	12.6826	12.6826	7.2208	14.4416	8.3103	2.417	3.9738	3.9738	6.3545	12.7091	8.7765	3.08
24	3.9738	3.9738	5.6564	11.3129	8.7765	3.08	12.6826	12.6826	7.2208	14.4416	8.3103	2.417	3.9738	3.9738	6.5776	13.1551	8.7765	3.08
25	3.9738	3.9738	5.6564	11.3129	8.7765	3.08	12.6826	12.6826	7.2208	14.4416	8.3103	2.417	3.9738	3.9738	6.4380	12.8760	8.7765	3.08
26	3.9738	3.9738	5.6564	11.3129	8.7765	3.08	12.6826	12.6826	7.2208	14.4416	8.3103	2.417	3.9738	3.9738	6.0462	12.0923	8.7765	3.08
27	3.9738	3.9738	5.6564	11.3129	8.7765	3.08	12.6826	12.6826	7.2208	14.4416	8.3103	2.417	3.9738	3.9738	5.5391	11.2782	8.7765	3.08
28	3.9738	3.9738	5.6564	11.3129	8.7765	3.08	12.6826	12.6826	7.2208	14.4416	8.3103	2.417	3.9738	3.9738	5.2143	10.4285	8.7765	3.08
29	3.9738	3.9738	5.6564	11.3129	8.7765	3.08	12.6826	12.6826	7.2208	14.4416	8.3103	2.417	3.9738	3.9738	4.7659	9.5318	8.7765	3.08
30	3.9738	3.9738	5.6564	11.3129	8.7765	3.08	12.6826	12.6826	7.2208	14.4416	8.3103	2.417	3.9738	3.9738	4.2888	8.5777	8.7765	3.08
31	3.9738	3.9738	5.6564	11.3129	8.7765	3.08	12.6826	12.6826	7.2208	14.4416	8.3103	2.417	3.9738	3.9738	3.7720	7.5440	8.7765	3.08
32	3.9738	3.9738	5.6564	11.3129	8.7765	3.08	12.6826	12.6826	7.2208	14.4416	8.3103	2.417	3.9738	3.9738	3.1991	6.3982	8.7765	3.08
33	3.9738	3.9738	5.6564	11.3129	8.7765	3.08	12.6826	12.6826	7.2208	14.4416	8.3103	2.417	3.9738	3.9738	2.5376	5.0252	8.7765	3.08
34	3.9738	3.9738	5.6564	11.3129	8.7765	3.08	12.6826	12.6826	7.2208	14.4416	8.3103	2.417	3.9738	3.9738	1.5909	3.3818	8.7765	3.08
35	3.9738	3.9738	5.6564	11.3129	8.7765	3.08	12.6826	12.6826	7.2208	14.4416	8.3103	2.417	3.9738	3.9738	0	0	8.7765	3.08

Table C.21 - Section 9.6.12 MADM Results

Parameter Value (m)	Observer's Decision	TOPSIS				AHP				ANP			
		Lane 1	Lane 2	Lane 3	Decision	Lane 1	Lane 2	Lane 3	Decision	Lane 1	Lane 2	Lane 3	Decision
7	1	0.9657	0.0343	NaN	1	0.4052	0.5948	NaN	1	0.4609	0.5391	NaN	1
8	1	0.6417	0.1762	0.4972	1	0.2766	0.4074	0.3161	1	0.3235	0.3601	0.3163	3
9	1	0.6357	0.0491	0.5620	1	0.2813	0.4159	0.3028	1	0.3207	0.3601	0.3193	3
10	1	0.6548	0.0309	0.6330	1	0.2850	0.4225	0.2925	1	0.3186	0.3608	0.3206	1
11	3	0.6793	0.0313	0.7118	3	0.2878	0.4276	0.2846	3	0.3174	0.3627	0.3200	1
12	3	0.7203	0.0312	0.9688	3	0.2985	0.4477	0.2538	3	0.3221	0.3737	0.3042	3
13	3	0.7507	0.0322	0.9678	3	0.2967	0.4443	0.2590	3	0.3208	0.3730	0.3062	3
14	3	0.7815	0.0332	0.9668	3	0.2951	0.4412	0.2637	3	0.3197	0.3724	0.3079	3
15	3	0.8133	0.0341	0.9659	3	0.2935	0.4383	0.2682	3	0.3187	0.3719	0.3094	3
16	3	0.8460	0.0350	0.9650	3	0.2921	0.4356	0.2723	3	0.3179	0.3714	0.3108	3
17	3	0.8796	0.0359	0.9641	3	0.2907	0.4330	0.2763	3	0.3171	0.3710	0.3120	3
18	3	0.9135	0.0367	0.9633	3	0.2894	0.4306	0.2800	3	0.3163	0.3706	0.3131	3
19	3	0.9453	0.0374	0.9626	3	0.2882	0.4282	0.2836	3	0.3156	0.3703	0.3141	3
20	1	0.9619	0.0381	0.9619	1	0.2870	0.4260	0.2870	1	0.3150	0.3700	0.3150	1
21	1	0.9616	0.0384	0.9451	1	0.2859	0.4239	0.2903	1	0.3144	0.3697	0.3159	1
22	1	0.9613	0.0387	0.9147	1	0.2848	0.4218	0.2935	1	0.3139	0.3695	0.3167	1
23	1	0.9611	0.0389	0.8835	1	0.2837	0.4198	0.2965	1	0.3133	0.3692	0.3174	1
24	1	0.9608	0.0392	0.8538	1	0.2827	0.4179	0.2995	1	0.3128	0.3690	0.3181	1
25	1	0.9610	0.0390	0.8723	1	0.2833	0.4191	0.2976	1	0.3131	0.3692	0.3177	1
26	1	0.9614	0.0386	0.9257	1	0.2851	0.4225	0.2924	1	0.3140	0.3696	0.3164	1
27	3	0.9618	0.0381	0.9619	3	0.2871	0.4262	0.2868	3	0.3150	0.3700	0.3149	3
28	3	0.9204	0.0368	0.9632	3	0.2892	0.4301	0.2807	3	0.3162	0.3705	0.3133	3
29	3	0.8620	0.0354	0.9646	3	0.2914	0.4344	0.2742	3	0.3175	0.3712	0.3113	3
30	3	0.8053	0.0339	0.9661	3	0.2939	0.4390	0.2671	3	0.3190	0.3720	0.3090	3
31	3	0.7513	0.0322	0.9678	3	0.2967	0.4442	0.2591	3	0.3208	0.3730	0.3062	3
32	3	0.6991	0.0304	0.9696	3	0.2998	0.4502	0.2499	3	0.3231	0.3743	0.3026	3
33	3	0.6470	0.0284	0.9716	3	0.3037	0.4575	0.2389	3	0.3261	0.3762	0.2977	3
34	3	0.5907	0.0261	0.9739	3	0.3088	0.4672	0.2240	3	0.3309	0.3793	0.2898	3
35	3	0.5031	0.0223	0.9777	3	0.3201	0.4885	0.1914	3	0.3453	0.3898	0.2649	3

C - Section 9.6.13 Vehicles Ahead Inputted Deceleration

Table C.22 - Section 9.6.13 Simulation Results

Parameter Value (m/s²)	Lane 1							Lane 2							Lane 3						
	Impact Velocity VA (m/s)	Impact Velocity HV1 (m/s)	Impact Velocity HV2 (m/s)	Impact Velocity VB (m/s)	Manoeuvre Acceleration (m/s²)	TTC (s)	Lane Open	Impact Velocity VA (m/s)	Impact Velocity HV1 (m/s)	Impact Velocity HV2 (m/s)	Impact Velocity VB (m/s)	Manoeuvre Acceleration (m/s²)	TTC (s)	Lane Open	Impact Velocity VA (m/s)	Impact Velocity HV1 (m/s)	Impact Velocity HV2 (m/s)	Impact Velocity VB (m/s)	Manoeuvre Acceleration (m/s²)	TTC (s)	Lane Open
6.5	9.1192	13.1322	3.6921	12.6888	8.7765	3.08	1	0	11.4561	10.3582	21.4249	8.3103	2.417	1	0	0	3.6921	12.6888	8.7765	4.248	1
6.6	9.1192	13.1322	3.6921	12.6888	8.7765	3.08	1	0	11.4561	10.3582	21.4249	8.3103	2.417	1	4.5721	6.1584	3.6921	12.6888	8.7765	3.938	1
6.7	9.1192	13.1322	3.6921	12.6888	8.7765	3.08	1	0	11.4561	10.3582	21.4249	8.3103	2.417	1	6.5538	8.9842	3.6921	12.6888	8.7765	3.59	1
6.8	9.1192	13.1322	3.6921	12.6888	8.7765	3.08	1	0	11.4561	10.3582	21.4249	8.3103	2.417	1	7.7138	10.7642	3.6921	12.6888	8.7765	3.371	1
6.9	9.1192	13.1322	3.6921	12.6888	8.7765	3.08	1	0	11.4561	10.3582	21.4249	8.3103	2.417	1	8.5177	12.0821	3.6921	12.6888	8.7765	3.209	1
7	9.1192	13.1322	3.6921	12.6888	8.7765	3.08	1	0	11.4561	10.3582	21.4249	8.3103	2.417	1	9.1192	13.1322	3.6921	12.6888	8.7765	3.08	1
7.1	9.1192	13.1322	3.6921	12.6888	8.7765	3.08	1	0	11.4561	10.3582	21.4249	8.3103	2.417	1	9.5947	14.0120	3.6921	12.6888	8.7765	2.972	1
7.2	9.1192	13.1322	3.6921	12.6888	8.7765	3.08	1	0	11.4561	10.3582	21.4249	8.3103	2.417	1	9.9747	14.7619	3.6921	12.6888	8.7765	2.88	1
7.3	9.1192	13.1322	3.6921	12.6888	8.7765	3.08	1	0	11.4561	10.3582	21.4249	8.3103	2.417	1	10.2913	15.4224	3.6921	12.6888	8.7765	2.799	1
7.4	9.1192	13.1322	3.6921	12.6888	8.7765	3.08	1	0	11.4561	10.3582	21.4249	8.3103	2.417	1	10.5489	16.0017	3.6921	12.6888	8.7765	2.728	1
7.5	9.1192	13.1322	3.6921	12.6888	8.7765	3.08	1	0	11.4561	10.3582	21.4249	8.3103	2.417	1	10.7671	16.5241	3.6921	12.6888	8.7765	2.664	1
7.6	9.1192	13.1322	3.6921	12.6888	8.7765	3.08	1	0	11.4561	10.3582	21.4249	8.3103	2.417	1	10.9595	17.0059	3.6921	12.6888	8.7765	2.605	1
7.7	9.1192	13.1322	3.6921	12.6888	8.7765	3.08	1	0	11.4561	10.3582	21.4249	8.3103	2.417	1	11.1166	17.4389	3.6921	12.6888	8.7765	2.552	1
7.8	9.1192	13.1322	3.6921	12.6888	8.7765	3.08	1	0	11.4561	10.3582	21.4249	8.3103	2.417	1	11.2526	17.8393	3.6921	12.6888	8.7765	2.503	1
7.9	9.1192	13.1322	3.6921	12.6888	8.7765	3.08	1	0	11.4561	10.3582	21.4249	8.3103	2.417	1	11.3661	18.2072	3.6921	12.6888	8.7765	2.458	1
8	9.1192	13.1322	3.6921	12.6888	8.7765	3.08	1	0	11.4561	10.3582	21.4249	8.3103	2.417	1	11.4724	18.5589	3.6921	12.6888	8.7765	2.415	1
8.1	9.1192	13.1322	3.6921	12.6888	8.7765	3.08	1	0	11.4561	10.3582	21.4249	8.3103	2.417	1	11.5542	18.8779	3.6921	12.6888	8.7765	2.376	1
8.2	9.1192	13.1322	3.6921	12.6888	8.7765	3.08	1	0	11.4561	10.3582	21.4249	8.3103	2.417	1	11.6272	19.1807	3.6921	12.6888	8.7765	2.339	1
8.3	9.1192	13.1322	3.6921	12.6888	8.7765	3.08	1	0	11.4561	10.3582	21.4249	8.3103	2.417	1	11.6906	19.4671	3.6921	12.6888	8.7765	2.304	1
8.4	9.1192	13.1322	3.6921	12.6888	8.7765	3.08	1	0	11.4561	10.3582	21.4249	8.3103	2.417	1	11.7439	19.7373	3.6921	12.6888	8.7765	2.271	1
8.5	9.1192	13.1322	3.6921	12.6888	8.7765	3.08	1	0	11.4561	10.3582	21.4249	8.3103	2.417	1	11.7865	19.9912	3.6921	12.6888	8.7765	2.24	1
8.6	9.1192	13.1322	3.6921	12.6888	8.7765	3.08	1	0	11.4561	10.3582	21.4249	8.3103	2.417	1	11.8265	20.2369	3.6921	12.6888	8.7765	2.21	1
8.7	9.1192	13.1322	3.6921	12.6888	8.7765	3.08	1	0	11.4561	10.3582	21.4249	8.3103	2.417	1	11.8548	20.4664	3.6921	12.6888	8.7765	2.182	1
8.8	9.1192	13.1322	3.6921	12.6888	8.7765	3.08	1	0	11.4561	10.3582	21.4249	8.3103	2.417	1	11.8797	20.6876	3.6921	12.6888	8.7765	2.155	1
8.9	9.1192	13.1322	3.6921	12.6888	8.7765	3.08	1	0	11.4561	10.3582	21.4249	8.3103	2.417	1	11.8919	20.8926	3.6921	12.6888	8.7765	2.13	1
9	9.1192	13.1322	3.6921	12.6888	8.7765	3.08	1	0	11.4561	10.3582	21.4249	8.3103	2.417	1	11.9091	21.0975	3.6921	12.6888	8.7765	2.105	1
9.1	9.1192	13.1322	3.6921	12.6888	8.7765	3.08	1	0	11.4561	10.3582	21.4249	8.3103	2.417	1	11.9127	21.2852	3.6921	12.6888	8.7765	2.082	1
9.2	9.1192	13.1322	3.6921	12.6888	8.7765	3.08	1	0	11.4561	10.3582	21.4249	8.3103	2.417	1	11.9210	21.4748	3.6921	12.6888	8.7765	2.059	1
9.3	9.1192	13.1322	3.6921	12.6888	8.7765	3.08	1	0	11.4561	10.3582	21.4249	8.3103	2.417	1	11.9149	21.6471	3.6921	12.6888	8.7765	2.038	1
9.4	9.1192	13.1322	3.6921	12.6888	8.7765	3.08	1	0	11.4561	10.3582	21.4249	8.3103	2.417	1	11.9130	21.7827	3.6921	12.6888	8.7765	2.017	0

Table C.23 - Section 9.6.13 Collision Modelling Results

Parameter Value (m/s²)	Lane 1						Lane 2						Lane 3					
	Collision Acceleration VA (g)	Collision Acceleration HV1 (g)	Collision Acceleration HV2 (g)	Collision Acceleration VB (g)	Manoeuvre Acceleration (m/s²)	TTC (s)	Collision Acceleration VA (g)	Collision Acceleration HV1 (g)	Collision Acceleration HV2 (g)	Collision Acceleration VB (g)	Manoeuvre Acceleration (m/s²)	TTC (s)	Collision Acceleration VA (g)	Collision Acceleration HV1 (g)	Collision Acceleration HV2 (g)	Collision Acceleration VB (g)	Manoeuvre Acceleration (m/s²)	TTC (s)
6.5	3.9738	3.9738	5.6564	11.3129	8.7765	3.08	12.6826	12.6826	7.2208	14.4416	8.3103	2.417	0	0	9.5915	9.5915	8.7755	4.248
6.6	3.9738	3.9738	5.6564	11.3129	8.7765	3.08	12.6826	12.6826	7.2208	14.4416	8.3103	2.417	1.5171	1.5171	5.6564	11.3129	8.7755	3.938
6.7	3.9738	3.9738	5.6564	11.3129	8.7765	3.08	12.6826	12.6826	7.2208	14.4416	8.3103	2.417	2.3523	2.3523	5.6564	11.3129	8.7755	3.59
6.8	3.9738	3.9738	5.6564	11.3129	8.7765	3.08	12.6826	12.6826	7.2208	14.4416	8.3103	2.417	2.9789	2.9789	5.6564	11.3129	8.7755	3.371
6.9	3.9738	3.9738	5.6564	11.3129	8.7765	3.08	12.6826	12.6826	7.2208	14.4416	8.3103	2.417	3.5066	3.5066	5.6564	11.3129	8.7755	3.209
7	3.9738	3.9738	5.6564	11.3129	8.7765	3.08	12.6826	12.6826	7.2208	14.4416	8.3103	2.417	3.9738	3.9738	5.6564	11.3129	8.7755	3.08
7.1	3.9738	3.9738	5.6564	11.3129	8.7765	3.08	12.6826	12.6826	7.2208	14.4416	8.3103	2.417	4.3998	4.3998	5.6564	11.3129	8.7755	2.972
7.2	3.9738	3.9738	5.6564	11.3129	8.7765	3.08	12.6826	12.6826	7.2208	14.4416	8.3103	2.417	4.7940	4.7940	5.6564	11.3129	8.7755	2.88
7.3	3.9738	3.9738	5.6564	11.3129	8.7765	3.08	12.6826	12.6826	7.2208	14.4416	8.3103	2.417	5.1642	5.1642	5.6564	11.3129	8.7755	2.799
7.4	3.9738	3.9738	5.6564	11.3129	8.7765	3.08	12.6826	12.6826	7.2208	14.4416	8.3103	2.417	5.5140	5.5140	5.6564	11.3129	8.7755	2.728
7.5	3.9738	3.9738	5.6564	11.3129	8.7765	3.08	12.6826	12.6826	7.2208	14.4416	8.3103	2.417	5.8477	5.8477	5.6564	11.3129	8.7755	2.664
7.6	3.9738	3.9738	5.6564	11.3129	8.7765	3.08	12.6826	12.6826	7.2208	14.4416	8.3103	2.417	6.1679	6.1679	5.6564	11.3129	8.7755	2.605
7.7	3.9738	3.9738	5.6564	11.3129	8.7765	3.08	12.6826	12.6826	7.2208	14.4416	8.3103	2.417	6.4756	6.4756	5.6564	11.3129	8.7755	2.552
7.8	3.9738	3.9738	5.6564	11.3129	8.7765	3.08	12.6826	12.6826	7.2208	14.4416	8.3103	2.417	6.7730	6.7730	5.6564	11.3129	8.7755	2.503
7.9	3.9738	3.9738	5.6564	11.3129	8.7765	3.08	12.6826	12.6826	7.2208	14.4416	8.3103	2.417	7.0612	7.0612	5.6564	11.3129	8.7755	2.458
8	3.9738	3.9738	5.6564	11.3129	8.7765	3.08	12.6826	12.6826	7.2208	14.4416	8.3103	2.417	7.3412	7.3412	5.6564	11.3129	8.7755	2.415
8.1	3.9738	3.9738	5.6564	11.3129	8.7765	3.08	12.6826	12.6826	7.2208	14.4416	8.3103	2.417	7.6138	7.6138	5.6564	11.3129	8.7755	2.376
8.2	3.9738	3.9738	5.6564	11.3129	8.7765	3.08	12.6826	12.6826	7.2208	14.4416	8.3103	2.417	7.8797	7.8797	5.6564	11.3129	8.7755	2.339
8.3	3.9738	3.9738	5.6564	11.3129	8.7765	3.08	12.6826	12.6826	7.2208	14.4416	8.3103	2.417	8.1396	8.1396	5.6564	11.3129	8.7755	2.304
8.4	3.9738	3.9738	5.6564	11.3129	8.7765	3.08	12.6826	12.6826	7.2208	14.4416	8.3103	2.417	8.3938	8.3938	5.6564	11.3129	8.7755	2.271
8.5	3.9738	3.9738	5.6564	11.3129	8.7765	3.08	12.6826	12.6826	7.2208	14.4416	8.3103	2.417	8.6431	8.6431	5.6564	11.3129	8.7755	2.24
8.6	3.9738	3.9738	5.6564	11.3129	8.7765	3.08	12.6826	12.6826	7.2208	14.4416	8.3103	2.417	8.8874	8.8874	5.6564	11.3129	8.7755	2.21
8.7	3.9738	3.9738	5.6564	11.3129	8.7765	3.08	12.6826	12.6826	7.2208	14.4416	8.3103	2.417	9.1275	9.1275	5.6564	11.3129	8.7755	2.182
8.8	3.9738	3.9738	5.6564	11.3129	8.7765	3.08	12.6826	12.6826	7.2208	14.4416	8.3103	2.417	9.3634	9.3634	5.6564	11.3129	8.7755	2.155
8.9	3.9738	3.9738	5.6564	11.3129	8.7765	3.08	12.6826	12.6826	7.2208	14.4416	8.3103	2.417	9.5963	9.5963	5.6564	11.3129	8.7755	2.13
9	3.9738	3.9738	5.6564	11.3129	8.7765	3.08	12.6826	12.6826	7.2208	14.4416	8.3103	2.417	9.8244	9.8244	5.6564	11.3129	8.7755	2.105
9.1	3.9738	3.9738	5.6564	11.3129	8.7765	3.08	12.6826	12.6826	7.2208	14.4416	8.3103	2.417	10.0504	10.0504	5.6564	11.3129	8.7755	2.082
9.2	3.9738	3.9738	5.6564	11.3129	8.7765	3.08	12.6826	12.6826	7.2208	14.4416	8.3103	2.417	10.2720	10.2720	5.6564	11.3129	8.7755	2.059
9.3	3.9738	3.9738	5.6564	11.3129	8.7765	3.08	12.6826	12.6826	7.2208	14.4416	8.3103	2.417	10.4923	10.4923	5.6564	11.3129	8.7755	2.038
9.4	3.9738	3.9738	5.6564	11.3129	8.7765	3.08	12.6826	12.6826	7.2208	14.4416	8.3103	2.417	10.6629	10.6629	5.6564	11.3129	8.7755	2.017

Table C.24 - Section 9.6.13 MADM Results

Parameter Value (m/s²)	Observer's Decision	TOPSIS				AHP				ANP			
		Lane 1	Lane 2	Lane 3	Decision	Lane 1	Lane 2	Lane 3	Decision	Lane 1	Lane 2	Lane 3	Decision
6.5	3	0.6910	0.1148	0.8244	3	0.2989	0.4473	0.2538	3	0.3195	0.3951	0.2854	3
6.6	3	0.7825	0.0300	0.9700	3	0.2970	0.4439	0.2591	3	0.3182	0.3830	0.2988	3
6.7	3	0.8435	0.0323	0.9677	3	0.2935	0.4376	0.2690	3	0.3167	0.3775	0.3057	3
6.8	3	0.8945	0.0343	0.9657	3	0.2909	0.4330	0.2761	3	0.3159	0.3742	0.3098	3
6.9	3	0.9386	0.0363	0.9637	3	0.2888	0.4292	0.2819	3	0.3154	0.3719	0.3127	3
7	1	0.9619	0.0381	0.9619	1	0.2870	0.4260	0.2870	1	0.3150	0.3700	0.3150	1
7.1	1	0.9617	0.0383	0.9391	1	0.2854	0.4231	0.2915	1	0.3147	0.3685	0.3168	1
7.2	1	0.9616	0.0384	0.9015	1	0.2839	0.4205	0.2956	1	0.3145	0.3672	0.3184	1
7.3	1	0.9615	0.0385	0.8631	1	0.2826	0.4181	0.2994	1	0.3143	0.3661	0.3197	1
7.4	1	0.9613	0.0387	0.8261	1	0.2813	0.4158	0.3029	1	0.3141	0.3651	0.3208	1
7.5	1	0.9612	0.0388	0.7906	1	0.2801	0.4137	0.3062	1	0.3139	0.3642	0.3218	1
7.6	1	0.9610	0.0390	0.7565	1	0.2790	0.4117	0.3093	1	0.3138	0.3635	0.3227	1
7.7	1	0.9609	0.0391	0.7238	1	0.2779	0.4098	0.3123	1	0.3137	0.3628	0.3235	1
7.8	1	0.9607	0.0393	0.6924	1	0.2769	0.4080	0.3151	1	0.3136	0.3621	0.3243	1
7.9	1	0.9606	0.0394	0.6621	1	0.2760	0.4062	0.3178	1	0.3135	0.3615	0.3249	1
8	1	0.9605	0.0395	0.6329	1	0.2750	0.4046	0.3204	1	0.3135	0.3610	0.3256	1
8.1	1	0.9603	0.0398	0.6047	1	0.2742	0.4030	0.3229	1	0.3134	0.3605	0.3261	1
8.2	1	0.9602	0.0402	0.5775	1	0.2733	0.4014	0.3253	1	0.3133	0.3600	0.3267	1
8.3	1	0.9600	0.0407	0.5512	1	0.2725	0.3999	0.3276	1	0.3133	0.3596	0.3271	1
8.4	1	0.9599	0.0413	0.5257	1	0.2717	0.3985	0.3299	1	0.3132	0.3592	0.3276	1
8.5	1	0.9597	0.0420	0.5010	1	0.2709	0.3971	0.3320	1	0.3132	0.3588	0.3280	1
8.6	1	0.9596	0.0428	0.4773	1	0.2701	0.3957	0.3342	1	0.3131	0.3584	0.3284	1
8.7	1	0.9594	0.0437	0.4543	1	0.2694	0.3944	0.3362	1	0.3131	0.3581	0.3288	1
8.8	1	0.9593	0.0446	0.4322	1	0.2687	0.3931	0.3382	1	0.3131	0.3578	0.3292	1
8.9	1	0.9591	0.0455	0.4108	1	0.2680	0.3918	0.3402	1	0.3130	0.3574	0.3295	1
9	1	0.9590	0.0465	0.3905	1	0.2673	0.3906	0.3421	1	0.3130	0.3572	0.3298	1
9.1	1	0.9588	0.0474	0.3709	1	0.2666	0.3894	0.3440	1	0.3130	0.3569	0.3301	1
9.2	1	0.9587	0.0485	0.3523	1	0.2660	0.3882	0.3458	1	0.3130	0.3566	0.3304	1
9.3	1	0.9585	0.0494	0.3346	1	0.2653	0.3871	0.3476	1	0.3129	0.3564	0.3307	1
9.4	1	0.9657	0.0343	NaN	1	0.4068	0.5932	NaN	1	0.4599	0.5401	NaN	1

C - Section 9.6.14 Vehicles Behind Inputted Deceleration

Table C.25 - Section 9.6.14 Simulation Results

Parameter Value (m/s²)	Lane 1							Lane 2							Lane 3						
	Impact Velocity VA (m/s)	Impact Velocity HV1 (m/s)	Impact Velocity HV2 (m/s)	Impact Velocity VB (m/s)	Manoeuvre Acceleration (m/s²)	TTC (s)	Lane Open	Impact Velocity VA (m/s)	Impact Velocity HV1 (m/s)	Impact Velocity HV2 (m/s)	Impact Velocity VB (m/s)	Manoeuvre Acceleration (m/s²)	TTC (s)	Lane Open	Impact Velocity VA (m/s)	Impact Velocity HV1 (m/s)	Impact Velocity HV2 (m/s)	Impact Velocity VB (m/s)	Manoeuvre Acceleration (m/s²)	TTC (s)	Lane Open
0	9.1192	13.1322	3.6921	12.6888	8.7765	3.08	1	0	11.4561	10.3582	21.4249	8.3103	2.417	1	9.1192	13.1322	16.1405	30.6687	8.7765	2.744	1
0.25	9.1192	13.1322	3.6921	12.6888	8.7765	3.08	1	0	11.4561	10.3582	21.4249	8.3103	2.417	1	9.1192	13.1322	15.8385	30.1456	8.7765	2.78	1
0.5	9.1192	13.1322	3.6921	12.6888	8.7765	3.08	1	0	11.4561	10.3582	21.4249	8.3103	2.417	1	9.1192	13.1322	15.5285	29.5037	8.7765	2.818	1
0.75	9.1192	13.1322	3.6921	12.6888	8.7765	3.08	1	0	11.4561	10.3582	21.4249	8.3103	2.417	1	9.1192	13.1322	15.2022	29.0411	8.7765	2.858	1
1	9.1192	13.1322	3.6921	12.6888	8.7765	3.08	1	0	11.4561	10.3582	21.4249	8.3103	2.417	1	9.1192	13.1322	14.8516	28.4552	8.7765	2.9	1
1.25	9.1192	13.1322	3.6921	12.6888	8.7765	3.08	1	0	11.4561	10.3582	21.4249	8.3103	2.417	1	9.1192	13.1322	14.4847	27.8452	8.7765	2.945	1
1.5	9.1192	13.1322	3.6921	12.6888	8.7765	3.08	1	0	11.4561	10.3582	21.4249	8.3103	2.417	1	9.1192	13.1322	14.0935	27.2079	8.7765	2.98	1
1.75	9.1192	13.1322	3.6921	12.6888	8.7765	3.08	1	0	11.4561	10.3582	21.4249	8.3103	2.417	1	9.1192	13.1322	13.6780	26.5412	8.7765	2.98	1
2	9.1192	13.1322	3.6921	12.6888	8.7765	3.08	1	0	11.4561	10.3582	21.4249	8.3103	2.417	1	9.1192	13.1322	13.2300	25.8406	8.7765	2.98	1
2.25	9.1192	13.1322	3.6921	12.6888	8.7765	3.08	1	0	11.4561	10.3582	21.4249	8.3103	2.417	1	9.1192	13.1322	12.7577	25.1056	8.7765	3.08	1
2.5	9.1192	13.1322	3.6921	12.6888	8.7765	3.08	1	0	11.4561	10.3582	21.4249	8.3103	2.417	1	9.1192	13.1322	12.2448	24.3283	8.7765	3.08	1
2.75	9.1192	13.1322	3.6921	12.6888	8.7765	3.08	1	0	11.4561	10.3582	21.4249	8.3103	2.417	1	9.1192	13.1322	11.6996	23.5092	8.7765	3.08	1
3	9.1192	13.1322	3.6921	12.6888	8.7765	3.08	1	0	11.4561	10.3582	21.4249	8.3103	2.417	1	9.1192	13.1322	11.1058	22.6378	8.7765	3.08	1
3.25	9.1192	13.1322	3.6921	12.6888	8.7765	3.08	1	0	11.4561	10.3582	21.4249	8.3103	2.417	1	9.1192	13.1322	10.4715	21.7134	8.7765	3.08	1
3.5	9.1192	13.1322	3.6921	12.6888	8.7765	3.08	1	0	11.4561	10.3582	21.4249	8.3103	2.417	1	9.1192	13.1322	9.7724	20.7214	8.7765	3.08	1
3.75	9.1192	13.1322	3.6921	12.6888	8.7765	3.08	1	0	11.4561	10.3582	21.4249	8.3103	2.417	1	9.1192	13.1322	9.0004	19.6521	8.7765	3.08	1
4	9.1192	13.1322	3.6921	12.6888	8.7765	3.08	1	0	11.4561	10.3582	21.4249	8.3103	2.417	1	9.1192	13.1322	8.1637	18.5030	8.7765	3.08	1
4.25	9.1192	13.1322	3.6921	12.6888	8.7765	3.08	1	0	11.4561	10.3582	21.4249	8.3103	2.417	1	9.1192	13.1322	7.2299	17.2506	8.7765	3.08	1
4.5	9.1192	13.1322	3.6921	12.6888	8.7765	3.08	1	0	11.4561	10.3582	21.4249	8.3103	2.417	1	9.1192	13.1322	6.1909	15.8816	8.7765	3.08	1
4.75	9.1192	13.1322	3.6921	12.6888	8.7765	3.08	1	0	11.4561	10.3582	21.4249	8.3103	2.417	1	9.1192	13.1322	5.0224	14.3718	8.7765	3.08	1
5	9.1192	13.1322	3.6921	12.6888	8.7765	3.08	1	0	11.4561	10.3582	21.4249	8.3103	2.417	1	9.1192	13.1322	3.6921	12.6888	8.7765	3.08	1
5.25	9.1192	13.1322	3.6921	12.6888	8.7765	3.08	1	0	11.4561	10.3582	21.4249	8.3103	2.417	1	9.1192	13.1322	2.1674	10.7965	8.7765	3.08	1
5.5	9.1192	13.1322	3.6921	12.6888	8.7765	3.08	1	0	11.4561	10.3582	21.4249	8.3103	2.417	1	9.1192	13.1322	0.3917	8.6378	8.7765	3.08	1
5.75	9.1192	13.1322	3.6921	12.6888	8.7765	3.08	1	0	11.4561	10.3582	21.4249	8.3103	2.417	1	9.1192	13.1322	0	5.9668	8.7765	3.08	1
6	9.1192	13.1322	3.6921	12.6888	8.7765	3.08	1	0	11.4561	10.3582	21.4249	8.3103	2.417	1	9.1192	13.1322	0	0	8.7765	3.08	1

Table C.26 - Section 9.6.14 Collision Modelling Results

Parameter Value (m/s²)	Lane 1 VA (g)	Lane 1 HV1 (g)	Lane 1 HV2 (g)	Lane 1 VB (g)	Lane 1 Manoeuvre Accel (m/s²)	Lane 1 TTC (s)	Lane 2 VA (g)	Lane 2 HV1 (g)	Lane 2 HV2 (g)	Lane 2 VB (g)	Lane 2 Manoeuvre Accel (m/s²)	Lane 2 TTC (s)	Lane 3 VA (g)	Lane 3 HV1 (g)	Lane 3 HV2 (g)	Lane 3 VB (g)	Lane 3 Manoeuvre Accel (m/s²)	Lane 3 TTC (s)
0	3.9738	3.9738	5.6564	11.3129	8.7755	3.08	12.6826	12.6826	7.2208	14.4416	8.3103	2.417	19.7796	9.8898	16.8794	16.8794	8.7765	2.744
0.25	3.9738	3.9738	5.6564	11.3129	8.7755	3.08	12.6826	12.6826	7.2208	14.4416	8.3103	2.417	19.0614	9.5307	16.5640	16.5640	8.7765	2.78
0.5	3.9738	3.9738	5.6564	11.3129	8.7755	3.08	12.6826	12.6826	7.2208	14.4416	8.3103	2.417	18.3304	9.1652	16.2356	16.2356	8.7765	2.818
0.75	3.9738	3.9738	5.6564	11.3129	8.7755	3.08	12.6826	12.6826	7.2208	14.4416	8.3103	2.417	17.5806	8.7903	15.9033	15.9033	8.7765	2.858
1	3.9738	3.9738	5.6564	11.3129	8.7755	3.08	12.6826	12.6826	7.2208	14.4416	8.3103	2.417	16.8011	8.4006	15.5748	15.5748	8.7765	2.9
1.25	3.9738	3.9738	5.6564	11.3129	8.7755	3.08	12.6826	12.6826	7.2208	14.4416	8.3103	2.417	16.0027	8.0014	15.2379	15.2379	8.7765	2.945
1.5	3.9738	3.9738	5.6564	11.3129	8.7755	3.08	12.6826	12.6826	7.2208	14.4416	8.3103	2.417	15.1750	7.5875	14.8993	14.8993	8.7765	2.98
1.75	3.9738	3.9738	5.6564	11.3129	8.7755	3.08	12.6826	12.6826	7.2208	14.4416	8.3103	2.417	14.3232	7.1616	14.5564	14.5564	8.7765	2.98
2	3.9738	3.9738	5.6564	11.3129	8.7755	3.08	12.6826	12.6826	7.2208	14.4416	8.3103	2.417	13.4324	6.7162	14.2141	14.2141	8.7765	2.98
2.25	3.9738	3.9738	5.6564	11.3129	8.7755	3.08	12.6826	12.6826	7.2208	14.4416	8.3103	2.417	3.9738	3.9738	8.2473	16.4945	8.7765	3.08
2.5	3.9738	3.9738	5.6564	11.3129	8.7755	3.08	12.6826	12.6826	7.2208	14.4416	8.3103	2.417	3.9738	3.9738	8.0319	16.0639	8.7765	3.08
2.75	3.9738	3.9738	5.6564	11.3129	8.7755	3.08	12.6826	12.6826	7.2208	14.4416	8.3103	2.417	3.9738	3.9738	7.8103	15.6207	8.7765	3.08
3	3.9738	3.9738	5.6564	11.3129	8.7755	3.08	12.6826	12.6826	7.2208	14.4416	8.3103	2.417	3.9738	3.9738	7.5882	15.1764	8.7765	3.08
3.25	3.9738	3.9738	5.6564	11.3129	8.7755	3.08	12.6826	12.6826	7.2208	14.4416	8.3103	2.417	3.9738	3.9738	7.3584	14.7169	8.7765	3.08
3.5	3.9738	3.9738	5.6564	11.3129	8.7755	3.08	12.6826	12.6826	7.2208	14.4416	8.3103	2.417	3.9738	3.9738	7.1288	14.2575	8.7765	3.08
3.75	3.9738	3.9738	5.6564	11.3129	8.7755	3.08	12.6826	12.6826	7.2208	14.4416	8.3103	2.417	3.9738	3.9738	6.8980	13.7961	8.7765	3.08
4	3.9738	3.9738	5.6564	11.3129	8.7755	3.08	12.6826	12.6826	7.2208	14.4416	8.3103	2.417	3.9738	3.9738	6.6582	13.3163	8.7765	3.08
4.25	3.9738	3.9738	5.6564	11.3129	8.7755	3.08	12.6826	12.6826	7.2208	14.4416	8.3103	2.417	3.9738	3.9738	6.4163	12.8325	8.7765	3.08
4.5	3.9738	3.9738	5.6564	11.3129	8.7755	3.08	12.6826	12.6826	7.2208	14.4416	8.3103	2.417	3.9738	3.9738	6.1685	12.3369	8.7765	3.08
4.75	3.9738	3.9738	5.6564	11.3129	8.7755	3.08	12.6826	12.6826	7.2208	14.4416	8.3103	2.417	3.9738	3.9738	5.9151	11.8301	8.7765	3.08
5	3.9738	3.9738	5.6564	11.3129	8.7755	3.08	12.6826	12.6826	7.2208	14.4416	8.3103	2.417	3.9738	3.9738	5.6564	11.3129	8.7765	3.08
5.25	3.9738	3.9738	5.6564	11.3129	8.7755	3.08	12.6826	12.6826	7.2208	14.4416	8.3103	2.417	3.9738	3.9738	5.3901	10.7802	8.7765	3.08
5.5	3.9738	3.9738	5.6564	11.3129	8.7755	3.08	12.6826	12.6826	7.2208	14.4416	8.3103	2.417	3.9738	3.9738	5.1163	10.2325	8.7765	3.08
5.75	3.9738	3.9738	5.6564	11.3129	8.7755	3.08	12.6826	12.6826	7.2208	14.4416	8.3103	2.417	3.9738	3.9738	3.5584	7.1167	8.7765	3.08
6	3.9738	3.9738	5.6564	11.3129	8.7755	3.08	12.6826	12.6826	7.2208	14.4416	8.3103	2.417	3.9738	0	0	0	8.7765	3.08

Table C.27 - Section 9.6.14 MADM Results

Parameter Value (m/s²)	Observer's Decision	TOPSIS Lane 1	TOPSIS Lane 2	TOPSIS Lane 3	TOPSIS Decision	AHP Lane 1	AHP Lane 2	AHP Lane 3	AHP Decision	ANP Lane 1	ANP Lane 2	ANP Lane 3	ANP Decision
0	1	0.9691	0.4886	0.1181	1	0.2418	0.3412	0.4169	1	0.2956	0.3389	0.3655	1
0.25	1	0.9686	0.4734	0.1363	1	0.2433	0.3441	0.4126	1	0.2960	0.3397	0.3643	1
0.5	1	0.9679	0.4574	0.1556	1	0.2449	0.3470	0.4080	1	0.2965	0.3405	0.3631	1
0.75	1	0.9672	0.4405	0.1764	1	0.2466	0.3501	0.4033	1	0.2970	0.3413	0.3618	1
1	1	0.9664	0.4232	0.1990	1	0.2484	0.3534	0.3983	1	0.2974	0.3422	0.3604	1
1.25	1	0.9656	0.4053	0.2233	1	0.2502	0.3568	0.3930	1	0.2980	0.3432	0.3589	1
1.5	1	0.9647	0.3875	0.2497	1	0.2521	0.3604	0.3875	1	0.2986	0.3443	0.3572	1
1.75	1	0.9636	0.3704	0.2781	1	0.2541	0.3641	0.3819	1	0.2993	0.3457	0.3550	1
2	1	0.9626	0.3551	0.3094	1	0.2562	0.3680	0.3759	1	0.3001	0.3472	0.3527	1
2.25	1	0.9610	0.1556	0.6793	1	0.2754	0.4042	0.3204	1	0.3096	0.3678	0.3225	1
2.5	1	0.9607	0.1288	0.6978	1	0.2763	0.4059	0.3178	1	0.3100	0.3680	0.3220	1
2.75	1	0.9605	0.1002	0.7178	1	0.2772	0.4076	0.3151	1	0.3104	0.3681	0.3215	1
3	1	0.9603	0.0713	0.7390	1	0.2782	0.4094	0.3124	1	0.3108	0.3682	0.3210	1
3.25	1	0.9601	0.0460	0.7623	1	0.2792	0.4113	0.3095	1	0.3112	0.3684	0.3204	1
3.5	1	0.9601	0.0399	0.7871	1	0.2802	0.4132	0.3066	1	0.3117	0.3686	0.3197	1
3.75	1	0.9604	0.0396	0.8138	1	0.2812	0.4151	0.3037	1	0.3122	0.3688	0.3191	1
4	1	0.9607	0.0393	0.8434	1	0.2823	0.4172	0.3005	1	0.3127	0.3690	0.3184	1
4.25	1	0.9610	0.0390	0.8752	1	0.2834	0.4192	0.2973	1	0.3132	0.3692	0.3176	1
4.5	1	0.9613	0.0387	0.9090	1	0.2846	0.4214	0.2940	1	0.3138	0.3694	0.3168	1
4.75	1	0.9616	0.0384	0.9425	1	0.2858	0.4237	0.2906	1	0.3144	0.3697	0.3159	1
5	1	0.9619	0.0381	0.9619	1	0.2870	0.4260	0.2870	1	0.3150	0.3700	0.3150	1
5.25	3	0.9426	0.0374	0.9626	3	0.2883	0.4285	0.2833	3	0.3157	0.3703	0.3140	3
5.5	3	0.9074	0.0365	0.9635	3	0.2896	0.4310	0.2793	3	0.3164	0.3707	0.3129	3
5.75	3	0.7310	0.0315	0.9685	3	0.2978	0.4465	0.2557	3	0.3216	0.3734	0.3050	3
6	3	0.5031	0.0223	0.9777	3	0.3201	0.4885	0.1914	3	0.3453	0.3898	0.2649	3